UNIVERSITE PARIS–IX DAUPHINE
U.F.R. MATHEMATIQUES DE LA DECISION

THESE

pour l'obtention du titre de
DOCTEUR EN SCIENCES
spécialité : Mathématiques Appliquées
(arrêté du 30 Mars 1992)

présentée et soutenue publiquement
par

Simon MASNOU

le 15 Décembre 1998

Titre :

FILTRAGE ET DESOCCLUSION D'IMAGES PAR METHODES D'ENSEMBLES DE NIVEAU

Directeur de thèse :

Jean-Michel MOREL

JURY

Président :	M.	**Yves MEYER**
Rapporteur :	M.	**Luigi AMBROSIO**
Rapporteur :	M.	**Vicent CASELLES**
	Mme.	**Françoise DIBOS**
	M.	**Jean-Michel MOREL**
	M.	**David MUMFORD**
	M.	**Bernard ROUGE**
	M.	**Leonid YAROSLAVSKY**

à Delphine,
à mes parents,

Je souhaiterais d'abord remercier Yves Meyer de l'honneur qu'il me fait en acceptant la présidence de ce jury.

Je suis très reconnaissant à Luigi Ambrosio et Vicent Caselles d'avoir accepté d'être les rapporteurs sur cette thèse. Leurs suggestions et leurs remarques, l'aide qu'ils m'ont apportée dans la compréhension du sujet m'ont été extrêmement utiles et je les en remercie vivement.

David Mumford a accepté de participer au jury et je lui en suis très reconnaissant.

J'ai eu grand plaisir à travailler avec Bernard Rougé sur des problèmes issus de l'imagerie satellitaire et je le remercie d'avoir accepté d'être membre du jury.

J'aimerais assurer de ma gratitude Leonid Yaroslavsky pour les précieux conseils qu'il m'a donnés et les remarques qu'il a su me faire lors de la réalisation de ce travail. Je le remercie d'avoir accepté de participer au jury.

Jean-Michel Morel a dirigé ce travail durant trois années. Sa disponibilité, son ouverture d'esprit, son sens de l'innovation et sa qualité d'écoute m'ont permis d'effectuer cette thèse dans des conditions exceptionnelles et je lui en suis infiniment reconnaissant.

Françoise Dibos a codirigé la partie de cette thèse consacrée au problème de la désocclusion. Elle a énormément contribué par ses remarques précieuses et sa disponibilité aux résultats qui sont présentés ici et je lui adresse mes plus sincères remerciements.

J'ai effectué cette thèse au sein du groupe de traitement d'images réuni autour de Jean-Michel Morel. La qualité des échanges au sein de ce groupe m'a été précieuse et je remercie vivement Denis Pasquignon, Francine Catté, Christian Lopez, Georges Koepfler, Jacques Froment, Pascal Monasse, Frédéric Guichard, François Malgouyres, Agnès Desolneux, Frédéric Cao, Yann Gousseau et Jose-Luis Lisani.

Ce travail a été réalisé au Centre de Recherches de Mathématiques de la Décision à l'Université Paris-IX Dauphine, dirigé par Maria Esteban. J'ai eu plaisir à côtoyer les membres de ce laboratoire et je souhaiterais en particulier assurer de toute mon amitié Céline Gelperowic, Géraldine Polaillon, Jacques Giacomoni, Frédéric Vautrain, Agnès Tourin, Antonin Chambolle, Jacques-Olivier Moussafir et Michel Vanbreugel.

Table des matières

Chapitre 1

Introduction

Une image numérique en niveaux de gris u est en général dans la technologie actuelle une application d'un sous-ensemble de $\mathbb{N} \times \mathbb{N}$ dans l'intervalle $[0, 255]$ associant à chaque point de la grille discrète une valeur entière de niveau de gris. Une image numérique peut donc comporter 256 niveaux de gris s'échelonnant de 0 à 255, le noir étant représenté par la valeur 0 et le blanc par la valeur 255. Les images en couleurs sont généralement codées sous la forme (u_r, u_g, u_b) où u_r est une image en niveaux de gris correspondant au canal rouge, u_g est l'image correspondant au canal vert et u_b est associée au canal bleu. Le processus de formation d'une image à partir d'une scène naturelle est extrêmement complexe et la formule suivante n'en est qu'un modèle simple:

$$u = \mathrm{Q}\left\{\mathrm{g}[(k * O).\Pi_\Gamma.F_{N,M} + n]\right\}.d \qquad (*)$$

où

- O est le flux de photons.
- k est le noyau de convolution optique du capteur.
- Π_Γ est le maillage régulier du plan Γ composé de cellules à l'intérieur desquelles on mesure l'énergie lumineuse reçue.
- $F_{N,M}$ est la fenêtre d'observation de taille $N \times M$.
- n désigne le bruit photonique et électronique qui s'ajoute à l'énergie lumineuse mesurée.
- g est un opérateur de changement de contraste qui représente la fonction de transfert non linéaire du capteur.
- Q est un opérateur de quantification uniforme dans l'intervalle discret $[0, 255]$ des valeurs réelles d'énergie lumineuse.
- d, enfin, est le bruit destructif lié à la transmission qui se caractérise par la présence de taches dans l'image.

Le nombre et la complexité des opérations qui apparaissent dans la formule $(*)$ font

que le problème inverse consistant à retrouver le flux optique original O à partir de l'image u est impossible à résoudre. Il existe en revanche plusieurs méthodes et théories qui permettent de résoudre partiellement ce problème inverse. Citons par exemple la théorie de Shannon qui, sous l'hypothèse que le flux optique a un spectre à support borné et que le maillage Π_Γ est suffisamment fin, permet de reconstruire totalement le signal $k*O$ à partir du signal échantillonné $(k*O).\Pi_\Gamma$. La théorie morphologique de Matheron-Serra a, quant à elle, trait à la présence de l'opérateur de changement de contraste g. Cet opérateur est rarement connu et peut différer considérablement d'un capteur à l'autre. On ne peut donc le déduire de la simple observation de l'image u. En revanche, ainsi que nous le verrons plus loin, Georges Matheron et Jean Serra ont montré comment l'utilisation des ensembles de niveau de l'image permettent de la caractériser et de la traiter indépendamment de la fonction de changement de contraste utilisée.

Cette thèse a pour objet l'étude de deux problèmes distincts. Dans le premier, nous supposons que l'image observée s'écrit soit sous la forme $u = Q[g(v+n)]$ où n est un bruit additif blanc à distribution gaussienne ou uniforme, soit sous la forme $u = Q[g(v)].d_f$ où d_f désigne un bruit impulsionnel de fréquence f. Rappelons qu'un bruit impulsionnel de fréquence f remplace le niveau de gris d'un pourcentage f de points uniformément répartis dans l'image par une valeur aléatoire entre 0 et 255 suivant une loi uniforme, tandis que les autres points restent inchangés. Dans les deux expressions précédentes, g désigne une fonction de changement de contraste strictement croissante entre ses deux niveaux inférieur et supérieur de saturation et Q un opérateur de quantification uniforme. Notre problème est alors de définir un opérateur T tel que Tu soit le plus proche possible de $Q[g(v)]$. Il s'agit donc de filtrer l'image en vue de la restaurer, c'est-à-dire d'éliminer le bruit.

Le second problème que nous aborderons est un problème d'interpolation. Partant d'une image $u.d$ où d est un bruit destructif, quel opérateur peut-on définir de sorte que l'image résultante soit proche de u ? Plus précisément, l'image $u.d$ se caractérise par la présence de taches dans l'image qui occultent partiellement ou totalement certains objets présents dans la scène. Notre but est de définir une *désocclusion*, c'est-à-dire une opération de restauration des objets partiellement occultés. L'approche que nous développerons ne s'applique pas exclusivement au bruit destructif mais aussi bien à toute source d'occlusion quelle qu'elle soit. En particulier, elle permet de résoudre le problème consistant à restaurer un objet dans l'image partiellement occulté par d'autres objets.

Dans un souci de plus grande généralité, nous désignerons par image en niveaux de gris toute application $\mathcal{L}^N$-mesurable de $\mathbb{R}^N$ dans $\mathbb{R}$, où $\mathcal{L}^N$ désigne la mesure de Lebesgue dans $\mathbb{R}^N$. L'emploi d'un espace continu de préférence à une grille discrète permet en effet une bien meilleure caractérisation des propriétés d'un opérateur agissant sur les images. Le passage de la grille discrète au plan continu se fait très naturellement en considérant

qu'une image est une fonction constante par morceaux.

Dans le modèle d'acquisition d'une image que nous avons présenté, nous n'avons fait apparaître comme seuls termes de bruit qu'un bruit additif et un bruit destructif. En fait, la notion de bruit en traitement d'images est extrêmement vague car elle recouvre des phénomènes très variés. Ainsi, la saisie, la transmission, la manipulation des images sont autant de facteurs susceptibles d'introduire des modifications dans l'image originale qui peuvent être de natures très différentes. Ce peut être un flou dans l'image dû à une mauvaise mise au point du capteur utilisé pour saisir la scène; ou encore une perte d'informations qui survient lors de la transmission d'une image satellitaire entre le satellite et le sol. Les exemples sont également nombreux de signaux altérés par un bruit gaussien ou impulsionnel lors de leur transmission. Citons enfin l'exemple de l'impression d'une image sur un papier de mauvaise qualité : dans l'image résultante, la texture du papier sera étroitement mélée aux informations contenues dans l'image originale. Tous ces exemples, absolument pas exhaustifs, permettent de comprendre en quoi le "bruit" dans une image, c'est-à-dire l'information qui ne correspond pas à ce que l'on souhaiterait voir, est une notion parfaitement subjective et totalement dépendante de l'application traitée. En conséquence, la définition d'un opérateur universel de restauration d'images est illusoire car il n'y a pas de définition universelle du bruit. C'est la raison pour laquelle nous nous limiterons dans la première partie de cette thèse au problème de restauration d'une image altérée soit par un bruit additif blanc, soit par un bruit impulsionnel.

Revenons à présent sur le terme g qui modélise la fonction de transfert du capteur dans l'équation $(*)$. Comme nous l'avons dit, cette fonction peut varier considérablement d'un capteur à l'autre sans que pour autant la scène observée ait changé. De façon plus générale, c'est le problème de la pertinence du niveau de gris observé qui est en cause. Max Wertheimer, le fondateur de l'école de la Gestalt, a initié de nombreux travaux sur la perception visuelle. Il faisait remarquer dès 1923 [40] que l'attribution d'une valeur précise de niveau de gris aux objets contenus dans une scène est tout à fait arbitraire. En revanche, c'est l'ordre dans lequel ces valeurs sont prises qui est pertinent. Pour être plus précis, nous sommes capables de dire que le ciel est plus clair que la forêt dans un paysage donné, mais il n'y a pas plus de raison d'attribuer au ciel et à la forêt les valeurs respectives 120 et 230 que 90 et 150. Il faut par ailleurs rappeler que les conditions d'illumination d'une scène peuvent considérablement évoluer d'un moment à l'autre sans que pour autant la nature des objets présents dans la scène ait changé. Matheron [25] et Serra [36] ont déduit des travaux de Wertheimer un principe que doivent vérifier les méthodes d'analyse en traitement des images : le principe d'invariance par changement de contraste, ou principe morphologique. En vertu de ce principe, un opérateur de filtrage ne doit dépendre que de l'ordre des niveaux de gris et non du contraste. Cela revient à considérer qu'une image u est en fait un représentant d'une classe d'équivalence dont chaque élément v peut être

déduit de u par application d'un changement de contraste. Insistons sur ce point : pour Matheron et Serra, l'image observée n'est pas pertinente et il faut la caractériser d'une façon qui ne dépende ni du capteur utilisé ni des conditions d'illumination de la scène. On peut en déduire une relation que doit satisfaire tout opérateur de filtrage T vérifiant le principe d'invariance par changement de contraste :

$$T(g(u)) = g(T(u))$$

où u est l'image observée et g, par souci de simplicité, tout changement de contraste continu et strictement croissant.

La plupart des opérateurs de restauration généralement utilisés en traitement des images ne satisfont pas le principe morphologique. Il en va ainsi des méthodes linéaires ou non-linéaires basées sur la caractérisation d'une image à l'aide de ses contours, ou "edges" [6, 22, 23, 24, 41]. On peut adresser deux reproches à la théorie de l'*edge detection*. Le premier est que la définition des contours d'une image est fragile et qu'ils n'en sont pas une bonne caractérisation. Il est en effet connu que la simple donnée des contours de permet pas de reconstruire l'image. Par ailleurs, les contours dépendent du gradient dans l'image et sont donc incompatibles avec la théorie morphologique. A la suite des travaux de Marr-Hildreth s'est développée la théorie du filtrage "espace-échelle" (ou *scale-space filtering*) qui a pour objet la description d'une image à différentes échelles d'analyse. D'importants travaux d'axiomatisation [1] ont montré le rôle fondamental en traitement des images de deux équations : la *mean curvature motion* $\frac{\partial u}{\partial t} = |Du|\text{curv}(u)$ à laquelle se ramène asymptotiquement le filtre médian itéré, et l'*affine invariant curvature motion* $\frac{\partial u}{\partial t} = |Du|(\text{curv}(u))^{1/3}$. Ces deux équations vérifient le principe morphologique mais induisent une évolution des lignes de niveau de l'image en fonction de leur courbure et ne permettent donc pas de préserver les structures de l'image tout en éliminant le bruit.

L'analyse de Fourier ainsi que sa généralisation, l'analyse par ondelettes [26], permettent une caractérisation complète de l'image sous la forme d'une combinaison linéaire d'ondes élémentaires. Toutes les méthodes d'analyse d'image qui en résultent ne rentrent cependant pas dans le cadre de notre étude car la linéarité des transformations utilisées est incompatible avec l'invariance par changement de contraste.

Quels sont alors les éléments qui permettent de caractériser entièrement une image de façon morphologique? Matheron et Serra ont montré que les ensembles de niveau ont cette propriété. Rappelons que si u est une fonction $\mathcal{L}^N$-mesurable de $\mathbb{R}^N$ dans $\mathbb{R}$ alors l'ensemble supérieur de niveau λ est $X_\lambda := \{x \in \mathbb{R}^N : u(x) \geq \lambda\}$ tandis que l'ensemble inférieur de niveau λ est $X'_\lambda := \{x \in \mathbb{R}^N : u(x) \leq \lambda\}$. On peut facilement vérifier que la famille constituée de tous les ensembles supérieurs – le résultat est bien sûr identique pour les ensembles inférieurs – est globalement invariante pour tout changement de contraste

continu et strictement croissant. En outre les deux formules de reconstruction

$$\begin{array}{lrcll} & u(x) & := & \sup\{\lambda : x \in X_\lambda\} & \text{p.p. } x \in \mathbb{R}^N \\ \text{et} & u(x) & := & \inf\{\lambda : x \in X'_\lambda\} & \text{p.p. } x \in \mathbb{R}^N \end{array}$$

assurent que les ensembles de niveau caractérisent complètement l'image. Les frontières des ensembles de niveau sont appelées de façon générique "lignes de niveau", bien que ce terme soit abusif lorsque $N > 2$. La "carte topographique" d'une image est l'ensemble de ses lignes de niveau. Nous avons représenté dans la figure 1.1 certaines lignes de niveau d'une image et la reconstruction que l'on peut déduire par interpolation [9] de cette carte topographique simplifiée.

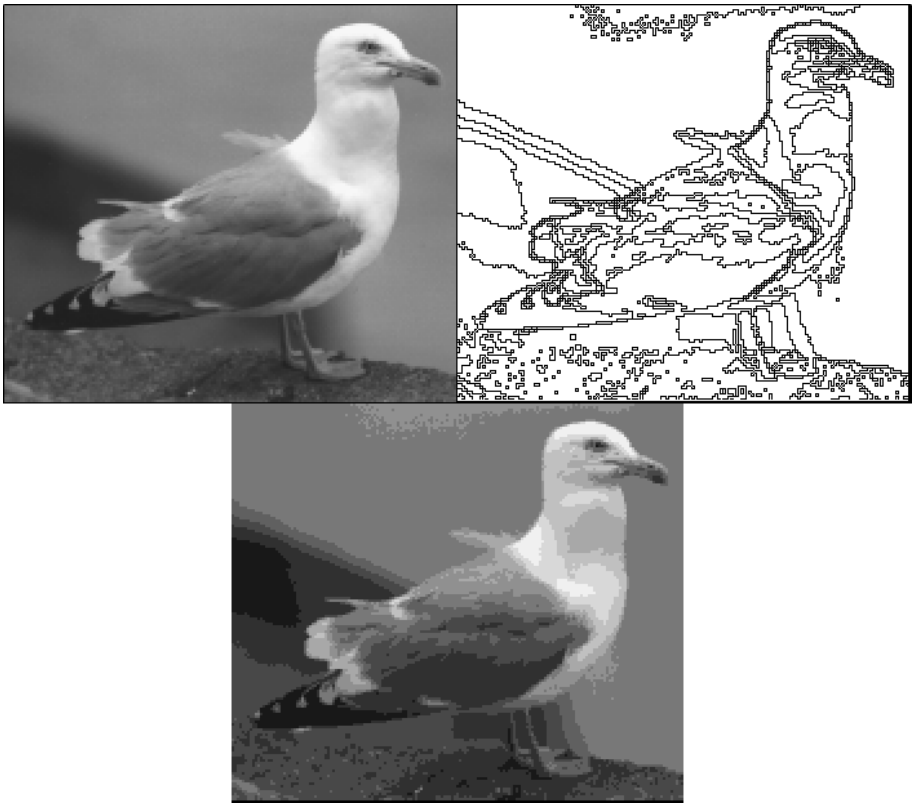

FIG. 1.1: *En haut : une image et sa carte topographique simplifiée (lignes de niveau de 24 en 24). En bas, l'image reconstruite à partir de cette carte topographique : même si l'on ne prend en compte que quelques lignes de niveau, on a déjà une très bonne représentation de l'image.*

La première partie de cette thèse a pour objet la restauration des images bruitées à l'aide d'opérateurs morphologiques à voisinage. L. Yaroslavsky [42, 43] a développé une approche synthétique des techniques de filtrage local qui consistent à régulariser une image

u en chaque point en fonction des valeurs dans un voisinage autour du point considéré. Génériquement, ces voisinages sont de deux types :

1. les voisinages définis en chaque point x du domaine de l'image comme un sous-ensemble $N_1(x)$ du disque $B_a(x)$ de rayon a tel que

$$N_1(x) = \{y \in B_a(x) : u(x) - \epsilon_v^- \leq u(y) \leq u(x) + \epsilon_v^+\}$$

   où ϵ_v^-, $\epsilon_v^+ \in \mathbb{R}^+$ sont deux constantes données.

2. les voisinages définis comme un sous-ensemble de $B_a(x)$ s'écrivant

$$N_2(x) = \{y \in B_a(x) : R(u(x)) - \epsilon_R^- \leq R(u(y)) \leq R(u(x)) + \epsilon_R^+\}$$

   où $R(u(x)) := |\{z \in B_a(x) : u(z) < u(x)\}|$ désigne le rang de $u(x)$ et ϵ_R^-, $\epsilon_R^+ \in \mathbb{R}^+$ sont deux constantes données.

Il est clair que les voisinages du type N_1 ne sont pas morphologiques car ils font intervenir le gradient dans l'image, alors que les voisinages du type N_2 sont morphologiques. Une fois le voisinage sélectionné, on peut choisir différents types d'opérateur, tels le médian, l'inf, le sup, la moyenne et tous les filtres pondérés qui en découlent. Les filtres morphologiques qui font intervenir un voisinage du type N_2 sont appelés "filtres de rang".

Le chapitre 2 de cette thèse est consacré à l'étude de différents opérateurs locaux de restauration d'images vérifiant le principe morphologique. Dans la section 2.1, nous rappelons d'abord qu'une image doit être considérée comme représentant d'une classe d'équivalence au regard de plusieurs types de perturbations. Puis nous montrons que tout filtre de rang équivaut au simple calcul du médian sur un mode de l'histogramme. La section 2.2 est consacrée au rappel des définitions et propriétés de l'espace des fonctions à variation bornée dans $\mathbb{R}^N$ et des ensembles de périmètre fini, que nous faisons intervenir dans la suite de la thèse. Dans la section 2.3, nous nous intéressons au filtre médian, le plus classique des filtres morphologiques. Nous montrons qu'il n'est pas un projecteur sur l'espace des fonctions à variation bornée et qu'il peut même augmenter la variation totale d'une fonction BV. La section 2.4 est consacrée à la définition et à l'étude d'un filtre médian particulier, qui ne s'applique plus sur un disque mais sur un voisinage s'adaptant à la structure locale des lignes de niveau. Ce filtre, MFCN (Median Filter on a Connected Neighborhood), a la particularité d'admettre une plus grande classe de points fixes que le filtre médian classique ce qui le rend plus apte à préserver les structures de l'image tout en éliminant le bruit. Nous comparons par ailleurs ses performances avec celles d'autres méthodes de restauration.

Nous introduisons dans la section 2.5 une notion faible de connexité, plus pertinente lorsque l'on s'intéresse aux ensembles de périmètre fini que la connexité au sens topologique

classique. Cette notion va nous être utile tout au long des sections 2.6 et 2.7. Dans la section 2.6 nous nous intéressons à deux filtres morphologiques introduits par Luc Vincent qui consistent à éliminer les composantes connexes d'ensembles de niveau d'aire trop petite, et qui peuvent être considérés comme une simplification du filtre MFCN introduit à la section 2.4. Nous proposons de les définir comme opérateurs morphologiques agissant sur l'espace des fonctions à variation bornée et nous montrons leurs propriétés de monotonie, de continuité et d'idempotence. Nous montrons par ailleurs qu'ils font décroître la variation totale.

La section 2.7 a pour objet l'introduction et l'étude du filtre de grains, qui peut être vu comme une adaptation des filtres de Luc Vincent à la structure de la carte topographique d'une image. Les ensembles considérés ne sont plus les composantes connexes des ensembles de niveau mais les grains de l'image, c'est-à-dire ces ensembles "sans trous" dont la frontière est une ligne de niveau. Nous montrons qu'en tant qu'opérateur agissant sur l'espace des fonctions à variation bornée dans une boule bornée de $\mathbb{R}^N$, ce filtre est morphologique, idempotent et fait décroître la variation totale. En outre, nous proposons une définition qui, contrairement aux filtres de Luc Vincent, permet de traiter indifféremment les ensembles de niveau inférieur ou supérieur lorsque la fonction à variation bornée considérée est très régulière. Nous présentons ensuite quelques expériences où nous comparons le filtre de grain et les filtres de Luc Vincent à d'autres filtres de restauration.

Le chapitre 3 est entièrement consacré à l'étude du problème de désocclusion, que nous introduisons dans la section 3.1. Nous montrons dans la section 3.2 l'existence d'une désocclusion optimale qui respecte le principe de "complétion amodale" de Kanizsa lorsque la fonction à interpoler est à variation bornée. Nous décrivons dans la section 3.3 l'algorithme permettant en pratique de réaliser la désocclusion d'une partie d'une image et nous présentons quelques expériences dans la section 3.4.

L'annexe A contient une étude numérique dont l'objet est la représentation de l'image par le filtre médian de la fonction utilisée pour le contre-exemple de la section 2.3.3. Il est montré à la section 2.3.3 que la fonction résultante a une plus grande variation totale que la fonction initiale. Nous donnons par approximation numérique dans l'annexe A le graphe de cette fonction résultante.

Enfin, nous effectuons dans l'annexe B l'étude asymptotique d'un filtre local non linéaire et non morphologique défini sur un voisinage du type N_1 (voir ci-dessus) dans le cas particulier où la fonction traitée est régulière et où ses lignes de niveau sont des paraboles au voisinage du point considéré. Nous montrons en particulier que le filtre est, dans ce cas, asymptotiquement équivalent à une équation qui ne diffère de la *mean curvature motion* qu'à un terme correctif près.

Chapitre 2

Filtrage local récursif à voisinage

2.1 Morphological filters, rank filters and histograms.

In the sequel, we shall call neighborhood (in a wide sense) of a point $x \in \mathbb{R}^N$ any $\mathcal{L}^N$-measurable subset $\mathcal{V} \subset \mathbb{R}^N$ containing x. Notice that we do not assume x to be in the interior of $\mathcal{V}$. In addition, unless specified, $\mathcal{V}$ will generally be taken bounded and closed. Given a $\mathcal{L}^N$-measurable function defined on $\mathbb{R}^N$, we address here the following problem : assuming that we only know the values of u on a neighborhood $\mathcal{V}$ of x, what is the "best estimate" of $u(x)$. Let us once more emphasize that images are not reliable data : the information they contained depends of course on the original scene that was captured but, in addition, also on the sensor characteristics as well as on the capture conditions. Therefore, we shall consider that the values of u within $\mathcal{V}$ are representatives of equivalence classes under several groups of perturbations :

Contrast rearrangements : any perturbation of the type $u \to g \circ u$ where g is an arbitrary increasing continuous function.

Combinatorial rearrangements : when captured at a very local scale, the gray level is not a reliable information. This can be checked by simply looking at a photograph with a lens or by zooming on a digital image. It is therefore reasonable to think that the "true value" of u at x depends on a small neighborhood $\mathcal{V}$ of x. How this neighborhood must be chosen is a deep question which we shall discuss later. However, we can assume that the "true value" $\tilde{u}(x)$ depends upon all values of u inside $\mathcal{V}$. Since $\mathcal{V}$ is small, it is reasonable to think that any redistribution of those values on $\mathcal{V}$ shall not alter $\tilde{u}(x)$. In other words, we consider all possible maps $\mathcal{C} : \mathcal{V} \to \mathcal{V}$ which are measure-preserving and we assume that the observed u is the result of those perturbations

$$u_{|\mathcal{V}} \to u_{\mathcal{V}} \circ \mathcal{C} \tag{2.1.1}$$

Projective views we mean here the transformations $u(x) \to u(Px)$ where P is a projective map. As a simplified case we may consider $u(x) \to u(Ax)$ where A is an affine map.

Occlusion the image formation process entails drastic consequences when one is concerned with the correct estimate of $u(x)$. Indeed, in the case of real world images ($N = 2$) or in the case of movies ($N = 2+1$), we know that boundaries appear in an image because most physical objects simply occlude what is behind them. The result of this operation can be written as (calling $u(x)$ the final image, $v(x)$ the original image without the occluding object A and u_A the image of the object A, defined on a subset $A \subset \mathbb{R}^2$) :

$$\begin{array}{ll} u(x) = u_A(x) & \text{if } x \in A \\ u(x) = v(x) & \text{otherwise} \end{array} \tag{2.1.2}$$

Clearly, the boundary of A, ∂A, separates on the image two regions where values of $u(x)$ have nothing to do with each other, so that computing the "estimated" value $\tilde{u}(x)$ as a mean on a ball would be nonsense if x is close to ∂A.

Transparency this is another perturbation that occurs in the formation of images and is more generally related to the shadowing. Physical objects cannot only overlap, they also can intercept the light coming from light sources so that their shadow is projected on other objects. We can state that by a rough (but somehow reliable) generic model of shadowing. We call $S \in \mathbb{R}^2$ the domain of the shadow spot. Inside this spot, the original gray level is altered by a contrast change $u \to g \circ u$, where of course g is increasing and $g(s) \leq s$. Calling, as for the occlusion, $v(x)$ the image without shadowing, we have

$$\begin{array}{ll} u(x) = g \circ v(x) & \text{if } x \in S \\ u(x) = v(x) & \text{otherwise} \end{array} \tag{2.1.3}$$

Clearly, as in the occlusion process, a new discontinuity front, ∂S, is added to the image. Now the structure of v is somehow preserved since for example the level lines of v inside S are not altered in shape, but shifted in gray level.

Like previously said in the introduction, the nature of perturbations and the formation of images itself lead us to the following definition.

Definition 2.1.1 *We call "morphological filter" any operator $T : u \to T(u)$ mapping the space of $\mathcal{L}^N$-measurable functions onto itself and which is covariant with respect to any increasing continuous contrast change g, that is*

$$T(g \circ u)(x) = g(T(u)(x)), \quad \forall x \in \mathbb{R}^N \tag{2.1.4}$$

We shall denote by $u_{|\mathcal{V}}$ the restriction of u to the "neighborhood" $\mathcal{V}$ and shall assume that $|\mathcal{V}| < \infty$.

2.1.1 Repartition functions and rank filters.

Definition 2.1.2 *We call repartition function of u on $\mathcal{V}$ and denote by $H = H_{u,\mathcal{V}}$ the real function $H(\lambda) = |\{x \in \mathcal{V} : u(x) \leq \lambda\}|$.*

It is easily seen that H is nondecreasing and satisfies $H(-\infty) = 0$, $H(+\infty) = |\mathcal{V}|$. If u is in $\mathrm{L}^\infty(\mathcal{V})$ then, denoting respectively by $\sup_{\mathcal{V}} u$ and $\inf_{\mathcal{V}} u$ the essential sup and inf of u on $\mathcal{V}$, we also have

$$\begin{aligned} H(\lambda) &= 0 \qquad \text{on } (-\infty, \inf_{\mathcal{V}} u) \\ H(\lambda) &= |\mathcal{V}| \quad \text{on } [\sup_{\mathcal{V}}, +\infty) \end{aligned}$$

Among the elementary and useful properties of the repartition function, we have the morphological covariance. Indeed, if g is a continuous increasing real function, we have

$$H_{g\circ u}(\lambda) = |\{x : g \circ u(x) \leq \lambda\}|,$$

$$H_{g\circ u}(\lambda) = \left|\{x : u(x) \leq g^{-1}(\lambda)\}\right|, \text{ so that}$$

$$H_{g\circ u}(\lambda) = H_u(g^{-1}(\lambda)) \text{ and therefore,}$$

$$H_{g\circ u}(g(\lambda)) = H_u(\lambda) \tag{2.1.5}$$

Definition 2.1.3 *We call histogram of u on $\mathcal{V}$ the distributional derivative of H on $\mathbb{R}$. We shall denote it by $h = h_{u,\mathcal{V}}$.*

Since H is nondecreasing with respect to the gray level, h is a positive measure, $h = H'$ and if u is in L^∞, the support of h is $[\inf_{\mathcal{V}} u, \sup_{\mathcal{V}} u]$. An example of histogram is illustrated in figure 2.1. In order to see how histograms change with contrast changes g, we can derive the relation (2.1.5) in the sense of distributions and obtain

$$H'_{g\circ u}(g(\lambda))g'(\lambda) = H'_u(\lambda), \text{ so that}$$

$$h_{g\circ u}(g(\lambda))g'(\lambda) = h_u(\lambda) \tag{2.1.6}$$

Note that this relation is much less easy to deal with than relation (2.1.5).

Definition 2.1.4 *We call "rank filter" any map $T : (u, \mathcal{V}) \to T_{\mathcal{V}}(u)$ such that, for every $x \in \mathbb{R}^{\mathrm{N}}$, $T_{\mathcal{V}}(u)(x)$ only depends upon the repartition function of u on $x + \mathcal{V}$ and satisfies :*

$$T_{\mathcal{V}}(u)(x) \in u(\mathcal{V} + x) \qquad \textit{(no new gray level is created)} \tag{2.1.7}$$

$$T_{\mathcal{V}}(g \circ u)(x) = g(T_{\mathcal{V}}(u)(x)), \qquad \textit{for any real continuous increasing function } g \tag{2.1.8}$$

Given a point $x \in \mathbb{R}^{\mathrm{N}}$, the map $: (u, \mathcal{V}) \to T_{\mathcal{V}}(u)(x) \in \mathbb{R}$ is called rank filter at x.

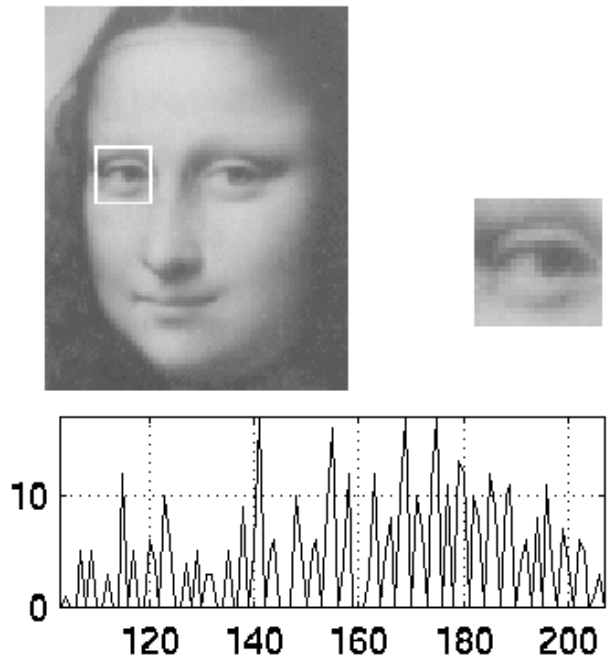

Figure 2.1: Top-left : original image
Top-right : fragment
Bottom : histogram of the fragment

Relations (2.1.7) and (2.1.8) mean that $T_{\mathcal{V}}(u)(x)$ is one of the values of u on $x + \mathcal{V}$, this value being picked out in a covariant way with respect to contrast changes. We see with this definition that rank filters are morphological filters.

In general, rank filters are defined on functions assuming a finite number of values on a finite set of arguments. In the case of digital images, $\mathcal{V}$ is a union of pixels, all with the same size, and u assumes a constant value on each pixel. Since at a small scale, values assumed on pixels tend to be randomly distributed, we can ensure stability of a rank filter by imposing that it be invariant under every combinatorial rearrangement $\mathcal{C}$ of $\mathcal{V}$. In other terms, $\mathcal{C}$ being an arbitrary perturbation of the pixels of $\mathcal{V}$, we assume that

$$T_{\mathcal{V}}(u \circ \mathcal{C}) = T_{\mathcal{V}}(u) \tag{2.1.9}$$

It is easily seen, in this discrete framework, that (2.1.9) is equivalent to the fact that $T_{\mathcal{V}}$ only depends on the histogram of u, which is invariant with respect to permutations. Indeed, in this case, the histogram h of u is a finite sum of Dirac masses, $h_u = \sum_{i=1}^{N} n_i \delta_i$ where n_i represents the number of pixels where u assumes the value i. Thus, if u and v have the same histogram, one can easily find a permutation $\mathcal{C}$ of $\mathcal{V}$ such that $u = v \circ \mathcal{C}$. Since the repartition function is uniquely determined by the histogram (and conversely), we deduce that the combinatorial invariance (2.1.9) is equivalent, in the case of discrete filters, to the fact that $T(u)$ only depends upon the histogram of u. In the continuous case, it is clear that if $T(u)$ only depends on H_u, then (2.1.9) is satisfied for any measure-preserving map

$\mathcal{C} : \mathcal{V} \to \mathcal{V}$. We do not know under which assumptions the converse implication is true.

Definition 2.1.5 (Histogram's modes)
Let u be a bounded measurable function defined on a measurable set $\mathcal{V} \subset \mathbb{R}^N$. We call mode of u any maximal interval I such that

$$\forall \phi \in C_c(I, [0, +\infty)),\ \phi \not\equiv 0, \qquad \int_I \phi \, dh > 0$$

Remark 2.1.6 If I_1 and I_2 are two modes of u, then $I_1 \cap I_2 = \emptyset$. Indeed, if I_1 and I_2 meet, then $I_1 \cup I_2$ also is a mode, which contradicts the maximality. Since u is bounded, the number of modes is either finite or countable. Before starting with the classification of rank filters, let us give some basic examples.

Example 1 : The maps defined for every $x \in \mathbb{R}^N$ by $T_{\mathcal{V}}(u)(x) = \sup_{x+\mathcal{V}} u$ or $T_{\mathcal{V}}(u)(x) = \inf_{x+\mathcal{V}} u$ are rank filters.

Example 2 : Let $r \in [0, 1]$ and define

$$\mathrm{med}^r_{\mathcal{V}}(u)(x) = \inf\{\lambda \in \mathbb{R} : \ |\{y \in x + \mathcal{V} : \ u(y) \le \lambda\}| \ge r\,|\mathcal{V}|\} \tag{2.1.10}$$

As a particular case, we define the "lower median filter" as $\mathrm{med}_{\mathcal{V}}(u) = \mathrm{med}^{\frac{1}{2}}_{\mathcal{V}}$ which shall be more precisely studied later. Moreover, it is worth noticing that

$$\mathrm{med}^0_{\mathcal{V}}\, u(x) = \inf_{x+\mathcal{V}} u \quad \text{and} \quad \mathrm{med}^1_{\mathcal{V}}\, u(x) = \sup_{x+\mathcal{V}} u \tag{2.1.11}$$

Example 3 : **Modal rank filters**
Assume that for every $x \in \mathbb{R}^N$, u is bounded on $x + \mathcal{V}$. Let us call $(M_i(x))_{i \in I}$ the set of modes of u in $x + \mathcal{V}$ and assume that some choice, depending upon H_u, has been made in I, which selects one of the modes, say $M_{i_0}(x)$. As an example, $M_{i_0}(x)$ can be chosen as the mode containing a fixed value, $u(x_0)$ attained by u on $x + \mathcal{V}$, where of course $x_0 \in x + \mathcal{V}$. Then we define a modal rank filter as

$$T(u)(x) = \mathrm{med}^r_{x+\mathcal{V} \cap u^{-1}(M_{i_0}(x))}(u)(x), \tag{2.1.12}$$

In the sequel and without loss of generality, we shall denote for the sake of simplicity $\mathcal{V} := x + \mathcal{V}$, $M_i := M_i(x)$ and $T(u) := T(u)(x)$. Remark that $T(u)$ is simply the median value computed over the mode M_{i_0}.

2.1.2 Classification of rank filters – Special rank filters

We are now in a position to classify the rank filters, assuming that the number of modes of u on $\mathcal{V}$ is finite and equal to K. Let us order them so that $M_i = [u_{2i-1}, u_{2i}]$, $i = 1, \ldots, K$ and $u_{2i} < u_{2i+1}$. Then, we set for $i = 1, \ldots, K$,

$$m_i := |\{x : \ u_{2i-1} \le u(x) \le u_{2i}\}|$$

Thus, the repartition function H_u of u on $\mathcal{V}$ is constant on each interval (u_{2i}, u_{2i+1}) and equal to $m_1 + ... + m_i$.

Let $\mathcal{F}_\mathcal{V}$ be the set of all bounded measurable functions u with a finite set of modes on $\mathcal{V}$. For every such function u, we call $(M_i)_{i=1,...,K}$ its modes and $m_1, ..., m_K$ the measures of the domains of the modes, $m_i = |\{x : u(x) \in M_i\}|$.

Theorem 2.1.7 (Rank filters are modal rank filters)
Let $x \in \mathbb{R}^N$. Let $T : \mathcal{F}_\mathcal{V} \to \mathbb{R}$ be a rank filter at x. Then, for every $u \in \mathcal{F}_\mathcal{V}$, there exist two functions

$$\begin{aligned} i : \quad & (\mathbb{R}^+)^K \to \mathbb{N} \\ & (m_1, ..., m_K) \to i(m_1, ..., m_K) \in \{1, ..., K\} \end{aligned}$$

$$\begin{aligned} r : \quad & (\mathbb{R}^+)^K \to [0, 1] \\ & (m_1, ..., m_K) \to r(m_1, ..., m_K) \in [0, 1] \end{aligned}$$

such that

$$T_\mathcal{V}(u) = \mathrm{med}^r_{\mathcal{V} \cap u^{-1}(M_i)}\, u.$$

In other words, all rank filters are "modal rank filters" as defined in example 3.

This theorem states that any filter that depends only on the repartition function and is covariant with respect to any continuous increasing contrast change, reduces to a median filter over some particular mode of the histogram. In particular, such filters are covariant with respect to any measure-preserving map of the neighborhood $\mathcal{V}$ onto itself.

PROOF : Since $T_\mathcal{V}(u)$ only depends upon the histogram of u on $\mathcal{V}$, H_u, there is no loss of generality in writing $T(H_u)$ instead of $T_\mathcal{V}(u)$. Equality (2.1.4) states that for every continuous increasing real function g, $T_\mathcal{V}(g \circ u) = g(T_\mathcal{V}(u))$. In addition, recall from (2.1.5) that $H_{g \circ u}(g(\lambda)) = H_u(\lambda)$, thus

$$H_u(g(\lambda)) = H_{g^{-1} \circ u}(\lambda)$$

From (2.1.4) we can deduce that

$$T(H_u \circ g) = T(H_{g^{-1} \circ u}) = T(g^{-1} \circ u) = g^{-1}(T(u)) = g^{-1}(T(H_u))$$

and finally

$$T(H_u) = g(T(H_u \circ g)) \tag{2.1.13}$$

for any continuous increasing real function g. In order to prove the theorem, we shall choose g so that the function $H_u \circ g$ depends only on the measures of the modes' domains,

$m_1, ..., m_K$. More precisely, we shall construct a continuous increasing function g such that

$$H_u \circ g = \tilde{H}_{m_1,...,m_K} = \tilde{H}, \qquad \text{where (see figure 2.2)} \tag{2.1.14}$$

$$\tilde{H}(s) = \begin{cases} 0 & \text{if } s \leq 1 \\ m_1(s-1) & \text{on } [1,2] \\ m_1 & \text{on } [2,3] \\ m_1 + m_2(s-3) & \text{on } [3,4] \\ \ldots\ldots & \\ m_1 + ... + m_{i-1} + m_i(s-2i+1)) & \text{on } [2i-1,\ 2i] \\ m_1 + ... + m_i & \text{on } [2i, 2i+1] \\ \ldots\ldots & \\ m_1 + ... + m_K & \text{if } s \geq 2K+1 \end{cases} \tag{2.1.15}$$

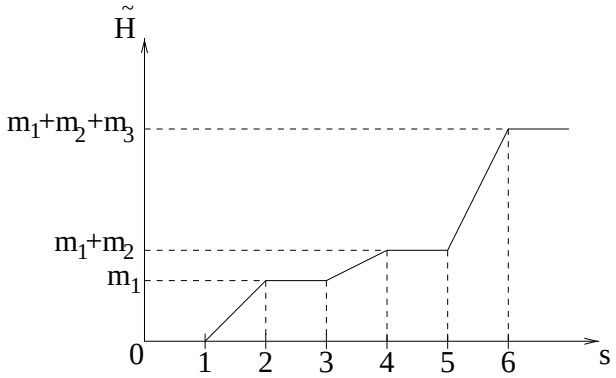

Figure 2.2: Normalized $\tilde{H}$ of the repartition function H_u

In order to obtain (2.1.14), it is enough to define g as a pseudo inverse of H_u :

$$g(s) = \begin{cases} u_1 + s - 1 & \text{if } s \leq 1 \\ H_u^{-1}(m_1(s-1)) & \text{on } [1,2] \\ u_2 + (u_3 - u_2)(s-2) & \text{on } [2,3] \\ \ldots\ldots & \\ H_u^{-1}(m_1 + ... + m_{i-1} + m_i(s-2i+1)) & \text{on } [2i-1,\ 2i] \\ u_{2i} + (u_{2i+1} - u_{2i})(s-2i) & \text{on } [2i,\ 2i+1] \\ \ldots\ldots & \\ s + u_{2K+1} & \text{if } s \geq 2K+1 \end{cases} \tag{2.1.16}$$

It is easily checked that (2.1.14) is satisfied and from (2.1.13) we deduce that

$$T(u) = T(H_u) = g(T(\tilde{H}_{m_1,...,m_K})) \tag{2.1.17}$$

The formula (2.1.17) must now be interpreted. First of all, we notice that $\tilde{H}_{m_1,...,m_K}$ only depends upon the values $m_1, ..., m_K$ and, therefore, so does $T(\tilde{H}_{m_1,...,m_K})$. In addition, we know from (2.1.7) that $\rho := T_{\mathcal{V}}(I_{m_1,...,m_K})$ belongs to $[0, 2K-1]$. Now, let us define $j = j(m_1, ..., m_K) := [\rho]$, where $[\rho]$ denotes the largest integer j such that $j \leq \rho$, and $r = r(m_1, ..., m_K) := \rho - [\rho] \in [0, 1)$. Two cases arise :

1) If j is even, e.g $j = 2i$, then $\rho \in [2i, 2i+1)$ and we get from (2.1.16) and (2.1.17) :

$$T_{\mathcal{V}}(u) = u_{2i} + (u_{2i+1} - u_{2i})(\rho - 2i)$$

Now, if $\rho > 2i$, $u_{2i} + (u_{2i+1} - u_{2i})(\rho - 2i)$ is not attained by u, since the range of u is contained in the intervals $[u_{2i-1}, u_{2i}]$ and this is contradictory with (2.1.7). Therefore, this case cannot happen for a rank filter.

2) If j is odd, e.g. $j = 2i - 1$, then ρ belongs to $[2i-1, 2i)$ and we get from (2.1.16) and (2.1.17) :

$$T(u) = H_u^{-1}(m_1 + ... + m_i + m_{i+1}r) \tag{2.1.18}$$

It must be emphasized that $H_u^{-1}(m_1 + ... + m_i + m_{i+1}r)$ is well defined in the sense that it is not an interval since H_u is increasing on $[2i-1, 2i]$. Set $\lambda := H_u^{-1}(m_1 + ... + m_i + m_{i+1}r)$ and remark that

$$|\{x \in \mathcal{V} : u(x) \leq \lambda\}| = m_1 + ... + m_i + m_{i+1}r$$

In addition

$$\mathrm{med}^r_{\mathcal{V} \cap u^{-1}(M_{i+1})} u = \inf\{\lambda' : \left|\{x \in \mathcal{V} \cap u^{-1}(M_{i+1}) : u(x) \leq \lambda'\}\right| \geq r \left|\mathcal{V} \cap u^{-1}(M_{i+1})\right|\}$$

Since $\left|\mathcal{V} \cap u^{-1}(M_{i+1})\right| = m_{i+1}$ we deduce from the uniqueness of λ that

$$T(u) = \mathrm{med}^r_{\mathcal{V} \cap u^{-1}(M_{i+1})} u$$

This achieves the proof, since both r and i only depend upon $(m_1, ..., m_K)$. □

We now consider an important class of rank filters. Recall from the definition of a rank filter T that, given a bounded measurable subset $\mathcal{V} \subset \mathbb{R}^N$ and a point $x \in \mathbb{R}^N$, the value $T_{\mathcal{V}}(u)(x)$ is chosen among all the values in $u(x + \mathcal{V})$ in a way covariant with respect to increasing contrast changes. We wish now to give a specific role to x. The interpretation is simple and was given at the beginning of this section : we wish the rank filter to give an "estimate", a "truer value" to $u(x)$ than $u(x)$ itself. The original value $u(x)$ may have a special role to play in the evaluation. For instance, when x is close to an edge due to an occlusion, we would like to pay more attention to points belonging to the same object as x and therefore where u take values "comparable" to $u(x)$.

Definition 2.1.8 *Let $\mathcal{V}$ be a bounded measurable subset of $\mathbb{R}^N$ and u a bounded measurable function defined on $\mathbb{R}^N$. We call "special rank filter with neighborhood $\mathcal{V}$" any map $T : (u, \mathcal{V}) \to T_{\mathcal{V}}(u)$ such that for all $x \in \mathbb{R}^N$, $T_{\mathcal{V}}(u)(x)$ only depends upon the repartition function $H = H_u$ of u on $x + \mathcal{V}$ and upon the index i_0 of the mode $M_{i_0}(u)$ containing $u(x)$. In addition we assume that $T_{\mathcal{V}}(u)$ satisfies the relations (2.1.7) and (2.1.8) defining rank filters, that is*

$$T_{\mathcal{V}}(u)(x) \in u(x + \mathcal{V})$$
$$T_{\mathcal{V}}(g \circ u)(x) = g(T_{\mathcal{V}}(u)(x)) \quad \textit{for any continuous increasing real function } g$$

As in the definition of rank filters, we shall call "special rank filter at x with neighborhood $\mathcal{V}$" the map associating with a bounded measurable function u the real number $T_{\mathcal{V}}(u)(x)$. To summarize, the special rank filter at x is like the rank filter at x, except that we allow in addition an i_0-dependence of $T_{\mathcal{V},x}(u)$. Clearly, the mode containing $u(x)$ may have some privilege for fixing the "true value".

Theorem 2.1.7 can be easily adapted to special rank filters.

Theorem 2.1.9 *Let $\mathcal{V}$ be a bounded subset of $\mathbb{R}^N$, $x \in \mathcal{V}$, u a bounded measurable function on $\mathbb{R}^N$ with a finite number K of modes on $\mathcal{V}$ and i_0 the index of the mode containing $u(x)$. Let $T : \mathcal{F}_{\mathcal{V}} \to \mathbb{R}$ be a special rank filter at x. Then there exist two functions*

$$\begin{aligned} i : \quad & (\mathbb{R}^+)^K \times \mathbb{N} \to \mathbb{N} \\ & (m_1, ..., m_K, i_0) \to i(m_1, ..., m_K, i_0) \in \{1, 2, ..., K\} \end{aligned}$$

$$\begin{aligned} r : \quad & (\mathbb{R}^+)^K \times \mathbb{N} \to [0, 1] \\ & (m_1, ..., m_K, i_0) \to i(m_1, ..., m_K, i_0) \in [0, 1] \end{aligned}$$

such that

$$T_{\mathcal{V}}(u) = \mathrm{med}^r_{\mathcal{V} \cap u^{-1}(I_i)} u.$$

PROOF : The proof is identical to the proof of Theorem 2.1.7. We only need to replace everywhere $T(u)$, $T(H_u)$ and $T(\tilde{H})$ by respectively $T(u, i_0)$, $T(H_u, i_0)$ and $T(\tilde{H}, i_0)$ and to notice that i_0 is unaltered by any increasing continuous contrast change g. □

2.2 BV functions and sets of finite perimeter

Roughly speaking, a function of bounded variation is an integrable function which is not too much oscillating (see the definition below) and which has a finite energy when defined in the plane. Because of these properties, it is very natural to identify an image with a function of bounded variation. In contrast with other functional spaces that might be used, the space of functions of bounded variation (BV) allows a geometric characterization of the level sets structure.

The total variation of a function measures in some way its oscillations. It is therefore logical to think that a denoising filter which introduces more regularity in an image should decrease the total variation. This approach has been used by L. Rudin and S. Osher [34] to perform a global denoising of an image u_0, assuming that u_0 is blurry and corrupted by a Gaussian white noise. More precisely, their problem was to recover the function u_1 such that $u_0 = Au_1 + n$ where A is the blurring operator and n is a noise with zero mean and standard deviation σ. They consequently introduced the following minimization problem

$$\text{Minimize} \quad \int_\Omega |Du|$$

with the assumptions that $\int_\Omega Au = \int_\Omega u_0$ and $\int_\Omega |Au - u_0|^2 = \sigma^2$. The results obtained by Rudin and Osher and later by A. Chambolle and P.L. Lions [10] showed that this method works well for Gaussian noise removal. However, the results may look somewhat artificial with very strong edges due to the total variation that prefers high steps to slowly increasing slopes. It appears anyway that the total variation is a good characterization of the presence of noise in an image and we shall take it as a criterion for the quality of denoising.

We now recall the definition and main properties of BV functions and sets of finite perimeter.

Notations

- $A \sim B$ means that the symmetric difference of A and B, $A \Delta B$, is Lebesgue negligible.
- $|A|$ is the Lebesgue measure of A.
- Unless otherwise specified, Ω shall denote either an open bounded subset of $\mathbb{R}^N$ with Lipschitz boundary or $\mathbb{R}^N$ itself.

For each $k \geq 0$, $\delta > 0$ and $A \subset \mathbb{R}^N$ one defines

$$\mathcal{H}^k_\delta(A) := \frac{w_k}{2^k} \inf \left\{ \sum_{i \in I} (\operatorname{diam} A_i)^k : A \subset \bigcup_{i \in I} A_i, \operatorname{diam} A_i < \delta \right\}$$

where I is finite or countable, $\operatorname{diam} A_i = \sup\{|x-y| : x, y \in A_i\}$ and w_k is the volume of the unit ball in $\mathbb{R}^k$. The k-dimensional Hausdorff measure of A is defined as

$$\mathcal{H}^k(E) := \lim_{\delta \to 0} \mathcal{H}^k_\delta(E)$$

The Hausdorff dimension of A is given by

$$\dim_{\mathcal{H}}(A) := \inf\{k \geq 0 : \mathcal{H}^k(E) = 0\}$$

with the property that if $h \equiv \dim_{\mathcal{H}}(A)$,

$$\begin{aligned} &k < h \Rightarrow \mathcal{H}^k(A) = +\infty \\ &0 \leq \mathcal{H}^h(A) \leq +\infty \\ &k > h \Rightarrow \mathcal{H}^k(A) = 0 \end{aligned}$$

and for any Borel set $B \subset \mathbb{R}^{\mathrm{N}}$

$$|B| = \mathcal{H}^N(B)$$

Let Ω be an open subset of $\mathbb{R}^{\mathrm{N}}$. The space of functions of bounded variation on Ω is the set $\mathrm{BV}(\Omega)$ of all those functions $u \in \mathrm{L}^1(\Omega)$ whose distributional derivative can be represented by a $\mathbb{R}^{\mathrm{N}}$-valued measure $Du = (D_1 u, \ldots, D_N u)$ in Ω, i.e.

$$\int_\Omega u \operatorname{div} \phi \, dx = -\sum_{i=1}^{N} \int_\Omega \phi_i dD_i u \quad \forall \phi \in [\mathrm{C}^1_c(\Omega)]^N$$

The total variation of a function of bounded variation u is defined as the total variation of Du

$$|Du|(\Omega) = \sup\{\int_\Omega u \operatorname{div} \phi \, dx, \ \phi \in \mathrm{C}^1_{\mathrm{c}}(\Omega; \mathbb{R}^{\mathrm{N}}), \ |\phi| \leq 1\}$$

The total variation is also denoted by $\int_\Omega |Du| dx$. The space $\mathrm{BV}(\Omega)$ is endowed with the norm

$$\|u\|_{\mathrm{BV}} = \|u\|_{\mathrm{L}^1} + |Du|(\Omega)$$

For any function u of bounded variation and from the Radon-Nikodým Theorem, the measure Du can be decomposed in an absolute continuous part Du_{ac} and a singular part Du_{s} with respect to the Lebesgue measure $\mathcal{L}^N$. Moreover $Du_{\mathrm{ac}} = \mathcal{L}^N \llcorner \nabla u$ where ∇u is the Radon-Nikodým derivative of u with respect to $\mathcal{L}^N$. As a consequence, ∇u exactly coincides with the distributional derivative of u when $u \in \mathrm{W}^{1,1}(\Omega)$.

The reader may refer to [3, 13, 15, 44] for more details on the following properties of functions of bounded variation.

Theorem 2.2.1 (Lower semicontinuity of variation measure)
Suppose $\{u_n\}_{n \in \mathbb{N}} \subset \mathrm{BV}(\Omega)$ *and* $u_n \to u$ *in* $\mathrm{L}^1_{\mathrm{loc}}(\Omega)$. *Then*

$$|Du|(\Omega) \leq \liminf_{n \to \infty} |Du_n|(\Omega)$$

Theorem 2.2.2 (Approximation by smooth functions)
Assume $u \in \mathrm{BV}(\Omega)$. *There exist functions* $\{u_n\}_{n=1}^{\infty} \subset \mathrm{BV}(\Omega) \cap C^{\infty}(\Omega)$ *such that*

$$u_n \to u \text{ in } \mathrm{L}^1(\Omega) \text{ and}$$
$$|Du_n|(\Omega) \to |Du|(\Omega) \text{ as } n \to \infty$$

Theorem 2.2.3 (Compactness)
Let Ω *be open and bounded, with* $\partial\Omega$ *Lipschitz. Assume that* $\{u_n\}_{n=1}^{\infty}$ *is a sequence in* $\mathrm{BV}(\Omega)$ *satisfying*

$$\sup_n \|u_n\|_{\mathrm{BV}} < \infty$$

Then there exists a subsequence $\{u_{n_k}\}_{k=1}^{\infty}$ *and a function* $u \in \mathrm{BV}(\Omega)$ *such that*

$$u_{n_k} \to u \text{ in } \mathrm{L}^1(\Omega) \text{ as } k \to \infty \quad \text{and} \quad \|u\|_{\mathrm{BV}} \leq \liminf_{k\to\infty} \|u_{n_k}\|_{\mathrm{BV}}$$

A consequence of the next theorem is that any function of bounded variation defined in $\mathbb{R}^2$ has finite energy.

Theorem 2.2.4 (Sobolev's inequality) *Let* $u \in \mathrm{BV}(\mathbb{R}^{\mathrm{N}})$. *Then, there exists a constant* C *such that*

$$\|u\|_{\mathrm{L}^{N/N-1}} \leq C|Du|(\mathbb{R}^{\mathrm{N}})$$

The perimeter in Ω of a $\mathcal{L}^N$-measurable subset $E \subset \mathbb{R}^{\mathrm{N}}$ is defined as the total variation of the indicator function of E, i.e.

$$P(E,\Omega) := |\chi_E|(\Omega) = \sup\{\int_E \operatorname{div}\phi\, dx,\ \phi \in \mathrm{C}_{\mathrm{c}}^1(\Omega;\mathbb{R}^{\mathrm{N}}),\ |\phi| \leq 1\}$$

If $P(E,\Omega) < +\infty$ then we shall say that E has finite perimeter in Ω. If we can only state that $P(E,U) < +\infty$ for each open set $U \subset\subset \Omega$ then E is said to have locally finite perimeter in Ω.

Theorem 2.2.5 (Isoperimetric inequality) *Let* $N > 1$. *For any set of finite perimeter in* $\mathbb{R}^{\mathrm{N}}$, *either* E *or* $\mathbb{R}^{\mathrm{N}} \setminus E$ *has finite Lebesgue measure and*

$$\min\{|E|,\ |\mathbb{R}^{\mathrm{N}} \setminus E|\} \leq C[P(E,\mathbb{R}^{\mathrm{N}})]^{N/(N-1)}$$

for some dimensional constant C.

The upper level sets of a measurable function u defined on Ω are given by

$$U_t := \{x \in \Omega :\ u(x) \geq t\}$$

and the lower level sets by

$$L_t := \{x \in \Omega :\ u(x) \geq t\}$$

Theorem 2.2.6 (Coarea formula)
Let $u \in \mathrm{BV}(\Omega)$. Then U_t, L_t have finite perimeter in Ω for L^1-a.e. $t \in \mathbb{R}$ and

$$|Du|(\Omega) = \int_{-\infty}^{+\infty} P(U_t, \Omega)dt = \int_{-\infty}^{+\infty} P(L_t, \Omega)dt$$

Conversely, if $u \in \mathrm{L}^1(\Omega)$ and $\int_{-\infty}^{+\infty} P(U_t, \Omega)dt < +\infty$ (or $\int_{-\infty}^{+\infty} P(L_t, \Omega)dt < +\infty$) then $u \in \mathrm{BV}(\Omega)$

The coarea formula associated with the reconstruction formula and the following property ensure that the level sets offer a complete representation of a function of bounded variation. If u^+ and u^- respectively denote the positive and negative parts of u so that $u = u^+ - u^-$ and since

$$\int_\Omega |u^+|dx = \int_0^{+\infty} |\{u^+ > t\}|dt \quad \text{and} \quad \int_\Omega |u^-|dx = \int_0^{+\infty} |\{u^- > t\|dt$$

we deduce that

$$\int_\Omega |u|dx = \int_0^{+\infty} (|\{u > t\}| + |\{u < -t\}|)\, dt$$

If E is a set of locally finite perimeter in Ω, one defines the reduced boundary $\partial^* E$ as all those points $x \in \mathbb{R}^{\mathrm{N}}$ such that

$$\begin{array}{ll} (i) & P(E, B_\rho(x)) \equiv |D\chi_E|(B_\rho(x)) > 0 \text{ for all } \rho > 0 \\ (ii) & \nu_E(x) := -\lim_{\rho \downarrow 0} \dfrac{D\chi_E(B_\rho(x)}{|D\chi_E|(B_\rho(x))} \text{ exists in } \mathbb{R}^{\mathrm{N}} \text{ and satisfies} \\ (iii) & |\nu_E(x)| = 1 \end{array}$$

The function ν_E is called the generalized outer normal to E and

$$D\chi_E = -\nu_E |D\chi_E|$$

A fundamental property of the reduced boundary is that $\partial^* E$ is a countably $(N-1)$-rectifiable set, that is

$$\partial^* E = \bigcup_{n=0}^{\infty} K_n$$

where $\mathcal{H}^{\mathrm{N}-1}(K_0) = 0$ and each K_n, $n \geq 1$ is a compact subset of an $(N-1)$-dimensional embedded C^1 submanifold of $\mathbb{R}^{\mathrm{N}}$. Moreover,

$$D\chi_E = -\nu_E \mathcal{H}^{\mathrm{N}-1} \llcorner \partial^* E$$

Theorem 2.2.7 (Gauss-Green's formula)
Let E be a set of locally finite perimeter in Ω. Then

$$\int_E div\, \phi\, dx = \int_{\partial^* E} \langle \nu_E, \phi \rangle d\mathcal{H}^{\mathrm{N}-1} \quad \forall \phi \in [\mathrm{C}_c^1(\Omega)]^N$$

Definition 2.2.8 (Points of density t and essential boundary)
For every $t \in [0,1]$ and every $\mathcal{L}^N$-measurable set $E \subset \mathbb{R}^N$ the set of all those points where E has density t is defined as

$$E^t := \{x \in \mathbb{R}^N : \lim_{\rho \downarrow 0} \frac{|E \cap B_\rho(x)|}{|B_\rho(x)|} = t\}$$

The essential boundary of E, $\partial_M E$, is the set $\mathbb{R}^N \setminus (E^0 \cup E^1)$ of all those points where E has density neither 0 nor 1.

Theorem 2.2.9 *Let E be a set of finite perimeter in Ω. Then*

$$\mathcal{H}^{N-1}(\partial_M E \setminus \partial^* E) = 0$$
$$\partial^* E \cap \Omega \subset E^{1/2} \subset \partial_M E \text{ and}$$
$$\mathcal{H}^{N-1}(\Omega \setminus (E^0 \cup \partial^* E \cup E^1)) = 0$$

In particular, E has density either 0, $1/2$ or 1 at $\mathcal{H}^{N-1}$-a.e. $x \in \Omega$

Definition 2.2.10 *Let u be a Lebesgue measurable function from Ω into $\mathbb{R}$.*
Define the lower approximate limit of u at x

$$u^-(x) := \sup\{t \in \mathbb{R} : \lim_{r \downarrow 0} \frac{|B(x,r) \cap \{u < t\}|}{|B(x,r)|} = 0\}$$

and the upper approximate limit of u at x

$$u^+(x) := \inf\{t \in \mathbb{R} : \lim_{r \downarrow 0} \frac{|B(x,r) \cap \{u > t\}|}{|B(x,r)|} = 0\}$$

We speak of the approximate limit of u at x in case

$$u^-(x) = u^+(x) \equiv \operatorname{ap}\lim_{y \to x} u(y)$$

u is said to be approximatively continuous at x if $\operatorname{ap}\lim_{y \to x} u(y) \equiv u(x)$.

$$S_u := \{x \in \mathbb{R}^N : u^-(x) < u^+(x)\}$$

is called the approximate discontinuity set.

It is worth noticing that $u^-(x)$ and $u^+(x)$ do not depend on the representative u for the reason they are defined with measures and not pointwise values. Moreover, it is a consequence of the Lebesgue Theorem that a Lebesgue measurable function defined on Ω is approximatively continuous at $\mathcal{L}^N$-a.e. $x \in \Omega$.

Theorem 2.2.11 (Rectifiability of S_u) *Let $u \in \mathrm{BV}(\Omega; \mathbb{R})$. Then*

$$S_u \text{ is countably } (N-1)\text{-rectifiable and}$$
$$-\infty < u^-(x) \le u^+(x) < +\infty \quad \text{for } \mathcal{H}^{N-1}\text{-almost every } x \in \Omega$$

Theorem 2.2.12 (Boundary trace) *Let $\Omega \subset \mathbb{R}^N$ be an open, bounded set with Lipschitz boundary and $u \in \mathrm{BV}(\Omega)$. There exists a bounded linear mapping*

$$T : \mathrm{BV}(\Omega) \to \mathrm{L}^1(\partial\Omega, \mathcal{H}^{N-1})$$

such that for $\mathcal{H}^{N-1}$-almost every $x \in \partial\Omega$

$$\lim_{r \downarrow 0} \fint_{\Omega \cap B_r(x)} |u(y) - Tu(y)| dy = 0$$

and so

$$Tu(x) = \lim_{r \to 0} \fint_{\Omega \cap B_r(x)} u(y) dy$$

Theorem 2.2.13 (Extensions) *Assume $\Omega \subset \mathbb{R}^N$ is open and bounded, with $\partial\Omega$ Lipschitz. Let $u_1 \in \mathrm{BV}(\Omega)$ and $u_2 \in \mathrm{BV}(\mathbb{R}^N \setminus \overline{\Omega})$. Define*

$$\tilde{u}(x) := \begin{cases} u_1(x) & \text{if } x \in \Omega \\ u_2(x) & \text{if } x \in \mathbb{R}^N \setminus \overline{\Omega} \end{cases}$$

Then $u \in \mathrm{BV}(\mathbb{R}^N)$ and

$$|Du|(\mathbb{R}^N) = |Du_1|(\Omega) + |Du_2|(\mathbb{R}^N \setminus \overline{\Omega}) + \int_{\partial\Omega} |Tu_1 - Tu_2| d\mathcal{H}^{N-1}$$

2.3 Median filter and total variation

Let u be a $\mathcal{L}^N$-measurable real function on $\mathbb{R}^N$. The median of u with respect to a bounded subset $B \subset \mathbb{R}^N$ is defined at every $x \in \mathbb{R}^N$ as the set of real numbers t such that

$$|(B+x) \cap \{y : u(y) > t\}| \leq \frac{|B|}{2} \quad \text{and} \quad |(B+x) \cap \{y : u(y) < t\}| \leq \frac{|B|}{2}$$

and denoted as $\mathrm{med}_B\, u(x)$. It is easily seen that $\mathrm{med}_B\, u(x)$ is a nonempty compact interval $[\mathrm{med}_B^-\, u(x), \mathrm{med}_B^+\, u(x)]$ where

$$\begin{aligned} \mathrm{med}_B^-\, u(x) &\equiv \inf\{t \in \mathbb{R} : |\{y \in B+x : u(y) \leq t\}| \geq \tfrac{|B|}{2}\} \\ \mathrm{med}_B^+\, u(x) &\equiv \sup\{t \in \mathbb{R} : |\{y \in B+x : u(y) \geq t\}| \geq \tfrac{|B|}{2}\} \end{aligned}$$

are respectively the lower and upper median values over B at x. In the sequel we shall call median filter the operator which maps every $\mathcal{L}^N$-measurable real function u on $\mathbb{R}^N$ onto the function $\mathrm{med}_B^-\, u$. It is worth noticing that the properties that shall be stated remain valid if one replaces $\mathrm{med}_B^-\, u(x)$ with any other value in the interval $[\mathrm{med}_B^-\, u(x), \mathrm{med}_B^+\, u(x)]$.

If $m := \mathrm{med}_B^-\, u(x)$ is such that $|(B+x) \cap \{u = m\}| = 0$ then

$$|\{y \in B+x : u(y) \leq m\}| = |\{y \in B+x : u(y) \geq m\}| = |B|/2$$

More generally, if u is continuous and B is connected then $\mathrm{med}_B^-\, u = \mathrm{med}_B^+\, u$. Indeed, let us assume that u is continuous but $\mathrm{med}_B^-\, u < \mathrm{med}_B^+\, u$. Let λ_1 and λ_2 be such that $\mathrm{med}_B^-\, u < \lambda_1 < \lambda_2 < \mathrm{med}_B^+\, u$. Then $|\{y \in B : u(y) \leq \lambda_1\}| \geq |B|/2$ and $|\{y \in B : u(y) \geq \lambda_2\}| \geq |B|/2$ so that $|\{y \in B : \lambda_1 < u(y) < \lambda_2\}| = 0$. Since u is continuous we deduce that $u^{-1}((\lambda_1, \lambda_2))$ is open and thus $u^{-1}((\lambda_1, \lambda_2)) = \emptyset$ which is in contradiction with the property of any continuous mapping to preserve connectedness.

We shall call in the sequel *conventional median filter* the median filter defined over a bounded ball B. This definition can be of course generalized by replacing the Lebesgue measure with any other positive measure on $\mathbb{R}^N$. As an example, the *weighted median filter* is defined by using the measure $k\mathcal{L}^N$ where k is a radial, positive and continuous function on $\mathbb{R}^N$ such that $\int_{\mathbb{R}^N} k(x)dx = 1$. The reader may refer to [16] for more details.

As pointed out in the general introduction, the iterated conventional median filter is asymptotically equivalent to the *mean curvature motion* $\frac{\partial u}{\partial t} = |Du|\mathrm{curv}(u)$ [16] under the assumption that u is smooth enough. This can be equivalently formulated by writing that the evolution of a level line C of u follows the equation $\frac{\partial C}{\partial t} = \mathrm{curv}(C)$ which clearly means that the level lines of u are evolving with respect to their curvature.

It is well-known that the median filter is a morphological monotone operator. However, it is not continuous with respect to the convergence in $\mathrm{L}^1_{\mathrm{loc}}(\mathbb{R}^N)$. Let us indeed consider the real step function f such that $f(x) = 0$ if $x < 0$ and $f(x) = 1$ if $x > 1$. Clearly, $\mathrm{med}^-_{B_1} f(0) = 0$ and $\mathrm{med}^+_{B_1} f(0) = 1$. Since the functions f_n such that

$$f_n(x) = \begin{cases} 0 & \text{if } x < -1/n \\ \frac{1+nx}{2} & \text{if } -1/n \leq x \leq 1/n \\ 1 & \text{if } x > 1/n \end{cases}$$

converge to f as $n \to \infty$ in $\mathrm{L}^1(\mathbb{R})$ and $\mathrm{med}^-_{B_1} f_n(0) = \mathrm{med}^+_{B_1} f_n(0) = 1/2$ we can infer that the median filter is not continuous with respect to the convergence in $\mathrm{L}^1_{\mathrm{loc}}(\mathbb{R})$. Analogous counter-examples can be found to prove that the median filter is more generally not continuous with respect to the convergence in $\mathrm{L}^1_{\mathrm{loc}}(\mathbb{R}^N)$. We shall now study the relationship between the median filter and the space of functions of bounded variation.

2.3.1 Median filter and projection onto BV

The regularizing effect of the median filter has already been pointed out. Then, the question occurs whether the median filter is a projector of $\mathrm{L}^1(\mathbb{R}^N)$ onto $\mathrm{BV}(\mathbb{R}^N)$. Unfortunately the answer is negative, as shown with the following example in $\mathbb{R}$. Define a partition of the interval $[0, \frac{4}{3}]$ by all those intervals $[s_n, s_{n+1}]$ with

$$s_1 = 0 \quad \text{and} \quad s_n = \sum_{k=2}^{n} (\frac{2}{3})^n, \;\; n \geq 2$$

and let f be the function such that

$$f(x) = \begin{cases} -1 & \text{on } [s_1, s_2) \\ \frac{5}{2}(-1)^n & \text{on } [s_n, s_{n+1}), \;\; n \geq 2 \end{cases}$$

Clearly, f is in $\mathrm{L}^1([0, \frac{4}{3}])$ and $\int_0^{\frac{4}{3}} |f(x)|dx = 24/9$ but f has an infinite total variation. Indeed, $P(\{f > t\}) = +\infty$ for any $t \in (-5/2, 5/2)$. Let us compute $\mathrm{med}_{B(x,\frac{2}{3})} f(x)$ for every $x \in [0, \frac{2}{3}]$. It is easily seen that $\mathrm{med}_{B(x,\frac{2}{3})} f(x)$ depends on the sign of $\int_0^{x+\frac{2}{3}} f(x)dx$. If it is positive then $\mathrm{med}_{B(x,\frac{2}{3})} f(x) = \frac{5}{2}$, otherwise $\mathrm{med}_{B(x,\frac{2}{3})} f(x) < 0$. Remark now that

$$\begin{aligned} \int_0^{s_n} f(x)dx &= \sum_{k=0}^{n-1} f(s_k)(s_{k+1} - s_k) \\ &= -(\tfrac{2}{3})^2 + \sum_{k=2}^{n-1} (-1)^k (\frac{2}{3})^{k+1} - (-1)^{k-1}(\frac{2}{3})^k \quad (\text{using } \tfrac{5}{2} = 1 + \tfrac{3}{2}) \\ &= (-1)^{n-1}(\tfrac{2}{3})^n \end{aligned}$$

Thus, any point $x \in [0, \frac{2}{3}]$ is associated with a median value alternatively positive and negative depending on which interval of the form $[s_k, s_{k+1})$ the point $x + \frac{2}{3}$ belongs to. Consequently $\mathrm{med}_{B_{\frac{2}{3}}} f$ is not a function of bounded variation.

2.3.2 The median filter decreases the perimeter of bounded and convex sets

Let E be a $\mathcal{L}^N$-measurable set in $\mathbb{R}^N$. We define

$$\mathrm{med}_r E := \{x : |B(x,r) \cap E| \geq \frac{|B(x,r)|}{2}\}$$

which is equivalent to let $u := \chi_E$ be the indicator function of E, $v := \mathrm{med}_r^+ u$ and define $\mathrm{med}_r E := \chi_v$

Lemma 2.3.1 *Let E be a convex set in $\mathbb{R}^N$. Then $\forall r > 0$, $\mathrm{med}_r E$ is a closed and convex set. Moreover, if E is closed then $\mathrm{med}_r E \subset E$.*

PROOF : The result is obvious when $\mathrm{med}_r E$ is empty so we assume that $\mathrm{med}_r E \neq \emptyset$. We now recall the Brunn-Minkowski Theorem (see [14])

Theorem 2.3.2 (Brunn-Minkowski) *If A and B are two nonempty subsets of $\mathbb{R}^N$ then*

$$|A + B|^{1/N} \geq |A|^{1/N} + |B|^{1/N}$$

where $A + B = \{x + y : x \in A,\, y \in B\}$

Let $x, y \in \mathrm{med}_r E$ and $z := tx + (1-t)y$ for some $t \in (0,1)$. Let $x' \in B(x,r)$, $y' \in B(y,r)$ and $z' = tx' + (1-t)y'$. Remark that $|z' - z| = |t(x'-x) + (1-t)(y'-y)| \leq t|x'-x| + (1-t)|y'-y| \leq r$ thus

$$B(z,r) \supset tB(x,r) + (1-t)B(y,r)$$

Since E is convex, if $x, y \in E$ then $tx + (1-t)y \in E$ and thus

$$B(z,r) \cap E \supset t(B(x,r) \cap E) + (1-t)(B(y,r) \cap E)$$

It follows from the Brunn-Minkowski Theorem that

$$|B(z,r) \cap E|^{1/n} \geq t^{1/n} |B(x,r) \cap E|^{1/n} + (1-t)^{1/n} |B(y,r) \cap E|^{1/n}$$

Since $|B(x,r) \cap E| \geq 1/2$ and $|B(y,r) \cap E| \geq 1/2$, we infer that

$$|B(z,r) \cap E| \geq \frac{(t^{1/n} + (1-t)^{1/n})^n}{2} \geq 1/2$$

and thus $z \in \mathrm{med}_r E$. Therefore, $\mathrm{med}_r E$ is convex. The property of $\mathrm{med}_r E$ to be closed follows from the Lebesgue measure continuity.

Assume now that E is closed and let $x \notin E$. Obviously, $\overline{B}(x,r) \cap E$ is convex, closed and does not contain x. Thus, the Hahn-Banach separation Theorem ([5]) gives $|B(x,r) \cap E| < 1/2$ so that $x \notin \mathrm{med}_r E$. Therefore, $\mathrm{med}_r E \subset E$. □

The following result is known (see for instance [2]).

Theorem 2.3.3 (Comparison Theorem) *For any set E of finite perimeter in $\mathbb{R}^N$ and any closed convex set $C \subset \mathbb{R}^N$ we have*

$$P(E \cap C) \leq P(E)$$

with equality if and only if $|E \setminus C| = 0$

A trivial consequence of this result is the following.

Proposition 2.3.4 *Let E be a bounded, closed and convex subset of $\mathbb{R}^N$. Then $\forall r > 0$,*

$$P(\mathrm{med}_r E) \leq P(E)$$

PROOF : Since E is bounded and convex, it has finite perimeter ([14], Thm. 3.2.35). It follows from Lemma 2.3.1 that $\mathrm{med}_r E$ is bounded and convex for all $r > 0$. Moreover, $\mathrm{med}_r E$ is closed and $\mathrm{med}_r E \subset E$. The proposition ensues by a simple application of Theorem 2.3.3. □

The question whether such a result could be established for any set of finite perimeter has not been solved in the general case. We shall exhibit in the next section a counter–example proving that the perimeter may increase if the set is not connected. We conjecture that there exist also counter-examples when the set is assumed to be connected.

2.3.3 The median filter may increase the total variation

Since the median filter is used for image denoising, a nice property of this filter would be that it decreases the total variation, and thus removes oscillations in image that may be due to noise. Unfortunately, the median filter does not have this property, mainly for the reason that even if E and F are of finite perimeter and such that $P(\mathrm{med}_r E) < P(E)$ and $P(\mathrm{med}_r F) < P(F)$ it may happen that $P(\mathrm{med}_r(E \cup F)) > P(E \cup F)$. As a consequence, we can find a counter-example where the median filter does increase the image total variation.

Let $u \equiv u_{h,\theta_0}$ be the characteristic function of the gray set shown in figure 2.3a. We shall prove that there exists some $0 < h < 1$ and some $0 < \theta_0 < \frac{\pi}{4}$ such that the level lines of the function $v := \mathrm{med}_1^+ u$ are longer than the level lines of u. A similar argument could be developed for $\mathrm{med}_1^- u$. From the coarea formula this will imply that the total variation

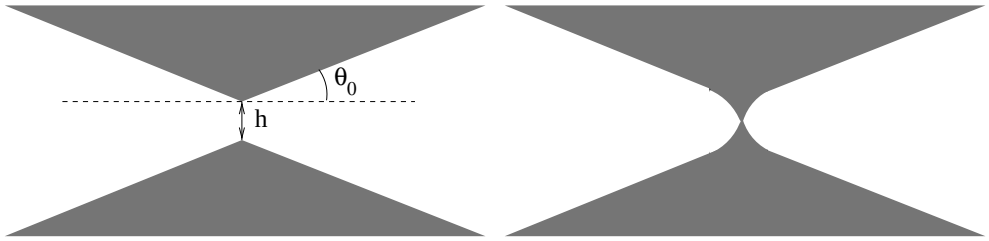

Figure 2.3: Left(a) – density plot of u, Right(b) – density plot of $\mathrm{med}_1\, u$

of v is larger than the total variation of u. Practically, we shall see in Appendix A with a numerical argument that v is the characteristic function of the gray set in figure 2.3b.

Let the apex of the lower angular sector be the origin of our coordinates system. Let us denote the upper and lower angular sectors by S_1 and S_2 respectively. For obvious symmetry reasons, the problem may reduce to find the set of points (x, y) in $\mathbb{R}^+ \times (-\infty, \frac{h}{2}]$ such that the area $A(x, y)$ of the intersection between the ball $B_1(x, y)$ and the angular sectors is more than $\frac{\pi}{2}$. Let us begin with the following lemma

Lemma 2.3.5 *Let $h = 0.5$. There exists some θ_0 such that*
$v(0, y) = 1$ *for every* $y \in \mathbb{R}$
$v(x, 0.25) = 0$ *for every* $y \in \mathbb{R} \setminus \{0\}$
$v(x, y) = 1$ *if* $(x, y) \in S_1 \cup S_2$ *and* $\inf(x^2 + y^2, x^2 + (y - 0.25)^2) \geq 1$
$v(x, y) = 0$ *if* $(x, y) \notin S_1 \cup S_2$ *and* $\inf(x^2 + y^2, x^2 + (y - 0.25)^2) \geq 1$

PROOF : Let us begin with proving that

$$\forall y \in \mathbb{R}, \quad A(0, y) \geq A(0, \frac{h}{2}) \tag{2.3.1}$$

This arises from figure 2.4. Let $\frac{h}{2} \leq y_1 < y_2 \leq 1$. For obvious symmetry reasons

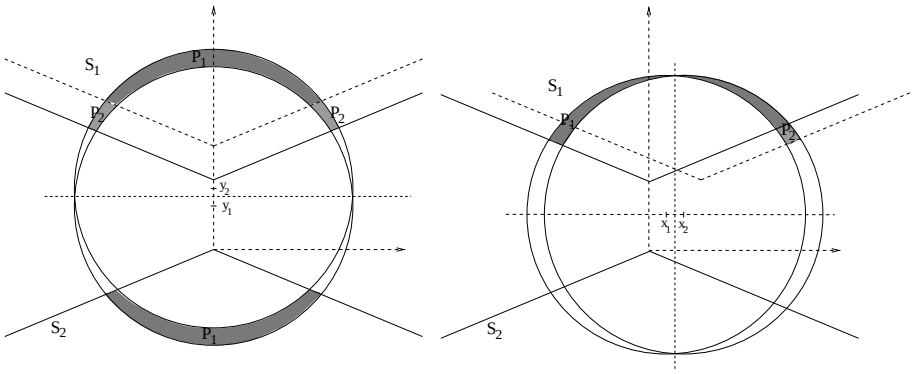

Figure 2.4:

$A(0, y_2) - A(0, y_1) = P_1 + 2P_2 - P_1 = 2P_2 > 0$ so that $A(0, y_2) > A(0, y_1)$. If $1 \leq y_1 < y_2$

then the ball does not intersect anymore the lower angular sector. On the other hand, the area of the intersection between the ball and the upper angular sector is clearly increasing. Therefore $A(0,y_2) > A(0,y_1)$ and thus $A(0,y)$ is increasing on $[\frac{h}{2},+\infty)$. By a symmetry argument, $A(0,y)$ is decreasing on $(-\infty,\frac{h}{2}]$ and (2.3.1) ensues. Now, a similar argument yields

$$\forall x \in \mathbb{R},\quad A(x,\frac{h}{2}) \leq A(0,\frac{h}{2}) \tag{2.3.2}$$

Indeed when $0 \leq x_1 \leq x_2$ and $d((0,h);(x_2,\frac{h}{2})) \leq 1$ then $A(x_2,\frac{h}{2}) - A(x_1,\frac{h}{2}) = P_1 - P_2 - P_1 = -P_2 < 0$. If $d((0,h);(x_1,\frac{h}{2})) \geq 1$ then no area is added but only subtracted and (2.3.2) follows.
It will be shown in Appendix A that

$$A(0,\frac{h}{2},\theta_0) = \pi - 2\theta_{\frac{h}{2},\theta_0} - h\cos\theta_{\frac{h}{2},\theta_0}$$

where

$$\cos\theta_{y,\theta_0} = \cos\theta_0\left(\sqrt{1-y^2\cos^2\theta_0} - y\sin\theta_0\right)$$

θ_{y,θ_0} is a continuous function with respect to θ_0 on $[0,\frac{\pi}{2}]$. Since $\theta_{\frac{h}{2},0} = \arccos(\sqrt{1-\frac{h^2}{4}})$ and $\theta_{\frac{h}{2},\frac{\pi}{2}} = \frac{\pi}{2}$, we deduce when $h = 0.5$ that

$$A(0,0.25,0) - \frac{\pi}{2} \approx 0.581313 > 0 \text{ and } A(0,0.25,\frac{\pi}{2}) - \frac{\pi}{2} = -\frac{\pi}{2} < 0$$

thus there exists some θ_0 such that $A(0,0.25,\theta_0) = \frac{\pi}{2}$. For such a θ_0 we have

$$\begin{array}{ll} \forall x \in \mathbb{R}\setminus\{0\}, & A(x,0.25) < \frac{\pi}{2} \\ \forall y \in \mathbb{R}\setminus\{0.25\}, & A(0,y) > \frac{\pi}{2} \\ & A(0,0.25) = \frac{\pi}{2} \end{array}$$

Moreover we obviously have that $A(x,y) \geq \frac{\pi}{2}$ when (x,y) is in one of the angular sectors and $\inf(d((x,y);(0,0)), d((x,y);(0,\frac{h}{2}))) \geq 1$. When (x,y) is outside the angular sectors and $\inf(d((x,y);(0,0)), d((x,y);(0,\frac{h}{2}))) \geq 1$ then $A(x,y) < \frac{\pi}{2}$. The lemma finally follows from the statement

$$v(x,y) = 1 \Leftrightarrow A(x,y) \geq \frac{\pi}{2}$$

□

Lemma 2.3.6 *Under the assumptions of the previous lemma,*

$$|D\,\mathrm{med}_1\,u|\,(\mathbb{R}^2) > |Du|\,(\mathbb{R}^2)$$

PROOF : Let $a = (0, \frac{h}{2}) = (0, 0.25)$ and b, c like in figure 2.5. According to Lemma 2.3.5, the two paths (a, b) and (a, c) that we have represented contain only points (x, y) such that $v(x, y) = 1$. These two paths are in the connected component $\mathcal{C}$ of a in $\{(x, y),\ v(x, y) = 1\}$. Furthermore, according to Lemma 2.3.5, a, b and c belong to the boundary of $\mathcal{C}$. Let d denotes the apex of the upper angular sector and $\mathcal{L}(a, b)$ the length of the boundary of $\mathcal{C}$ between a and b. Obviously, $\mathcal{L}(a, b) = \mathcal{L}(a, c) \geq d(a, b) > d(d, b)$ thus the level lines of v are longer than the level lines of u and the result ensues from Coarea formula. □

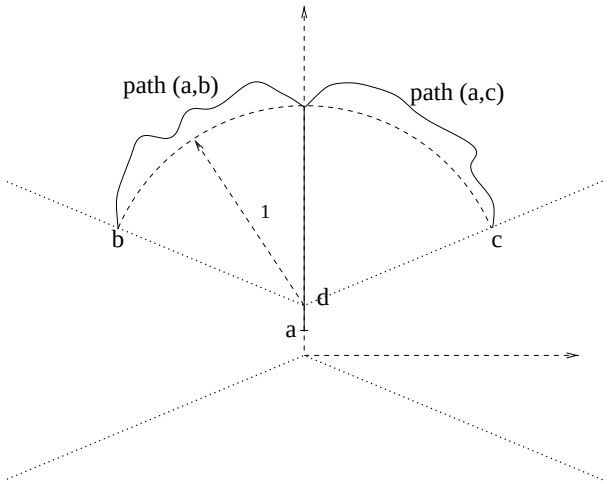

Figure 2.5:

2.4 Median filter on a connected neighborhood

Almost every local filter, linear or nonlinear, morphological or not, has generally to be iterated before it yields the desired solution. But too many iterations may result in a much too smooth image. Moreover, smoothing effect occurs even for initial smooth data. This is particularly confusing since the goal of image restoration is generally to denoise while preserving uncorrupted data. The lack of preservation is actually due to the definition of coherence which is implicitly related to each filter. Let us say that an image is coherent with respect to some operator if it is a fixed point for this operator.

A coherent image with respect to the conventional median filter (the morphological reference filter) in the continuous plane is such that curvature is zero at every point of any level line [16]. If it is with respect to the median filter computed over some N_2-like neighborhood (see the general introduction), then it can be easily checked that the curvature at any point of any level line does not exceed some upper limit. On the discrete grid, these last two conditions can be weakened due to numerical approximations. But the classes of coherent images with respect to both operators are still restricted to smooth images (the larger the size of working window, the smoother the image). Therefore, iterating one of these filters on a "natural" image until convergence often yields a result that is too smooth to be satisfactory.

Figure 2.6 illustrates why conventional median filter and median filter computed over some N_2-like neighborhood are associated with such a restricted class of coherent images: they involve a neighborhood that cannot fully fit the local conformation of level lines for it is constrained inside a disk. Now, is there a way to remove spatial constraint while letting filtering be local ? Simplest answer seems to be connectedness.

Since N_1-like neighborhoods are not morphological, we shall concentrate our study on local filtering involving N_2-like neighborhoods. We now examine how the definition of N_2 can be modified so that connectedness be involved. Recall that the neighborhood $N_2(x)$ at x is made of two subsets of a disk. A "monotone" set of area ϵ_R^+ made of points with gray level larger than $u(x)$ and a "monotone" set of area ϵ_R^- made of points with gray level less than $u(x)$. By "monotone" we mean that $N_2(x)$ can be constructed by progressively adding points y with respect to the distance $|u(y) - u(x)|$ (the lower this distance, the sooner y is added). The way we shall construct our neighborhood is equivalent, except that we combine the "monotone" characteristic with connectedness and that we set $\theta := \epsilon_R^+ = \epsilon_R^-$.

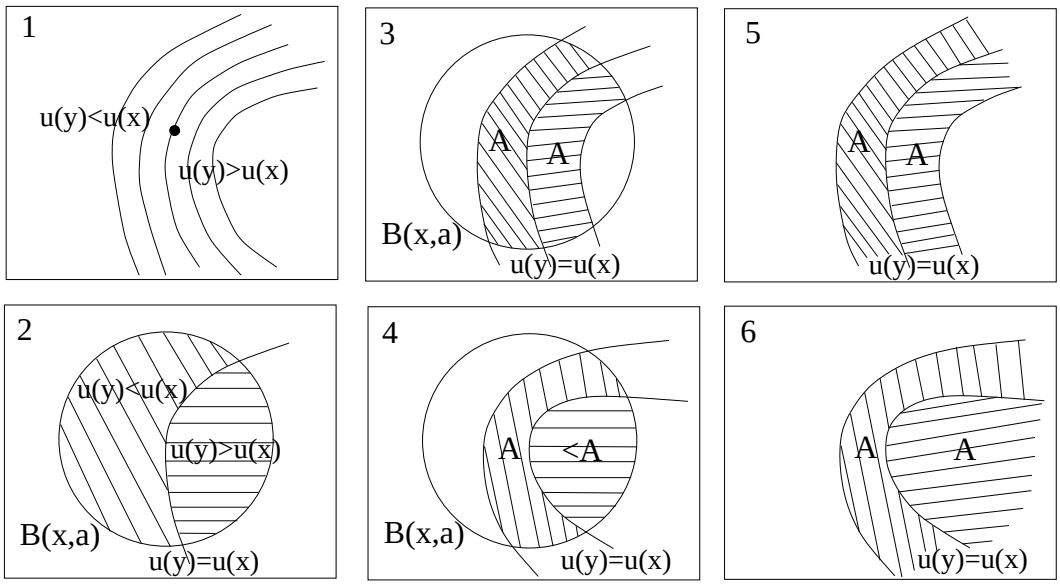

Figure 2.6: The evolution of a smooth function at a regular point (Figure 1) can be avoided only by removing spatial constraint

2 Conventional median filter: the level line $u(y) = u(x)$ evolves as soon as $|\text{curv}\, u(x)| > 0$ (indeed $|\{y,\, u(y) > u(x)\}| < |\{y,\, u(y) < u(x)\}|$)

3-4 Median filter on N_2 neighborhood: evolution as soon as $|\text{curv}\, u(x)| > C$.

5-6 Median filter on connected neighborhood: no evolution $\forall\, \text{curv}\, u(x)$.

2.4.1 Definitions

Let $\Omega \subset \mathbb{R}^N$ be an open subset of $\mathbb{R}^N$ with Lipschitz boundary.

Definition 2.4.1 *Let $\Gamma \subset \Omega$, a, $b \in \Gamma$ and $\mathcal{G} = (\gamma_i)$ be the set of all paths linking a to b and included in Γ. The* geodesic distance $\mathsf{d}_\Gamma(\mathsf{a},\mathsf{b})$ *between a and b is defined as :*

$$d_\Gamma(a,b) = \begin{cases} \inf L(\gamma_i) & \text{if } \mathcal{G} \neq \emptyset \\ +\infty & \text{else} \end{cases}$$

Moreover, the distance of any point $a \in \Gamma$ to some subset $E \subset \Omega$ with respect to Γ is defined as :

$$d_\Gamma(a,E) = \begin{cases} \inf\limits_{b \in E \cap \Gamma} d_\Gamma(a,b) & \text{if } E \cap \Gamma \neq \emptyset \\ +\infty & \text{else} \end{cases}$$

If $d_\Gamma(a,b) < +\infty$ there does not necessarily exist a path γ linking a to b and included in Γ such that $L(\gamma) = d_\Gamma(a,b)$ (take for instance Γ open and nonconvex). However, if Γ is closed and simply connected then this path exists and is unique.

In view of Definition 2.2.10 we now give the construction of the connected neighborhood on which the median value shall be computed.

Definition 2.4.2 *Let $u \in \mathrm{BV}(\Omega)$. For every $x \in \Omega$ and for all $\alpha \leq u^-(x)$ and $\beta \geq u^+(x)$ we define :*

$$\mathcal{L}_\alpha(x) = \{y \in \Omega :\ \alpha \leq u^-(y) \leq u^-(x)\}$$
$$\text{and} \quad \mathcal{U}_\beta(x) = \{y \in \Omega :\ u^+(x) \leq u^+(y) \leq \beta\}$$

We denote by $L_\alpha(x)$ and $U_\beta(x)$ the connected components of x in $\mathcal{L}_\alpha(x)$ and $\mathcal{U}_\beta(x)$, respectively.

Remark that $L_\alpha(x)$ and $U_\beta(x)$ are not empty since $x \in L_\alpha(x) \cap U_\beta(x)$.

Definition 2.4.3 (Connected neighborhood construction)
Let $\theta > 0$ and for every $x \in \Omega$:

$$W^=(x) = \text{connected component of } x \text{ in } \{y \in \Omega :\ u^-(y) = u^-(x) \text{ and } u^+(y) = u^+(x)\}$$

If $|W^=(x)| \geq \theta$ we define $\boxed{W_\theta(x) = W^=(x)}$
Else let :

$$\mathcal{I} = \{\alpha \in \mathbb{R} :\ \alpha \leq u^-(x),\ |L_\alpha(x)| \geq \theta\}$$
$$\text{and} \quad \mathcal{S} = \{\beta \in \mathbb{R} :\ \beta \geq u^+(x),\ |U_\beta(x)| \geq \theta\}$$

Let :

$$E_0(x) = \begin{cases} \text{connected component of } x \text{ in } \{y \in \Omega :\ u^-(y) \leq u^-(x)\} \text{ if } \mathcal{I} = \emptyset \\ L_{\sup \mathcal{I}}(x) \text{ else} \end{cases}$$
$$F_0(x) = \begin{cases} \text{connected component of } x \text{ in } \{y \in \Omega :\ u^+(y) \geq u^+(x)\} \text{ if } \mathcal{S} = \emptyset \\ U_{\inf \mathcal{S}}(x) \text{ else} \end{cases}$$

If $|E_0(x)| \geq \theta$ and $|F_0(x)| \geq \theta$ let $\boxed{W_\theta(x) = W^=(x)}$
Else :

- *If $|E_0(x)| < \theta$ and $|F_0(x)| < \theta$ let* $\boxed{W_\theta(x) = E_0(x) \cup F_0(x)}$
- *If $|E_0(x)| \geq \theta$ and $|F_0(x)| < \theta$ let :*

$$\mathcal{I}' = \{\alpha \in \mathbb{R} :\ \alpha \leq u^-(x),\ |L_\alpha(x) \backslash W^=(x)| \geq \theta\}$$

If $\mathcal{I}' = \emptyset$ then let

$$E_1(x) = \text{connected component of } x \text{ in } \{y \in \Omega :\ u^-(y) \leq u^-(x)\}$$

$$\text{and } \boxed{W_\theta(x) = E_1(x) \cup F_0(x)}$$

Else :

◇ *If* $\left|L_{\sup \mathcal{I}'}(x) \backslash W^{=}(x)\right| = \theta$ *let* $E_2(x) = L_{\sup \mathcal{I}'}(x)$

$$\text{and } \boxed{W_\theta(x) = E_2(x) \cup F_0(x)}$$

◇ *Else let* $\mathcal{I}'' = \{\alpha \in \mathbb{R} : \ \alpha \leq u^-(x), \ |L_\alpha(x) \backslash W^{=}(x)| < \theta\}$ *and* $\mathcal{A} := L_{\sup \mathcal{I}'}(x) \backslash L_{\inf \mathcal{I}''}(x)$. *Let* $(\mathcal{C}_\kappa)$ *be the lower level sets of the geodesic distance* $d_{L_{\sup \mathcal{I}'}(x)}(., L_{\inf \mathcal{I}''}(x))$. *We define*

$$E_3(x) = L_{\inf \mathcal{I}''}(x) \cup \mathcal{C}_\epsilon$$

where ϵ *is such that* $|E_3(x)| = \theta + |W^{=}(x)|$ *and finally*

$$\boxed{W_\theta(x) = E_3(x) \cup F_0(x)}$$

- *If* $|E_0(x)| < \theta$ *and* $|F_0(x)| \geq \theta$ *let :*

$$\mathcal{S}' = \{\beta \in \mathbb{R} : \ \beta \geq u^+(x), \ |U_\beta(x) \backslash W^{=}(x)| \geq \theta\}$$

If $\mathcal{S}' = \emptyset$ *then let*

$$F_1(x) = \text{connected component of } x \text{ in } \{y \in \Omega : \ u^+(y) \geq u^+(x)\}$$

$$\text{and } \boxed{W_\theta(x) = E_0(x) \cup F_1(x)}$$

Else :

◇ *If* $|U_{\inf \mathcal{S}'}(x) \backslash W^{=}(x)| = \theta$ *let* $F_2(x) = U_{\inf \mathcal{S}'}(x)$

$$\text{and } \boxed{W_\theta(x) = E_0(x) \cup F_2(x)}$$

◇ *Else let* $\mathcal{S}'' = \{\beta \in \mathbb{R} : \ \beta \geq u^+(x), \ |U_\beta(x) \backslash W^{=}(x)| < \theta\}$ *and* $\theta := U_{\inf \mathcal{S}'}(x) \backslash U_{\sup \mathcal{S}''}(x)$. *Let* $(\mathcal{C}_\kappa)$ *be the lower level sets associated with the geodesic distance* $d_{U_{\inf \mathcal{S}'}(x)}(., U_{\sup \mathcal{S}''}(x))$. *We define*

$$F_3(x) = U_{\sup \mathcal{S}''}(x) \cup \mathcal{C}_\epsilon$$

where ϵ *is such that* $|F_3(x)| = \theta + |W^{=}(x)|$ *and finally*

$$\boxed{W_\theta(x) = E_0(x) \cup F_3(x)}$$

When $W_\theta(x) = W^{=}(x)$ *we define* $W^+(x) = W^-(x) = W^{=}(x)$, *else* $W_\theta(x)$ *can be written as* $W_\theta(x) = E_i(x) \cup F_j(x)$ *thus we define* $W^-(x) = E_i(x)$ *and* $W^+(x) = F_j(x)$.

It must be emphasized that the previous construction involves connected components in the conventional topological sense which is not the most natural when dealing with BV functions (see Section 2.5). However, our filter construction is based on the continuity of the geodesic distance function within connected components, which cannot be stated if the components are defined up to Lebesgue negligible sets.

The construction of the connected neighborhood is based on the following idea : at each point of Ω we wish to find, whenever possible, a sub-neighborhood W^- and a super-neighborhood W^+ whose measures equal at most θ. Now, according to definitions of $\mathcal{I}$ and $\mathcal{S}$, and assuming that these sets are not empty, it might happen that $|L_{\sup \mathcal{I}}| > \theta$ and $|U_{\inf \mathcal{S}}| > \theta$. In such a case, by means of a geodesic distance like in the definition, we could select subsets of $L_{\sup \mathcal{I}}$ and $U_{\inf \mathcal{S}}$ having the right measure. But it is trivial in this case that the median value over the union of these two subsets equals $u(x)$. This is the reason why we define for simplicity in such a case $W_\theta(x) = W^=(x)$.

Remark now that $W_\theta(x)$ is not necessarily of measure less or equal to θ – take for instance its definition when $|W^=(x)| \geq \theta$. In case where $|E_0(x)| \geq \theta$ and $|F_0(x)| < \theta$ – argument is analogous when $|E_0(x)| < \theta$ and $|F_0(x)| \geq \theta$ – we do not extract a subset $E \subset E_0(x)$ such that $|E| = \theta$ but, if possible, such that $|E \setminus W^=(x)| = \theta$. The reason is that we want to put in agreement the processing of $\mathrm{C}^0 \cap \mathrm{BV}(\mathbb{R}^\mathrm{N}, \mathbb{R})$ functions with the processing of $\mathrm{C}^1 \cap \mathrm{BV}(\mathbb{R}^\mathrm{N}, \mathbb{R})$ functions (see below).

The following lemmas ensure the validity of Definition 2.4.3.

Lemma 2.4.4 *If* $\mathcal{I} := \{\alpha \in \mathbb{R} : \ \alpha \leq u^-(x), \ |L_\alpha(x)| \geq \theta\} \neq \emptyset$ *then* $\sup \mathcal{I} \in \mathcal{I}$

PROOF : Since u is measurable, the sets $L_\alpha(x)$ are measurable $\forall \alpha \in \mathcal{I}$ and $\alpha < \beta$ implies that $L_\beta(x) \subset L_\alpha(x)$. Let (α_n) be an increasing sequence of $\mathcal{I}$ tending to $\sup \mathcal{I}$. Then

$$\left| \bigcap_n L_{\alpha_n}(x) \right| = \lim_{n \to \infty} |L_{\alpha_n}(x)| \geq \theta$$

and the lemma ensues.
It might be proven analogously that if $\mathcal{S} \neq \emptyset$ then $\inf \mathcal{S} \in \mathcal{S}$ and similar results hold for $\mathcal{I}'$ and $\mathcal{S}'$. In contrast, $|L_{\inf \mathcal{I}''}(x) \setminus W^=(x)| \leq \theta$ and $\left|L_{\sup \mathcal{S}''}(x) \setminus W^=(x)\right| \leq \theta$ □

Lemma 2.4.5 *Whenever it needs to be defined, there exists some* $\epsilon > 0$ *such that*

$$L_{\inf \mathcal{I}''}(x) \cup \mathcal{C}_\epsilon$$

is a connected set of measure $\theta + |W^=(x)|$.

PROOF : Such an ϵ has to be defined whenever

$$\left|L_{\sup \mathcal{I}'}(x) \setminus W^=(x)\right| > \theta \text{ and } |L_{\inf \mathcal{I}''}(x) \setminus W^=(x)| < \theta$$

First, remark that the geodesic distance to $L_{\inf \mathcal{I}''}(x)$ within the connected set $L_{\sup \mathcal{I}'}(x)$ is continuous, hence any lower level set of the distance function is connected. For all $\delta > 0$ such that

$$\mathcal{C}_\delta := \{y \in L_{\sup \mathcal{I}'}(x) : \ d_{L_{\sup \mathcal{I}'}(x)}(y, L_{\inf \mathcal{I}''}(x)) = \delta\} \neq \emptyset,$$

it arises from the triangular inequality that $|\mathcal{C}_\delta| = 0$. Therefore, by the measure continuity, there exists some $\epsilon > 0$ such that $|L_{\inf \mathcal{I}''}(x) \cup \mathcal{C}_\epsilon \setminus W^=(x)| = \theta$, and lemma ensues. An analogous argument yields that there exists some ϵ such that $U_{\sup \mathcal{S}''}(x) \cup \mathcal{C}_\epsilon$ is a connected set of measure $\theta + |W^=(x)|$. □

Definition 2.4.6 *For every $\theta > 0$ we define the* median filter on a connected neighborhood of measure θ *as the operator* MFCN_θ *such that for every $u \in \mathrm{BV}(\Omega)$ and $x \in \Omega$:*

$$\mathsf{MFCN}_\theta\, u(x) = \mathrm{med}^-_{W_\theta(x)}\, u = \inf\{\lambda \in \mathbb{R} : \ |\{y \in W_\theta(x) : \ u(y) \leq \lambda\}| \geq \frac{|W_\theta(x)|}{2}\}$$

For the sake of simplicity, we decided to restrict our definition by using $\mathrm{med}^-_{W_\theta(x)}\, u(x)$ but it is worth noticing that any result in the sequel still holds if we replace $\mathrm{med}^-_{W_\theta(x)}\, u(x)$ with any value in $[\mathrm{med}^-_{W_\theta(x)}\, u(x), \mathrm{med}^+_{W_\theta(x)}\, u(x)]$.

We have illustrated in figure 2.7 the general aspect of $W^-(x)$, $W^=(x)$ and $W^+(x)$ in the case of a piecewise smooth function u from $\mathbb{R}^2$ onto $\mathbb{R}$ and when x belongs to the constant part of the graph of u. As previously written, there is an adaptation of these neighborhoods to the local conformation of level lines so that median filtering on $W_\theta(x)$ lets structure invariant.

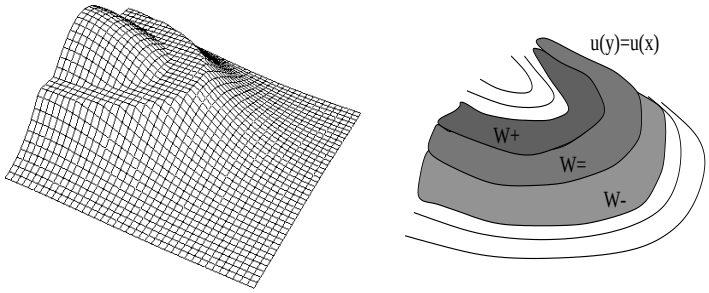

Figure 2.7: $W^-(x)$, $W^=(x)$ and $W^+(x)$ on a formal example
Left : 3D plot of a smooth function – Right : shapes of $W^-(x)$, $W^=(x)$ and $W^+(x)$

As wrote above, our definition allows to put in agreement the processing of $\mathrm{C}^0 \cap \mathrm{BV}(\mathbb{R}^N, \mathbb{R})$ functions with the processing of $\mathrm{C}^1 \cap \mathrm{BV}(\mathbb{R}^N, \mathbb{R})$ functions. Let us indeed assume that in any case we define W^- and W^+ such that their respective areas do not exceed θ and consider in $\mathbb{R}^2$ the two radial functions illustrated in figure 2.4.1. The radial

function u_2 is defined by

$$u_2(r) = \begin{cases} u_1(r) \text{ if } r \geq r_2 \\ u_1(r_2) \text{ else} \end{cases}$$

Let us set $\pi r_1^2 = \theta$ and $\pi r_2^2 = \frac{\theta+1}{2}$. With previous assumptions on W^- and W^+ we obtain $|L_{u_1}(r)| = \theta > |U_{u_1}(r)|$ if $r < r_1$ and $|L_{u_1}(r)| = |U_{u_1}(r)| = \theta$ else. Thereby $\text{med}(L_{u_1}(r) \cup U_{u_1}(r)) = u_1(r)$ if $r \geq r_1$ and $\text{med}(L_{u_1}(r) \cup U_{u_1}(r)) = u_1(r_1)$ else. Function u_1 shall therefore be truncated at level $u(r_1)$ through filtering.

On the other hand it can be proven that for every $r < r_2$, $L_{u_2}(r) = W^=_{u_2}(r) = \{(x,y) : x^2 + y^2 \leq r_2^2\}$ so that $|U_{u_2}(r)| = \frac{\theta+1}{2}$ whereas $\left|L_{u_2}(r) \backslash W^=_{u_2}(r)\right| = \frac{\theta-1}{2}$. Hence $\text{med}(L_{u_2}(r) \cup U_{u_2}(r)) = u_2(r_2)$ if $r < r_2$. Now for every $r \geq r_2$, $\text{med}(L_{u_2}(r) \cup U_{u_2}(r)) = u_2(r)$ so that u_2 remains identical.

Behaviours of both functions are consequently different for the only reason that $u_2(r)$ is constant for some values of r whereas $u_1(r)$ is not. This cannot be valid whenever we would our process to depend on the only connectedness and area and furthermore for the reason that different captors may generate various truncations in image so that our attempt to reduce dependence on image capture would be unsuccessful. Now it is easy to check that using Definition 2.4.3 shall yield the same result for $\mathsf{MFCN}_\theta u_1$ and $\mathsf{MFCN}_\theta u_2$.

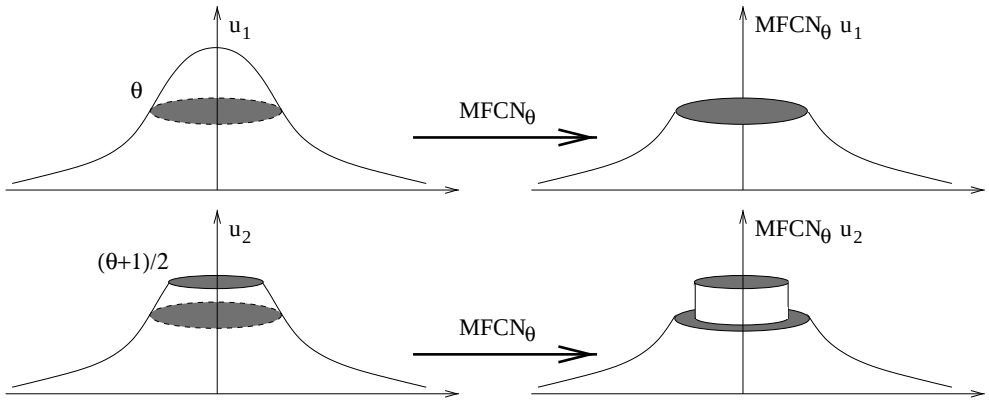

Figure 2.8: Adaptation of W^- and W^+ definitions for similar processing of $\mathrm{C}^1(\mathbb{R}^N, \mathbb{R})$ and $\mathrm{C}^0(\mathbb{R}^N, \mathbb{R})$ functions.

2.4.2 Properties

MFCN_θ is not continuous with respect to the convergence in $\mathrm{L}^1_{\mathrm{loc}}(\mathbb{R}^N)$ neither monotone on $\mathrm{BV}(\mathbb{R}^N)$. The noncontinuity property follows from the fact that, as proved in Section 2.3, the median filter is not continuous with respect to the convergence in $\mathrm{L}^1_{\mathrm{loc}}(\mathbb{R}^N)$. Now, the median filter is monotone but MFCN_θ does not inherit of this property as shown with the following counter-example : we have illustrated in figure 2.9 two radial functions u and v such that $u \leq v$ on some neighborhood. For every $x \in E$, for every $\theta > 0$, $|W^-_u(x)| = \theta$

and for some large enough value of θ, $|W_v^-(x)| < \theta$. Now, it is easily seen that $\forall x \in E$, $\mathsf{MFCN}_\theta u(x) > \mathsf{MFCN}_\theta v(x)$ whenever θ is large enough.

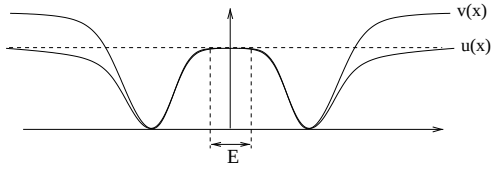

Figure 2.9: Counter-example for the non monotonicity of MFCN_θ

Proposition 2.4.7 MFCN_θ *is invariant with respect to any continuous increasing contrast change.*

PROOF : Let g be a real continuous increasing function.
For all $\alpha \leq u(x)$ and $\beta \geq u(x)$, we deduce from Definition 2.4.3 :

$$\begin{aligned} \mathcal{L}_\alpha(u)(x) &= \{y \in \mathbb{R}^2 :\ \alpha \leq u(y) \leq u(x)\} \\ &= \{y \in \mathbb{R}^2 :\ g(\alpha) \leq g \circ u(y) \leq g \circ u(x)\} = \mathcal{L}_{g(\alpha)}(g \circ u)(x) \\ \text{and}\quad \mathcal{U}_\beta(u)(x) &= \{y \in \mathbb{R}^2 :\ u(x) \leq u(y) \leq \beta\} \\ &= \{y \in \mathbb{R}^2 :\ g \circ u(x) \leq g \circ u(y) \leq g(\beta)\} = \mathcal{U}_{g(\beta)}(g \circ u)(x) \end{aligned}$$

Hence, the families of sets $\{\mathcal{L}_\alpha(u)(x)\}_{\alpha \leq u(x)}$ and $\{\mathcal{U}_\beta(u)(x)\}_{\beta \geq u(x)}$ are globally invariant with respect to any continuous increasing contrast change, inclusions and connectedness being preserved. Thus $W_\theta(u)(x) = W_\theta(g \circ u)(x)$ and :

$$\begin{aligned} \mathsf{MFCN}_\theta(g \circ u)(x) &= \inf\{\lambda :\ |\{y \in W_\theta(g \circ u)(x),\ g \circ u(y) \leq \lambda\}| \geq \tfrac{|W_\theta(g \circ u)(x)|}{2}\} \\ &= \inf\{g(\lambda) :\ |\{y \in W_\theta(x) :\ g \circ u(y) \leq g(\lambda)\}| \geq \tfrac{|W_\theta(x)|}{2}\} \\ &= \inf\{g(\lambda) :\ |\{y \in W_\theta(x) :\ u(y) \leq \lambda\}| \geq \tfrac{|W_\theta(x)|}{2}\} \\ &= g(\inf\{\lambda \in \mathbb{R} :\ |\{y \in W_\theta(x) :\ u(y) \leq \lambda\}| \geq \tfrac{|W_\theta(x)|}{2}\}) \\ &= g(\mathsf{MFCN}_\theta u(x)) \end{aligned}$$

□

Proposition 2.4.8 *For every Euclidean mapping* Φ *of* $\mathbb{R}^N$ *onto itself and for every* $x \in \Phi^{-1}(\Omega)$

$$\mathsf{MFCN}_\theta(\Phi u)(x) = \mathsf{MFCN}_\theta(u)(\Phi(x))$$

PROOF : Φ preserves the connectedness, the Lebesgue measure and the geodesic distance hence

$$W_\theta(\Phi u)(x) = \Phi^{-1}(W_\theta(u)(\Phi x))$$

and the proposition ensues. □

Proposition 2.4.9 MFCN_θ *may increase the total variation.*

PROOF : Let $u \in \mathrm{BV}$ be the image shown in figure 2.10. Let $\lambda > 2$ and $\theta = \pi r_1^2$. In view of the definitions, $\mathsf{MFCN}_\theta u$ is the right image in the figure if $2r_1^2 > r_3^2$ and $3r_1^2 > r_2^2 + r_3^2$.

Indeed, if x is such that $u(x) = \lambda$ then $\theta = \pi r_1^2$ implies that $\mathsf{MFCN}_\theta u(x) = \lambda$. If $u(x) = 1$ then $|W^=(x)| = \pi(r_2^2 - r_1^2)$, $|W^-(x) \setminus W^=(x)| = \pi(r_3^2 - r_2^2)$ and if $2r_1^2 > r_3^2$ then $W^+(x) = \{y : u(y) \geq 1\}$ thus $|W^+(x) \setminus W^=(x)| = \pi r_1^2$ and finally $\mathsf{MFCN}_\theta u(x) = \lambda$.

If $u(x) = 0$ then $|W^=(x)| = \pi(r_3^2 - r_2^2)$, $W^-(x) \setminus W^=(x) = \emptyset$ and thus $|W^+(x) \setminus W^=(x)| = \pi r_1^2$. The inequality $3r_1^2 > r_2^2 + r_3^2$ is enough to ensure that $\mathsf{MFCN}_\theta u(x) = 1 + \epsilon$. Finally $\{y : u(y) = 1 + \epsilon\}$ is supposed to be of measure large enough to ensure that if $u(x) = 1 + \epsilon$ then $\mathsf{MFCN}_\theta u(x) = 1 + \epsilon$. Let us now examine the total variation.

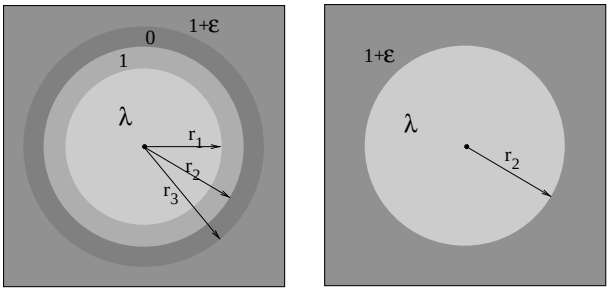

Original image u MFCN$_\theta$ (u)

Figure 2.10: There are values of r_1, r_2, r_3 and ϵ such that $|D(\mathsf{MFCN}_\theta u)| > |Du|$ with $\theta = \pi r_1^2$

$$|Du| = \int_1^\lambda 2\pi r_1 + \int_0^1 2\pi r_2 + \int_0^{1+\epsilon} 2\pi r_3 = 2\pi((\lambda - 1)r_1 + r_2 + (1 + \epsilon)r_3)$$

and

$$|D\mathsf{MFCN}_\theta u| = \int_{1+\epsilon}^\lambda 2\pi r_2 = 2\pi(\lambda - 1 - \epsilon)r_2$$

The total variation has increased if $(\lambda - 1 - \epsilon)r_2 > (\lambda - 1)r_1 + r_2 + (1 + \epsilon)r_3$ thus the counter-example is valid if the following conditions are satisfied

$$2r_1^2 > r_3^2, \quad 3r_1^2 > r_2^2 + r_3^2 \quad \text{and} \quad 0 < \epsilon < \frac{(\lambda - 1)(r_2 - r_1) - r_2 - r_3}{r_2 + r_3}$$

It can be checked that $r_1 = 2$ (thus $\theta = 4\pi$), $r_2 = 2.1$, $r_3 = 2.2$, $\epsilon = 0.1$ and $\lambda = 50$ are admissible values and the proposition ensues. □

The main difference between the conventional median filter and MFCN_θ is that the latter depends on the only area of the connected components of level sets whereas the former basically depends on the curvature of the level lines. We therefore conjecture the following result.

Conjecture 2.4.10 *Let $u \in \mathrm{BV}$. For every $\theta > 0$, there exists some $C > 0$ such that*

$$|D\mathsf{MFCN}_\theta u| \leq C\,|Du|$$

Moreover, there exists $n < +\infty$ such that $(\mathsf{MFCN}_\theta)^n(u)$ is a fixed point.

2.4.3 Experimental results

Recall that we have defined MFCN in order to avoid a systematic alteration of image structures. This is illustrated in figure 2.11, which shows the remarkable stability of unnoisy data through filtering. In contrast, conventional median filter with a working window of area approximatively 2θ yields after only two iterations much too smooth solutions which are not fixed points (other classic morphological filters have exactly the same drawback). Finally we deduce from these experiments that choosing a value for the parameter θ (generally taken between 5 and 20) is not a drawback in contrast to most of denoising filters for which the choice is often crucial and highly delicate.

In the following experiments we compare MFCN with reference filters. The conventional median filter is taken as the reference morphological filter. The Susan (Smallest Univalue Segment Assimilating Nucleus) filter [38], defined as

$$\text{Susan}\, u(x) = C \int_{B_a(x)} u(y) e^{-\frac{|y-x|^2}{d^2}} e^{-\frac{|u(y)-u(x)|^2}{\ell^2}} dy$$

where C is a normalization factor and a is taken large enough so that spatial limitation be mainly due to the term $e^{-\frac{|y-x|^2}{d^2}}$, can be considered as a synthesis of classic local and nonlinear filters involving average - and therefore non morphological. In view of Yaroslavsky neighborhoods N_1 and N_2 defined in the general introduction, this operator can be seen as the average over a neighborhood derived from N_1 by weighting in both spatial and brightness domains. We also shall compare MFCN with the Rudin-Osher global and nonlinear denoising method (see Section 2.2).

Figure 2.12 illustrates the performances of these filters when original image (detail of an aerial CNES photograph) is corrupted by a large amount of impulse noise ($f = 25\%$). The best result – which is also a fixed point in contrast to the other methods – is obviously performed by MFCN. This is not surprising in view of our approach. Indeed, a point is not modified through filtering if it belongs to some sub- and super-neighborhoods of same area; most of the points that do not satisfy this property are noisy points, so that filtering performs a real denoising while unnoisy points are not altered. The decay of total variation is particularly large since an impulse noise creates large and frequent variations.

In contrast, the Rudin–Osher method performs quite badly but this is not surprising for it was not designed for this kind of noise. Conventional median filter yields a solution that is too smooth when Susan filter does not succeed in removing noise (a less noisy result could be obtained but associated with a high loss of definition in image).

The ability of MFCN to preserve structure much better than other filters is due to its weak smoothing property. This may be a drawback on a qualitative point of view: the

Figure 2.11: [1] Original image u
[2] $(\mathsf{MFCN}_{10})^{11}(u)$ (fixed point) [3] $(\mathrm{med}_{B(.,2.5)})^2 u$ (compare with [2])
[4] $(\mathsf{MFCN}_{20})^{10}(u)$ (fixed point) [5] $(\mathrm{med}_{B(.,3.5)})^2 u$ (compare with [4])

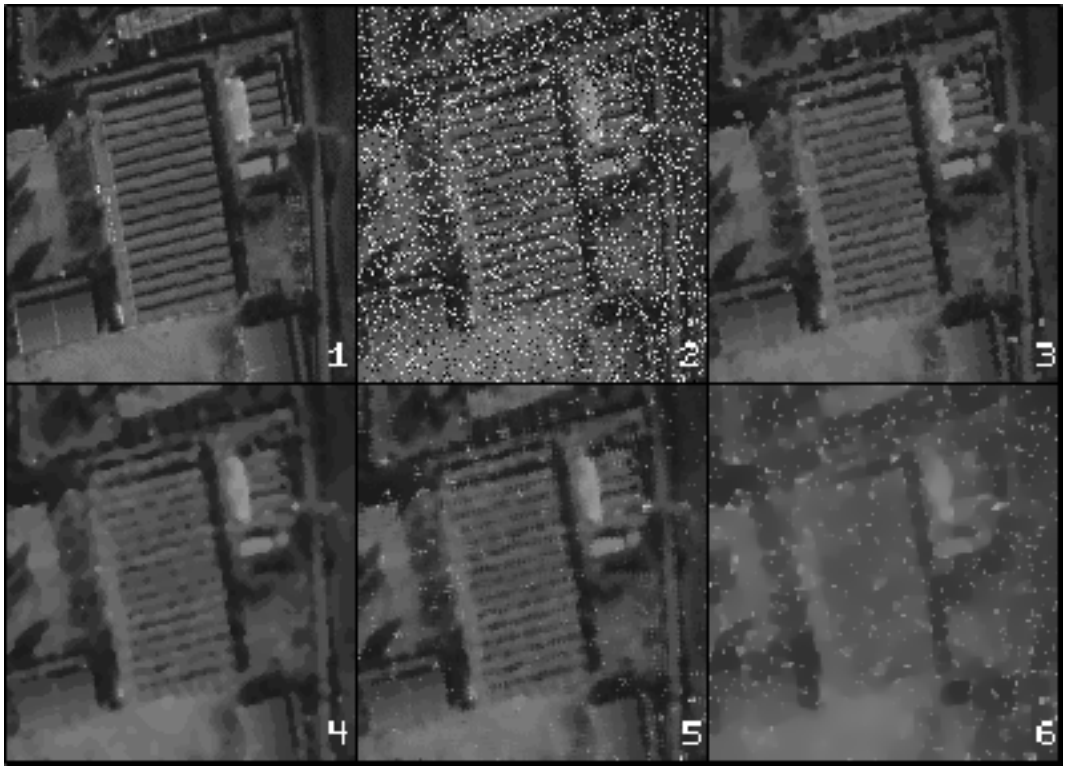

Figure 2.12: [1] Original image u_0 (aerial CNES photograph)
[2] Noisy image u (impulse noise, $f = 25\%$)
[3] $(\mathsf{MFCN}_5)^5(\mathrm{med}_{B(.,1)}\, u)$ (fixed point, 4-connectivity) [4] $(\mathrm{med}_{B(.,1.5)})^2(u)$
[5] $(\mathrm{Susan}_{(t=12,\, d=0.4)})u$ [6] Rudin-Osher ($\epsilon = 1,\ dt = 1,\ T_0 = 0,\ T = 40$)

original lack of smoothness of level lines or the one generated by noise will remain unless a smoothing process is introduced. Take for instance the example illustrated in figure 2.13.

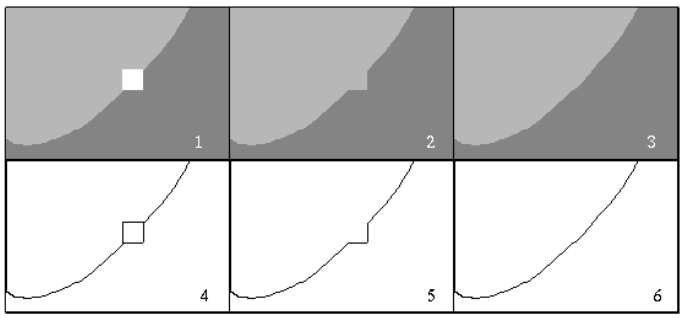

Figure 2.13: [1] Noisy image u – [2] $\mathsf{MFCN}_\theta^n u$
[3] $\mathrm{Cmed}_{D(.,r)}(\mathsf{MFCN}_\theta^n u)$ – [4-5-6] Level lines in images 1-2-3

The white square is processed by MFCN as a noisy region because of its small area and is correctly removed. But the local "deviation" of "the" main level line due to the square has been preserved. A solution consists in computing median filter inside the only region previously occupied by the square; the smoothness of the line is then recovered without any global evolution. A drawback of this post-smoothing method is that the fixed point property is lost and that two more parameters have to be introduced : the radius of the disk on which the median value is computed and the number of iterations. Now let us emphasize the difference between this method and a denoising with conventional iterated median filter. The latter induces a global diffusion from the only curvature of level lines. The former recovers local coherence from the area of bilevel sets – i.e. $X_{\lambda,\nu} = \{x \in \Omega,\ \lambda \leq u(x) \leq \nu\}$ – and points which have been modified are considered as noisy points; they are the only points where the diffusion process occurs, so that there is no global alteration of image structures.

Remark that the disocclusion method that shall be presented in the next chapter and which is idempotent, could replace the conventional iterated median for post-smoothing of modified zones since one might consider them as occlusions.

Another way of obtaining a smoother result without loosing the fixed point property consists in applying the conventional iterated median to the whole image before MFCN. Naturally, this pre-smoothing has to be slight in order to avoid a serious alteration of structures in image: radius of the structuring element and the number of iterations have to be small. It arises from our experiments that pre-smoothing is particularly interesting in case of images corrupted with white additive noises. The following equation summarizes the combination of MFCN with both pre-smoothing and post-smoothing – values of disk radius and iterations number are empirically the ones offering the best compromise between smoothing and structure preservation:

$$v(.) = \mathrm{Cmed}_{D(.,1.5)} \mathsf{MFCN}_\theta^n \, \mathrm{med}_{D(.,1)}(u)(.)$$

$$\text{where} \quad \mathrm{Cmed}_{D(.,1.5)} \Psi u(.) = \begin{cases} \mathrm{med}_{D(.,1.5)} \Psi u(.) & \text{if } \Psi u(.) \neq u(.) \\ \Psi u(.) & \text{else} \end{cases}$$

and n is the number of iterations until convergence. Let us however notice that we generally avoid using post-smoothing: we used for example the only pre-smoothing in figure 2.12 (one iteration of median filter on a ball $D(.,1)$).

Figure 2.14 illustrates the results obtained by applying the filters described above to an image corrupted with a white Gaussian additive noise of standard deviation 10. Rudin–Osher method performs obviously well – it was specifically designed for this type of noise – but it is not morphological, parameters are hardly adjustable, the solution is not a fixed point and too many iterations yield a piecewise constant solution made of large and artificial pieces. In contrast MFCN converges to a solution which is less fair but is a fixed point and therefore depends on a single parameter (θ). Moreover, MFCN is morphological and yields better result than the reference conventional median filter

Figure 2.14: [1] Original image
[2] Image u corrupted with white additive Gaussian noise ($\sigma = 10$)
[3] $(\mathsf{MFCN}_{10})^6(\mathrm{med}_{B(.,1)}\, u)$ (fixed point for MFCN_{10}) – [4] $(\mathrm{med}_{B(.,1.5)})^2 u$
[5] Rudin-Osher method ($\epsilon = 1,\ dt = 1,\ T_0 = 0,\ T = 6$) – [6] $\mathrm{Susan}_{(d=1.4,\, t=12)}(u)$

in view of preserving structures: details are sharper and there was no global diffusion. Finally Susan filter performs well in removing noise, but the use of average filter induces a strong regularization that makes the fine textures disappear : the result looks a bit artificial.

As already said, one of the main characteristic of MFCN is its ability to preserve functions at points where roughly speaking sub- and super-neighborhoods have the same area. In contrast, it is not possible to construct simultaneously such neighborhoods near any extreme value. Either W^- or W^+ are too small so that regions surrounding extrema will evolve as illustrated in figure 2.15 where a C^1 function in $\mathbb{R}$ becomes C^0 when iterating MFCN.

This simple remark yields two operators, denoted by $I_\theta S_\theta$ and $S_\theta I_\theta$. They were first introduced by Luc Vincent in [39] within the framework of Mathematical Morphology. The basic idea is to remove connected components of level sets having small area and this

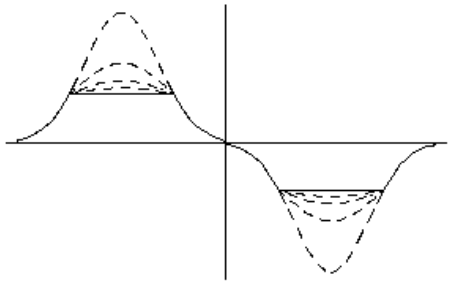

Figure 2.15: Evolution of a smooth function near the only extreme values by iterating MFCN.

can be done by combining two operators defined for every x in Ω in the following way :

$$I_\theta u(x) = \inf\{\lambda,\ \lambda \geq u(x),\ |\text{connected component of } x \text{ in } \{y \in \Omega,\ u(y) \leq \lambda\}| > \theta\}$$
$$S_\theta u(x) = \sup\{\lambda,\ \lambda \leq u(x),\ |\text{connected component of } x \text{ in } \{y \in \Omega,\ u(y) \geq \lambda\}| > \theta\}$$

It is easily seen that I_θ acts on the vicinity of the minima of u whereas S_θ acts on the vicinity of the maxima. Both filters have consequently to be combined for denoising a conventional image. However, when dealing with functions of bounded variation, the definition above can be adapted and improved in order to be more reliable and to take into account the structure of level sets as sets of finite perimeter. In the next section, we present a weak notion of connectedness which is well adapted and reliable when dealing with sets of finite perimeter. Then, we shall give a new definition of Luc Vincent's filters and study in detail their properties as operators acting on the space of functions of bounded variation.

2.5 Partitions of sets of finite perimeter

The following definition is related to the partition of a set into sets of finite perimeter (see [3]).

Definition 2.5.1 *Let $\Omega \subset \mathbb{R}^N$ be an open set and $I \subset \mathbb{N}$. We say that a partition $\{E_i\}_{i\in I}$ of Ω is a Caccioppoli partition if $\sum_{i\in I} P(E_i, \Omega) < \infty$. We say that a Caccioppoli partition $\{E_i\}_{i\in I}$ is ordered if $|E_i| \geq |E_j|$ whenever $i \leq j$.*

It must be emphasized that a Caccioppoli partition always induces an ordered one just by a permutation of the indexes in I if $|\Omega| < \infty$ or if $\Omega = \mathbb{R}^N$. In particular, due to the isoperimetric inequality, if $\{E_i\}_{i\in\mathbb{N}}$ is an ordered Caccioppoli partition of $\mathbb{R}^N$, only E_0 has infinite measure. In view of Theorem 2.2.9 we have the following result.

Theorem 2.5.2 (Local structure of Caccioppoli partitions [3])
Let $\{E_i\}_{i\in I}$ be a Caccioppoli partition of Ω. Then

$$\bigcup_{i\in I} (E_i)^1 \ \cup \bigcup_{i,j\in I, i\neq j} (E_i)^{1/2} \cap (E_j)^{1/2}$$

contains $\mathcal{H}^{N-1}$-almost all of Ω.

This is equivalent to say that $\mathcal{H}^{N-1}$-almost every $x \in \Omega$ belongs either to a unique E_i or to the intersection of two and only two sets $(E_i)^{1/2}$. The crucial result related to Caccioppoli partitions is the following compactness result. Recall that the convergence in measure of sets means the convergence in L^1 of the associated characteristic functions.

Theorem 2.5.3 (Compactness of Caccioppoli partitions [3])
Let $\{E_{i,h}\}_{i\in I}$, $h \in \mathbb{N}$, be Caccioppoli partitions of $\mathbb{R}^N$ satisfying

$$\sup\left\{\sum_{i\in I} P(E_{i,h}, \mathbb{R}^N) : h \in \mathbb{N}\right\} < \infty$$

Then, if either I is finite or the partitions are ordered, there exists a Caccioppoli partition $\{E_i\}_{i\in I}$ of $\mathbb{R}^N$ and a subsequence h_k such that (E_{i,h_k}) locally converges in measure to E_i for any $i \in I$.

This result holds for Caccioppoli partition of an open bounded set $\Omega \subset \mathbb{R}^N$ with Lipschitz boundary since

$$\sum_{i\in I} P(E_{i,h}, \mathbb{R}^N) = \sum_{i\in I} P(E_{i,h}, \Omega) + \mathcal{H}^{N-1}(\partial\Omega)$$

The notion of connected components in the conventional topology is not well-suited to the sets of finite perimeter for mainly three reasons : a set of finite perimeter is always

defined up to $\mathcal{L}^N$-negligible sets, there is no good compactness property for the conventional connected components and, finally, the perimeter of a set Ω may differ from the sum of the perimeters of its connected components. The notion of connected components for sets of finite perimeter was first used in a paper by G. Dolzmann and S. Müller [12] but existence and uniqueness were not proved. They appeared in a paper by B. Kirchheim [20] with different and, in our opinion, more complicated proofs that the ones we give below. Finally, in a recent paper [8], V. Caselles and J.M. Morel have proposed a different but equivalent definition of connectedness in $\mathbb{R}^2$. They proved as well the existence and the uniqueness of the decomposition into connected components and stated in addition an accurate decomposition of the essential boundary into "interior" and "exterior" oriented Jordan curves. To avoid any confusion with the conventional notion of connected components, we shall rather speak in the sequel of indecomposable components. The definition of indecomposability is now given.

Definition 2.5.4 *A set E with finite perimeter and finite measure is called indecomposable if $|E| > 0$ and E cannot be written as a disjoint union $F \cup G$ with $|F|.|G| > 0$ and $P(E) = P(F) + P(G)$.*

Theorem 2.5.5 (Indecomposable components of sets of finite perimeter) *Any set E with finite measure and finite perimeter in $\mathbb{R}^N$ can be written as a disjoint union of finitely or countably many indecomposable sets E_i such that $\sum_i P(E_i) = P(E)$. Moreover, this decomposition is unique.*

PROOF : Let us consider all those ordered partitions $\{E_i\}_{i\in I}$ of E in finitely or countably many sets with strictly positive Lebesgue measure such that

$$\sum_{i\in I} P(E_i) \leq P(E) \tag{2.5.1}$$

There exists at least one partition satisfying this inequality : the trivial partition of E by itself. Given an admissible partition, any other partition obtained by decomposing a decomposable set E_i into two disjoint sets E_{i_1} and E_{i_2} with strictly positive measures and such that $P(E_i) = P(E_{i_1}) + P(E_{i_2})$, satisfies also (2.5.1).

Assume now that $I = \mathbb{N}$, the proof being simpler if I is finite. From the subadditivity of perimeter, we can infer that for any finite subset $J \subset I$

$$P(\bigcup_{i\in J} E_i, \mathbb{R}^N) \leq \sum_{i\in J} P(E_i, \mathbb{R}^N) \tag{2.5.2}$$

and by the lower semicontinuity of perimeter it follows that the same inequality is true for any subset $J \subset I$.

Let $\{E_{i,h}\}_{i\in I}$, $h \in \mathbb{N}$ be a sequence of ordered partitions satisfying (2.5.1) and maximizing $\sum_{i\in I} |E_i|^\alpha$ where $\alpha \in (\frac{N-1}{N}, 1)$. Due to (2.5.1), all the partitions satisfy the assumptions of Theorem 2.5.3. In addition, remark that $(|F| + |G|)^\alpha < |F|^\alpha + |G|^\alpha$ whenever $|F|.|G| > 0$. Indeed, it is easily seen that the function $f(x) = (1+x)^\alpha - 1 - x^\alpha$ is decreasing and $f(0) = 0$.
Let $n \in \mathbb{N}$. Since $i \mapsto |E_{i,h}|$ is decreasing we infer that for every $h \in \mathbb{N}$,

$$|E_{n,h}| \leq \frac{1}{n} |\bigcup_{i=1}^{n} E_{i,h}|$$

From (2.5.2) and the isoperimetric inequality we deduce that

$$|E_{n,h}| \leq \frac{C L^{N/(N-1)}}{n}$$

where $L := P(E, \mathbb{R}^N)$ and, since the partitions are ordered, the inequality holds for any set $E_{i,h}$ with $i \geq n$, thus

$$|E_{n,h}|^{(\alpha - \frac{N-1}{N})} \leq \frac{C^{(\alpha-\frac{N-1}{N})} L^{\frac{\alpha N}{N-1}-1}}{n^{(\alpha-\frac{N-1}{N})}}$$

Therefore, $\forall \epsilon > 0$, using the isoperimetric inequality and $\alpha > \frac{N-1}{N}$

$$\begin{aligned}
\sum_{i=n}^{\infty} |E_{i,h}|^\alpha &= \sum_{i=n}^{\infty} |E_{i,h}|^{(\alpha-\frac{N-1}{N})} |E_{i,h}|^{(N-1)/N} \\
&\leq \frac{C^{(\alpha-\frac{N-1}{N})} L^{\frac{\alpha N}{N-1}-1}}{n^{(\alpha-\frac{N-1}{N})}} \sum_{i=n}^{\infty} |E_{i,h}|^{(N-1)/N} \\
&\leq \frac{C^{(\alpha-\frac{N-1}{N})} L^{\frac{\alpha N}{N-1}-1}}{n^{(\alpha-\frac{N-1}{N})}} \sum_{i=n}^{\infty} C^{(N-1)/N} P(E_{i,h}, \mathbb{R}^N) \\
&\leq \frac{C^\alpha L^{\frac{\alpha N}{N-1}-1}}{n^{(\alpha-\frac{N-1}{N})}} \sum_{i=n}^{\infty} P(E_{i,h}, \mathbb{R}^N) \\
&\leq \frac{C^\alpha L^{\frac{\alpha N}{N-1}}}{n^{(\alpha-\frac{N-1}{N})}} < \epsilon
\end{aligned}$$

for n large enough, independent of h. Thus there exists some upper bound M, independent of h such that

$$\sum_{i=0}^{\infty} |E_{i,h}|^\alpha = \sum_{i=0}^{n-1} |E_{i,h}|^\alpha + \sum_{i=n}^{\infty} |E_{i,h}|^\alpha < n|E|^\alpha + \epsilon < M$$

and since $A(h) := \sum_{i=0}^{\infty} |E_{i,h}|^\alpha$ is increasing with respect to h, we deduce that $A(h)$ converges as $h \to \infty$.

By Theorem 2.5.3, there exists some subsequence h_k and a partition $\{E_i\}_{i\in I}$ such that (E_{i,h_k}) converges in measure to (E_i) as $h_k \to \infty$. From the lower semicontinuity of perimeter, $P(E_i) \leq \liminf_{h_k\to\infty} P(E_{i,h_k})$ and thus

$$\sum_{i=0}^{\infty} P(E_i) \leq \liminf_{h_k\to\infty} \sum_{i=0}^{\infty} P(E_{i,h_k}) \leq P(E)$$

Combining with (2.5.2) we deduce that

$$P(E) = \sum_{i=0}^{\infty} P(E_i)$$

Moreover, any E_i is indecomposable, since otherwise there would exist a partition (F_i) satisfying (2.5.1) and such that $\sum_{i=0}^{\infty} |F_i|^\alpha > \sum_{i=0}^{\infty} |E_i|^\alpha$, thus $\sum_{i=0}^{\infty} |F_i|^\alpha > \lim_{h_k\to\infty} A(h_k)$, which is a contradiction. □

Lemma 2.5.6 *Let F be a set of finite perimeter and $\{F_i\}$ a partition of F in sets of finite perimeter with $\sum_i P(F_i) < \infty$. Then $P(F) = \sum_i P(F_i)$ if and only if*

$$(*) \qquad \mathcal{H}^{N-1}(\Omega \cap F_i^{1/2} \cap F_j^{1/2}) = 0, \quad \textit{whenever } i \neq j$$

PROOF : Assume that (*) holds. From Theorems 2.2.9 and 2.5.2 we can deduce that $\mathcal{H}^{N-1}$-almost every point of Ω either belongs to F^0, or

$$(\bigcup_i F^{1/2} \cap F_i^{1/2}) \cup (\bigcup_{i\neq j} F^{1/2} \cap (F_i^{1/2} \cap F_j^{1/2}))$$

or to

$$(\bigcup_i F_i^1) \cup (\bigcup_{i\neq j} F^1 \cap (F_i^{1/2} \cap F_j^{1/2}))$$

The intersections in (*) being $\mathcal{H}^{N-1}$-negligible one infers that $\mathcal{H}^{N-1}$-almost every point of Ω either belongs to $F^0 \cup \bigcup_i F_i^1$ or to $\bigcup_i F^{1/2} \cap F_i^{1/2}$. This implies

$$\Omega \cap F_i^{1/2} \subset \Omega \cap F^{1/2}$$

up to $\mathcal{H}^{N-1}$-negligible sets, hence, using (*) and $P(E_i, \Omega) = \mathcal{H}^{N-1}(\Omega \cap E_i^{1/2})$, we get $\sum P(F_i) \leq P(F)$ and the equality follows by the subadditivity of the perimeter.

Conversely, if $\sum_i P(F_i) = P(F)$, and (*) does not hold for some $i \neq j$, we set $E = F_i$ and $L = \cup_{j\neq i} F_j$ and notice that $P(L) = \sum_j P(F_i)$. Since otherwise $P(F) \leq P(E) + P(L) < P(F_i) + \sum_j P(F_i)$ which contradicts $\sum_i P(F_i) = P(F)$. Thus, $P(E) + P(L) = P(F)$ and F is the disjoint union of E and L. In addition, the negation of (*) implies that

$$\mathcal{H}^{N-1}(\Omega \cap E^{1/2} \cap L^{1/2}) > 0$$

because, since E and L are disjoint, $\mathcal{H}^{N-1}$-a.e. $x \in E^{1/2} \cap E_j^{1/2}$ belongs to $E^{1/2} \cap L^{1/2}$. In this way we reduced ourselves to the case of two sets only. Remark now that

$$\begin{aligned}
\mathcal{H}^{\mathrm{N}-1}(\Omega \cap (E^{1/2} \cup L^{1/2})) &= \mathcal{H}^{\mathrm{N}-1}(\Omega \cap E^{1/2}) + \mathcal{H}^{\mathrm{N}-1}(\Omega \cap L^{1/2}) \\
&\quad - \mathcal{H}^{\mathrm{N}-1}(\Omega \cap E^{1/2} \cap L^{1/2}) \\
&= P(E) + P(L) - \mathcal{H}^{\mathrm{N}-1}(\Omega \cap E^{1/2} \cap L^{1/2}) \\
&= P(F) - \mathcal{H}^{\mathrm{N}-1}(\Omega \cap E^{1/2} \cap L^{1/2}) \\
&= \mathcal{H}^{\mathrm{N}-1}(\Omega \cap F^{1/2}) - \mathcal{H}^{\mathrm{N}-1}(\Omega \cap E^{1/2} \cap L^{1/2})
\end{aligned}$$

and we get a contradiction since $F^{1/2} \subset E^{1/2} \cup L^{1/2}$, and therefore $\mathcal{H}^{\mathrm{N}-1}(\Omega \cap F^{1/2}) \leq \mathcal{H}^{\mathrm{N}-1}(\Omega \cap (E^{1/2} \cup L^{1/2}))$. □

Theorem 2.5.7 *If F is indecomposable, $F \subset E$ and a partition $\{E_i\}$ of E satisfies $\sum_i P(E_i) = P(E)$, then there exists a unique i such that $F \subset E_i$, up to Lebesgue negligible sets.*

PROOF : Let $F_i = E_i \cap F$. We shall first prove that F_i satisfies the assumptions of the previous lemma. Indeed, using the fact that $\mathcal{H}^{N-1}$-almost every point belongs to $E_i^0 \cup E_i^1 \cup E_i^{1/2}$ we obtain

$$\Omega \cap F_i^{1/2} \subset \Omega \cap (E_i^1 \cup E_i^{1/2})$$

up to $\mathcal{H}^{N-1}$-negligible sets. Hence

$$\Omega \cap F_i^{1/2} \cap F_j^{1/2} \subset \Omega \cap E_i^{1/2} \cap E_j^{1/2}$$

Since, by the previous lemma, the sets $E_i^{1/2}$ satisfy condition $(*)$, we infer that the sets $F_i^{1/2}$ satisfy $(*)$ as well. Moreover, since $\mathcal{H}^{N-1}$-almost every point is in $F^0 \cup F^1 \cup F^{1/2}$ we obtain also

$$\Omega \cap F_i^{1/2} \subset \Omega \cap (F^{1/2} \cup E_i^{1/2})$$

hence $\sum_i P(F_i) \leq P(F) + \sum_i P(E_i) < +\infty$. Applying Lemma 2.5.6, we infer that $\sum_i P(F_i) = P(F)$ and the indecomposability of F implies that only one of the sets $F_i = E_i \cap F$ can have strictly positive measure. Thus there exists a unique i such that $F \subset E_i$, up to Lebesgue negligible sets, and the theorem ensues. □

Using Theorem 2.5.7, it is easy to check that the family $\{E_i\}$ given by Theorem 2.5.5 is unique, modulo permutations of the sets and modifications of them by Lebesgue negligible sets. Indeed if $\{E_i\}$ and $\{F_j\}$ are two different decompositions of E into indecomposable components, then Theorem 2.5.7 implies that for every i, there exists a unique j such that $E_i \subset F_j$ and for every j there exists a unique i such that $F_j \subset E_i$. Since components are disjoint we deduce that $E_i = F_j$ up to Lebesgue negligible sets. In the sequel, we shall denote by $\{E_i\}_{i \in I}$ the indecomposable components of E.

Let us now come back to the filters defined by Luc Vincent. We shall prove that using Caccioppoli partitions into indecomposable sets of the level sets of a BV function , it is possible to give a reliable formulation of these filters. In addition, we shall derive new properties and in particular, the fact that these filters make the BV norm decrease.

2.6 Level sets area filtering

Let Ω be an open, bounded subset of $\mathbb{R}^N$ with Lipschitz boundary.

Definition 2.6.1 *Let E be a set of finite perimeter in Ω and $\theta \geq 0$. We define $T_\theta E$ as the union of the indecomposable components E_i of E such that $|E_i| > \theta$.*

Notice that $T_0 E = E$ and that T_θ is well defined only up to Lebesgue negligible sets. Moreover, by the subadditivity of perimeter, it follows that $P(T_\theta E) \leq P(E)$, with equality only if $T_\theta E \sim E$.

Proposition 2.6.2 *Let E, F be two sets of finite perimeter in Ω.*
$E \subset F$ implies $T_\theta E \subset T_\theta F$, where both inclusions are understood up to Lebesgue negligible sets. Moreover, if $E_h \uparrow E$ and $P(E_h) \to P(E)$, then $T_\theta E_h \uparrow T_\theta E$ and $P(T_\theta E_h) \to P(T_\theta E)$.

By $E_h \uparrow E$ we mean that (E_h) is an increasing sequence of sets converging in measure to E, i.e. $|E_h \setminus E_{h'}| = 0$ whenever $h < h'$ and $|E_h \Delta E| \to 0$. The continuity property stated in this proposition is not true for any sequence of sets locally converging in measure to E. Take indeed a decreasing sequence of indecomposable sets with measure always greater than θ that converges in measure and in perimeter to a set having two indecomposable components, one of them being of measure less than θ.

PROOF : If E_i is any indecomposable component of E with $|E_i| > \theta$, then by Theorem 2.5.7 there exists j such that $E_i \subset F_j$, with F_j indecomposable component of F. Since $|F_j| > \theta$ we conclude that $E_i \subset T_\theta F$, and since i is arbitrary the same is true for $T_\theta E$ and the first part of the proposition ensues.

Let $(E_{i,h})_{i \in I}$ be the ordered indecomposable components of E_h so that $P(E_h) = \sum_i P(E_{i,h})$. Since $P(E_h, \Omega) \to P(E, \Omega)$ we can assume without loss of generality that $\sup\{P(E_h),\ h \in \mathbb{N}\} < \infty$. By the compactness Theorem 2.5.3 and since (E_h) converges in measure to E, we obtain that $(E_{i,h})$ converges in measure to E_i for any $i \in I$ and $\{E_i\}_{i \in I}$ is a Caccioppoli partition of E. Moreover, since $E_h \uparrow E$, we deduce by Theorem 2.5.7 that $E_{i,h} \uparrow E_i$. In addition, by the lower semicontinuity of the perimeter,

$$(**) \qquad \sum_{i \in I} P(E_i, \Omega) \leq \sum_{i \in I} \liminf_{h \to \infty} P(E_{i,h}, \Omega) \leq \liminf_{h \to \infty} \sum_{i \in I} P(E_{i,h}, \Omega) \leq \liminf_{h \to \infty} P(E_h, \Omega)$$

Since $P(E_h, \Omega) \to P(E, \Omega)$ we deduce by the subadditivity of the perimeter that

$$\sum_i P(E_i, \Omega) = P(E, \Omega)$$

Let $i \in I$. By the monotonicity of T_θ we obtain that $T_\theta E_{i,h} \subset T_\theta E_{i,h'}$ whenever $h < h'$. Then, obviously, $|E_{i,h}| > \theta$ for some h implies that $|E_i| > \theta$. On the other hand, if $|E_i| > \theta$ for some i then by the continuity of the Lebesgue measure, it follows that $|E_{i,h}| > \theta$ as soon as h is large enough. Thus $(T_\theta E_h) \uparrow T_\theta E$. Finally, denoting $\{E_{j,h}\}_{j \in J}$ the indecomposable components of $T_\theta E_h$, $P(T_\theta E_h) \to P(T_\theta E)$ follows easily by replacing I by J in $(**)$ and noticing that $P(\cup_{j \in J} E_{j,h}, \Omega) \to P(\cup_{j \in J} E_j, \Omega)$. □

Now we want to extend T_θ to functions; to this aim, the following lemma will be useful.

Lemma 2.6.3 *For any monotone family of sets X_λ there exists a finite or countable set D such that*

$$\lim_{\mu \to \lambda} X_\mu = X_\lambda \qquad \forall \lambda \in \mathbb{R} \setminus D,$$

where convergence means convergence in measure.

PROOF : It is enough to notice that the map $\lambda \mapsto |X_\lambda|$ is monotone, thus has at most countably many discontinuity points, and to choose D as the set of those discontinuity points. We shall call D the set of discontinuity points of X_λ. □

Theorem 2.6.4
Let $u \in \mathrm{BV}(\Omega)$. Then, there exists a measurable function $u_{\mathrm{S}} : \Omega \to [-\infty, +\infty]$ (resp. $u_{\mathrm{I}} : \Omega \to [-\infty, +\infty]$) such that

$$\{u_{\mathrm{S}} \geq \lambda\} \sim T_\theta\{u \geq \lambda\} \qquad (\textit{resp. } \{u_{\mathrm{I}} \leq \lambda\} \sim T_\theta\{u \leq \lambda\})$$

with at most countably many exceptions. Any other measurable function v with the same property coincides with u_{S} (resp. u_{I}) almost everywhere in Ω.

PROOF : Let $X_\lambda = \{u \geq \lambda\}$. By the Coarea formula, for almost every $\lambda \in \mathbb{R}$, X_λ has finite perimeter in Ω and we can define $Y_\lambda := T_\theta X_\lambda$. Since $\lambda < \lambda'$ imply $X_\lambda \supset X'_\lambda$, we infer by Proposition 2.6.2 that (Y_λ) is decreasing. Let D be the set of discontinuity points of Y_λ, let $D' \subset \mathbb{R}$ countable and dense and define

$$u_{\mathrm{S}}(x) := \sup\{\lambda \in D' : \ x \in Y_\lambda\}.$$

We now prove that $\{u_{\mathrm{S}} \geq \lambda\} \sim Y_\lambda$ for any $\lambda \notin D$. In fact, we clearly have

$$Y_\eta \subset \{u_{\mathrm{S}} \geq \lambda\} \subset Y_\gamma$$

for any η, $\gamma \in D'$, $\eta > \lambda > \gamma$. If we choose sequences $\eta_h \downarrow \lambda$ and $\gamma_h \uparrow \lambda$ in D', Lemma 2.6.3 gives that Y_λ coincides with $\{u_{\mathrm{S}} \geq \lambda\}$ up to Lebesgue negligible sets. In particular, $\{u_{\mathrm{S}} \geq \lambda\}$ is measurable for any $\lambda \notin D$; by approximation the same is true for any real λ, hence u_{S} is measurable.

Finally, the uniqueness of u_{S} can be proved checking, by a similar argument, that for u_1, u_2 given, $\{u_1 \geq \lambda\} \sim \{u_2 \geq \lambda\}$ for a dense set of λ implies $u_1 = u_2$ almost everywhere in Ω.

The proof for u_{I} is analogous by remarking that the sets $X_\lambda = \{u \leq \lambda\}$, thus $Y_\lambda = T_\theta X_\lambda$, compose an increasing family and defining $u_{\mathrm{I}}(x) := \inf\{\lambda \in D' : \ x \in Y_\lambda\}$. □

From now, we shall denote by $\mathrm{S}_\theta u$ (resp. $\mathrm{I}_\theta u$) the function u_{S} (resp. u_{I}) of the previous theorem. Remark that $\{u \geq \lambda\} \sim \{-u \leq -\lambda\}$ thus

$$\begin{aligned} \{\mathrm{S}_\theta u \geq \lambda\} &\sim \{\mathrm{I}_\theta(-u) \leq -\lambda\} \\ &\sim \{-\mathrm{I}_\theta(-u) \geq \lambda\} \end{aligned}$$

Finally,

$$\mathrm{S}_\theta u = -\mathrm{I}_\theta(-u) \qquad \text{a.e. in } \Omega \tag{2.6.1}$$

In addition, since $T_\theta\{u \geq \lambda\} \subset \{u \geq \lambda\}$ and $T_\theta\{u \leq \lambda\} \subset \{u \leq \lambda\}$ we infer $\{\mathrm{S}_\theta u \geq \lambda\} \subset \{u \geq \lambda\}$ and $\{\mathrm{I}_\theta u \leq \lambda\} \subset \{u \leq \lambda\}$ for almost every λ, hence

$$\mathrm{S}_\theta u \leq u \leq \mathrm{I}_\theta u \qquad \text{a.e. in } \Omega \tag{2.6.2}$$

Remark 2.6.5 Recall that $\mathrm{I}_\theta\mathrm{S}_\theta$ and $\mathrm{S}_\theta\mathrm{I}_\theta$ can be seen as filters deriving from MFCN since the three of them tend to "erode" a BV function in the vicinity of its extrema. However, it can be easily checked with the counter-example given in Proposition 2.4.9 that these three operators are different.

Theorem 2.6.6 *Let $\theta \geq 0$. I_θ, S_θ, $\mathrm{I}_\theta\mathrm{S}_\theta$ and $\mathrm{S}_\theta\mathrm{I}_\theta$ are idempotent and monotone operators acting on* $\mathrm{BV}(\Omega)$. *Moreover, they are covariant with respect to any real continuous increasing contrast change and any affine mapping of $\mathbb{R}^{\mathrm{N}}$ onto itself preserving the Lebesgue measure.*

PROOF : The idempotence property of S_θ follows from the fact that if E is a set of finite perimeter and $\{E_i\}_{i\in I}$ its indecomposable components, then the indecomposable components of $T_\theta E$ are those sets E_j, $j \in J \subset I$ such that $|E_j| > \theta$. Thus $T_\theta(T_\theta E) \sim T_\theta E$. Therefore, if $u \in \mathrm{BV}(\Omega)$ then for almost every $\lambda \in \mathbb{R}$, $\{u \geq \lambda\}$ has finite perimeter and the argument above yields $T_\theta(T_\theta\{u \geq \lambda\}) \sim T_\theta\{u \geq \lambda\}$. By the uniqueness property

stated in Theorem 2.6.4 we deduce that $\mathrm{S}_\theta(\mathrm{S}_\theta u)$ and $\mathrm{S}_\theta u$ coincides almost everywhere in Ω. Relation (2.6.1) implies that I_θ is idempotent as well.

Now, from relation (2.6.2) we deduce that $\mathrm{S}_\theta u \leq \mathrm{I}_\theta \mathrm{S}_\theta u$ a.e. in Ω. Thus, using the definition of I_θ, for almost every $\lambda \in \mathbb{R}$ we get $\{\mathrm{I}_\theta \mathrm{S}_\theta u \geq \lambda\} \supset \{\mathrm{S}_\theta u \geq \lambda\}$. By definition of S_θ, $T_\theta\{S_\theta \geq \lambda\} \sim \{S_\theta \geq \lambda\}$ and by Proposition 2.6.2 and Theorem 2.5.7 every indecomposable component of $T_\theta\{\mathrm{I}_\theta \mathrm{S}_\theta u \geq \lambda\} \sim \{\mathrm{S}_\theta \mathrm{I}_\theta \mathrm{S}_\theta u \geq \lambda\}$ has Lebesgue measure greater than θ. Thus, $\mathrm{S}_\theta \mathrm{I}_\theta \mathrm{S}_\theta u = \mathrm{I}_\theta \mathrm{S}_\theta u$ almost everywhere in Ω. Since I_θ is idempotent, we deduce that $\mathrm{I}_\theta \mathrm{S}_\theta \mathrm{I}_\theta \mathrm{S}_\theta u = \mathrm{I}_\theta \mathrm{I}_\theta \mathrm{S}_\theta u = \mathrm{I}_\theta \mathrm{S}_\theta u$ a.e. in Ω thus $\mathrm{I}_\theta \mathrm{S}_\theta$ is idempotent. Same result holds for $\mathrm{S}_\theta \mathrm{I}_\theta$ since $\mathrm{I}_\theta \mathrm{S}_\theta(-u) = -\mathrm{S}_\theta \mathrm{I}_\theta u$ a.e. in Ω.

In the sequel of the proof we shall concentrate on the only operator S_θ since by relation (2.6.1) the results can be easily derived for I_θ, $\mathrm{S}_\theta \mathrm{I}_\theta$ and $\mathrm{I}_\theta \mathrm{S}_\theta$.

Let $u, v \in \mathrm{BV}(\Omega)$ such that $u \leq v$. Thus for almost every $\lambda \in \mathbb{R}$, $\{u \geq \lambda\} \subset \{v \geq \lambda\}$ and both sets have finite perimeter. Hence, by Proposition 2.6.2, $T_\theta\{u \geq \lambda\} \subset T_\theta\{v \geq \lambda\}$ for almost every λ so that $\mathrm{S}_\theta u \leq \mathrm{S}_\theta v$ almost everywhere in Ω and the monotonicity property ensues.

The covariance of S_θ with respect to any real continuous increasing contrast change is simply due to the fact that such a contrast change lets the level sets globally invariant. More precisely, if g is such a contrast change and $u \in \mathrm{BV}(\Omega)$ then for almost every $\lambda \in \mathbb{R}$, $\{g(u) \geq g(\lambda)\} = \{u \geq \lambda\}$ thus $T_\theta\{g(u) \geq g(\lambda)\} \sim T_\theta\{u \geq \lambda\}$ and, by definition, $\{\mathrm{S}_\theta g(u) \geq g(\lambda)\} \sim \{\mathrm{S}_\theta u \geq \lambda\}$. Thus $\{g^{-1}(\mathrm{S}_\theta g(u)) \geq \lambda\} \sim \{\mathrm{S}_\theta u \geq \lambda\}$ and we infer from the argument above related to the uniqueness of the representation by means of level sets that $\mathrm{S}_\theta g(u) = g(\mathrm{S}_\theta u)$ almost everywhere in Ω.

Denote by $\phi(x) = Ax + v$ where $A \in \mathrm{SL}(\mathbb{R}^\mathrm{N})$ and $v \in \mathbb{R}^\mathrm{N}$ an affine mapping of $\mathbb{R}^\mathrm{N}$ onto itself preserving the Lebesgue measure. Since both Lebesgue and Hausdorff measures are translation invariant, we just have to prove the property for the map $A : \mathbb{R}^\mathrm{N} \to \mathbb{R}^\mathrm{N}$. Let E be a set of finite perimeter in Ω and $\{E_i\}_{i \in I}$ its indecomposable components. From the lemma below, we deduce that $\{AE_i\}_{i \in I}$ is a Caccioppoli partition of AE into its indecomposable components. Moreover, $|AE_i| = |E_i|$ so that $T_\theta AE = AT_\theta E$. The conclusion follows for S_θ by using like above the decomposition of a function u of bounded variation into its upper level sets of finite perimeter. □

Lemma 2.6.7 *Let $A \in \mathrm{SL}(\mathbb{R}^\mathrm{N})$ and E a set of finite perimeter in Ω. If $\{E_i\}_{i \in I}$ is a Caccioppoli partition of E into its indecomposable components, then $\{AE_i\}_{i \in I}$ is a Caccioppoli partition of AE into its indecomposable components.*

PROOF : First remark that A is one-to-one so that $E = \cup_{i \in I} E_i$ implies that $AE = \cup_{i \in I} AE_i$ and the union is disjoint. In addition, by Theorem 3.16 and Remark 3.17 in [3] we infer that

$$D_\ell(A_\# \chi_{E_i}) = \sum_{k=1}^{N} (C_{\nabla A})_{k\ell} A_\#(D_k \chi_{E_i}), \qquad \forall \ell = 1, \ldots, N$$

where $A_{\#}u(x)$ denotes $u(A^{-1}(x))$ and $C_{\nabla A}$ is the matrix of cofactors of ∇A. Since $D\chi_{E_i}$ is supported by $E_i^{1/2}$ we deduce that for every Borel set $S \subset \mathbb{R}^N \setminus A(E_i^{1/2})$ and every $\ell \in [1, N]$, $D_\ell(A_{\#}\chi_{E_i})(S) = 0$. In addition, $A_{\#}\chi_{E_i}(x) = \chi_{E_i}(A^{-1}(x)) = \chi_{AE_i}(x)$ for every $x \in A\Omega$ and we can conclude that $(AE_i)^{1/2} \subset A(E_i^{1/2})$ up to $\mathcal{H}^{N-1}$-negligible sets. Applying the same formula with A^{-1} instead of A and AE_i instead of E_i yields the converse inclusion so that

$$(AE_i)^{1/2} = A(E_i^{1/2}) \tag{2.6.3}$$

up to $\mathcal{H}^{N-1}$-negligible sets. Now, assume that AE_i is decomposable into two disjoint sets F and G such that $|F|.|G| > 0$ and $P(AE_i, A\Omega) = P(F, A\Omega) + P(G, A\Omega)$, thus by Lemma 2.5.6, $\mathcal{H}^{N-1}(A\Omega \cap F^{1/2} \cap G^{1/2}) = 0$. Then, $E_i = A^{-1}F \cup A^{-1}G$ with $A^{-1}F$ and $A^{-1}G$ disjoint and $|A^{-1}F|.|A^{-1}G| > 0$. Moreover, we infer from the relation (2.6.3) above and from the properties of Hausdorff measures (see [3], p. 82) that

$$\begin{aligned} \mathcal{H}^{N-1}(\Omega \cap (A^{-1}F)^{1/2} \cap (A^{-1}G)^{1/2}) &= \mathcal{H}^{N-1}(A^{-1}(A\Omega \cap F^{1/2} \cap G^{1/2})) \\ &\leq [\mathrm{Lip}(A^{-1})]^{N-1}\mathcal{H}^{N-1}(A\Omega \cap F^{1/2} \cap G^{1/2})) \end{aligned}$$

Thus $\mathcal{H}^{N-1}(\Omega \cap (A^{-1}F)^{1/2} \cap (A^{-1}G)^{1/2}) = 0$ and this is contradictory since by Lemma 2.5.6 it would imply that E_i is decomposable. Hence, AE_i is an indecomposable set $\forall i \in I$. Now let $i, j \in I$ and $i \neq j$. Then, like above,

$$\begin{aligned} \mathcal{H}^{N-1}(A\Omega \cap (AE_i)^{1/2} \cap (AE_j)^{1/2}) &= \mathcal{H}^{N-1}(A(\Omega \cap E_i^{1/2} \cap E_j^{1/2})) \\ &\leq [\mathrm{Lip}(A)]^{N-1}\mathcal{H}^{N-1}(\Omega \cap E_i^{1/2} \cap E_j^{1/2}) \end{aligned}$$

and we deduce from Lemma 2.5.6 that $\mathcal{H}^{N-1}((AE_i)^{1/2} \cap (AE_j)^{1/2}) = 0$ whenever $i \neq j$, hence $\sum_{i\in I} P(AE_i) = P(AE)$ and $\{AE_i\}_{i\in I}$ is the Caccioppoli partition of AE into its indecomposable components. □

Theorem 2.6.8 *Let $u \in \mathrm{BV}(\Omega)$ and $\theta \geq 0$. Then $\mathrm{I}_\theta u, \mathrm{S}_\theta u \in \mathrm{BV}(\Omega)$. In addition*

$$\begin{aligned} & |D\mathrm{I}_\theta u|(\Omega) \leq |Du|(\Omega) \\ \textit{and} \quad & |D\mathrm{S}_\theta u|(\Omega) \leq |Du|(\Omega) \end{aligned}$$

PROOF : Once again the proofs for I_θ and S_θ are analogous. From the coarea formula, $\{u \geq \lambda\}$ is a set of finite perimeter for almost every $\lambda \in \mathbb{R}$. Thus, using the decomposition of $\{u \geq \lambda\}$ into indecomposable sets $(E_i)_{i\in I}$ and the fact that $\{\mathrm{S}_\theta u \geq \lambda\} \sim T_\theta\{u \geq \lambda\} = \bigcup_{j\in J\subset I} E_j$ with $E_j| > \theta$, we infer that $P(\{\mathrm{S}_\theta u \geq \lambda\}, \Omega) = \sum_{j\in J} P(E_j, \Omega) \leq \sum_{i\in I} P(E_i, \Omega)$ and thus $P(\{\mathrm{S}_\theta u \geq \lambda\}, \Omega) \leq P(\{u \geq \lambda, \Omega)$. Therefore

$$\int_{-\infty}^{+\infty} P(\{\mathrm{S}_\theta u \geq \lambda\}, \Omega)\, d\lambda \leq \int_{-\infty}^{+\infty} P(\{u \geq \lambda\}, \Omega)\, d\lambda$$

so that

$$|D\mathrm{S}_\theta u|(\Omega) \leq |Du|(\Omega)$$

and $\mathrm{S}_\theta u \in \mathrm{BV}(\Omega)$. □

It must be emphasized that I_θ and S_θ may increase the L^1 norm if for instance and respectively u has a negative or a positive part. However, if u is nonnegative then remark that for almost every λ, $T_\theta\{u \geq \lambda\} \subset \{u \geq \lambda\}$ so that

$$\begin{aligned}\int_\Omega |\mathrm{S}_\theta u| dx &= \int_0^{+\infty} |\{\mathrm{S}_\theta u \geq \lambda\}|\, d\lambda \\ &= \int_0^{+\infty} |T_\theta\{u \geq \lambda\}|\, d\lambda \\ &\leq \int_0^{+\infty} |\{u \geq \lambda\}|\, d\lambda \\ &\leq \int_\Omega |u| dx\end{aligned}$$

thus $\|\mathrm{S}_\theta u\|_{\mathrm{L}^1(\Omega)} \leq \|u\|_{\mathrm{L}^1(\Omega)}$. Analogously, if u is nonpositive then we get

$$\int_\Omega |\mathrm{I}_\theta u| dx = \int_{-\infty}^0 |\{\mathrm{I}_\theta u \leq \lambda\}|\, d\lambda \leq \int_{-\infty}^0 |\{u \leq \lambda\}|\, d\lambda \leq \int_\Omega |u| dx$$

thus $\|\mathrm{I}_\theta u\|_{\mathrm{L}^1(\Omega)} \leq \|u\|_{\mathrm{L}^1(\Omega)}$.

Theorem 2.6.9 *Let $u \in \mathrm{BV}(\Omega)$ and $(u_h) \subset \mathrm{BV}(\Omega)$ a sequence of nonnegative functions satisfying*

$$u_h \uparrow u \quad \text{a.e.}, \qquad \lim_{h\to\infty} |Du_h|(\Omega) = |Du|(\Omega).$$

Then there exists a subsequence such that $\mathrm{S}_\theta u_h \underset{\mathrm{L}^1(\Omega)}{\longrightarrow} \mathrm{S}_\theta u$ and $|D\mathrm{S}_\theta u_h|(\Omega) \to |D\mathrm{S}_\theta u|(\Omega)$.

If $v \in \mathrm{BV}(\Omega)$ and $(v_h) \subset \mathrm{BV}(\Omega)$ is a sequence of nonnegative functions satisfying

$$v_h \downarrow v \quad \text{a.e.}, \qquad \lim_{h\to\infty} |Dv_h|(\Omega) = |Dv|(\Omega),$$

then there exists a subsequence such that $\mathrm{I}_\theta v_h \underset{\mathrm{L}^1(\Omega)}{\longrightarrow} \mathrm{I}_\theta v$ and $|D\mathrm{I}_\theta v_h|(\Omega) \to |D\mathrm{I}_\theta v|(\Omega)$.

PROOF : By the Monotone Convergence Theorem, $u_h \to u$ in $\mathrm{L}^1(\Omega)$. This fact, together with the monotonicity of (u_h), yields that, for some subsequence, $\{u_h \geq t\} \uparrow \{u \geq t\}$ in measure for a.e. $t \in \mathbb{R}$, . Now, the Coarea formula implies that for a.e. $t \in \mathbb{R}$, $\{u_h \geq t\}$, $h \in \mathbb{N}$ and $\{u \geq t\}$ have finite perimeter, and we deduce from the lower semicontinuity of perimeter that $P(\{u \geq t\}) \leq \liminf_{h\to\infty} P(\{u_h \geq t\})$ for a.e. $t \in \mathbb{R}$, . Since, in addition, $\int_{-\infty}^{+\infty} P(\{u_h \geq t\})dt \to \int_{-\infty}^{+\infty} P(\{u \geq t\})dt$, we deduce from Lemma 2.6.10 below, which is a variant of the Dominated Convergence Theorem, that $P(\{u_h \geq t\}) \to P(\{u \geq t\})$ in $\mathrm{L}^1(\mathbb{R})$ and, therefore, a subsequence is converging to $P(\{u \geq t\})$ almost everywhere in $\mathbb{R}$. Recalling that $\{u_h \geq t\} \uparrow \{u \geq t\}$ in measure, we apply Proposition 2.6.2 to get that for

a.e. $t \in \mathbb{R}$, $\{S_\theta u_h \geq t\} \uparrow \{S_\theta u \geq t\}$ in measure – thus $\int_\Omega |\chi_{\{S_\theta u_h \geq t\}} - \chi_{\{S_\theta u \geq t\}}| dx \to 0$ and $\chi_{\{S_\theta u_h \geq t\}} \leq \chi_{\{S_\theta u \geq t\}}$ a.e. in Ω – and $\lim_{h\to\infty} P(\{S_\theta u_h \geq t\}) = P(\{S_\theta u \geq t\})$.

Remark now that $|\chi_{\{S_\theta u_h \geq t\}} - \chi_{\{S_\theta u \geq t\}}| \leq \chi_{\{S_\theta u \geq t\}}$ and $\int_0^{+\infty} \int_\Omega \chi_{\{S_\theta u \geq t\}} dx\, dt = \int_\Omega |S_\theta u| < +\infty$ since $S_\theta u \in L^1(\Omega)$. We deduce from the Dominated Convergence Theorem that $\int_0^{+\infty} \int_\Omega |\chi_{\{S_\theta u_h \geq t\}} - \chi_{\{S_\theta u \geq t\}}| dx\, dt \to 0$, thus $S_\theta u_h \to S_\theta u$ in $L^1(\Omega)$.

Now, since $P(\{S_\theta u_h \geq t\}) \leq P(\{u_h \geq t\})$, $P(\{S_\theta u_h \geq t\}) \to P(\{S_\theta u \geq t\})$ a.e., $P(\{u_h \geq t\}) \to P(\{u \geq t\})$ a.e. and $\int_{-\infty}^{+\infty} P(\{u_h \geq t\}) dt \to \int_{-\infty}^{+\infty} P(\{u \geq t\}) dt$, we deduce from a well-known variant of the Dominated Convergence Theorem (see for instance [13]) that $\int_{-\infty}^{+\infty} P(\{S_\theta u_h \geq t\}) dt \to \int_{-\infty}^{+\infty} P(\{S_\theta u \geq t\}) dt$ and the first part of the theorem ensues.

Notice that our result for I_θ is stated in the case where the functions are nonnegative. However, the result obtained for S_θ implies a similar result for I_θ only when (v_h) are nonpositive since $(v_h) \downarrow v$ implies $(-v_h) \uparrow -v$, $D(-v_h) = -Dv_h$ and $I_\theta v_h = -S_\theta(-v_h)$. In order to prove the result when the functions (v_h) are nonnegative, and this is the interesting case when dealing with images, remark that $\{v \leq \lambda\} = \Omega \setminus \{v > \lambda\}$. Assuming that $v_h \downarrow v$ a.e. and $\lim_{h\to\infty} |Dv_h|(\Omega) = |Dv|(\Omega)$ we obtain, possibly passing to some subsequence, that $\{v_h \leq t\} \uparrow \{v \leq t\}$ in measure for a.e. $t \in \mathbb{R}$ and, with the same argument as above, $\int_\Omega |\chi_{\{I_\theta v_h \leq t\}} - \chi_{\{I_\theta v \leq t\}}| dx \to 0$, $\chi_{\{I_\theta v_h \leq t\}} \leq \chi_{\{I_\theta v \leq t\}}$ a.e. in Ω and $\int_{-\infty}^{+\infty} P(\{I_\theta v_h \leq t\}) dt \to \int_{-\infty}^{+\infty} P(\{I_\theta v \leq t\}) dt$. The conclusion concerning the total variation is a direct consequence of the Coarea formula. Moreover, remark that $|\chi_{\{I_\theta v_h \leq t\}} - \chi_{\{I_\theta v \leq t\}}| = |\chi_{\{I_\theta v_h > t\}} - \chi_{\{I_\theta v > t\}}| \leq \chi_{\{I_\theta v_h > t\}} \leq \chi_{\{I_\theta v_0 > t\}}$ and $\int_0^{+\infty} \int_\Omega \chi_{\{I_\theta v_0 > t\}} dx\, dt < +\infty$ since $I_\theta v_0 \in L^1(\mathbb{R})$. The conclusion follows by the Dominated Convergence Theorem. □

Lemma 2.6.10 *Let $(f_h) \subset L^1(\mathbb{R})$ and $f \in L^1(\mathbb{R})$ be nonnegative functions satisfying*

$$\liminf_{h\to\infty} f_h(t) \geq f(t) \quad \text{a.e.}, \qquad \limsup_{h\to\infty} \int_{\mathbb{R}} f_h(t)\, dt \leq \int_{\mathbb{R}} f(t)\, dt.$$

Then $f_h \to f$ in $L^1(\mathbb{R})$.

PROOF : Let $g_h := \inf_{k\geq h} f_k$ and notice that $\sup_h g_h = \liminf_{h\to\infty} f_h \geq f$ and

$$\int_{\mathbb{R}} g_h(t)\, dt \leq \int_{\mathbb{R}} \liminf_{h\to\infty} f_h(t)\, dt \leq \liminf_{h\to\infty} \int_{\mathbb{R}} f_h(t)\, dt \leq \int_{\mathbb{R}} f(t)\, dt$$

Hence,

$$\int_{\mathbb{R}} f(t) dt \leq \int_{\mathbb{R}} \sup_h g_h(t)\, dt \leq \int_{\mathbb{R}} \lim_{h\to\infty} g_h(t)\, dt \leq \lim_{h\to\infty} \int_{\mathbb{R}} g_h(t)\, dt \leq \int_{\mathbb{R}} f(t)\, dt.$$

Therefore, $\sup_h g_h = f$ a.e. and, by the Dominated Convergence Theorem, $g_h \to f$ in L^1. Since $(f - f_h)^+ \leq (f - g_h)^+$ we conclude that $(f - f_h)^+$ tends to 0 in L^1. Finally, since

$$(f - f_h)^- = (f - f_h)^+ - (f - f_h)$$

we get that

$$\limsup_{h\to\infty} \int_{\mathbb{R}} (f-f_h)^-(t)\,dt \leq \limsup_{h\to\infty} \int_{\mathbb{R}} (f_h-f)(t)\,dt \leq 0$$

so that $(f-f_h)^- \to 0$ in L^1 and the conclusion follows. □

The reader may find in Section 2.7.3 experimental results related to Vincent's filters, jointly presented with results related to the grain filter of the next section.

A drawback of the filters $\mathrm{I}_\theta\mathrm{S}_\theta$ or $\mathrm{S}_\theta\mathrm{I}_\theta$ is that they do not process simultaneously the minima and the maxima of a function. Moreover, I_θ and S_θ do not commute in general as illustrated in figure 2.16 where the radii of the circles can be chosen such that the results shown in the figure are obtained for some value of θ. Remark in addition that the commutation property still does not hold when the sets $\{u < \lambda\}$ are used for the definition of I_θ instead of $\{u \leq \lambda\}$. In the next section we shall propose a filter, the grain filter, which removes only the small grains in an image. Roughly speaking and in view of figure 2.16, grains are those sets without holes whose boundary is a level line. This approach shall allow us to preserve the oscillations and is in a sense more naturally related to the topographic map. However, we shall see that due to the structure of a topographic map, it is not possible in general to deal indifferently with lower or upper level sets of a BV function, unless this function is highly differentiable.

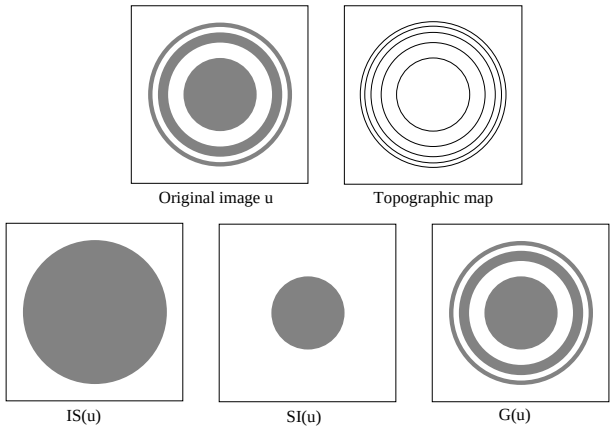

Figure 2.16: An image and its topographic map. I_θ and S_θ do not commute and remove the oscillations. In contrast, oscillations are preserved with the grain filter.

2.7 Grain filter

2.7.1 The "filling" operator

The operator that we are now going to define and study associates with any indecomposable set A the set, that we shall call grain, obtained by "filling the holes of A".

For the sake of simplicity, Ω shall denote in the sequel an open bounded ball in $\mathbb{R}^{\mathrm{N}}$.

Let $E \subset \Omega$ be a set of finite perimeter in Ω such that

$$E \subset\subset \Omega \quad \text{or} \quad \Omega \setminus E \subset\subset \Omega \tag{2.7.1}$$

The strict inclusion must be here understood in the following way : if A is a set of finite perimeter in Ω we say that $A \subset\subset \Omega$ if there exists some $\epsilon > 0$ such that $d(x, \mathbb{R}^N \setminus \Omega) \geq \epsilon$ for almost every $x \in A$. Let $\{E_i\}_{i \in I}$ denote the indecomposable components of E. Then, obviously, $E \subset\subset \Omega$ implies that $\forall i \in I$, $E_i \subset\subset \Omega$. Define $F_i = \Omega \setminus E_i$ and remark that $P(F_i, \Omega) = P(E_i, \Omega) < \infty$ and F_i has finite measure. Thus F_i can be partitioned into its indecomposable components $\{F_{i,j}\}_{j \in J}$ and we denote $F_{i,0}$ as the (unique) component satisfying $\partial\Omega \subset F_{i,0}^{1/2}$. The uniqueness of $F_{i,0}$ follows from the assumption $E \subset\subset \Omega$ and Lemma 2.5.6. Remark that $\forall j \in J \setminus \{0\}$ $F_{i,j} \subset\subset \Omega$, thus $\mathcal{H}^{N-1}(\partial\Omega \cap F_{i,j}^{1/2}) = 0$ up to $\mathcal{H}^{N-1}$-negligible sets. In view of the notations above we define

$$H_i := J \setminus \{0\} \quad \text{whenever } E_i \subset\subset \Omega$$

as the set of indexes associated to the "holes" enclosed by E_i. Assume now that $\Omega \setminus E \subset\subset \Omega$. With the same argument as above we infer that there exists a unique component E_i of E that is not strictly contained in Ω and such that $\partial\Omega \subset E_i^{1/2}$. Obviously $F_i = \Omega \setminus E_i \subset\subset \Omega$ and in view of the notations above we define

$$H_i := J \quad \text{whenever } \Omega \setminus E_i \subset\subset \Omega$$

Then we define the "filled set" associated with E_i with respect to Ω as

$$\tilde{E}_i := E_i \cup \bigcup_{j \in H_i} F_{i,j} \tag{2.7.2}$$

We deduce easily from the definition that $\Omega \setminus E_i \subset\subset \Omega$ implies $\tilde{E}_i = \Omega$ up to Lebesgue negligible sets thus $P(\tilde{E}_i, \Omega) = 0 \leq P(E_i, \Omega)$. If $E_i \subset\subset \Omega$ then $\tilde{E}_i = \Omega \setminus F_{i,0}$. Since $\Omega \setminus E_i = F_{i,0} \cup \bigcup_{j \in H_i} F_{i,j}$ we infer that $P(\tilde{E}_i, \Omega) = P(\Omega \setminus F_{i,0}, \Omega) = P(F_{i,0}, \Omega) = P(E_i, \Omega) - \sum_{j \in H_i} P(F_{i,j}, \Omega)$ thus $P(\tilde{E}_i, \Omega) \leq P(E_i, \Omega)$. This can be also proved by first remarking that $\Omega \cap \tilde{E}_i^{1/2} = \Omega \cap F_{i,0}^{1/2}$ and $\Omega \cap E_i^{1/2} = \Omega \cap F^{1/2}$ up to $\mathcal{H}^{N-1}$-negligible sets. Now, with the same argument as in the proof of Lemma 2.5.6, we get

$$\Omega \cap F_{i,j}^{1/2} \subset \Omega \cap F^{1/2} \quad \forall j \in J \tag{2.7.3}$$

and in particular $\Omega \cap F_{i,0}^{1/2} \subset \Omega \cap F^{1/2}$ which yields

$$\Omega \cap \tilde{E}_i^{1/2} \subset \Omega \cap E_i^{1/2} \tag{2.7.4}$$

thus $P(\tilde{E}_i, \Omega) \leq P(E_i, \Omega)$. In contrast, $|\tilde{E}_i| \geq |E_i|$. Finally, the "filled set" associated with E with respect to Ω is defined as

$$\tilde{E} := \bigcup_{i \in I} \tilde{E}_i$$

It is easily seen from the definitions that $\Omega \setminus E \subset\subset \Omega$ implies $\tilde{E} = \Omega$ up to Lebesgue negligible sets.

Lemma 2.7.1 *Let E, F be two indecomposable sets. Then $\Omega \cap E^{1/2} \subset \Omega \cap F^{1/2}$ implies that $E \cup F$ is an indecomposable set.*

PROOF : Assume that $E \cup F$ is decomposable, thus there exists a partition of $E \cup F$ into two disjoint sets G and H such that $|G|.|H| > 0$ and $P(E \cup F) = P(G) + P(H)$. Since E and F are indecomposable we obtain by Theorem 2.5.7 that each or them is either a subset of G or H. Since both of them cannot be contained in the same set, we can assume that for instance $E \subset G$ and $F \subset H$. Thus, by Theorem 2.2.9, $\Omega \cap E^{1/2} \subset \Omega \cap (G^1 \cup G^{1/2})$ and $\Omega \cap F^{1/2} \subset \Omega \cap (H^1 \cup H^{1/2})$. Hence, since G and H are disjoint,

$$\Omega \cap E^{1/2} \cap F^{1/2} \subset \Omega \cap G^{1/2} \cap H^{1/2}$$

By Lemma 2.5.6, $\mathcal{H}^{N-1}(\Omega \cap G^{1/2} \cap H^{1/2}) = 0$ thus $\mathcal{H}^{N-1}(\Omega \cap E^{1/2} \cap F^{1/2}) = 0$ and we get a contradiction since $\Omega \cap E^{1/2} \subset \Omega \cap F^{1/2}$ and $\mathcal{H}^{N-1}(\Omega \cap E^{1/2}) = P(E, \Omega) > 0$. □

Proposition 2.7.2 *Let E be a set of finite perimeter in Ω satisfying (2.7.1) and $\{E_i\}_{i\in I}$ the Caccioppoli partition of E into its indecomposable components. Then :*

- *$\forall i \in I$, $\tilde{E}_i$ is an indecomposable set.*
- *there exists $J \subset I$ such that $\{\tilde{E}_j\}_{j\in J}$ is a Caccioppoli partition of $\tilde{E}$ into its indecomposable components.*
- *$P(\tilde{E}, \Omega) \leq P(E, \Omega)$.*

PROOF : 1) Let $i \in I$. Assume that $E_i \subset\subset \Omega$ otherwise $\tilde{E}_i = \Omega$ up to Lebesgue negligible sets and the result is trivial since Ω is clearly an indecomposable set. Since $E_i \subset\subset \Omega$, using (2.7.3) and $\Omega \cap F^{1/2} = \Omega \cap E_i^{1/2}$ with the same notations as above, we obtain that

$$\Omega \cap F_{i,j}^{1/2} \subset \Omega \cap E_i^{1/2} \quad \forall j \in J \tag{2.7.5}$$

Let $j \in H_i$. Since $F_{i,j}$ and E_i are indecomposable sets, we deduce by the previous lemma that $E_i \cup F_{i,j}$ is indecomposable. Now, E_i and $F_{i,j}$ are disjoint and we remark that, given $r > 0$ and $x \in \Omega$

$$\begin{aligned} |B(x,r) \cap (E_i \cup F_{i,j})| &= |B(x,r) \cap E_i| + |B(x,r) \cap F_{i,j}| - |B(x,r) \cap E_i \cap F_{i,j}| \\ &= |B(x,r) \cap E_i| + |B(x,r) \cap F_{i,j}| \end{aligned}$$

Since $\Omega \cap F_{i,j}^{1/2} \subset \Omega \cap E_i^{1/2}$ we infer that

$$\Omega \cap (E_i \cup F_{i,j})^{1/2} = \Omega \cap (E_i^{1/2} \setminus F_{i,j}^{1/2}) \tag{2.7.6}$$

up to $\mathcal{H}^{N-1}$-negligible sets. Let $j' \neq j \in H_i$. By Lemma 2.5.6, $\mathcal{H}^{N-1}(\Omega \cap F_{i,j}^{1/2} \cap F_{i,j'}^{1/2}) = 0$ and by (2.7.3) $\Omega \cap F_{i,j'}^{1/2} \subset \Omega \cap E_i^{1/2}$. Hence, using (2.7.6), we get that

$$\Omega \cap F_{i,j'}^{1/2} \subset \Omega \cap (E_i \cup F_{i,j})^{1/2}$$

up to $\mathcal{H}^{N-1}$-negligible sets. A new call to Lemma 2.7.1 yields that $(E_i \cup F_{i,j} \cup F_{i,j'})$ is indecomposable. The same argument can be used for any $j \in H_i$ and we finally obtain that $\tilde{E}_i = E_i \cup \bigcup_{j\in H_i} F_{i,j}$ is an indecomposable set.

2) If $\Omega \setminus E \subset\subset \Omega$ then recall that there exists a unique component E_0 of E such that $\partial\Omega \subset E_0^{1/2}$ and $\tilde{E}_0 = \Omega$ up to Lebesgue negligible sets. In addition, $\forall i \in I$, $\tilde{E}_i \subset \tilde{E}_0$ and the second statement of the proposition ensues by simply setting $J := \{0\}$. Assume now that $E \subset\subset \Omega$, hence $\forall i \in I$, $E_i \subset\subset \Omega$. Let $i, j \in I$, $i \neq j$. We shall prove that either $\tilde{E}_i \subset \tilde{E}_j$, or $\tilde{E}_i \supset \tilde{E}_j$ or $\tilde{E}_i \cap \tilde{E}_j = \emptyset$ up to Lebesgue negligible sets. Since the E_i's are disjoint, we first have that $E_i \subset F_j = \Omega \setminus E_j$ and $E_j \subset F_i = \Omega \setminus E_i$. Then, because E_i and E_j are indecomposable sets, we deduce by Theorem 2.5.7 that there exists a unique component $F_{j,k}$ of F_j such that $E_i \subset F_{j,k}$ and a unique component $F_{i,\ell}$ of F_i such that $E_j \subset F_{i,\ell}$ up to Lebesgue negligible sets. Then, three cases arise : if $F_{j,k} = F_{j,0}$

and $F_{i,\ell} = F_{i,0}$ with the same notations as above, it is easily seen that $\tilde{E}_i \cap \tilde{E}_j = \emptyset$. If $F_{i,\ell} \neq F_{i,0}$ then $\tilde{E}_j \subset \tilde{E}_i$. Finally, $F_{j,k} \neq F_{j,0}$ implies $\tilde{E}_i \subset \tilde{E}_j$. Remark that we cannot have simultaneously $F_{i,\ell} \neq F_{i,0}$ and $F_{j,k} \neq F_{j,0}$ because $F_{i,\ell} \neq F_{i,0}$ and $E_j \subset F_{i,\ell}$ imply that $E_i \subset F_{j,0}$ thus $F_{j,k} = F_{j,0}$ up to Lebesgue negligible sets.

Now, let J be the subset of I such that $\forall i \in I$, $\exists j \in J$ such that $\tilde{E}_i \subset \tilde{E}_j$ and $\tilde{E}_j \cap \tilde{E}_k = \emptyset$, whenever $j, k \in J$, $j \neq k$. From above, such a set exists and $\{\tilde{E}_j\}_{j\in J}$ is a Caccioppoli partition of $\tilde{E}$ into indecomposable sets.

3) We shall now prove that this partition is actually a partition of $\tilde{E}$ into its indecomposable components. Recall that for every $i \in I$, $\Omega \cap \tilde{E}_i^{1/2} \subset \Omega \cap E_i^{1/2}$. Using Lemma 2.5.6, we get that

$$\mathcal{H}^{\mathrm{N}-1}(\Omega \cap E_i^{1/2} \cap E_j^{1/2}) = 0, \quad \text{whenever } i \neq j,\ i, j \in I$$

Hence,

$$\mathcal{H}^{\mathrm{N}-1}(\Omega \cap \tilde{E}_i^{1/2} \cap \tilde{E}_j^{1/2}) = 0, \quad \text{whenever } i \neq j,\ i, j \in J$$

By (2.7.4), $\sum_{j\in J} P(\tilde{E}_j, \Omega) \leq \sum_{j\in J} P(E_j, \Omega) < +\infty$ and a new call to Lemma 2.5.6 yields that the sets $\tilde{E}_j$, $j \in J$ are the indecomposable components of $\tilde{E}$.

4) If $\Omega \setminus E \subset\subset \Omega$ then $\tilde{E} = \Omega$ up to Lebesgue negligible sets thus $P(\tilde{E}, \Omega) = 0$ and the third statement ensues. Assume now that $E \subset\subset \Omega$. Since $P(\tilde{E}, \Omega) = \sum_{j\in J} P(\tilde{E}_j, \Omega) \leq \sum_{j\in J} P(E_j, \Omega) \leq \sum_{i\in I} P(E_i, \Omega)$ we finally get that

$$P(\tilde{E}, \Omega) \leq P(E, \Omega)$$

□

Proposition 2.7.3 *If E is a set of finite perimeter in Ω satisfying (2.7.1) then $\tilde{\tilde{E}} = \tilde{E}$.*

PROOF : In view of the previous proposition, it is enough to prove that if E_i is some indecomposable component of E, then $\tilde{\tilde{E}}_i = \tilde{E}_i$. The result is obvious if $\tilde{E}_i = \Omega$ up to Lebesgue negligible sets thus we assume that $E_i \subset\subset \Omega$. Recall from the definition of the "filling" operation that $\tilde{E}_i = \Omega \setminus F_{i,0}$ where $F_{i,0}$ is an indecomposable component of $\Omega \setminus E_i$. Since $\Omega \setminus \tilde{E}_i = F_{i,0}$ is indecomposable and recalling that $\partial\Omega \subset F_{i,0}^{1/2}$ we get that $\tilde{\tilde{E}}_i = \Omega \setminus F_{i,0} = \tilde{E}_i$ up to Lebesgue negligible sets, and the proposition ensues. □

Proposition 2.7.4 *Let $E \subset E'$ be two sets of finite perimeter in Ω satisfying (2.7.1). Then $\tilde{E} \subset \tilde{E}'$. Moreover, if $E \subset\subset \Omega$, $E_h \uparrow E$ and $P(E_h, \Omega) \to P(E, \Omega)$, then $\tilde{E}_h \uparrow \tilde{E}$ and $P(\tilde{E}_h, \Omega) \to P(\tilde{E}, \Omega)$, where convergence of sets means convergence in measure.*

PROOF : The monotonicity is obvious if $\Omega \setminus E' \subset\subset \Omega$ since $\tilde{E}' = \Omega$. Assume now that $E \subset E' \subset\subset \Omega$. Let $\{E_i\}_{i\in I}$ and $\{E'_j\}_{j\in J}$ be respectively the Caccioppoli partitions of E and E' into indecomposable components. From Theorem 2.5.7 we infer that $\forall i \in I$,

$\exists j \in J$ such that $E_i \subset E'_j$. Thus, $F'_j = \Omega \setminus E'_j \subset F'_i = \Omega \setminus E_i$. In particular, by a new call to Theorem 2.5.7, $F'_{j,0} \subset F_{i,0}$, hence $\tilde{E}_i \subset \tilde{E}'_j \subset \tilde{E}$ and the result ensues since i is arbitrary and $\tilde{E} = \bigcup_{i\in I} \tilde{E}_i$.

Let $E_h \uparrow E$ and $P(E_h, \Omega) \to P(E, \Omega)$. Obviously, $E_h \subset\subset \Omega$ for every $h \in \mathbb{N}$. Let $\{E_{i,h}\}_{i\in I}$ be the ordered indecomposable components of E_h. With the same argument as in the proof of Proposition 2.6.2 and in view of compactness Theorem 2.5.3 we get that for every $i \in I$, $E_{i,h} \uparrow E_i$ and $P(E_{i,h}, \Omega) \to P(E_h, \Omega)$. In addition, since $E_{i,h} \subset E_i$ and $E_{i,h}$ is an indecomposable set, it follows that E_i is an indecomposable set. Then, denoting $F_{i,h} = \Omega \setminus E_{i,h}$ it is easily seen that $F_{i,h} \downarrow F_i$ and $P(F_{i,h}, \Omega) \to P(F_i, \Omega)$. If $\{F^j_{i,h}\}_{j\in J}$ are the ordered indecomposable components of $F_{i,h}$ we obtain with the same argument as above that $F^j_{i,h} \to F^j_i$ and $P(F^j_{i,h}, \Omega) \downarrow P(F^j_i, \Omega)$. Finally, if $F^k_{i,h}$ is the only component such that $\partial\Omega \subset (F^k_{i,h})^{1/2}$ we get in particular and because E_i is indecomposable that $F^k_{i,h} \downarrow F^k_i$, $P(F^k_{i,h}, \Omega) \to P(F^k_i, \Omega)$ and F^k_i is the only component of F_i such that $\partial\Omega \subset (F^k_i)^{1/2}$. Consequently, $\tilde{E}_{i,h} = \Omega \setminus F^k_{i,h} \uparrow \tilde{E}_i = \Omega \setminus F^k_i$ and $P(\tilde{E}_{i,h}, \Omega) \to P(\tilde{E}_i, \Omega)$. Since the convergence holds for any $i \in I$, the final result ensues by a simple application of Proposition 2.7.2. □

Remark 2.7.5 The "filling" operator is not continuous in general as illustrated in figure 2.17 where the sets E_h in gray converge to the set E with four indecomposable components. Obviously $\tilde{E}_h$ contains the central part whereas $\tilde{E} = E$ does not.

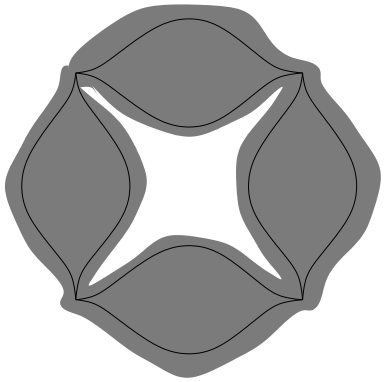

Figure 2.17: The "filling" operator is not continuous with respect to the strict convergence of a decreasing sequence of sets like the gray one in the figure, to the set composed of four indecomposable components

Proposition 2.7.6 *Let $\Omega_{\mathrm{E}} \subset \mathbb{R}^{\mathrm{N}}$ be an open bounded ball such that $\Omega \subset\subset \Omega_{\mathrm{E}}$. If $E \subset \Omega$ is a set of finite perimeter in Ω and $\{E_i\}_{i\in I}$ the partition of E into its indecomposable components, then $\forall i \in I$*

$$\partial\Omega \cap E_i^{1/2} = \partial\Omega \cap \tilde{E}_i^{1/2}$$

where the "filling" operation must be understood here with respect to Ω_{E}. Moreover,

$$P(\tilde{E}, \Omega) \leq P(E, \Omega)$$

PROOF : Since $\partial\Omega$ is Lipschitz,

$$P(E,\Omega_{\mathrm{E}}) = P(E,\Omega) + \mathcal{H}^{\mathrm{N}-1}(\partial\Omega \cap E^{1/2})$$

Thus E has finite perimeter in Ω_{E}. Let us first prove that $\forall i \in I$, $\partial\Omega \cap E_i^{1/2} = \partial\Omega \cap \tilde{E}_i^{1/2}$ up to $\mathcal{H}^{\mathrm{N}-1}$-negligible sets.

Recall that $\tilde{E}_i = \Omega_{\mathrm{E}} \setminus F_{i,0}$ where $F_{i,0}$ is the unique indecomposable component of $\Omega_{\mathrm{E}} \setminus E_i = \bigcup_{j\in J} F_{i,j}$ such that $\partial\Omega_{\mathrm{E}} \subset F_{i,0}^{1/2}$. Since $\Omega \subset\subset \Omega_{\mathrm{E}}$ it is easily seen that $\Omega_{\mathrm{E}} \setminus \Omega$ is indecomposable and from $E_i \subset \Omega$ and a call to Theorem 2.5.7 we infer that $\Omega_{\mathrm{E}} \setminus \Omega \subset F_{i,0}$ up to $\mathcal{H}^{\mathrm{N}-1}$-negligible sets. Now, $\mathcal{H}^{\mathrm{N}-1}$-almost every point in Ω_{E} belongs either to $F_{i,0}^0$, $F_{i,0}^1$ or $F_{i,0}^{1/2}$ thus $(\Omega_{\mathrm{E}} \setminus \Omega)^{1/2} \subset F_{i,0}^{1/2} \cup F_{i,0}^1$ and in particular, since $\partial\Omega$ is Lipschitz,

$$\partial\Omega = \Omega_{\mathrm{E}} \cap (\Omega_{\mathrm{E}} \setminus \Omega)^{1/2} \subset F_{i,0}^{1/2} \cup F_{i,0}^1 \tag{2.7.7}$$

By definition, $\tilde{E}_i = E_i \cup \bigcup_{j\in J\setminus\{0\}} F_{i,j}$ and since the $F_{i,j}$'s are disjoint subsets of $\Omega_{\mathrm{E}} \setminus E_i$ we get that $\{E_i\} \cup \{F_{i,j}\}_{j\in J\setminus\{0\}}$ is a Caccioppoli partition of $\tilde{E}_i$. By Theorem 2.5.2, it follows that

$$E_i^1 \cup \bigcup_{j\in J\setminus\{0\}} F_{i,j}^1 \cup \bigcup_{\substack{j,k\in J\setminus\{0\}\\ j\neq k}} F_{i,j}^{1/2} \cap F_{i,k}^{1/2} \cup \bigcup_{j\in J\setminus\{0\}} E_i^{1/2} \cap F_{i,j}^{1/2}$$

contains $\mathcal{H}^{\mathrm{N}-1}$-almost all of $\tilde{E}_i$. By Lemma 2.5.6, $\mathcal{H}^{\mathrm{N}-1}(\Omega_{\mathrm{E}} \cap F_{i,j}^{1/2} \cap F_{i,k}^{1/2}) = 0$ whenever $j \neq k$. Using (2.7.7), we get

$$\partial\Omega \cap \tilde{E}_i^{1/2} = \partial\Omega \cap E_i^{1/2}$$

up to $\mathcal{H}^{\mathrm{N}-1}$-negligible sets.

In view of Theorem 2.7.2, let $J \subset I$ be such that $\{\tilde{E}_j\}_{j\in J}$ are the indecomposable components of $\tilde{E}$, where the "filling" operation holds with respect to Ω_{E}. By (2.7.4), $\forall j \in J$, $P(\tilde{E}_j,\Omega_{\mathrm{E}}) \leq P(E_j,\Omega_{\mathrm{E}})$. Hence, $P(\tilde{E}_j,\Omega) + \mathcal{H}^{\mathrm{N}-1}(\partial\Omega \cap \tilde{E}_j^{1/2}) \leq P(E_j,\Omega) + \mathcal{H}^{\mathrm{N}-1}(\partial\Omega \cap E_j^{1/2})$ and using the relation above, we obtain $P(\tilde{E}_j,\Omega) \leq P(E_j,\Omega)$. Now, remark that $\tilde{E}^{1/2} \subset \bigcup_{j\in J} \tilde{E}_j^{1/2}$ and by Lemma 2.5.6 $\mathcal{H}^{\mathrm{N}-1}(\Omega_{\mathrm{E}} \cap \tilde{E}_j^{1/2} \cap \tilde{E}_k^{1/2}) = 0$ whenever $j \neq k$. Thus,

$$\mathcal{H}^{\mathrm{N}-1}(\partial\Omega \cap \tilde{E}^{1/2}) = \sum_{j\in J} \mathcal{H}^{\mathrm{N}-1}(\partial\Omega \cap \tilde{E}_j^{1/2})$$

Analogously, it can be proved that

$$\mathcal{H}^{\mathrm{N}-1}(\partial\Omega \cap E^{1/2}) = \sum_{i\in I} \mathcal{H}^{\mathrm{N}-1}(\partial\Omega \cap E_i^{1/2})$$

Therefore,

$$\begin{aligned}
P(\tilde{E},\Omega) &= P(\tilde{E},\Omega_{\mathrm{E}}) - \mathcal{H}^{\mathrm{N}-1}(\partial\Omega \cap \tilde{E}^{1/2}) \\
&= \textstyle\sum_{j\in J}[P(\tilde{E}_j,\Omega_{\mathrm{E}}) - \mathcal{H}^{\mathrm{N}-1}(\partial\Omega \cap \tilde{E}_j^{1/2})] \\
&\leq \textstyle\sum_{j\in J}[P(E_j,\Omega_{\mathrm{E}}) - \mathcal{H}^{\mathrm{N}-1}(\partial\Omega \cap E_j^{1/2})] \\
&\leq \textstyle\sum_{i\in I}[P(E_i,\Omega_{\mathrm{E}}) - \mathcal{H}^{\mathrm{N}-1}(\partial\Omega \cap E_i^{1/2})] \\
&\leq P(E,\Omega)
\end{aligned}$$

2.7.2 Grain filter

The grain filter that we are now going to define precisely can be seen as an operator associating with any set of finite perimeter E the set obtained by adding to E its small "holes".

Definition 2.7.7 *Let $\theta > 0$. We call grain filter of size θ, and denote by G_θ, the map which associates with any subset E of finite perimeter in Ω and satisfying (2.7.1)*

$$\mathrm{G}_\theta E := \bigcup_{i\in I} (T_\theta \tilde{E}_i) \setminus T_\theta(\tilde{E}_i \setminus E_i)$$

where $\{E_i\}_{i\in I}$ is the Caccioppoli partition of E into its indecomposable components.

Recall from (2.7.2) that $\tilde{E}_i = E_i \cup \bigcup_{j\in H_i} F_{i,j}$. Then, it is easily seen that G_θ acts on E_i in the following way :

- if $|\tilde{E}_i| \leq \theta$ then $\mathrm{G}_\theta E_i = \emptyset$
- otherwise $\mathrm{G}_\theta E_i = E_i \cup \bigcup_{k\in K} F_{i,k}$ with $\forall k \in K \subset H_i$, $|F_{i,k}| \leq \theta$.

where both equalities hold up to Lebesgue negligible sets.

Proposition 2.7.8 *Assume that $|\Omega| > \theta$. Let K be the maximal subset of I such that $\forall k \in K$, $\mathrm{G}_\theta E_k = (T_\theta \tilde{E}_k) \setminus T_\theta(\tilde{E}_k \setminus E_k) \neq \emptyset$. Then each $\mathrm{G}_\theta E_k$ is an indecomposable set and $\{\mathrm{G}_\theta E_k\}_{k\in K}$ is the Caccioppoli partition of $\mathrm{G}_\theta E$ into its indecomposable components.*

PROOF : In view of the remark above, it follows by Lemma 2.7.1 and (2.7.5) that if $\mathrm{G}_\theta E_k \neq \emptyset$ then $\mathrm{G}_\theta E_k$ is an indecomposable set. Let $i, j \in I$, $i \neq j$. Recall from the proof of Proposition 2.7.2 that either $\tilde{E}_i \cap \tilde{E}_j = \emptyset$, or $\tilde{E}_i \subset \tilde{E}_j$ or $\tilde{E}_j \subset \tilde{E}_i$ up to Lebesgue negligible sets. In the first case, obviously $\mathrm{G}_\theta E_i \cap \mathrm{G}_\theta E_j = \emptyset$. Let $\{F_{i,k}\}_{k\in J}$ be the Caccioppoli partition of $\Omega \setminus E_i$ into its indecomposable components. $\tilde{E}_j \subset \tilde{E}_i$ – the case $\tilde{E}_i \subset \tilde{E}_i$ can be addressed analogously – is satisfied when there exists $k \in H_i$ such that $E_j \subset F_{i,k}$. Now, since E_i is indecomposable and, by (2.7.5), $\forall k \in H_i$, $F_{i,k}^{1/2} \subset E_i^{1/2}$ we deduce that $\tilde{F}_{i,k} = F_{i,k}$ for every $k \in H_i$. Thus, by the monotonicity of the "filling" operator, $\tilde{E}_j \subset F_{i,k}$. Then, $F_{i,k} \subset \mathrm{G}_\theta E_i$ implies that $|F_{i,k}| \leq \theta$ thus $|\tilde{E}_j| \leq \theta$ and finally $\mathrm{G}_\theta E_j = \emptyset$. On the other hand, if $|F_{i,k}| > \theta$ then obviously $\mathrm{G}_\theta E_j \cap \mathrm{G}_\theta E_i = \emptyset$ up to Lebesgue negligible sets. Finally, $\forall i, j \in I$, $\mathrm{G}_\theta E_i \cap \mathrm{G}_\theta E_j = \emptyset$ up to Lebesgue negligible sets. Let K be the maximal subset of I such that $\forall k \in K$, $\mathrm{G}_\theta E_k \neq \emptyset$. Then, $\{\mathrm{G}_\theta E_k\}_{k\in K}$ is a Caccioppoli partition of $\mathrm{G}_\theta E$ into indecomposable sets. Now, if $\mathrm{G}_\theta E_k = E_k \cup \bigcup_{\ell\in L} F_{k,\ell}$ remark that

$$\Omega \cap (\mathrm{G}_\theta E_k)^{1/2} \subset \Omega \cap (E_k^{1/2} \cup \bigcup_{\ell\in L} F_{k,\ell}^{1/2})$$

and using (2.7.5) we obtain $\Omega \cap (\mathrm{G}_\theta E_k)^{1/2} \subset \Omega \cap E_k^{1/2}$. By Proposition 2.7.2 and Lemma 2.5.6 it follows that

$$\mathcal{H}^{\mathrm{N}-1}(\Omega \cap (\mathrm{G}_\theta E_k)^{1/2} \cap (\mathrm{G}_\theta E_i)^{1/2}) = 0 \quad \text{whenever } i \neq k$$

Thus, by Lemma 2.5.6, $P(\mathrm{G}_\theta E, \Omega) = \sum_{k\in K} P(\mathrm{G}_\theta E_k, \Omega)$ and we can conclude by the uniqueness of the decomposition into indecomposable components that $\{\mathrm{G}_\theta E_k\}_{k\in K}$ is the Caccioppoli partition of $\mathrm{G}_\theta E$ into its indecomposable components. □

Remark 2.7.9 T_θ and the "filling" operator are continuous with respect to the strict convergence of increasing sequences of sets but the grain filter does not inherit of this property as illustrated in figure 2.18. This is due to the fact that $(\tilde{E}_{i,h} \setminus E_{i,h})_{h\in\mathbb{N}}$ is a decreasing sequence for which the continuity of T_θ does not hold.

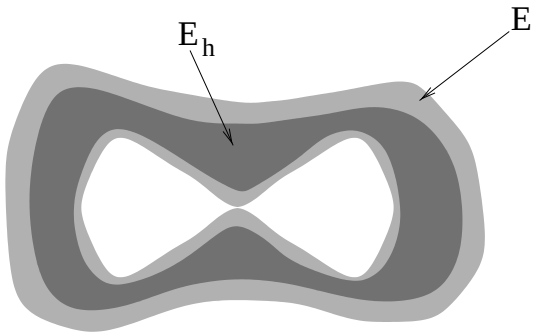

Figure 2.18: The grain filter is not continuous with respect to the strict convergence of an increasing sequence of sets E_h like the gray one in the figure, to the set E such that $\tilde{E} \setminus E$ is the union of two indecomposable components, one of measure $> \theta$, the other (F) of measure $< \theta$. Indeed, $\mathrm{G}_\theta E_h = E_h \to E$ but $\mathrm{G}_\theta E = E \cup F$

Proposition 2.7.10 *Let E, E' be two sets of finite perimeter in Ω satisfying (2.7.1). Then $E \subset E'$ implies $\mathrm{G}_\theta E \subset \mathrm{G}_\theta E'$, where both inclusions are understood up to Lebesgue negligible sets.*

PROOF : Let $\{E_i\}_{i\in I}$ and $\{E'_j\}_{j\in J}$ be the Caccioppoli partitions of E and E' into indecomposable components. By Theorem 2.5.7 we get that to each $i \in I$ can be associated a unique $j \in J$ such that $E_i \subset E'_j$. Obviously, it is enough to prove that $\mathrm{G}_\theta E_i \subset \mathrm{G}_\theta E'_j$ so that we reduce ourselves to the case of two indecomposable sets only. In the sequel we shall denote by $T'_\theta E$ the union of the indecomposable components of E such that $|E_i| \leq \theta$.

Let $L \subset K$ be two indecomposable subsets of Ω. Let $\{L_i\}_{i\in I}$ and $\{K_j\}_{j\in j}$ be respectively the Caccioppoli partitions of $\Omega \setminus L$ and $\Omega \setminus K$ into their indecomposable components. Since $\Omega \setminus K \subset \Omega \setminus L$ we deduce by Theorem 2.5.7 that for all $j \in J$ there exists a unique $i \in I$ such that $K_j \subset L_i$. Obviously, $|L_i| \leq \theta$ implies that $|K_j| \leq \theta$. Now, let $i \in I$ and remark that $L_i \setminus \bigcup_{j\in J} K_j \subset K$ since $K \cup \bigcup_{j\in J} K_j = K \cup (\Omega \setminus K) = \Omega$. It follows that $T'_\theta(\Omega \setminus L) \subset K \cup T'_\theta(\Omega \setminus K)$, hence $L \cup T'_\theta(\Omega \setminus L) \subset K \cup T'_\theta(\Omega \setminus K)$ and thus $\mathrm{G}_\theta L \subset \mathrm{G}_\theta K$ since the previous inclusion can be restricted to those components of $\Omega \setminus L$ and $\Omega \setminus K$ strictly contained in Ω. □

In view of Theorem 2.6.4 we now state :

Theorem 2.7.11 *Let $\Omega \subset\subset \Omega_{\rm E}$ be open and bounded balls in $\mathbb{R}^{\rm N}$ with $|\Omega| > \theta$. Let $u \in {\rm BV} \cap {\rm L}^\infty(\Omega)$ and define its extensions $u_{\rm E_S}$ and $u_{\rm E_I}$ on $\Omega_{\rm E}$ as*

$$u_{\rm E_S}(x) := \begin{cases} u(x) & on\ \Omega \\ \inf_\Omega u - 1 & on\ \Omega_{\rm E} \setminus \Omega \end{cases} \quad and \quad u_{\rm E_I}(x) := \begin{cases} u(x) & on\ \Omega \\ \sup_\Omega u + 1 & on\ \Omega_{\rm E} \setminus \Omega \end{cases}$$

Then, there exist two measurable functions $u_{\rm G_S} : \Omega_{\rm E} \to [-\infty, +\infty]$ and $u_{\rm G_I} : \Omega_{\rm E} \to [-\infty, +\infty]$ such that for almost every $\lambda \in \mathbb{R}$

$$\{u_{\rm G_S} \geq \lambda\} \sim {\rm G}_\theta\{u_{\rm E_S} \geq \lambda\} \quad and \quad \{u_{\rm G_I} < \lambda\} \sim {\rm G}_\theta\{u_{\rm E_I} < \lambda\}$$

where the "filling" operation is made with respect to $\Omega_{\rm E}$. In addition, any other measurable function v with the same property as $u_{\rm G_S}$ (resp. $u_{\rm G_I}$) coincides with $u_{\rm G_S}$ (resp. $u_{\rm G_I}$) almost everywhere on $\Omega_{\rm E}$.

PROOF : Notice that by Theorem 2.2.13 we get that $u_{\rm E} \in {\rm BV}(\Omega_{\rm E})$. Let us first prove the theorem for $u_{\rm G_S}$. Remark that, by definition, for every $\lambda > \inf_\Omega u - 1$, $X_\lambda := \{u_{\rm E} \geq \lambda\} = \{u \geq \lambda\} \subset\subset \Omega_{\rm E}$ whereas for every $\lambda \leq \inf_\Omega u - 1$, $X_\lambda = \Omega_{\rm E}$. By the Coarea formula, X_λ has finite perimeter for almost every $\lambda \in \mathbb{R}$ and we can define $Y_\lambda := {\rm G}_\theta X_\lambda$. Clearly, for almost every $\lambda \leq \inf_\Omega u - 1$, $Y_\lambda = \Omega_{\rm E}$. Since (X_λ) is decreasing, we get by Proposition 2.7.10 that (Y_λ) is decreasing and in view of Lemma 2.6.3 we call D the set (at most countable) of its discontinuity points. Let $D' \subset \mathbb{R}$ countable and dense, and define for every $x \in \Omega_{\rm E}$

$$u_{\rm G_S}(x) := \sup\{\lambda \in D' : x \in Y_\lambda\}$$

By the same argument as in Theorem 2.6.4, we get that $\{u_{\rm G_S} \geq \lambda\} \sim Y_\lambda$ for any $\lambda \notin D$. In addition, $u_{\rm G_S}$ is measurable and unique up to modifications on Lebesgue negligible sets.

Remark that $E \subset \Omega$ implies that ${\rm G}_\theta E \subset \Omega$ since ${\rm G}_\theta\Omega = \Omega$ under the assumption that $|\Omega| > \theta$. Therefore, the function $u_{\rm G_S}$ does not depend on a particular choice for $\Omega_{\rm E}$. Moreover, we define ${\rm G}^{\rm s}_\theta$ as the operator associating with u the restriction of $u_{\rm G_S}$ to Ω and remark that for almost every $\lambda \geq \inf_\Omega u$,

$$\{{\rm G}^{\rm s}_\theta u \geq \lambda\} \sim {\rm G}_\theta\{u \geq \lambda\}$$

because ${\rm G}_\theta\{u \geq \lambda\} \subset \Omega$ and where it must be kept in mind that the filling operation is made with respect to $\Omega_{\rm E}$. Remark in addition that the use of the value $\inf_\Omega u - 1$ is purely arbitrary. It is actually enough to extend u by any value strictly less than $\inf_\Omega u$ so that $\{u \geq \inf_\Omega\} = \Omega$, $\forall \lambda \geq \lambda\ \{u \geq \lambda\} \subset \Omega$ and the function ${\rm G}^{\rm s}_\theta u$ shall be the same. In addition, it is easily seen that for almost every $x \in \Omega$, $\inf_\Omega u \leq {\rm G}^{\rm s}_\theta u(x) \leq \sup_\Omega u$. Notice that the use of an extension is necessary since it is not true in general for an image that the level sets X_λ satisfy (2.7.1).

The theorem may be proven analogously for $u_{\mathrm{E_I}}$. Let X_λ denote the lower level sets of u_{E}, i.e $X'_\lambda := \{u_{\mathrm{E}} < \lambda\}$ and $Y'_\lambda := \mathrm{G}_\theta X'_\lambda$. Then, if D denotes the discontinuity set of (Y'_λ) and D' a countable and dense subset of $\mathbb{R}$, we define for every $x \in \Omega_{\mathrm{E}}$

$$u_{\mathrm{G_I}}(x) := \inf\{\lambda \in D' : x \in Y'_\lambda\}$$

and we obtain that $\{u_{\mathrm{G_S}} < \lambda\} \sim Y'_\lambda$ for every $\lambda \notin D$. Again, $u_{\mathrm{G_I}}$ is measurable and unique up to modifications on Lebesgue negligible sets.
Defining $\mathrm{G}^{\mathrm{i}}_\theta$ as the operator associating with u the restriction of $u_{\mathrm{G_I}}$ on Ω we get that the lower level sets of $\mathrm{G}^{\mathrm{i}}_\theta u$ coincide with Y'_λ for every $\lambda \leq \sup_\Omega u$ up to Lebesgue negligible sets. Remark here again that the choice of $\sup_\Omega u + 1$ for extending u outside Ω is arbitrary and the result would be the same if we choose any other value strictly larger than $\sup_\Omega u$. Furthermore, remark that for almost every $x \in \Omega$, $\inf_\Omega u \leq \mathrm{G}^{\mathrm{i}}_\theta u(x) \leq \sup_\Omega u$. Finally let us emphasize an easy consequence of the definition that shall be useful in the sequel :

$$\{u_{\mathrm{E_S}} \geq \lambda\} = \Omega \setminus \{u_{\mathrm{E_I}} < \lambda\} \quad \text{a.e. in } [\inf_\Omega u, \sup_\Omega u)$$

where the equality holds up to Lebesgue negligible sets. □

Theorem 2.7.12 *$\mathrm{G}^{\mathrm{i}}_\theta$, $\mathrm{G}^{\mathrm{s}}_\theta$, $\mathrm{G}^{\mathrm{i}}_\theta\mathrm{G}^{\mathrm{s}}_\theta$, $\mathrm{G}^{\mathrm{s}}_\theta\mathrm{G}^{\mathrm{i}}_\theta$ are idempotent and monotone operators acting on $\mathrm{BV} \cap \mathrm{L}^\infty(\Omega)$. Moreover, they are covariant with respect to any real continuous increasing contrast change and any affine mapping of $\mathbb{R}^{\mathrm{N}}$ onto itself preserving the Lebesgue measure.*

PROOF : Let E be a set of finite perimeter in Ω and Ω_{E} a set with the same properties as in Theorem 2.7.11. Let $\{E_i\}_{i\in I}$ be the indecomposable components of E such that $\mathrm{G}_\theta E_i \neq \emptyset$. It follows easily from the definitions that $\widetilde{(\mathrm{G}_\theta E_i)} = \tilde{E}_i$, where the "filling" operation hold with respect to Ω_{E}, and since $T'_\theta(\tilde{E}_i \setminus \mathrm{G}_\theta E_i) = \emptyset$ we obtain that $\mathrm{G}_\theta\mathrm{G}_\theta E_i = \mathrm{G}_\theta E_i$. Now, let $u \in \mathrm{BV} \cap \mathrm{L}^\infty(\Omega)$. It follows by Theorem 2.7.11 that for almost every $\lambda \geq \inf_\Omega u$,

$$\{\mathrm{G}^{\mathrm{s}}_\theta\mathrm{G}^{\mathrm{s}}_\theta u \geq \lambda\} \sim \mathrm{G}_\theta\{\mathrm{G}^{\mathrm{s}}_\theta u \geq \lambda\} \sim \mathrm{G}_\theta\mathrm{G}_\theta\{u \geq \lambda\} \sim \mathrm{G}_\theta\{u \geq \lambda\} \sim \{\mathrm{G}^{\mathrm{s}}_\theta u \geq \lambda\}$$

and we obtain by the uniqueness property stated in Theorem 2.7.11 that $\mathrm{G}^{\mathrm{s}}_\theta\mathrm{G}^{\mathrm{s}}_\theta u$ and $\mathrm{G}^{\mathrm{s}}_\theta u$ coincide almost everywhere on Ω. The result can be proven analogously for $\mathrm{G}^{\mathrm{i}}_\theta u$.
Now, let us prove that $\mathrm{G}^{\mathrm{s}}_\theta\mathrm{G}^{\mathrm{i}}_\theta\mathrm{G}^{\mathrm{s}}_\theta u = \mathrm{G}^{\mathrm{i}}_\theta\mathrm{G}^{\mathrm{s}}_\theta u$. Actually, it is enough to prove that $\mathrm{G}^{\mathrm{i}}_\theta$ does not create grains of measure less than θ associated with upper level sets, which follows from the definitions and the fact that $\{u_{\mathrm{E_I}} < \lambda\} = \Omega \setminus \{u_{\mathrm{E_S}} \geq \lambda\}$ for a.e. $\lambda \in (\inf_\Omega u, \sup_\Omega u]$. Then, $\mathrm{G}^{\mathrm{i}}_\theta\mathrm{G}^{\mathrm{s}}_\theta\mathrm{G}^{\mathrm{i}}_\theta\mathrm{G}^{\mathrm{s}}_\theta u = \mathrm{G}^{\mathrm{i}}_\theta\mathrm{G}^{\mathrm{i}}_\theta\mathrm{G}^{\mathrm{s}}_\theta u = \mathrm{G}^{\mathrm{i}}_\theta\mathrm{G}^{\mathrm{s}}_\theta u$, using the fact that $\mathrm{G}^{\mathrm{i}}_\theta$ is idempotent. The idempotence of $\mathrm{G}^{\mathrm{s}}_\theta\mathrm{G}^{\mathrm{i}}_\theta$ can be proved with an analogous argument.

The monotonicity property of both operators $\mathrm{G}^{\mathrm{s}}_\theta$ and $\mathrm{G}^{\mathrm{i}}_\theta$ follows from a decomposition of $u \in \mathrm{BV} \cap \mathrm{L}^\infty(\Omega)$ into its level sets like above and a simple application of Proposition 2.7.10.

The covariance property with respect to any continuous increasing contrast change can be proved the same way as in Theorem 2.6.6.

Finally, the covariance with respect to any affine map of $\mathbb{R}^N$ onto itself follows from a call to Theorem 2.6.6 and the fact that if E is indecomposable then $\widetilde{(AE)} = A\tilde{E}$ where the "filling" operations are made respectively with respect to $A\Omega_E$ and Ω_E. Indeed, in view of the definition of the "filling" operator, $A\tilde{E} = A(\Omega_E \setminus F_0)$ where F_0 is the only indecomposable component of $\Omega_E \setminus E$ such that $\partial\Omega_E \subset F_0^{1/2}$. Since A is one to one we get that $A(\Omega_E \setminus F_0) = A\Omega_E \setminus AF_0$. In addition, we infer from (2.6.3) that $A\partial\Omega_E = \partial A\Omega_E$ and $AF_0^{1/2} = (AF_0)^{1/2}$ and since $\partial\Omega_E \subset F_0^{1/2}$ it follows that $\partial A\Omega_E \subset (AF_0)^{1/2}$. By Lemma 2.6.7, AF_0 is an indecomposable component of $A(\Omega_E \setminus E) = A\Omega_E \setminus AE$ and finally, $\widetilde{(AE)} = A\Omega_E \setminus AF_0 = A(\Omega_E \setminus F_0) = A\tilde{E}$. Then, using Theorem 2.6.6, we obtain

$$T_\theta(\widetilde{AE}) \setminus T_\theta((\widetilde{AE}) \setminus AE) = T_\theta(A\tilde{E}) \setminus T_\theta(A\tilde{E} \setminus AE) = A(T_\theta\tilde{E} \setminus T_\theta(\tilde{E} \setminus E))$$

Thus $G_\theta AE = AG_\theta E$ and the result follows for $u \in BV \cap L^\infty(\Omega)$ by using like above its decomposition into either upper or lower level sets and by a call to Proposition 2.7.8. □

Theorem 2.7.13 *Let $u \in BV \cap L^\infty(\Omega)$. Then $G_\theta^i u$, $G_\theta^s u \in BV \cap L^\infty(\Omega)$. In addition,*

$$|DG_\theta u|(\Omega) \leq |Du|(\Omega)$$

PROOF : We shall prove the theorem for G_θ^s, the proof being analogous for G_θ^i. From the Coarea formula, $\{u \geq \lambda\}$ is a set of finite perimeter in Ω for almost every $\lambda \geq \inf_\Omega u$ and $\{u \geq \lambda\} \subset \Omega \subset\subset \Omega_E$. Denoting $E := \{u \geq \lambda\}$ and $\{E_i\}_{i\in I}$ its indecomposable components, recall that the indecomposable components of $G_\theta E$ are simply all the sets $G_\theta E_k$, $k \in K \subset I$, that are not empty and can be written as $G_\theta E_k = E_k \cup \bigcup_{j\in J} F_{k,j}$ with $|F_{k,j}| \leq \theta$. Using Proposition 2.7.6 and Relation (2.7.5) we deduce that

$$\partial\Omega \cap (G_\theta E_k)^{1/2} = \partial\Omega \cap E_k^{1/2}$$

In addition, by Lemma 2.5.6,

$$\mathcal{H}^{N-1}(\partial\Omega \cap (G_\theta E_k)^{1/2} \cap (G_\theta E_{k'})^{1/2}) = 0 \quad \text{whenever } k \neq k'$$

Now, since $G_\theta E \subset \Omega$, it follows from Theorem 2.5.2, the two equalities above and Proposition 2.7.8 that

$$\mathcal{H}^{N-1}(\partial\Omega \cap (G_\theta E)^{1/2}) = \sum_{k\in K} \mathcal{H}^{N-1}(\partial\Omega \cap (G_\theta E_k)^{1/2})$$

and thus,

$$\begin{aligned} P(\mathrm{G}_\theta E, \Omega) &= P(\mathrm{G}_\theta E, \Omega_\mathrm{E}) - \mathcal{H}^{\mathrm{N}-1}(\partial\Omega \cap (\mathrm{G}_\theta E)^{1/2}) \\ &= \textstyle\sum_{k\in K}[P(\mathrm{G}_\theta E_k, \Omega_\mathrm{E}) - \mathcal{H}^{\mathrm{N}-1}(\partial\Omega \cap (\mathrm{G}_\theta E_k)^{1/2})] \\ &\leq \textstyle\sum_{k\in K}[P(E_k, \Omega_\mathrm{E}) - \mathcal{H}^{\mathrm{N}-1}(\partial\Omega \cap E_k^{1/2})] \\ &\leq \textstyle\sum_{i\in I}[P(E_i, \Omega_\mathrm{E}) - \mathcal{H}^{\mathrm{N}-1}(\partial\Omega \cap E_i^{1/2})] \\ &\leq P(E, \Omega_\mathrm{E}) - \mathcal{H}^{\mathrm{N}-1}(\partial\Omega \cap E^{1/2}) \\ &\leq P(E, \Omega) \end{aligned}$$

Remark that the last three expressions are actually equal and it follows in particular that

$$P(E, \Omega) = \sum_{i\in I} P(E_i, \Omega)$$

The inequality $P(\mathrm{G}_\theta E, \Omega) \leq P(E, \Omega)$ holds for any $E := \{u \geq \lambda\}$ with $\lambda \geq \inf_\Omega u$. In addition, for almost every $\lambda < \inf_\Omega u$, $\{u \geq \lambda\} = \Omega_\mathrm{E}$ thus $\mathrm{G}_\theta\{u \geq \lambda\} = \Omega_\mathrm{E}$ and it follows that $P(\mathrm{G}_\theta E, \Omega) = P(E, \Omega) = 0$. Then, a call to Coarea formula yields

$$|D\mathrm{G}^\mathrm{s}_\theta u|(\Omega) \leq |Du|(\Omega)$$

and $\mathrm{G}^\mathrm{s}_\theta u \in \mathrm{BV}(\Omega)$. We obtain in addition that $\mathrm{G}^\mathrm{s}_\theta u \in \mathrm{L}^\infty(\Omega)$ by simply remarking that $\{u_{\mathrm{E_S}} \geq \inf_\Omega u\} = \Omega$, so that $\mathrm{G}^\mathrm{s}_\theta u(x) \geq \inf_\Omega u$ almost everywhere on Ω, and $\mathrm{G}^\mathrm{s}_\theta(x) \leq \sup_\Omega u$ almost everywhere on Ω since by Theorem 2.7.11

$$\{\mathrm{G}^\mathrm{s}_\theta u \geq \lambda\} \sim \mathrm{G}_\theta\{u \geq \lambda\}$$

for almost every $\lambda \geq \inf_\Omega u$ and the conclusion follows by remarking that

$$\mathrm{G}_\theta\{u > \sup_\Omega u\} = \mathrm{G}_\theta\emptyset = \emptyset$$

It must be emphasized that like I_θ and S_θ, $\mathrm{G}^\mathrm{s}_\theta$ or $\mathrm{G}^\mathrm{i}_\theta$ do not necessarily decrease the L^1 norm. Consider indeed the following counter-example in $\mathbb{R}^2$ with $\Omega = B_2(0)$, $\Omega_\mathrm{E} = B_3(0)$ and the radial function u defined by

$$u(x) = \begin{cases} 0 & \text{if } |x| > 1 \\ 2 & \text{if } \frac{1}{2} < |x| \leq 1 \\ 1 & \text{if } |x| \leq \frac{1}{2} \end{cases}$$

Then, with $\theta = |B_{1/2}(0)| + \epsilon$ and $\epsilon \ll 1$ we get that

$$\mathrm{G}^\mathrm{s}_\theta u(x) = \begin{cases} 0 & \text{if } |x| > 1 \\ 2 & \text{if } |x| \leq 1 \end{cases}$$

Thus,

$$\|\mathrm{G}^\mathrm{s}_\theta u\|_{\mathrm{L}^1(\Omega)} = \int_0^2 \pi dx = 2\pi$$

whereas

$$\|u\|_{\mathrm{L}^1(\Omega)} = \int_0^1 \pi + \int_1^2 3\pi/4 dx = 7\pi/4$$

□

Since, in order to perform the denoising of an image, we combine $\mathrm{G}_\theta^{\mathrm{s}}$ and $\mathrm{G}_\theta^{\mathrm{i}}$, the question arises whether it would be enough to simply define $\mathrm{G}_\theta E = \bigcup_{i\in I} T_\theta \tilde{E}_i$. Indeed, it can be check that such a definition yields analogous results when the operators associated with either upper or lower sets are combined. Now, the main interest of $\mathrm{G}_\theta^{\mathrm{s}}$ or $\mathrm{G}_\theta^{\mathrm{i}}$ like they were defined is stated in the following theorem, which establishes that in contrast to $\mathrm{I}_\theta\mathrm{S}_\theta$ or $\mathrm{I}_\theta\mathrm{S}_\theta$, it is equivalent to filter grains of a highly differentiable function of bounded variation by either $\mathrm{G}_\theta^{\mathrm{i}}$ and $\mathrm{G}_\theta^{\mathrm{s}}$. In other words, minima and maxima are processed simultaneously and it is equivalent to use either lower or upper level sets.

Theorem 2.7.14 *Let $u \in \mathrm{C}^{\mathrm{N}}(\Omega, \mathbb{R})$ be a nonnegative function compactly supported in Ω. Then $\mathrm{G}_\theta^{\mathrm{i}} u = \mathrm{G}_\theta^{\mathrm{s}} u$ almost everywhere in Ω.*

PROOF : First remark that obviously $u \in \mathrm{BV}(\Omega)$ since u is compactly supported in Ω. We now recall the Morse Theorem ([30]) for the critical set of a function.

Theorem 2.7.15 (Morse) *Let Ω be an open subset of $\mathbb{R}^{\mathrm{N}}$ and let $u \in \mathrm{C}^{\mathrm{N}}(\Omega, \mathbb{R})$. Then u transforms its critical set in a set of linear measure zero.*

In other words, denoting $C(u) = \{x \in \Omega : \mathrm{rank}(Du(x)) = 0\}$, the Morse Theorem states that $\{C(u) \cap u^{-1}(t)\}$ is empty for almost every $t \in \mathbb{R}$. Let $\mathcal{R}$ denotes this dense set of t's and for $t \in \mathcal{R}$, let $X^t := \{u \geq t\}$ and $X_t := \{u < t\} \equiv \Omega \setminus X^t$. Since u is supposed to have compact support in Ω we get that X^t and X_t satisfy (2.7.1) for every $t \in \mathcal{R}$. Now let $t \in \mathcal{R}$, $\{E_i\}_{i\in I}$ be the indecomposable components of X^t and $\{E'_j\}_{j\in J}$ the indecomposable components of X_t. Since $\{C(u) \cap u^{-1}(t)\} = \emptyset$ for every $t \in \mathcal{R}$, we infer that for every $i \in I$, $K_i := \tilde{E}_i \setminus \bigcup_{\tilde{E}_j \subset \tilde{E}_i} \tilde{E}_j$ is indecomposable. Therefore, by Theorem 2.5.7, there exists a unique $j \in J$ such that $K_i \subset E'_j$ and even more, by (2.7.4), that $K_i = E'_j$. Thus, $K_i \in \mathrm{G}_\theta E_i$ implies $|\tilde{E}'_j| \leq \theta$ and $K_i \cap \mathrm{G}_\theta E_i = \emptyset$ implies $|\tilde{E}'_j| > \theta$. Since the role of E'_j and E_i can be exchanged we finally infer that $\cup_{i\in I} \mathrm{G}_\theta E_i = \Omega \setminus \cup_{j\in J} \mathrm{G}_\theta E'_j$. Hence, $\mathrm{G}_\theta X^t = \Omega \setminus \mathrm{G}_\theta X_t$ and since t is arbitrary in $\mathcal{R}$, Theorem 2.7.14 ensues. □

Remark 2.7.16 It is unfortunately not equivalent to deal either with upper or lower level sets for a general function u of bounded variation as shown with the counter-example of figure 2.19. Actually this is mainly due to the structure of upper and lower level sets whose boundaries can cross like for instance $\partial\{u \geq 1\}$ and $\partial\{u < 2\}$ with u the function of figure 2.19.

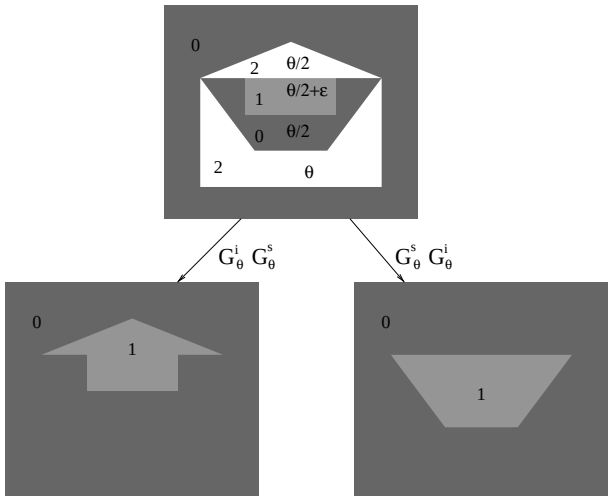

Figure 2.19: An example of function of bounded variation for which G^s_θ and G^i_θ do not commute.

Remark 2.7.17 It can be checked that G_θ differs from $S_\theta I_\theta$ as well as from $I_\theta S_\theta$, like for instance when operating on the function of Proposition 2.4.9. More generally, when dealing with concentric curves, $S_\theta I_\theta$ and $I_\theta S_\theta$ depend on the measure of each ring between two successive curves whereas G_θ depends on the measure of the sets enclosed by the curves. As a consequence, the grain filter ($G^s_\theta G^i_\theta$ or $G^i_\theta G^s_\theta$) is more able to preserve oscillations in contrast to $S_\theta I_\theta$ and $I_\theta S_\theta$. This is the main reason why it is more reliable from a topographic point of view.

Remark 2.7.18 By Theorem 2.6.4, Vincent's filters can be written as

$$\begin{aligned} S_\theta u(x) &= \sup\{t \in \mathcal{R} : x \in T_\theta\{u \geq t\}\} \\ I_\theta u(x) &= \inf\{t \in \mathcal{R} : x \in T_\theta\{u \leq t\}\} \end{aligned}$$

for almost every $x \in \Omega$, with $\mathcal{R}$ a countable and dense set of levels t such that $\{u \geq t\}$ has finite perimeter in Ω. Analogously it may be checked that the combination $G^s_\theta G^i_\theta$ or $G^i_\theta G^s_\theta$ is equivalent to combine the two filters

$$\begin{aligned} {G_\theta}^1 u(x) &:= \sup\{t \in \mathcal{R} : x \in F_\theta(\{u_{E_S} \geq t\})\} \\ {G_\theta}^2 u(x) &:= \inf\{t \in \mathcal{R} : x \in F_\theta(\{u_{E_I} < t\})\} \end{aligned}$$

where F_θ denotes the operator which associates a set A of finite perimeter in Ω satisfying (2.7.1) with $\bigcup_{i\in I} T_\theta \tilde{A}_i$, $\{A_i\}_{i\in I}$ being the Caccioppoli partition of A into its indecomposable components. However, remark that ${G_\theta}^1$ and ${G_\theta}^2$ differ from G^s_θ and G^i_θ, since they necessarily have to be combined even when dealing with highly differentiable functions.

2.7.3 Experimental results

In contrast to Vincent's filters, the implementation of the grain filter is far from being easy since it requires to take into account simultaneously the lower and upper level

sets. In [29], P. Monasse and F. Guichard have proposed a very fair method to compute the decomposition of an image into the connected components of its level lines, where the components are structured into a tree representing their geometric inclusions. This decomposition is equivalent to a hierarchical representation of the grains ordered with respect to the inclusion relation. Grain filtering can be easily derived from this representation, since it is enough to remove from the tree all the grains whose Lebesgue measure does not exceed some threshold θ, and then to reconstruct the filtered image. The reader may refer to [29] for more details.

In the following experiment we compare the performances of the conventional median filter, MFCN_θ, $\mathrm{I}_\theta\mathrm{S}_\theta$, the grain filter and a rank filter due to L. Yaroslavsky. This rank filter first identifies the noisy points as those points whose rank computed over a 3×3 neighborhood is either less than 1 or larger than 7 (on such a neighborhood the rank goes only between 0 and 8). Then the gray level of each noisy point is replaced by the median value computed over the neighborhood. In figure 2.20 we show an image extracted from a baboon image and we shall concentrate on this part enclosed by a white rectangle where two baboon whiskers intersect. Figure 2.21 shows a 3D representation of this part

Figure 2.20: Part of a baboon image. The results shown in figure 2.21 are related to the part of the image enclosed by the white rectangle.

of the image and it is compared with the corresponding representation for the image corrupted by an impulse noise with frequency 20% and the results performed by several filters : the conventional median filter computed over a disk with radius 1.5 and iterated twice, the rank filter described above, the Vincent's filter $\mathrm{I}_{10}\mathrm{S}_{10}$, the same filter combined with a post-regularization by the conditional median filter iterated twice over a disk with radius 1.5 (see Section 2.4.3), MFCN_{10} (see Section 2.4.1), the grain filter with threshold 10 and, finally, the grain filter combined with a post-regularization like above. Statistics are presented in figure 2.22. Vincent's filters and the grain filter perform clearly well at noise detection but are not as good as the median filter or the rank filter at estimating the

"true value" at each noisy point. However, the higher probability for these latter filters to wrongly detect a noisy point explains why, as shown in figure 2.21, MFCN, the Vincent's filter and the grain filter are better for structure preserving. In addition, and this property is particularly relevant for automation, they yield fixed points, in contrast to the median filter and the rank filter. Actually, these latter filters induce a smoothing effect that is very corrupting for image structure (the two whiskers of the baboon have been nearly removed). In contrast, if median filter is simply used in a post-regularization process, it is worth noticing that structures are well regularized without being too much altered.

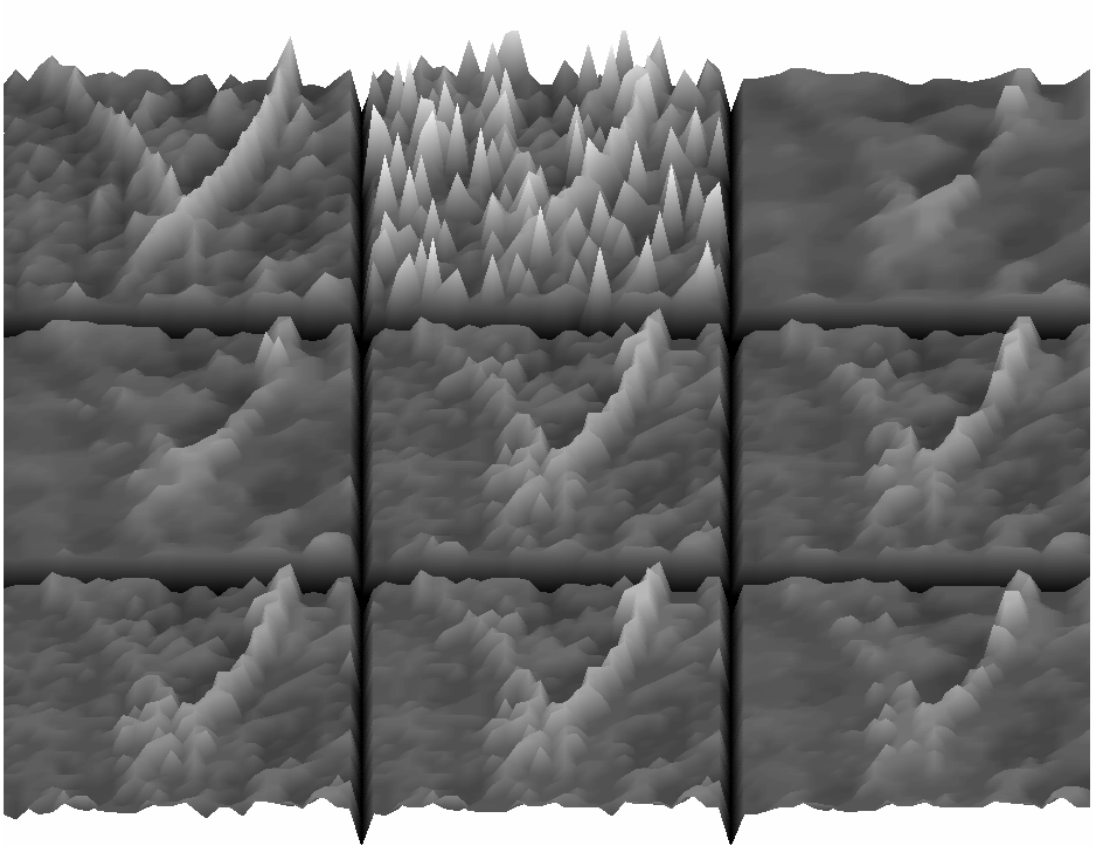

Figure 2.21: 3D representations of the following images :
Original image u_0 | Noisy image u ($f = 20\%$) | $\mathrm{med}^2_{1.5}\, u$
$\mathrm{rank}^2_{3,3,1,7}(u)$ | $\mathrm{I}_{10}\mathrm{S}_{10}(u)$ | $\mathrm{Cmed}^{\,2}_{1.5} \circ \mathrm{I}_{10}\mathrm{S}_{10}(u)$
$\mathrm{Cmed}^{\,2}_{1.5} \circ \mathrm{I}_{10}\mathrm{S}_{10}(u)$ | $\mathrm{G}_{10}(u)$ | $\mathrm{Cmed}^{\,2}_{1.5} \circ \mathrm{G}_{10}(u)$
(from left to right and top to bottom)

MFCN_θ, grain filter as well as Vincent's filters are mainly based on the adaptation of noisy points to some underlying local coherence. This approach is particularly efficient for denoising images corrupted with impulse noise since this kind of noise does not totally

	Prob. of missing a noisy point	Std. dev. of errors due to missing noise	Prob. of false detection	Std. dev. of errors due to false detection
$\mathrm{med}^2_{1.5}$	0.0117	2.5725	0.6375	16.1609
$\mathrm{rank}^2_{3,3,1,7}$	0.0242	4.3791	0.45	15.0261
$\mathrm{I}_{10}\mathrm{S}_{10}$	0.0392	6.5722	0.2850	7.2260
$\mathrm{Cmed}^2_{1.5} \circ \mathrm{I}_{10}\mathrm{S}_{10}$	0.0392	6.5722	0.2850	10.0371
MFCN_{10}	0.0383	6.4889	0.3242	9.2757
G_{10}	0.0300	4.9662	0.3875	8.6084
$\mathrm{Cmed}^2_{1.5} \circ \mathrm{G}_{10}$	0.0300	4.9662	0.3875	14.4390

	Std. dev. of residual noise	Std. dev. of detected corrupted pixel estimation errors
$\mathrm{med}^2_{1.5}$	19.0905	9.8878
$\mathrm{rank}^2_{3,3,1,7}$	17.8812	8.6563
$\mathrm{I}_{10}\mathrm{S}_{10}$	15.9141	12.5426
$\mathrm{Cmed}^2_{1.5} \circ \mathrm{I}_{10}\mathrm{S}_{10}$	15.0827	9.1361
MFCN_{10}	16.5968	12.0918
G_{10}	15.9245	12.6184
$\mathrm{Cmed}^2_{1.5} \circ \mathrm{G}_{10}$	17.5512	8.6579

Figure 2.22: Denoising statistics performed by the filters of figure 2.21

corrupt the image local coherence. This is illustrated in figure 2.23, where grain filter and $\mathrm{I}_\theta\mathrm{S}_\theta$ perform particularly well in removing an impulse noise with a high frequency (25%). In contrast, any white additive noise introduces a new coherence (images corrupted with white additive Gaussian noise look quite natural) to which these filters shall remain fastened so that their performances are limited (see figure 2.24). A strong smoothing filter like Susan – but it is not morphological – is more adapted to this kind of noise because of its ability to force the construction of a coherence quite different from the one in corrupted image. The drawback is, however, that some fine details or texture may be lost. A strong smoothing effect seems actually not to be compatible with a real preservation of structures.

The quality of the results obtained in figure 2.24 with Rudin-Osher global method originates, as we wrote before, in the fact that it was specifically designed for Gaussian noise removal. The difference between images 2.24-5 and 2.24-6 shows, however, that this method is highly sensitive to the choice of parameters. Now, if we ask a denoising filter to have a small number of parameters easily adjustable, to perform well with both additive and impulse noise and to yield a fixed point, then MFCN_A, G_θ or Vincent's filters should be preferred to the Rudin–Osher method.

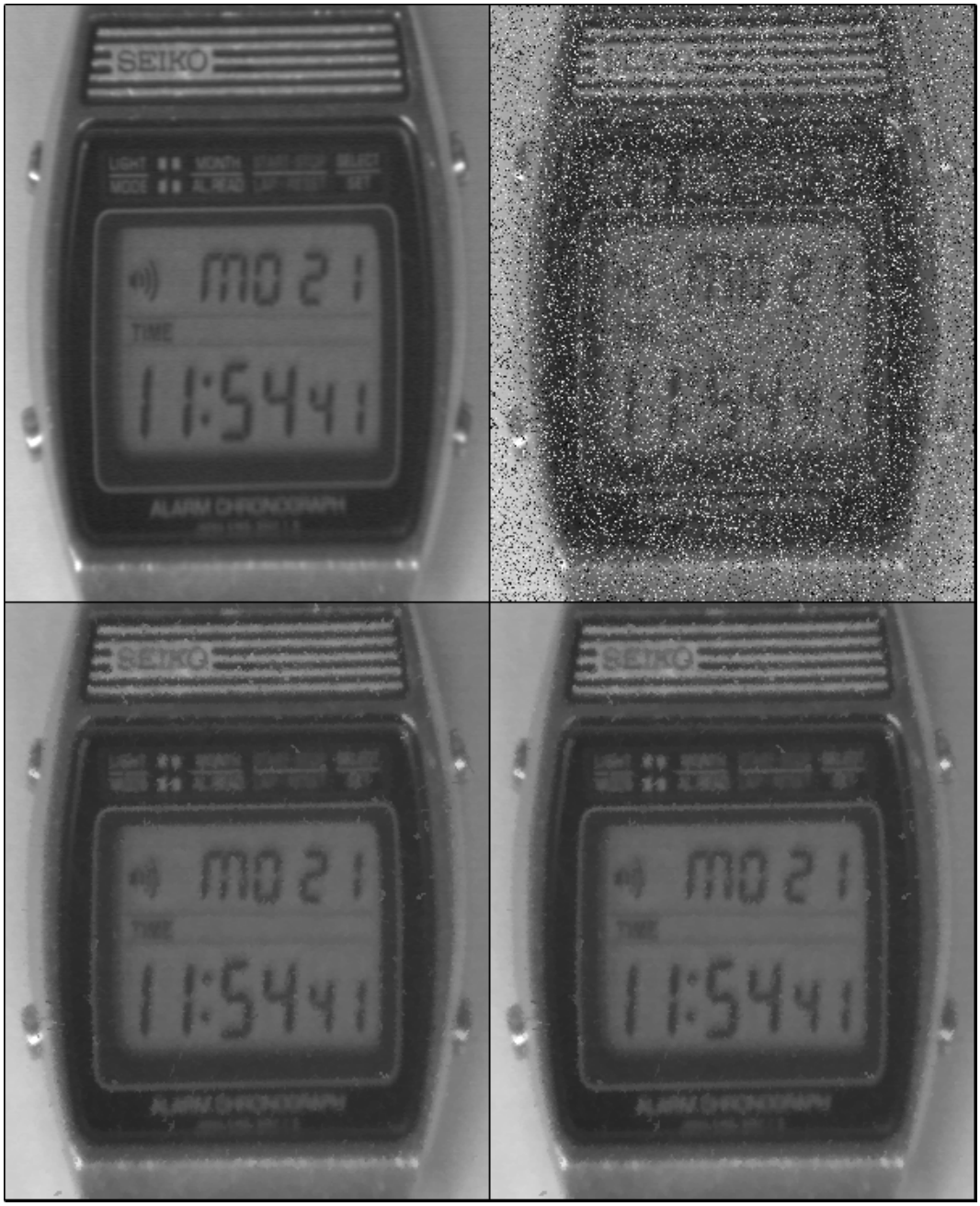

Figure 2.23: Performances of the grain filter and Vincent's filters on impulse noise
Top-left : original image Top-right : image u (impulse noise, $f = 25\%$).
Bottom-left : $\mathrm{G}_{10}(\mathrm{med}_1\, u)$ Bottom-right : $\mathrm{I}_{10}\mathrm{S}_{10}(\mathrm{med}_1\, u)$

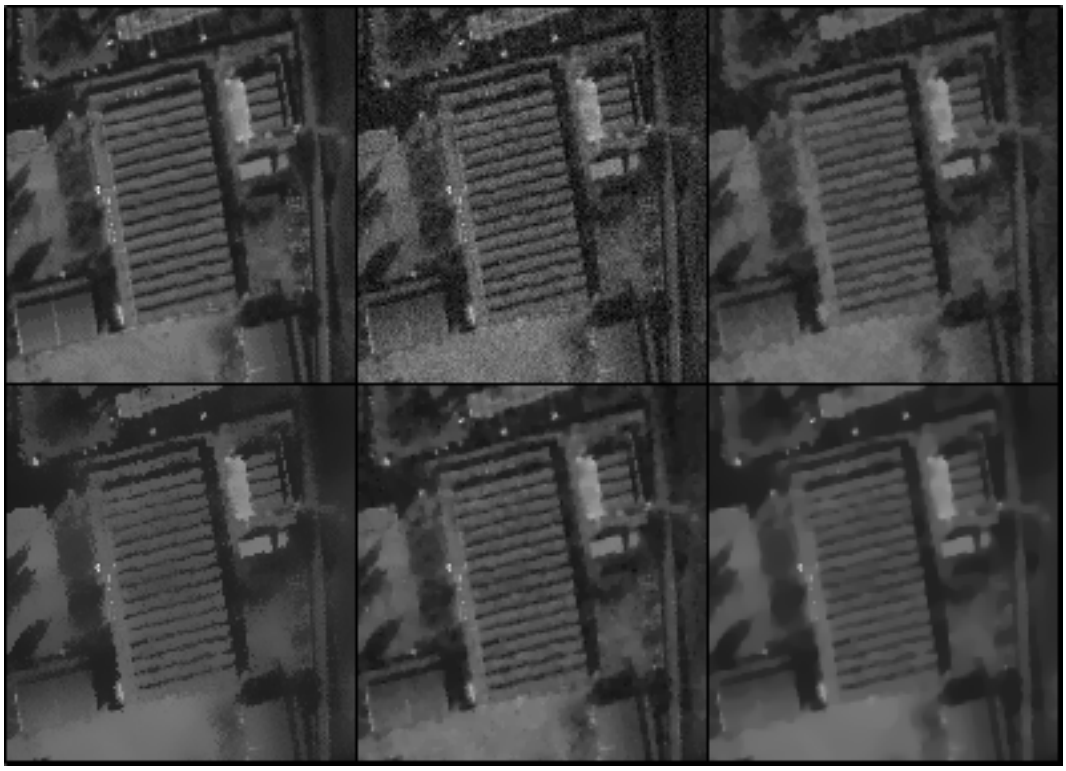

Figure 2.24: From left to right and up to bottom
1 Original image (aerial CNES photograph)
2 Noisy image u (white additive Gaussian noise ; $\sigma = 10$)
3 $G_5(\text{med}_{D(.,1)}\, u)$ (fixed point) 4 $\text{Susan}^2_{(d=5,\, l=12)} u$
5 Rudin-Osher ($\epsilon = 0.5,\ dt = 1;\ T_0 = 0;\ T_1 = 6$)
6 Rudin-Osher ($\epsilon = 0.5,\ dt = 1;\ T_0 = 0;\ T_1 = 13$)

Chapitre 3

Désocclusion

3.1 Introduction

Le problème qui nous occupe ici est le suivant : étant donné une image u et une tache Ω dans l'image dont on connaît la position, est-il possible de supprimer la tache ? En d'autres termes, peut-on à l'aide des informations au voisinage de la tache reconstruire l'image de la meilleure façon possible ? Il s'agit clairement d'un problème d'interpolation avec conditions de bord. Plus généralement, ce problème est lié au processus de complétion amodale, qui est un processus fondamental de la perception visuelle. Dans une scène naturelle, un objet est rarement totalement visible; il est presque toujours partiellement recouvert, ou occulté, par d'autres objets. Cependant, notre système visuel est capable, sous certaines conditions géométriques, de reconstruire la partie cachée en prolongeant artificiellement les bords des objets ; c'est ce qu'on appelle la complétion amodale. Nous avons illustré ce processus dans la figure 3.1, où notre système visuel reconstruit un rectangle qui, *a priori*, n'existe pas.

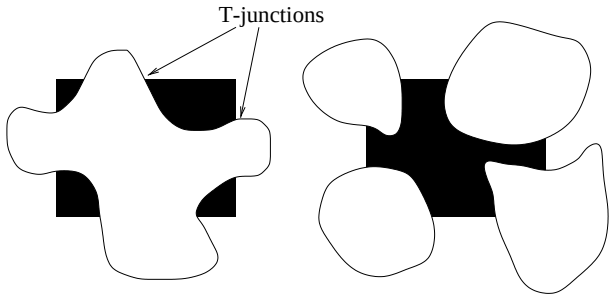

Figure 3.1: Le principe de complétion amodale de Kanizsa explique que nous percevions un rectangle dans les deux figures.

Cette capacité qu'à notre système visuel à reconstruire l'information manquante a été largement étudiée par les psychophysiciens, en particulier Gaetano Kanizsa [18, 19].

Il a ainsi été montré expérimentalement que ce ne sont pas des considérations globales faisant appel à notre connaissance de formes géométriques précises qui entrent en compte, mais plutôt la présence au bord de l'occlusion d'éléments très localisés, les jonctions en T [7, 18, 19]. On appelle jonctions en T ces points de la frontière de l'occlusion où les bords des objets présentent une configuration similaire à la lettre T. Les travaux des psychophysiciens ont permis d'établir que seule la présence des jonctions en T rend possible la reconstruction par le système visuel. Plus précisément, cette reconstruction consiste à créer artificiellement des contours reliant deux à deux les jonctions en T. La forme de ces contours artificiels dépend alors de la forme des contours au voisinage de chaque jonction en T, de sorte que les bords de l'objet reconstruit soient le plus possible courts et réguliers [18, 19].

Le problème de désocclusion qui nous occupe peut clairement être ramené à celui de la complétion amodale si l'on parvient à définir quels sont les objets occultés par la tache. Il y a quelques années, David Mumford et Mark Nitzberg [32] ont proposé une méthode pour retrouver la forme et la profondeur relative des objets contenus dans une image. Sans rentrer dans les détails de l'algorithme, une étape intermédiaire consiste, après avoir identifié les parties d'objet par segmentation, à regrouper ces parties en prolongeant leurs contours entre les jonctions en T – c'est-à-dire les points d'intersection entre la frontière de l'objet occulté et celle des objets occultants – à l'aide de courbes qui soient le plus possible courtes et peu oscillantes. La méthode utilisée est cependant peu satisfaisante pour la raison principale que les contours d'une image n'en sont pas une représentation complète, comme nous l'avons déjà vu, et dépendent autant de l'opérateur mis en œuvre pour les détecter que de la structure de l'image elle-même. Par ailleurs, la méthode de Mumford et Nitzberg ne permet de toute façon pas de résoudre le problème que nous nous posons, dans la mesure où la segmentation entraîne une perte considérable d'informations qui empêche toute reconstruction satisfaisante de l'image.

La méthode que nous proposons est basée sur l'utilisation des ensembles de niveau de l'image comme étant les objets occultés par la tache à éliminer. Pour restaurer ces objets, nous allons chercher à prolonger leurs frontières, c'est-à-dire les lignes de niveau, entre deux jonctions en T définies comme les points d'intersection des lignes de niveau avec l'occlusion. Cette méthode va nous permettre de restaurer des discontinuités et nous la comparerons à une méthode d'interpolation régulière proposée par V. Caselles, J.M. Morel et C. Sbert [9]. Leurs travaux ont permis d'établir le résultat suivant : si l'on connaît une fonction Lipschitz sur un bord qui peut être composé aussi bien de courbes que de points, alors la seule interpolation isotrope, stable, régulière et vérifiant le principe du maximum est donnée par l'équation AMLE (Absolute Minimizing Lipschitz Extension), qui s'écrit :

$$D^2u(\frac{Du}{|Du|}, \frac{Du}{|Du|}) = 0$$

3.2 A variational approach to image singular interpolation

In the following, we denote by Ω the part of the image plane occupied by the occluding object. We shall assume that Ω is open, bounded and simply connected and we denote by $\partial\Omega$ its boundary which we assume to be a Jordan curve.

The next lemmas ensure that there exists a simple rectifiable curve Γ arbitrarily close to Ω such that the one-dimensional restriction of u to Γ has bounded variation and such that the level lines of u are transverse to Γ.

Lemma 3.2.1 [Trace of BV-functions]
Let $\Omega \subset \mathbb{R}^2$ be an occlusion and $u \in \mathrm{BV}(\mathbb{R}^2 \setminus \overline{\Omega})$. For all $\eta > 0$, there exists an open, bounded and simply connected set $\tilde{\Omega}$ such that $\Omega \subset\subset \tilde{\Omega}$, $\partial\tilde{\Omega}$ is C^∞ and $d_{\mathcal{H}}(\Omega, \tilde{\Omega}) < \eta$. Define for every $h > 0$

$$\Gamma_h = \{x \in \mathbb{R}^2 \setminus \tilde{\Omega} : d(x, \tilde{\Omega}) = h\}$$

Then for almost every $h > 0$, the one-dimensional restriction $\tilde{u}$ of u to Γ_h is a function of bounded variation, i.e.

$$\int_{\Gamma_h} |\tilde{u}| d\mathcal{H}^1 < \infty \quad \text{and} \quad TV_{[0,\mathcal{L}(\Gamma_h)]}\tilde{u} = \int_0^{\mathcal{L}(\Gamma_h)} |\tilde{u}'| < \infty$$

Proof : Recall that the occlusion Ω is supposed to be an open, bounded and simply connected set such that $\partial\Omega$ is a rectifiable Jordan curve. Therefore, there exists $\epsilon > 0$ and a covering of Ω by finitely many balls B_i, $i = 1, ..., p$ with radius less than ϵ, such that the exterior boundary $\mathcal{C}$ of $\bigcup_{i=1}^p B_i$ is a piecewise C^∞ Jordan curve. By exterior boundary we mean the boundary that encloses Ω. $\mathcal{C}$ has singularities at points where two balls intersect. Since there are finitely many singularities, one can replace arcs of $\mathcal{C}$ in the vicinity of singularities by C^∞ arcs in order to obtain a C^∞ Jordan curve Γ_0 that encloses Ω (see figure 3.2). Obviously the set $\tilde{\Omega}$ enclosed by Γ_0 satisfies the properties of the lemma. Let us now define for every $h > 0$, $\Gamma_h = \{x \in \mathbb{R}^2 \setminus \tilde{\Omega} : d(x, \Gamma_0) = h\}$ so that $\Gamma_h \supset\supset \tilde{\Omega}$ and let $\Gamma_0 = \partial\tilde{\Omega}$. Γ_0 is a C^∞ curve and therefore has bounded curvature. Consequently, for h small enough, every point M of Γ_h can be associated with a unique point $m(s) \in \Gamma_0$ such that $\overrightarrow{mM} = h\vec{N}(s)$ where $N(s)$ denotes the outer normal to Γ_0 at $m(s)$ and s is the arc-length. Thus

$$\overrightarrow{\mathrm{OM}}(s, h) = \overrightarrow{\mathrm{OM}}(s) + h\vec{N}(s)$$

and Γ_h is C^∞ with respect to s. Moreover,

$$\frac{\partial\overrightarrow{\mathrm{OM}}}{\partial s} = \vec{T} + h\frac{d\vec{N}}{ds} = (1 - ch)\vec{T}$$

with $\vec{T}$ the tangent and c the curvature at $m(s)$. In addition

$$\frac{\partial\overrightarrow{\mathrm{OM}}}{\partial h} = \vec{N}$$

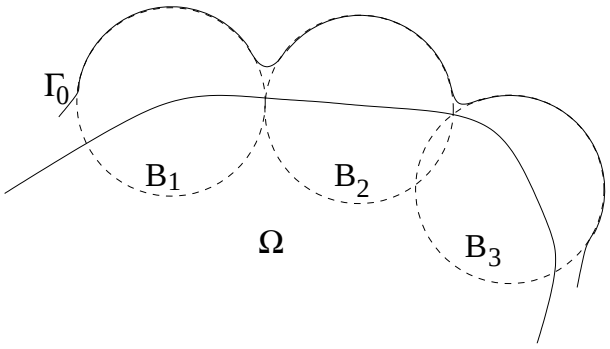

Figure 3.2: Ω can be enclosed by a C^∞ Jordan curve Γ

so that

$$||\frac{\partial\overrightarrow{OM}}{\partial s} \wedge \frac{\partial\overrightarrow{OM}}{\partial h}|| = |1 - ch|$$

Since the curvature of Γ_0 is uniformly bounded we can ensure that for h less than some threshold ϵ, $1 - ch \geq a > 0$. Let $E = \bigcup_{|h|<\epsilon} \Gamma_h$. Since u is a function of bounded variation in E, by Theorem 2.2.2 it can be approximated by a sequence of functions (u_n) in $BV \cap C^\infty(E)$ such that

$$u_n \longrightarrow u \quad \text{in } L^1$$
$$\int_E |\nabla u_n| \longrightarrow \int_E |Du|$$

Set $u_h(s) = u(M(s,h))$ and $u_h^n(s) = u_n(M(s,h))$. We deduce from the change of variables formula that

$$\begin{aligned}\int_{-\epsilon}^{\epsilon}\left(\int_0^{\mathcal{L}(\Gamma_h)} |u_h^n| ds\right) dh &\leq \tfrac{1}{a}\int_{-\epsilon}^{\epsilon}\int_0^{\mathcal{L}(\Gamma_h)} |u_n|.||\tfrac{\partial\overrightarrow{OM}}{\partial s} \wedge \tfrac{\partial\overrightarrow{OM}}{\partial h}||\, ds\, dh \\ &\leq \tfrac{1}{a}\int_E |u_n| dx \\ &< +\infty\end{aligned}$$

Thus $\int_0^{\mathcal{L}(\Gamma_h)} |u_h^n| dh \in L^1([-\epsilon,\epsilon])$ so that $u_h^n \in L^1(0, \mathcal{L}(\Gamma_h))$ for almost every $h \in [-\epsilon,\epsilon]$. Analogously we can write

$$\begin{aligned}\lim_{n\to\infty}\int_E |u_n - u| dx &= 0 \\ &= \lim_{n\to\infty}\int_{-\epsilon}^{\epsilon}\int_0^{\mathcal{L}(\Gamma_h)} |u_n - u|.||\tfrac{\partial\overrightarrow{OM}}{\partial s} \wedge \tfrac{\partial\overrightarrow{OM}}{\partial h}||\, ds\, dh \\ &= \lim_{n\to\infty}\int_{-\epsilon}^{\epsilon}\left(\int_0^{\mathcal{L}(\Gamma_h)} |1 - ch|.|u_h^n - u_h| ds\right) dh \qquad \text{(Fubini)}\end{aligned}$$

For every $h \in [-\epsilon, \epsilon]$, define $\phi_n(h) = \displaystyle\int_0^{\mathcal{L}(\Gamma_h)} |1 - ch|.|u_h^n - u_h| ds \geq a \int_0^{\mathcal{L}(\Gamma_h)} |u_h^n - u_h| ds.$
ϕ_n tends to zero in $\mathrm{L}^1([-\epsilon, \epsilon])$ so there exists a subsequence, still denoted by ϕ_n, that tends to 0 for almost every $h \in [-\epsilon, \epsilon]$. Therefore

$$\text{for a.e. } h \in [-\epsilon, \epsilon] \quad u_h^n \longrightarrow u_h \quad \text{in } \mathrm{L}^1(0, \mathcal{L}(\Gamma_h))$$

thus $u_h \in \mathrm{L}^1(0, \mathcal{L}(\Gamma_h))$.

Since u_n has bounded variation in E and

$$\frac{du_h^n}{ds} = \frac{\partial u_n(M(s,h))}{\partial s} = \nabla u_n(M).\frac{\partial M}{\partial s} = (1 - ch)\nabla u_n(M).\vec{T}$$

we have furthermore

$$\begin{aligned} \int_{-\epsilon}^{\epsilon} \left(\int_0^{\mathcal{L}(\Gamma_h)} |\frac{du_h^n}{ds}| ds \right) dh &\leq \int_{-\epsilon}^{\epsilon} \int_0^{\mathcal{L}(\Gamma_h)} |1 - ch|.|\nabla u_n| ds\, dh \\ &\leq \int_E |\nabla u_n| dx\, dy \\ &< +\infty \end{aligned}$$

and therefore

$$\int_0^{\mathcal{L}(\Gamma_h)} |\frac{du_h^n}{ds}| ds < +\infty \quad \text{for a.e. } h \in [-\epsilon, \epsilon]$$

To sum up

$$\begin{aligned} \text{for a.e. } h \in [-\epsilon, \epsilon] \quad & u_h^n \longrightarrow u_h \quad \text{in } \mathrm{L}^1(0, \mathcal{L}(\Gamma_h)) \\ \text{and} \quad & u_h^n \in \mathrm{BV}((0, \mathcal{L}(\Gamma_h))) \end{aligned}$$

From the lower semicontinuity of variation measure we obtain for a.e. $h \in [-\epsilon, \epsilon]$

$$\int_0^{\mathcal{L}(\Gamma_h)} |u_h'| ds \leq \liminf_{n \to \infty} \int_0^{\mathcal{L}(\Gamma_h)} |\frac{du_h^n}{ds}| ds$$

Thus

$$\begin{aligned} \int_{-\epsilon}^{\epsilon} \int_0^{\mathcal{L}(\Gamma_h)} |u_h'| ds\, dh &\leq \int_{-\epsilon}^{\epsilon} \liminf_{n \to \infty} \int_0^{\mathcal{L}(\mathcal{C})} |\frac{du_h^n}{ds}| ds\, dh \\ &\leq \liminf_{n \to \infty} \int_{-\epsilon}^{\epsilon} \int_0^{\mathcal{L}(\mathcal{C})} |\frac{du_h^n}{ds}| ds\, dh \quad \text{(Fatou)} \\ &\leq \liminf_{n \to \infty} \int_E |\nabla u_n| dx\, dy \\ &< +\infty \end{aligned}$$

Finally

$$\int_0^{\mathcal{L}(\Gamma_h)} |u_h'| ds < +\infty \quad \text{a.e. } h \in [-\epsilon, \epsilon]$$

and the lemma ensues by choosing some value of h realizing this inequality and setting $\tilde{u} = u_h$.

It must be emphasized that in order to ensure that u has finite values almost everywhere on Γ_h, thus is well defined, it is enough to apply the lemma with the representative u_r of u defined by $u_r(x) = u^+(x) = u^-(x)$ at every point x of approximate continuity of u and $u_r(x) = +\infty$ on S_u. □

In view of Definition 2.2.8 we can define for each $\mathcal{H}^1$-measurable K set the lower 1-dimensional density of K at $x \in \mathbb{R}^2$ as

$$\underline{\mathrm{D}}^1(x, K) = \liminf_{r \downarrow 0} \frac{\mathcal{H}^1(B(x, r) \cap K)}{2r}$$

The definition of the upper 1-dimensional density $\overline{\mathrm{D}}^1$ follows by replacing lim inf by lim sup. In case both limits coincide we define

$$\mathrm{D}^1(x, K) := \underline{\mathrm{D}}^1(x, K) = \overline{\mathrm{D}}^1(x, K)$$

Assuming that K is $\mathcal{H}^1$-rectifiable we get (see [3]) that

$$\begin{aligned} &\mathrm{D}^1(x, K) = 0 \quad \text{for } \mathcal{H}^1\text{-a.e. } x \in \mathbb{R}^2 \setminus K \\ &\mathrm{D}^1(x, K) = 1 \quad \text{for } \mathcal{H}^1\text{-a.e. } x \in K \end{aligned}$$

and we define the essential boundary of K as

$$\partial_M K = \{x \in \mathbb{R}^2 : \overline{\mathrm{D}}^1(x, K) > 0 \text{ and } \underline{\mathrm{D}}^1(x, K) > 0\}$$

The next lemma shall allow us to select a dense set with suitable properties among all the values λ taken by u on the occlusion boundary. Recall that there is no loss of generality in taking a dense set of λ since $u(x) = \sup\{\lambda : x \in X_\lambda u\}$ for almost every $x \in \mathbb{R}^2 \setminus \overline{\Omega}$.

Lemma 3.2.2 and Definition *Let $\Omega \subset \mathbb{R}^2$ be an occlusion and $u \in \mathrm{BV}(\mathbb{R}^2 \setminus \overline{\Omega})$. There exists a C^∞ Jordan curve Γ arbitrarily close to Ω such that, denoting by $\tilde{u}$ the restriction of u to Γ,*

$$\begin{aligned} & \tilde{u} \in \mathrm{BV}(\Gamma) && (i) \\ \exists \mathcal{R} \subset \mathbb{R}, \quad & \mathcal{H}^1(\mathbb{R} \setminus \mathcal{R}) = 0 \quad \textit{and} && \\ \forall \lambda \in \mathcal{R}, \quad & \bullet\ \mathcal{H}^1(\partial_{\mathrm{M}} X_\lambda u) < +\infty && (ii) \\ & \bullet\ \mathcal{H}^0(\partial_{\mathrm{M}} X_\lambda \tilde{u}) < +\infty && (iii) \\ & \bullet\ X_\lambda \tilde{u} = \lim_{\mu \to \lambda} X_\mu \tilde{u} && (iv) \\ & \bullet\ \mathcal{H}^0(\partial_{\mathrm{M}} X_\lambda u \cap \Gamma) < +\infty && (v) \\ & \bullet\ \forall x \in \partial_{\mathrm{M}}(X_\lambda \tilde{u}),\ D^1(x, \partial_{\mathrm{M}}(X_\lambda u)) = 1 && (vi) \end{aligned}$$

If $x \in A_\lambda := \partial_{\mathrm{M}}(X_\lambda \tilde{u})$ for some λ, we say that x is admissible.

PROOF : The existence of the curve Γ and the point (i) of the lemma are direct consequences of Lemma 3.2.1. Claims (ii), (iii), (iv), (v) and (vi) that we shall now prove roughly mean that we can find a dense set of values (λ) assumed by u such that :

1. the lines of level λ converging to the occlusion have finite length (claim (ii))
2. they can be associated with a finite number of points on the occlusion boundary (claims (iii), (v)) where they have density 1 (claim (vi)).
3. these points can be approximated by sequences of points associated with lower and greater levels (claim (iv)).

By the coarea formula

$$\int_{-\infty}^{\infty} P(X_\lambda u) d\lambda < +\infty$$

thus there exists $\mathcal{R}_0 \subset \mathbb{R}$ such that $\mathcal{H}^1(\mathbb{R} \setminus \mathcal{R}_0) = 0$ and for every $\lambda \in \mathcal{R}_0$, $P(X_\lambda u) = \mathcal{H}^1(\partial^* X_\lambda u) < +\infty$. Since $\mathcal{H}^1(\partial_{\mathrm{M}} X_\lambda u \setminus \partial^* X_\lambda u) = 0$ we deduce that $\mathcal{H}^1(\partial_{\mathrm{M}} X_\lambda u) < \infty$ for every $\lambda \in \mathcal{R}_0$ and (ii) ensues. The coarea formula applied to $\tilde{u}$ yields

$$\int_{\mathcal{R}_0} P(X_\lambda \tilde{u}) d\lambda \leq \int_{-\infty}^{\infty} P(X_\lambda \tilde{u}) d\lambda < \infty$$

thus there exists $\mathcal{R}_1 \subset \mathcal{R}_0$ such that $\mathcal{H}^1(\mathbb{R} \setminus \mathcal{R}_1) = 0$ and for every $\lambda \in \mathcal{R}_1$, $P(X_\lambda \tilde{u}) = \mathcal{H}^0(\partial^* X_\lambda \tilde{u}) < +\infty$. Since $\partial_{\mathrm{M}} X_\lambda \tilde{u} = \partial^* X_\lambda \tilde{u}$ we deduce that $\forall \lambda \in \mathcal{R}_1$, $\mathcal{H}^0(\partial_{\mathrm{M}} X_\lambda \tilde{u}) < +\infty$ which establishes (iii).

Claim (iv), where convergence means convergence with respect to Hausdorff measure $\mathcal{H}^1$, can be proven with the same argument as in Lemma 2.6.3 and ensures that we can restrict to those level sets of $\tilde{u}$ that can be approximated from below as well as from above. More precisely it ensures that there exists some dense set $\mathcal{R}_2 \subset \mathcal{R}_1$ of levels such that

$$X_\lambda \tilde{u} = \bigcap_{\nu < \lambda} X_\nu \tilde{u} = \bigcup_{\nu > \lambda} X_\nu \tilde{u}$$

up to $\mathcal{H}^1$-negligible sets.

It is worth noticing that in general $A_\lambda = \partial_{\mathrm{M}}(X_\lambda \tilde{u})$ may differ from $\partial_{\mathrm{M}}(X_\lambda u) \cap \Gamma$ by more than a $\mathcal{H}^1$-negligible set. This can happen when Γ coincides with some (or part of) level lines of u. Furthermore we do not even necessarily have that $\partial_{\mathrm{M}}(X_\lambda \tilde{u}) \subset \partial_{\mathrm{M}}(X_\lambda u) \cap \Gamma$. Take for instance u with some level lines crossing Γ at a cusp point. We shall now prove claim (v) which implies that each level line associated with a level in $\mathcal{R}$ intersects Γ at finitely many points. Let us recall from the proof of Lemma 3.2.1 that there exists some $h > 0$ such that $\Gamma = \Gamma_h := \{x : d(x, \tilde{\Omega}) = h\}$ where $\tilde{\Omega}$ strictly contains the original occlusion Ω and has C^∞ boundary. Now, for almost every $\lambda \in \mathbb{R}$, $X_\lambda u = \{u \geq \lambda\}$ has finite perimeter in $\mathbb{R}^2 \setminus \overline{\Omega}$, thus $\partial_{\mathrm{M}}\{u \geq \lambda\}$ is countably $\mathcal{H}^1$-rectifiable. Denoting $f := d$

the distance function with respect to $\tilde{\Omega}$, recall that f is 1-Lipschitz and we deduce from the Coarea formula for Lipschitz functions [3, 2.93] that for almost every $\lambda \in \mathbb{R}$,

$$\int_0^{+\infty} \mathcal{H}^0(\partial_{\mathrm{M}} X_\lambda u \cap f^{-1}(h))\, dh \leq \int_{\partial_{\mathrm{M}} X_\lambda u} |\nabla f(x)|\, d\mathcal{H}^1(x) \leq \mathcal{H}^1(\partial_{\mathrm{M}} X_\lambda u)$$

thus

$$\begin{aligned} \int_{\mathbb{R}} \int_0^{+\infty} \mathcal{H}^0(\partial_{\mathrm{M}} X_\lambda u \cap \Gamma_h)\, dh\, d\lambda &\leq \int_{\mathbb{R}} \mathcal{H}^1(\partial_{\mathrm{M}} X_\lambda u)\, d\lambda \\ &\leq |Du|(\mathbb{R}^2 \setminus \overline{\Omega}) \\ &< +\infty \end{aligned}$$

By Fubini's Theorem we deduce that

$$\int_0^{+\infty} \int_{\mathbb{R}} \mathcal{H}^0(\partial_{\mathrm{M}} X_\lambda u \cap \Gamma_h)\, d\lambda\, dh < +\infty$$

thus for almost every $h > 0$, $\int_{\mathbb{R}} \mathcal{H}^0(\partial_{\mathrm{M}} X_\lambda u \cap \Gamma_h)\, d\lambda$ is finite. Hence, we can select a dense set of levels $\mathcal{R} \subset \mathcal{R}_2$ such that $\forall \lambda \in \mathcal{R}$, $\mathcal{H}^0(\partial_{\mathrm{M}} X_\lambda u \cap \Gamma_h) < +\infty$. Claim (v) ensues by simply selecting some h satisfying this property as well as Lemma 3.2.1. Let us now prove that $\forall \lambda \in \mathcal{R}$, $\forall x \in A_\lambda$, $D^1(x, \partial_{\mathrm{M}}(X_\lambda u)) > 0$. First recall the following result ([8], Lemma 8) :

Lemma 3.2.3 *Let E be a set of finite perimeter and $y, z \in \mathbb{R}^2$ such that $D(y, E) = 1$, $D(z, E) = 0$, $D^1(y, \partial_{\mathrm{M}} E) = 0$ and $D^1(z, \partial_{\mathrm{M}} E) = 0$. Then any curve joining y and z will intersect $\{t : D^1(t, \partial_{\mathrm{M}} E) = 1\}$.*

Let $E := X_\lambda u$. Since $x \in A_\lambda = \partial_{\mathrm{M}} X_\lambda \tilde{u}$, $\overline{D}^1(x, X_\lambda \tilde{u}) > 0$ and $\overline{D}^1(x, (X_\lambda \tilde{u})^{\mathrm{c}}) > 0$. From (iv) above we deduce that there exist two points y and z arbitrarily close to x such that $\tilde{u}(y) > \lambda$ and $\tilde{u}(z) < \lambda$. From our assumption that $u_{|S_u} = +\infty$ and since $\int_\Gamma |\tilde{u}| dx < +\infty$, we infer that y and z can be chosen in order to be points of approximate continuity for u, thus $u^-(y) = u^+(y) > \lambda$ and $u^-(z) = u^+(z) < \lambda$. Hence, $D(y, X_\lambda u) = 1$ and $D(z, X_\lambda u) = 0$. In addition, we deduce from (iii) that $D^1(y, A_\lambda) = D^1(z, A_\lambda) = 0$ and the assumptions of the previous lemma are satisfied. Since y and z are arbitrarily close to x and, by (v), $\mathcal{H}^0(\partial_{\mathrm{M}} X_\lambda u \cap \Gamma) < +\infty$, it follows that $D^1(x, \partial_{\mathrm{M}}(X_\lambda u)) = 1$ and (vi) ensues. Let us finally emphasize that (iii) implies that A_λ is a finite set for every $\lambda \in \mathcal{R}$. □

In the sequel, we shall call admissible occlusion any set whose boundary has the properties of Lemma 3.2.2. By Lemma 3.2.1, we can deduce an admissible occlusion from any occlusion.

Let x be an admissible point in Γ. In view of previous lemmas we can define for almost every $\lambda \in [\tilde{u}(x-), \tilde{u}(x+)]$ an average direction

$$\nu_\lambda(x) := \nu_{\lambda,B}(x) = \fint_B \nu_{X_\lambda}\, d|\partial X_\lambda| = \frac{1}{\mathcal{H}^1(\partial^* X_\lambda \cap B)} \int_{\partial^* X_\lambda \cap B} \nu_{X_\lambda}\, d\mathcal{H}^1 \tag{3.2.1}$$

where $B = B(x, r_0)$, r_0 is such that $d(\Gamma, \Omega) > r_0$ and ν_{X_λ} denotes the outer normal at every point of the reduced boundary $\partial^* X_\lambda$. Without loss of generality, we can assume that the integral goes over the "connected component" of x within $B \cap \partial^* X_\lambda$, that is the set $C \subset B \cap \partial^* X_\lambda$ such that for $\mathcal{H}^1$-almost every $y \in C$, $D^1(y, C) = 1$ and C contains a curve joining x to y. Consequently, each admissible point x is associated for almost every $\lambda \in [\tilde{u}(x-), \tilde{u}(x+)]$ with an average direction $\nu_\lambda(x)$ and the orientation $o_\lambda(x) = \pm 1$, which refers to the orientation of the normal along C. We take as a convention that when C is watched from the occlusion boundary, $o_\lambda = 1$ if ν points toward the left of the curve and $o_\lambda = -1$ otherwise. Now, recall from Lemma 3.2.2 that for every $\lambda \in \mathcal{R}$, A_λ is a finite set. Moreover, we deduce from the properties of level lines that $\#A_\lambda$, the cardinal of A_λ, is even and

$$\#\{x \in A_\lambda : o_\lambda(x) = 1\} = \#\{x \in A_\lambda : o_\lambda(x) = -1\}$$

In the sequel we shall denote

$$\begin{aligned} A_\lambda^1 &:= \{x \in A_\lambda : o_\lambda(x) = 1\} \\ A_\lambda^{(-1)} &:= \{x \in A_\lambda : o_\lambda(x) = -1\} \end{aligned}$$

A logical variational criterion for the interpolant u is

$$E(u) = \int |Du|(1 + |\mathrm{curv} u|^p), \quad p \geq 1,$$

as proposed in [32], since this criterion yields short and not too curvy level lines compatible with Kanizsa's theory. Now, as shown in Bellettini *et al* [4], this criterion is not lower semicontinuous. Bellettini *et al* studied relaxed versions of E. We shall propose another relaxed version of E, which is compatible with Kanizsa's amodal completion theory. According to this theory, *an amodal completion is not a function*, but a set of lines or contours extending the contours of the image below the occluded part. These contours may even cross, but we shall exclude this possibility here, since we want a disocclusion as close as possible to a function. Indeed, from a noncrossing set of contours interpolating level lines, we can easily reconstruct a single function u whose level lines coincide almost everywhere with the contours (see figure 3.3). It must be emphasized that the solution to the equation $|Du|\mathrm{curv} u = D^2 u(\frac{Du^\perp}{|Du|}, \frac{Du^\perp}{|Du|}) = 0$ can be obtained in the particular case where $p = 1$. Whenever $p > 1$ the interpolating level lines are smooth curves and no more straight in general.

In order to solve the disocclusion problem we need to distinguish the cases when $p = 1$ and $p > 1$. If $p > 1$ we define $\mathcal{F}_p$ as the set of all measurable functions $\gamma : [0, 1] \to \overline{\Omega}$ such that $\gamma(0), \gamma(1) \in \Gamma$, $\gamma \in \mathrm{W}^{1,1}(0, 1)$, $|\gamma'(t)|$ is constant and strictly positive almost everywhere on $[0, 1]$, and the curvature of γ as a function of arc-length belongs to $\mathrm{L}^p(0, \mathcal{L}(\gamma))$. In addition, we assume that the trace of γ in $\overline{\Omega}$, also denoted by γ, is a

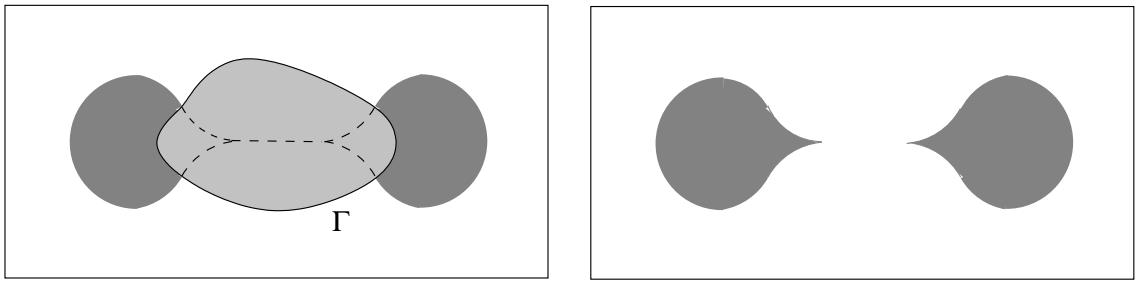

Figure 3.3: Left : disocclusion as a set of contours, $E(\mathcal{D}) < \infty$
Right : the associated solution u, $E(u) = +\infty$ if $p > 1$.

simple curve. Recall that $\gamma' \in \mathrm{L}^1(0,1)$ implies that γ has finite length and we can define the arc-length as

$$s(t) = \int_0^t |\gamma\prime(z)|dz$$

Since $|\gamma'(t)|$ is assumed to be constant almost everywhere on $[0,1]$ we infer that for almost every $t \in [0,1]$, $s(t) = t\mathcal{L}(\gamma)$ with $\mathcal{L}(\gamma)$ the curve length. In addition, the curve admits almost everywhere a tangent vector $\overrightarrow{T} = \gamma'(s) = \frac{\gamma'(t)}{|\gamma'(t)|}$. The curvature of γ at t is given by

$$\mathrm{curv}(t) = \frac{\det(\gamma'(t), \gamma''(t))}{|\gamma'(t)|^3}$$

and its absolute value can be written with respect to arc-length as

$$|\mathrm{curv}(s)| = |\gamma''(s)|$$

where $\gamma''(s)$ denotes here the second distributional derivative of γ with respect to s. From our assumptions, it is equivalent to say that γ as a function of s is in $\mathrm{W}^{2,p}(0, \mathcal{L}(\gamma))$ which implies

$$\int_0^{\mathcal{L}(\gamma)} (1 + |\gamma''(s)|^p)ds < +\infty$$

From $s(t) = t\mathcal{L}(\gamma)$ we deduce that

$$\frac{d^2\gamma}{ds^2} = \frac{1}{[\mathcal{L}(\gamma)]^2}\frac{d^2\gamma}{dt^2},$$

thus

$$\int_0^{\mathcal{L}(\gamma)} (1 + |\gamma''(s)|^p)ds = \int_0^1 \left(|\frac{d\gamma}{dt}| + [\mathcal{L}(\gamma)]^{1-2p} \left|\frac{d^2\gamma}{dt^2}\right|^p \right) dt \qquad (3.2.2)$$

and finally $\gamma \in \mathrm{W}^{2,p}(0,1)$. In order to deal with those curves of null length whose endpoints coincide on Γ, we add to $\mathcal{F}_p$ those trivial measurable functions $\gamma : [0,1] \to \overline{\Omega}$ such that

$\gamma(0) = \gamma(1) \in \Gamma$ and $|\frac{d\gamma}{dt}| = |\frac{d^2\gamma}{dt^2}| = 0$ everywhere in $(0,1)$. Obviously, these curves belong to $\mathrm{W}^{2,p}(0,1)$. Then we define

$$\mathcal{M}_p = \quad \{\gamma \in \mathcal{F}_p : \exists \lambda \in \mathcal{R} \text{ such that } \gamma(0) \in A^1_\lambda,\ \gamma(1) \in A^{(-1)}_\lambda\}$$

and each curve of $\mathcal{M}_p$ shall be referred as $\gamma(x,\lambda)$ with $x = \gamma(0) \in A^1_\lambda$. It is worth noticing that $\gamma \in \mathrm{W}^{2,p}(0,\mathcal{L}(\gamma))$ implies that γ is continuously differentiable on $[0,\mathcal{L}(\Gamma)]$. Then we associate any γ in $\mathcal{M}_p$ with the energy

$$E_p(\gamma) = \begin{cases} \displaystyle\int_0^{\mathcal{L}(\gamma)} (1 + |\gamma''(s)|^p) ds + \langle \tau(0)\widehat{,\gamma'}(0)\rangle + \langle \tau(1)\widehat{,\gamma'}(1)\rangle & \text{if } \mathcal{L}(\Gamma) > 0 \\ \langle \tau(0)\widehat{,\gamma'}(0)\rangle + \langle \tau(1)\widehat{,\gamma'}(1)\rangle & \text{otherwise} \end{cases} \tag{3.2.3}$$

where $\tau(0) = \nu_\lambda(\gamma(0))^\perp$ and $\tau(1) = \nu_\lambda(\gamma(1))^\perp$ in view of (3.2.1). By $\widehat{(v,w)}$ we denote the absolute value of the angle modulo 2π between two vectors v and w in $\mathbb{R}^2$. The use of two angular terms is due to the impossibility to extend outside Ω the regularity of the level lines (γ). Take indeed the case where two level lines join at a point x of Γ without being tangential at x. It is not possible to find two smooth curves continuing these lines without crossing.

The case $p = 1$ must be treated apart since the space $\mathrm{W}^{1,1}$ lacks of fair properties due to the fact that L^1 is not reflexive. Indeed, it is well known that if $p > 1$ and (f_k) is a sequence in $\mathrm{W}^{1,p}(U)$ with U bounded, ∂U Lipschitz and $\sup \|f_k\|_{\mathrm{W}^{1,p}(U)} < \infty$ then there exists a subsequence converging in $\mathrm{L}^1(U)$ to a function $f \in \mathrm{W}^{1,p}(U)$. This result does not hold if $p = 1$ since we can only ensure that $f \in \mathrm{BV}(U)$. Consequently, we define $\mathcal{F}_1$ as the set of all measurable functions $\gamma : [0,1] \to \overline{\Omega}$ such that $\gamma \in \mathrm{W}^{1,1}(0,1)$, $|\gamma'(t)|$ is constant and strictly positive almost everywhere on $[0,1]$ and the curvature of γ as a function of the arc-length is a vector-valued Radon measure with finite total variation, or, in other words, γ' as a function of the arc-length s is in $\mathrm{BV}(0,\mathcal{L}(\gamma))$. In addition, we assume here again that the trace of γ in $\overline{\Omega}$ is a simple curve. Remark that we can deduce from our assumptions that $\gamma \in \mathrm{W}^{1,1}(0,1)$ and $\gamma' \in \mathrm{BV}(0,1)$.
Denoting by $\int_0^{\mathcal{L}(\gamma)} |\gamma''(s)| ds$ the total variation of $\gamma''(s)$ in $[0,\mathcal{L}(\gamma)]$, we deduce that

$$\int_0^{\mathcal{L}(\gamma)} (1 + |\gamma''(s)|) ds = \int_0^1 \left(|\frac{d\gamma}{dt}| + \frac{1}{\mathcal{L}(\gamma)} |\frac{d^2\gamma}{dt^2}| \right) dt < +\infty \tag{3.2.4}$$

Like $\mathcal{F}_p$, we add to $\mathcal{F}_1$ all those curves of null length whose endpoints coincide on Γ and finally we define

$$\mathcal{M}_1 = \quad \{\gamma \in \mathcal{F}_1 : \exists \lambda \in \mathcal{R} \text{ such that } \gamma(0) \in A^1_\lambda,\ \gamma(1) \in A^{(-1)}_\lambda\}$$

and each curve of $\mathcal{M}_1$ shall be referred as $\gamma(x,\lambda)$ with $x = \gamma(0) \in A^1_\lambda$. Let us now emphasize that in contrast with the case $p > 1$, we can not ensure that γ is continuously

differentiable on $[0,1]$. Thus, the behavior of the angular terms at endpoints for a subsequence of curves is hardly controllable. The simplest way to avoid this problem is to artificially modify the boundary conditions. For every $\lambda \in \mathcal{R}$ and $x \in A_\lambda$ we define the line of level λ arriving at x as the segment $S(x,\lambda)$ of length $\alpha \ll 1$ making the angle $\tau(0)$ with Γ at x. To each curve $\gamma \in \mathcal{M}_1$ related to the level λ we associate the curve $\tilde{\gamma} : [0, \mathcal{L}(\gamma) + 2\alpha] \to \mathbb{R}^2$ with respect to arc-length such that

$$\text{if } \mathcal{L}(\gamma) > 0 \quad \begin{cases} \tilde{\gamma} = S(\gamma(0),\lambda) & \text{on } [0,\alpha] \\ \tilde{\gamma} = \gamma & \text{on } [\alpha, \mathcal{L}(\gamma)+\alpha] \\ \tilde{\gamma} = S(\gamma(1),\lambda) & \text{on } [\mathcal{L}(\gamma)+\alpha, \mathcal{L}(\gamma)+2\alpha] \end{cases}$$

$$\text{if } \mathcal{L}(\gamma) = 0 \quad \begin{cases} \tilde{\gamma} = S(\gamma(0),\lambda) & \text{on } [0,\alpha] \\ \tilde{\gamma} = S(\gamma(1),\lambda) & \text{on } [\alpha, 2\alpha] \end{cases}$$

and we define the energy of γ as

$$E_1(\gamma) = \int_0^{\mathcal{L}(\gamma)+2\alpha} (1 + |\tilde{\gamma}''(s)|) ds \tag{3.2.5}$$

Remark that

$$E_1(\gamma) \leq \int_0^{\mathcal{L}(\gamma)} (1 + |\gamma''(s)|) ds + 2\alpha + 2\pi$$

so that $\gamma \in \mathrm{W}^{1,1}(0,1)$ and $\gamma' \in \mathrm{BV}(0,1)$ imply $E_1(\gamma) < +\infty$. In the sequel, unless specified, we shall implicitly deal with the extension $\tilde{\gamma}$ of any curve $\gamma \in \mathcal{M}_1$.

Let us consider a set of curves in $\mathcal{M}_p$, $p \geq 1$, connecting the admissible points of Γ two by two – or possibly with themselves – and such that two different curves do not cross within Ω. Remark that the noncrossing property holds as well at curves endpoints in the sense that the sign of $\tilde{u}'$ along Γ determines the relative position of two curves starting at x. Now, observe that by Lemma 3.2.2, each level $\lambda \in \mathcal{R}$ is associated with a finite number of curves $(\gamma_{i,\lambda})$ where $i \in I$ and $\#I < +\infty$. For any $i \in I$, $\gamma_{i,\lambda}$ induces a partition of Ω in two sets. Walking the curve $\gamma_{i,\lambda}$ from $\gamma_{i,\lambda}(0)$, we define $X_{i,\lambda}$ as the left set if $o_\lambda(\gamma_{i,\lambda}(0)) = 1$ and the right set otherwise. Then we define :

$$X_\lambda := \cup_{i \in I} X_{i,\lambda} \tag{3.2.6}$$

and the reconstructed function u_d can be obtained by setting for every $x \in \Omega$,

$$u_d(x) := \sup\{\lambda \in \tilde{\mathcal{R}} : \, x \in X_\lambda\} \tag{3.2.7}$$

where $\tilde{\mathcal{R}}$ is a countable and dense subset of $\mathcal{R}$. By Theorem 2.6.4, u_d is a measurable function on Ω whose upper level sets coincide with the X_λ's up to Lebesgue negligible sets. Finally we define the reconstructed function associated with u as

$$u_r(x) = \begin{cases} u(x) & \text{if } x \in \mathbb{R}^2 \setminus \overline{\Omega} \\ u_d(x) & \text{if } x \in \Omega \end{cases} \tag{3.2.8}$$

We call p-disocclusion of u with respect to Ω any reconstructed function u_d obtained like above and such that the associated set of curves, denoted by $\mathcal{D}$ has finite total energy $E_p(\mathcal{D})$ with

$$E_p(\mathcal{D}) = \int_{\mathcal{R}} \sum_{x \in A^1_\lambda} E_p(\gamma(x,\lambda)) d\lambda \tag{3.2.9}$$

where we restrict to A^1_λ in order to avoid redundancy. For simplicity we shall also call $\mathcal{D}$ a disocclusion.

Theorem 3.2.4 *Let $E \subset \mathbb{R}^N$ be an occlusion and $u \in \mathrm{BV}(\mathbb{R}^2 \setminus \overline{E})$ such that $|u| < M$. Let $\Omega \supset\supset E$ be an admissible occlusion. Then there exists a 1-disocclusion of u with minimal energy and the extended function $u_r \in \mathrm{BV}(\mathbb{R}^2)$.*
If $p > 1$ and $\tilde{u}$ assume a finite number of levels on $\Gamma = \partial\Omega$ then there exists a p-disocclusion of u with minimal energy and the extended function $u_r \in \mathrm{BV}(\mathbb{R}^2)$.

PROOF : If $\tilde{u}$ assume a finite number of values $(\lambda) = I$, with $\#I < +\infty$ then we shall replace $E_p(\mathcal{D})$ with

$$E_p(\mathcal{D}) = \sum_{\lambda \in I} \sum_{x \in A^1_\lambda} E_p(\gamma(x,\lambda)) d\lambda$$

However, Claim#1, Claim#2 and Claim#3 remain valid without this assumption and we shall use for proving them the original definition of $E_p(\mathcal{D})$. Furthermore, notice that we shall keep for simplicity the notation $\mathcal{R}$ to denote the dense set defined in Lemma 3.2.2, despite the fact that u takes now its values only in $(-M, M)$.

CLAIM#1 : $\forall p \geq 1$, *there exists at least a trivial (non optimal) p-disocclusion $\mathcal{D}_0$.*

Remark first that the occlusion boundary $\Gamma = \partial\Omega$ is smooth and set $u_{|\Omega} = -M$. Let $C = \sup_{s \in (0, \mathcal{L}(\Gamma))} |\kappa(s)|$ with κ the curvature along Γ with respect to arc-length.

• If $p > 1$ one gets $\forall \lambda \in \mathcal{R}$,

$$\sum_{x \in A^1_\lambda} \int_0^{\mathcal{L}(\gamma)} (1 + |\gamma''(s)|^p) ds \leq \sum_{x \in A^1_\lambda} (1 + C^p)\mathcal{L}(\Gamma) = (1 + C^p)\mathcal{L}(\Gamma) \# A^1_\lambda$$

Moreover

$$\int_{\mathcal{R}} \sum_{x \in A^1_\lambda} \langle \tau_{\lambda,x}(0), \widehat{\gamma'_{x,\lambda}(0_+)} \rangle + \langle \tau_{\lambda,x}(1), \widehat{\gamma'_{x,\lambda}(1-)} \rangle < 2\pi \int_{\mathcal{R}} \# A^1_\lambda$$

Thus

$$\begin{aligned} E_p(\mathcal{D}_0) &\leq (2\pi + (1+C^p)\mathcal{L}(\Gamma)) \int_{\mathcal{R}} \#A^1_\lambda \\ &\leq (2\pi + (1+C^p)\mathcal{L}(\Gamma)) \int_{\mathbb{R}} \mathcal{H}^0(\partial_M X_\lambda \tilde{u}) \\ &\leq (2\pi + (1+C^p)\mathcal{L}(\Gamma)) \int_{\Gamma} |\tilde{u}'| dx \\ &< +\infty \end{aligned}$$

since $\tilde{u}$ has bounded variation and Claim#1 ensues for the case $p > 1$.

• If $p = 1$ then

$$\begin{aligned} \sum_{x \in A^1_\lambda} \int_0^{\mathcal{L}(\gamma)+2\alpha} (1 + |\tilde{\gamma}''(s)|) ds &= \sum_{x \in A^1_\lambda} \left(\int_0^{\mathcal{L}(\gamma)} (1 + |\gamma''(s)|) ds + 2\alpha \right. \\ &\quad \left. + (\langle \tau_{\lambda,x}(0), \widehat{\gamma'_{x,\lambda}(0_+)} \rangle + \langle \tau_{\lambda,x}(1), \widehat{\gamma'_{x,\lambda}(1-)} \rangle) \right) \end{aligned}$$

In view of argument above and since $\sum_{x \in A^1_\lambda} (2\alpha) = 2\alpha \# A^1_\lambda$ and $\int_{\mathcal{R}} \# A^1_\lambda < +\infty$ we infer that $E_1(\mathcal{D}_0) < +\infty$. Therefore, $\forall p \geq 1$, there exists a minimizing sequence $\mathcal{D}_n$ of p-disocclusions whose first element has finite total energy. Each p-disocclusion $\mathcal{D}_n$ consists of those curves $\gamma^n(x,\lambda)$ where $\lambda \in \mathcal{R}$ and $x \in A^1_\lambda$ and its energy is

$$E_p(\mathcal{D}_n) = \int_{\mathcal{R}} \sum_{x \in A^1_\lambda} E_p(\gamma^n(x,\lambda))$$

CLAIM#2 : $\forall p \geq 1$, *there exists a subsequence* $\mathcal{D}_m$, *and a countable and dense set* $\Lambda \in \mathcal{R}$ *such that*

$$\forall \lambda \in \Lambda,\ \forall x \in A^1_\lambda,\ \sup_m E_p(\gamma^m(x,\lambda)) < +\infty$$

This claim ensues from the following lemma with $f_n(\lambda) = \sum_{x \in A^1_\lambda} E_p(\gamma^n(x,\lambda))$ and remarking that $\|f_n\|_{\mathrm{L}^1} = E_p(\mathcal{D}_n)$ and $\sup_n \|f_n\|_{L^1} \leq E_p(\mathcal{D}_0) < +\infty$.

Lemma 3.2.5 *Let* $f_n \in \mathrm{L}^1(\mathbb{R})$ *such that* $\sup_n \|f_n\|_{L^1} < +\infty$. *Then there exists a subsequence* (f_m) *and a countable and dense set* $\Lambda \subset \mathbb{R}$ *such that*

$$\forall \lambda \in \Lambda,\ \sup_m |f_m(\lambda)| < +\infty$$

PROOF : Let us first prove that for every interval I in $\mathbb{R}$, $\exists \lambda \in I$ and a subsequence $(f_{m(\lambda)})$ such that $\sup_m |f_{m(\lambda)}(\lambda)| < +\infty$. It is true, otherwise for every $\lambda \in I$, $|f_n(\lambda)| \to +\infty$ which is in contradiction with Fatou's Lemma. Indeed,

$$\int_I \liminf |f_n| d\lambda \leq \liminf \int_I |f_n| d\lambda \leq \sup_n \|f_n\|_{L^1} < +\infty$$

Now let us consider all those dyadic intervals $(k2^{-j}, (k+1)2^{-j})$, $k \in \mathbb{N}$, $j \in \mathbb{Z}$, which form a countable and dense covering of $\mathbb{R}$. From the argument above, there exists in each of these intervals some λ and a sequence $f_{m(\lambda)}$ such that $\sup_m |f_{m(\lambda)}(\lambda)| < +\infty$. Then, the lemma ensues by a diagonal extraction. □

From now on $\mathcal{D}_m$ denotes the subsequence and $\Lambda = (\lambda_k)$ the countable and dense set defined in Claim#2.

CLAIM#3 : $\forall p \geq 1$, *there exists a subsequence* $\mathcal{D}_k$ *of* $\mathcal{D}_m$ *such that* $\forall \lambda \in \Lambda$ *and* $x \in A^1_\lambda$, $\gamma^k(x,\lambda)$ *is converging to some curve* $\gamma(x,\lambda)$.

Since $\sup_m E_p(\gamma^m(x,\lambda)) < +\infty$, and in particular $\sup_m \mathcal{L}(\gamma^m(x,\lambda)) < +\infty$ one gets

$$\begin{aligned} &\sup_m \|\gamma^m\|_{W^{2,p}(0,1)} < +\infty && \text{if } p > 1 \\ &\sup_m (\|\gamma^m\|_{W^{1,1}(0,1)} + \|(\gamma^m)'\|_{\mathrm{BV}(0,1)}) < +\infty && \text{if } p = 1 \end{aligned}$$

We deduce from the compactness properties of $W^{1,p}$ and BV and by a diagonal extraction argument that there exists a subsequence $\mathcal{D}_k$ such that $\forall \lambda \in \Lambda$, $\forall x \in A^1_\lambda$:

- if $p > 1$, $(\gamma^k(x,\lambda))$ converges weakly in $W^{2,p}(0,1)$ to $\gamma(x,\lambda)$, thus uniformly in $\mathrm{C}^1(0,1)$
- if $p = 1$, $(\gamma^k(x,\lambda))$ converges in $W^{1,1}(0,1)$ to $\gamma(x,\lambda)$
  $\gamma'(x,\lambda) \in \mathrm{BV}(0,1)$
  $$\int_0^1 |\gamma''(x,\lambda)|dt \leq \liminf_{k\to\infty} \int_0^1 |(\gamma^k)''(x,\lambda)|dt$$

In particular, and in both cases, $\mathcal{L}(\gamma^k) \to \mathcal{L}(\gamma)$ since $((\gamma^k)'(x,\lambda)) \to \gamma'(x,\lambda)$ in $\mathrm{L}^1(0,1)$. In addition, possibly up to a new diagonal extraction, we can ensure that $|(\gamma^k)'(x,\lambda)| \to |\gamma'(x,\lambda)|$ almost everywhere on $[0,1]$, hence $|\gamma'(x,\lambda)|$ is constant almost everywhere on $[0,1]$ so that each curve $\gamma(x,\lambda)$ is parametrized with constant velocity. Recall now that if I is an open interval of $\mathbb{R}$ (either bounded or not), then $W^{1,1}(I) \subset \mathrm{C}(\overline{I})$ with continuous injection and that any bounded sequence (u_n) in $W^{1,1}(I)$ admits a subsequence which converges everywhere on I [5]. In our case, this implies that $\gamma(x,\lambda)$ is a well-defined simple curve and that the limit curves do not cross within Ω since the curves (γ^k) do not cross. This result is more obvious when $p > 1$ since the convergence is uniform in $\mathrm{C}^1(0,1)$.

At this point of the proof and for the case $p > 1$ with $\tilde{u}$ assuming a finite number of values on Γ, we can state that there exists a limit p-disocclusion $\mathcal{D}$. The fact that this disocclusion has minimal energy shall be established in Claim#5. Claim#4 shall allow us to define in the case $p = 1$ the limit curves $\gamma(x,\lambda)$ for a dense set of $\lambda \in \mathcal{R}\backslash\Lambda$ and $x \in A^1_\lambda$.

CLAIM#4 : *Let* $p = 1$. *For almost every* $\lambda \in \mathcal{R}$ *and every* $x \in A^1_\lambda$, *the limit curve* $\gamma(x,\lambda)$ *can be defined as limit of curves* $\gamma(x,\lambda)$ *where* $\lambda \in \Lambda$.

First remark that any 1-disocclusion $\mathcal{D}_n$ can be replaced with a 1-disocclusion made only of geodesic paths in $\overline{\Omega}$ and with smaller total energy – by geodesic paths we mean those curves of minimal length totally included in $\overline{\Omega}$. Indeed, if γ is a curve joining two points x and y on Γ, the geodesic path γ_G between x and y has obviously the property that $\mathcal{L}(\gamma_G) \leq \mathcal{L}(\gamma)$ and

$$\int_0^{\mathcal{L}(\gamma_g)+2\alpha} |\tilde{\gamma}_g''(s)|ds \leq \int_0^{\mathcal{L}(\gamma)+2\alpha} |\tilde{\gamma}''(s)|ds$$

Moreover, since Γ is C^∞ it is easily seen that $\gamma_g \in C^\infty(0,1)$. In addition, if $C = \sup_{s\in(0,\mathcal{L}(\Gamma))} |\kappa(s)|$ denotes the supremum of the curvature along Γ and $L = \mathcal{L}(\Gamma)$ it follows that

$$\int_0^{\mathcal{L}(\gamma_g)+2\alpha} (1 + |\tilde{\gamma}_g''(s)|)ds \leq L + 2\alpha + LC + 2\pi$$

and

$$\int_0^1 \left(|\frac{d\tilde{\gamma}_g}{dt}| + |\frac{d^2\tilde{\gamma}_g}{dt^2}| \right) dt \leq L + 2\alpha + L(LC + 2\pi) \tag{3.2.10}$$

Moreover, from a given set of noncrossing curves constituting a 1-disocclusion, we can replace all these curves by geodesic paths with same endpoints. Obviously these geodesic paths do not cross and from the argument above we infer that the total energy is less than the energy of the original 1-disocclusion. Furthermore, and this is the crucial point, we deduce from relation (3.2.10) that all these new curves have uniformly bounded energy. Consequently, we shall consider from now that we are actually dealing with a minimizing sequence of disocclusions $\mathcal{D}_n$, each of them made only of geodesic paths, and everything that was stated above remains valid. In particular, the limit curves $\gamma(x,\lambda)$ for $\lambda \in \Lambda$ and $x \in A^1_\lambda$ are geodesic paths. This ensues from the following result : if (x_n) and (y_n) are two sequences of points in $\overline{\Omega}$ converging to $x, y \in \overline{\Omega}$ with respect to the geodesic distance in $\overline{\Omega}$, if $g_n : [0,1] \to \overline{\Omega}$ denotes the geodesic path between x_n and y_n parametrized with constant velocity, then g_n uniformly converges to some geodesic path g [35].

It must be noticed that when $p > 1$, we have restricted ourselves to the case where $\tilde{u}$ assumes finitely many values on Γ because we were unable to find any uniform bound for the energy of each curve of a p-disocclusion. Remark that we do not claim that this bound does not exist. Actually, the fact that the sequence minimizes the energy and that curves do not intersect let us think that a minimal p-disocclusion exists even when $\tilde{u}$ assume infinitely many values on Γ.

Let us now come back to the proof of Claim#4 and consider $\lambda \in \mathcal{R}$. From the definition of $\mathcal{R}$ there exist two sequences $(\lambda_{k_l^-})$ and $(\lambda_{k_l^+})$ in Λ such that $\lambda_{k_l^-} \to \lambda^-$ and $\lambda_{k_l^+} \to \lambda^+$. Since $\mathcal{R} \subset \{\lambda : X_\lambda \tilde{u} = \lim_{\mu\to\lambda} X_\mu \tilde{u}\}$, there exist two sequences of points $x_l^+ \in A^1_{\lambda_{k_l^+}}$

and $x_l^- \in A^1_{\lambda_{k_l^-}}$ converging to x. From (3.2.10) we infer that the curves $(\gamma(x_l^-, \lambda_{k_l^-}))_{l\in\mathbb{N}}$ and $(\gamma(x_l^+, \lambda_{k_l^+}))_{l\in\mathbb{N}}$ are uniformly bounded in $\mathrm{W}^{1,1}(0,1)$ whereas $(\gamma'(x_l^-, \lambda_{k_l^-}))_{l\in\mathbb{N}}$ and $(\gamma'(x_l^+, \lambda_{k_l^+}))_{l\in\mathbb{N}}$ are uniformly bounded in $\mathrm{BV}(0,1)$. Using the compactness properties of $\mathrm{W}^{1,1}(0,1)$ and $\mathrm{BV}(0,1)$ and a diagonal extraction argument, we can define

$$\begin{aligned} \gamma^-(x,\lambda) &= \lim_{l\to\infty} \gamma(x_l^-, \lambda_{k_l^-}) \text{ in } \mathrm{W}^{1,1}(0,1) \\ \gamma^+(x,\lambda) &= \lim_{l\to\infty} \gamma(x_l^+, \lambda_{k_l^+}) \text{ in } \mathrm{W}^{1,1}(0,1) \end{aligned} \tag{3.2.11}$$

where $(\gamma^-)'(x,\lambda)$, $(\gamma^+)'(x,\lambda) \in \mathrm{BV}(0,1)$ and

$$\begin{aligned} \int_0^1 |(\gamma^-)''(x,\lambda)|dt &\le \liminf_{l\to\infty} \int_0^1 |\gamma''(x_l^-, \lambda_{k_l^-})|dt \\ \int_0^1 |(\gamma^+)''(x,\lambda)|dt &\le \liminf_{l\to\infty} \int_0^1 |\gamma''(x_l^+, \lambda_{k_l^+})|dt \end{aligned} \tag{3.2.12}$$

Since $\gamma'(x_l^-, \lambda_{k_l^-}) \to (\gamma^-)'(x,\lambda)$ in $\mathrm{L}^1(0,1)$ we get that, up to some subsequence, $|\gamma'(x_l^-, \lambda_{k_l^-})| \to |(\gamma^-)'(x,\lambda)|$ almost everywhere on $[0,1]$, hence $\gamma^-(x,\lambda)$ is parametrized with constant velocity and the same result holds for $\gamma^+(x,\lambda)$.

Then, two cases arise :
1) If $\gamma^+(x,\lambda) = \gamma^-(x,\lambda) \equiv \gamma^\pm(x,\lambda)$ then let l, N such that

$$\begin{aligned} &d_{\mathcal{H}}(\gamma(x_l^+, \lambda_{k_l^+}); \gamma(x_l^-, \lambda_{k_l^-})) < \epsilon \\ &d_{\mathcal{H}}(\gamma^N(x_l^+, \lambda_{k_l^+}); \gamma(x_l^+, \lambda_{k_l^+})) < \epsilon \\ &d_{\mathcal{H}}(\gamma^N(x_l^-, \lambda_{k_l^-}); \gamma(x_l^-, \lambda_{k_l^-})) < \epsilon \end{aligned}$$

where $d_{\mathcal{H}}$ denotes the Hausdorff distance. Since $\gamma^k(x,\lambda)$ is in between $\gamma^k(x_l^+, \lambda_{k_l^+})$ and $\gamma^k(x_l^-, \lambda_{k_l^-})$ and $\gamma^\pm(x,\lambda)$ is in between $\gamma(x_l^+, \lambda_{k_l^+})$ and $\gamma(x_l^-, \lambda_{k_l^-})$, we deduce that for $k > N$, $d_{\mathcal{H}}(\gamma^k(x,\lambda); \gamma^\pm(x,\lambda)) < 2\epsilon$. Thus $\gamma^k(x,\lambda) \to \gamma^\pm(x,\lambda)$ in $\mathrm{L}^1(0,1)$ and from (3.2.11) and (3.2.12) we infer that $\gamma^\pm(x,\lambda) \in W^{1,1}(0,1)$ and $(\gamma^\pm)'(x,\lambda) \in \mathrm{BV}(0,1)$. Finally we define $\gamma(x,\lambda) := \gamma^\pm(x,\lambda)$ as the limit curve of the sequence $(\gamma^k(x,\lambda))_{k\in\mathbb{N}}$ and remark that

$$\mathcal{L}(\gamma^k) \to \mathcal{L}(\gamma) \tag{3.2.13}$$

Indeed, we deduce from (3.2.11) that $\mathcal{L}(\gamma(x_l^-, \lambda_{k_l^-})) \to \mathcal{L}(\gamma(x,\lambda))$ and $\mathcal{L}(\gamma(x_l^+, \lambda_{k_l^+})) \to \mathcal{L}(\gamma(x,\lambda))$, and (3.2.13) follows from the fact that the restriction of the curves to Ω - recall that we implicitly deal with extensions $\tilde{\gamma}$ – are geodesic paths of class C^∞. Moreover, we get from (3.2.10) that

$$\int_0^1 |\gamma''(x,\lambda)|dt \le \liminf_{k\to\infty} \int_0^1 |(\gamma^k)''(x,\lambda)|dt \tag{3.2.14}$$

2) If $\gamma^+(x,\lambda) \neq \gamma^-(x,\lambda)$ then (see figure 3.4) :

- either the subset of Ω enclosed in between $\gamma^+(x,\lambda)$ and $\gamma^-(x,\lambda)$ has positive area,
- or the geodesic distance on Γ between endpoints y^+ and y^- is positive.

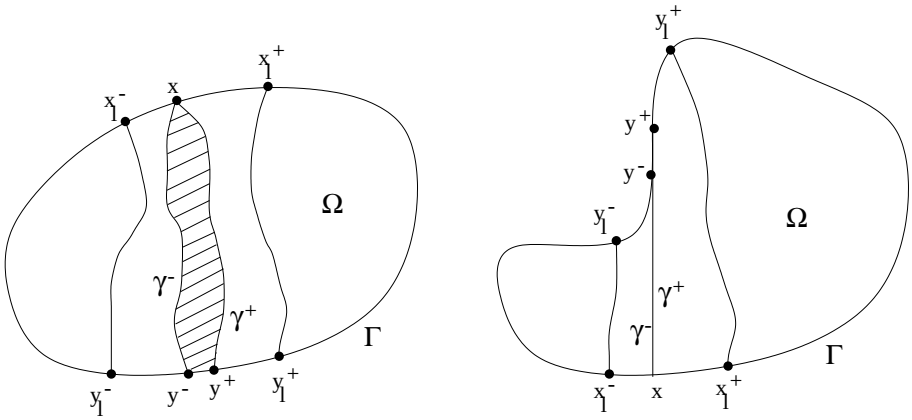

Figure 3.4:

Since Ω is bounded, Γ is rectifiable and the curves cannot cross, we deduce that there are at most countably many points x for which this situation arises. It is actually easily seen that there are at most countably many pairs (x,λ) for which $\gamma^-(x,\lambda) \neq \gamma^+(x,\lambda)$. Indeed, limit curves do not cross, so that if λ_0 and λ_1 are such that $x \in A_{\lambda_0}$, $x \in A_{\lambda_1}$, $\gamma^-(x,\lambda_0) \neq \gamma^+(x,\lambda_0)$ and $\gamma^-(x,\lambda_1) \neq \gamma^+(x,\lambda_1)$ then necessarily the regions enclosed by these curves do not overlap since these curves are limits of noncrossing curves. With the same argument as above we deduce that this situation can happen for at most countably many λ's. Then, we remove this countable set $\mathcal{R}_0$ from $\mathcal{R}$ and remark that this shall not change the reconstructed function u_d as well as the limit energy. Finally the limit 1-disocclusion $\mathcal{D}$ is defined as the set of all those limit curves $\gamma(x,\lambda)$ where $\lambda \in \mathcal{R} \setminus \mathcal{R}_0$ and $x \in A^1_\lambda$.

Claim#5 : *If $p = 1$ the limit disocclusion $\mathcal{D}$ is the disocclusion with minimal energy. If $p > 1$ and $\tilde{u}$ assume a finite number of values on Γ then $\mathcal{D}$ is the disocclusion with minimal energy.*

• Let $p > 1$ and assume that I is the finite set of values taken by $\tilde{u}$ on Γ. Recall from Claim#3 that for every $\lambda \in I$ and $x \in A^1_\lambda$, the sequences of curves $(\gamma^k(x,\lambda))$ converges weakly in $\mathrm{W}^{2,p}(0,1)$ to $\gamma(x,\lambda)$ thus uniformly in $\mathrm{C}^1(0,1)$. Since I is finite, there exists N such that, given $\lambda \in I$ and $x \in A^1_\lambda$, the curves $\gamma^k(x,\lambda)$ with $k > N$ have same endpoints

$x = \gamma^k(0)$ and $y = \gamma^k(1)$. Since the convergence is uniform in $\mathrm{C}^1(0,1)$, we infer that

$$\mathcal{L}(\gamma^k(x,\lambda)) \to \mathcal{L}(\gamma(x,\lambda)), \tag{3.2.15}$$

$$\langle \tau(0)\widehat{,\gamma^n}'(0)\rangle \to \langle \tau(0)\widehat{,\gamma}'(0)\rangle \quad \text{and} \quad (\tau(1)\widehat{,\gamma^n}'(1)) \to (\tau(1)\widehat{,\gamma}'(1)) \tag{3.2.16}$$

In addition, since the curves weakly converge in $\mathrm{W}^{2,p}(0,1)$ we get

$$\int_0^1 |\frac{d^2\gamma(x,\lambda)}{dt^2}|dt \le \liminf_{k\to\infty} \int_0^1 |\frac{d^2\gamma^k(x,\lambda)}{dt^2}|dt$$

Thus, if $\mathcal{L}(\gamma) = 0$ then, in view of (3.2.3), it is an obvious consequence of (3.2.16) that $E_p(\gamma(x,\lambda)) \le \liminf_{k\to\infty} E_p(\gamma^k(x,\lambda))$. If $\mathcal{L}(\gamma) > 0$ then by (3.2.15),

$$\begin{aligned}\liminf_{k\to\infty} \int_0^1 \left(|\frac{d\gamma^k}{dt}| + [\mathcal{L}(\gamma^k)]^{1-2p}\left|\frac{d^2\gamma^k}{dt^2}\right|^p\right)dt &\ge \liminf_{k\to\infty}\int_0^1 |\frac{d\gamma^k}{dt}|dt \\ &\quad + [\mathcal{L}(\gamma)]^{1-2p}\liminf_{k\to\infty}\int_0^1 \left|\frac{d^2\gamma^k}{dt^2}\right|^p dt \\ &\ge \int_0^1 \left(|\frac{d\gamma}{dt}|dt + [\mathcal{L}(\gamma)]^{1-2p}\left|\frac{d^2\gamma}{dt^2}\right|^p\right)dt\end{aligned}$$

and using (3.2.2) and (3.2.16) we deduce finally that for every $\lambda \in I$ and $x \in A^1_\lambda$,

$$E_p(\gamma(x,\lambda)) \le \liminf_{k\to\infty} E_p(\gamma^k(x,\lambda))$$

Consequently,

$$\begin{aligned}\liminf_{k\to\infty} \sum_{\lambda\in I}\sum_{x\in A^1_\lambda} E_p(\gamma^k(x,\lambda)) &\ge \sum_{\lambda\in I}\sum_{x\in A^1_\lambda} \liminf_{k\to\infty} E_p(\gamma^k(x,\lambda)) \\ &\ge \sum_{\lambda\in I}\sum_{x\in A^1_\lambda} E_p(\gamma(x,\lambda))\end{aligned}$$

and finally

$$E(\mathcal{D}) \le \liminf_{k\to\infty} E(\mathcal{D}_k)$$

so that the limit p-disocclusion is the disocclusion of minimal energy.

• If $p = 1$ then we deduce from (3.2.13) and (3.2.14) that $\forall\lambda \in \mathcal{R}\setminus\mathcal{R}_0$, $\forall x \in A^1_\lambda$ and denoting $\gamma := \gamma(x,\lambda)$, $\gamma^k := \gamma^k(x,\lambda)$,

$$\begin{aligned}\liminf_{k\to\infty} \int_0^1 \left(|\frac{d\tilde\gamma^k}{dt}| + \frac{1}{\mathcal{L}(\tilde\gamma^k)}\left|\frac{d^2\tilde\gamma^k}{dt^2}\right|\right)dt &\ge \liminf_{k\to\infty}\int_0^1 |\frac{d\tilde\gamma^k}{dt}|dt \\ &\quad + \frac{1}{\mathcal{L}(\tilde\gamma)}\liminf_{k\to\infty}\int_0^1 \left|\frac{d^2\tilde\gamma^k}{dt^2}\right| dt \\ &\ge \int_0^1 \left(|\frac{d\tilde\gamma}{dt}|dt + \frac{1}{\mathcal{L}(\tilde\gamma)}\left|\frac{d^2\tilde\gamma}{dt^2}\right|\right)dt\end{aligned}$$

and recall that from our definition of $\tilde{\gamma}$, $\mathcal{L}(\tilde{\gamma}) > 0$. Using (3.2.4) we infer that

$$E_1(\gamma(x,\lambda)) \leq \liminf_{k\to\infty} E_1(\gamma^k(x,\lambda))$$

Consequently,

$$\begin{aligned}\liminf_{k\to\infty} \int_{\mathcal{R}\setminus\mathcal{R}_0} \sum_{x\in A^1_\lambda} E_1(\gamma^k(x,\lambda)) &\geq \int_{\mathcal{R}\setminus\mathcal{R}_0} \sum_{x\in A^1_\lambda} \liminf_{k\to\infty} E_1(\gamma^k(x,\lambda)) \\ &\geq \int_{\mathcal{R}\setminus\mathcal{R}_0} \sum_{x\in A^1_\lambda} E_1(\gamma(x,\lambda))\end{aligned}$$

and finally

$$E(\mathcal{D}) \leq \liminf_{k\to\infty} E(\mathcal{D}_k)$$

so that the limit 1-disocclusion is the disocclusion of minimal energy.

In both cases, $p > 1$ and $p = 1$, we are now in position to define the reconstructed function u_d on Ω following (3.2.6) and (3.2.7). Since $E(\mathcal{D}) < +\infty$ we deduce from Coarea formula that $u_d \in \mathrm{BV}(\Omega)$. Indeed, if $p = 1$ then

$$\begin{aligned}|Du_d|(\Omega) &= \int_{\mathcal{R}\setminus\mathcal{R}_0} P(\{u \geq \lambda\}, \Omega) d\lambda \\ &\leq \int_{\mathcal{R}\setminus\mathcal{R}_0} \sum_{x\in A^1_\lambda} \mathcal{L}(\gamma(x,\lambda)) d\lambda \\ &\leq E(\mathcal{D})\end{aligned}$$

If $p > 1$ and $\{\lambda_1, \lambda_2, \ldots, \lambda_n\}$ is the finite set of all ordered values assumed by $\tilde{u}$ on Γ then

$$\begin{aligned}|Du_d|(\Omega) &= \int_{\lambda_1}^{\lambda_n} P(\{u \geq \lambda\}, \Omega) d\lambda \\ &= \sum_{i=1}^{n-1} |\lambda_{i+1} - \lambda_i| \sum_{x\in A^1_{\lambda_i}} \mathcal{L}(\gamma(x,\lambda)) \\ &\leq |\lambda_n - \lambda_1| \sum_{i=1}^{n-1} \sum_{x\in A^1_{\lambda_i}} \mathcal{L}(\gamma(x,\lambda)) \\ &\leq |\lambda_n - \lambda_1| E(\mathcal{D})\end{aligned}$$

Now, first remark that the set Ω we are dealing with satisfies the assumptions of Theorem 2.2.12. In addition, we assumed that $u \in \mathrm{BV}(\mathbb{R}^2 \setminus \overline{E})$ where $E \subset\subset \Omega$, so that $u \in \mathrm{BV}(\mathbb{R}^2 \setminus \overline{\Omega})$, and we proved that $u_d \in \mathrm{BV}(\Omega)$. Applying Theorems 2.2.12 and 2.2.13,

we infer that the reconstructed function u_r defined by (3.2.8) belongs to $\mathrm{BV}(\mathbb{R}^2)$ and Theorem 3.2.4 ensues. □

Remark 3.2.6 It must be emphasized that Theorem 3.2.4 still holds – and the proof can be trivially adapted – if one replaces the curve energy $E_p(\gamma)$ with

$$E_p(\gamma) := \int_0^{\mathcal{L}(\gamma)} (\alpha + \beta|\gamma''(s)|^p) ds$$

where $\alpha, \beta > 0$ are constants that weight the cost for the length relative to the cost for the curvature term.

Remark 3.2.7 In case $\tilde{u}$ is constant on Γ, say $\tilde{u} \equiv \lambda_0$, which means that there is no T-junction, it can be easily checked that the unique solution to our interpolation problem is obtained by simply setting $u_{|\Omega} \equiv \lambda_0$.

Remark 3.2.8 The optimal solution is not necessarily unique, as illustrated in the following example (figure 3.5) where the curve energy is defined as $E(\gamma) = \int_0^{\mathcal{L}(\gamma)} |\gamma''(s)|\, ds$ – remark that this example can be easily generalized to the case $p > 1$. Notice that the cross is no more an optimal solution when the length is taken into account in the energy formulation. Actually our method does not suit with "second-order" disocclusion problems, where new occlusions has to be generated. This kind of problems remains open within the framework of level lines interpolation.

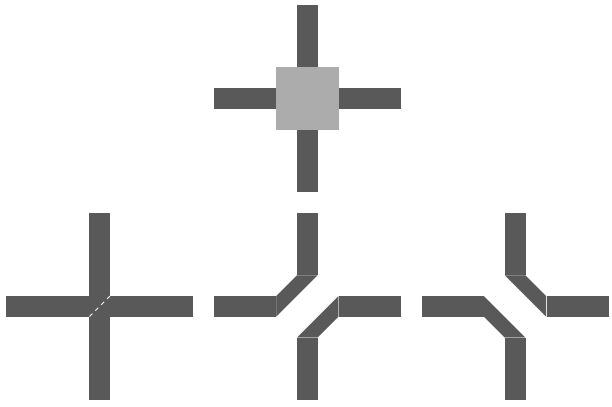

Figure 3.5: Top : an occlusion problem; Bottom : three optimal solutions for the curve energy $E(\gamma) = \int_0^{\mathcal{L}(\gamma)} |\gamma''(s)|\, ds$. The white dashed line in the left figure indicates the level lines connections.

We now conjecture that an optimal p-disocclusion exists for every $p \geq 1$.

Conjecture 3.2.9 *Let $E \subset \mathbb{R}^N$ be an occlusion and $u \in \mathrm{BV}(\mathbb{R}^2 \setminus \overline{E})$ such that $|u| < M$. Let $\Omega \supset\supset E$ be an admissible occlusion. Then for every $p \geq 1$, there exists a p-disocclusion of u with minimal energy and the extended function $u_r \in \mathrm{BV}(\mathbb{R}^2)$.*

3.3 Un algorithme pratique de désocclusion

L'algorithme que nous présentons maintenant permet de déterminer une 1-désocclusion optimale. Notons que la détermination d'une p-désocclusion optimale pour $p > 1$ est un problème encore ouvert pour plusieurs raisons. La première est que l'on ne connaît déjà pas de représentation exacte de la courbe qui minimise

$$\int_0^{\mathcal{L}(\gamma)} (1 + |\gamma''(s)|^p) ds$$

lorsque les tangentes aux extrémités sont prescrites. Dans le cas où $p = 2$ – il s'agit alors du problème d'Euler et les courbes minimales sont appelées "elastiques" – D. Mumford [31] a ainsi montré que la solution peut s'écrire comme dérivée logarithmique de la fonction θ mais ce résultat reste générique. Un schéma numérique d'approximation est proposé dans [32] mais il a l'inconvénient d'être très instable. E. Sharon, A. Brandt et R. Basri [37] ont introduit un modèle qui fournit une bonne approximation de la courbe optimale lorsque l'on suppose que les tangentes aux extrémités sont similaires. Rappelons cependant que notre problème diffère de celui d'Euler dans la mesure où l'on veut trouver la courbe de plus faible énergie contenue dans le domaine délimité par l'occlusion, ce que ne permettent pas les schémas précédents. La seconde raison pour laquelle la détermination d'une p-désocclusion reste un problème ouvert tient au fait que notre approche nécessite une minimisation globale d'une somme d'énergies portant sur des courbes auxquelles on interdit le croisement, problème pour lequel, à notre connaissance, il n'existe pas de solution numérique hormis dans le cas $p = 1$ que nous présentons ici. Nous verrons cependant que le seul cas $p = 1$ offre déjà des solutions satisfaisantes.

Détermination de la frontière de l'occlusion

On suppose que l'occlusion ne comporte aucun trou. Nous allons utiliser pour décrire l'image une grille de points à coordonnées entières et semi-entières. Chaque pixel est associé à un point de coordonnées entières et il est entouré de huit points dont au moins une coordonnée est semi-entière. Ces points permettent de définir des droites passant entre les pixels de l'image et l'on peut représenter la frontière de l'occlusion à l'aide d'une ligne polygonale dont les sommets sont des points à coordonnées semi-entières.

Afin que cette ligne polygonale soit une courbe de Jordan – ce qui sera utile pour la recherche d'un plus court chemin entre deux points de la frontière – les coordonnées des points où la frontière présente une concavité doivent être légèrement perturbées. Plus précisément, nous allons décrire la frontière à l'aide des seuls points à coordonnées semi-entières où la ligne polygonale change de direction. Toutefois, en chaque point de concavité, on stockera les coordonnées d'un point très proche – à une distance inférieure à 10^{-3} par exemple – se trouvant à l'extérieur de l'occlusion. Ainsi, si l'occlusion est formée de seulement deux pixels voisins en diagonale, cela revient à considérer que le sommet commun aux deux pixels est d'épaisseur non nulle.

Voyons cela sur un exemple. Dans la figure 3.6, l'occlusion à analyser est en blanc. Les grands disques noirs sont les centres des pixels de l'image, tandis que les petits disques marquent les points dont au moins une coordonnée est semi-entière. La frontière de l'occlusion a été représentée en trait plein. Partant de $(1.5, 3.5)$, un parcours de la frontière dans le sens trigonométrique nous donne une première liste des points de changement de direction

$$\{(1.5, 3.5),\ (1.5, 2.5),\ (2.5, 2.5),\ (2.5, 1.5),\ (4.5, 1.5), (4.5, 2.5),\ (2.5, 2.5),\ (2.5, 3.5)\}$$

Après traitement des concavités, la liste que nous retiendrons pour décrire la frontière de l'occlusion est

$$\{(1.5, 3.5),\ (1.5, 2.5),\ (2.4999, 2.4999),\ (2.5, 1.5),\ (4.5, 1.5),\\ (4.5, 2.5),\ (2.5001, 2.5001),\ (2.5, 3.5)\}$$

qui décrit une ligne polygonale simple et fermée.

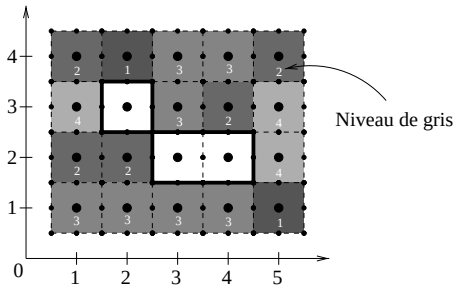

Fig. 3.6: *L'utilisation d'une grille à coordonnées semi-entières permet de décrire la frontière de l'occlusion composée ici des pixels blancs.*

Détermination des jonctions en T de la frontière

L'autre structure qui va nous permettre de décrire l'occlusion est l'ensemble des jonctions en T. Ce sont les points de la frontière qui sont un sommet commun à deux pixels n'appartenant pas à l'occlusion et de niveaux de gris différents. La liste de ces points est établie en deux étapes. La première étape recense simplement tous les points ayant cette propriété, la seconde étape insère les niveaux de gris intermédiaires. En d'autres termes,

une ligne séparant les niveaux 1 et 4 contient en fait 3 lignes de niveau, la ligne séparant les niveaux 1 et 2, celle séparant les niveaux 2 et 3, et enfin celle qui sépare les niveaux 3 et 4. Chaque jonction en T est décrite par ses coordonnées, les deux niveaux de gris auxquels elle est associée et l'angle que fait avec l'horizontale la ligne de niveau (rentrante) à laquelle est associée la jonction. Il faut cependant tenir compte du fait que la direction de la ligne de niveau au point de jonction avec l'occlusion n'est pas nécessairement pertinente du fait de l'échantillonnage spatial et du bruit et il est donc préférable de calculer une direction moyenne sur un voisinage autour de la jonction en T considérée. Dans l'exemple qui nous occupe, on obtient finalement la liste, présentée dans le tableau de la figure 3.7, des jonctions en T que l'on rencontre en parcourant la frontière dans le sens trigonométrique à partir du point $(1.5, 3.5)$ – on notera que les niveaux de gris sont donnés par ordre d'apparition.

# Jonction	Coordonnées	Niveaux de gris		Angle
1	(1.5 ; 3.5)	1	2	$-\frac{\pi}{2}$
2	(1.5 ; 3.5)	2	3	0
3	(1.5 ; 3.5)	3	4	0
4	(1.5 ; 2.5)	4	3	0
5	(1.5 ; 2.5)	3	2	0
6	(2.5 ; 1.5)	2	3	0
7	(4.5 ; 1.5)	3	2	$\pi/2$
8	(4.5 ; 1.5)	2	1	$\pi/2$
9	(4.5 ; 1.5)	1	2	π
10	(4.5 ; 1.5)	2	3	π
11	(4.5 ; 1.5)	3	4	π
12	(4.5 ; 2.5)	4	3	$-\pi/2$
13	(4.5 ; 2.5)	3	2	$-\pi/2$
14	(3.5 ; 2.5)	2	3	$-\pi/2$
15	(2.5 ; 3.5)	3	2	$-\pi/2$
16	(2.5 ; 3.5)	2	1	$-\pi/2$

FIG. 3.7: *Liste des jonctions en T*

Règles pour l'interpolation et énergie d'interpolation

Dans la mesure où une ligne de niveau qui atteint l'occlusion en repart nécessairement, il est important de noter qu'il y a un nombre pair de jonctions en T par niveau dans la liste précédente. Il suffit pour s'en assurer de faire l'analogie entre les lignes de niveau d'une image et les lignes de niveau d'un relief. Le principe de la désocclusion consiste à relier ces jonctions en T deux à deux en respectant deux règles de construction liées aux

propriétés mathématiques des lignes de niveau.

1. Deux jonctions en T ne peuvent être reliées par une ligne de niveau que si elles sont associées aux mêmes niveaux de gris et ont la même orientation, de sorte que le gradient conserve le même sens le long de la ligne. De telles jonctions en T sont dites compatibles.

2. Deux lignes de niveau reliant deux couples de jonctions en T ne peuvent pas se croiser.

La première règle nous permet de limiter le problème de mise en relation des jonctions en T deux à deux. A partir de la liste précédente, on peut établir deux colonnes distinctes de jonctions en T (voir figure 3.8). Chaque jonction de la première colonne peut être mise en relation avec n'importe quelle autre jonction de la seconde colonne appartenant au même sous-groupe.

Coordonnées	Niveaux de gris		Angle	Coordonnées	Niveaux de gris		Angle
(1.5 ; 3.5)	1	2	$-\pi/2$	(4.5 ; 1.5)	2	1	$\pi/2$
(4.5 ; 1.5)	1	2	π	(2.5 ; 3.5)	2	1	$-\pi/2$
(1.5 ; 3.5)	2	3	0	(1.5 ; 2.5)	3	2	0
(2.5 ; 1.5)	2	3	0	(4.5 ; 1.5)	3	2	$\pi/2$
(4.5 ; 1.5)	2	3	π	(4.5 ; 2.5)	3	2	$-\pi/2$
(3.5 ; 2.5)	2	3	$-\pi/2$	(2.5 ; 3.5)	3	2	$-\pi/2$
(1.5 ; 3.5)	3	4	0	(1.5 ; 2.5)	4	3	0
(4.5 ; 1.5)	3	4	π	(4.5 ; 2.5)	4	3	$-\pi/2$

Fig. 3.8: *Toute jonction en T de la première colonne peut être mise en relation avec une jonction en T associée aux mêmes niveaux de gris dans la seconde colonne*

Une solution admissible à notre problème de désocclusion est un ensemble de lignes de niveau établissant une bijection entre les deux colonnes précédentes, vérifiant les deux règles de construction et telles que toute ligne de niveau appartienne à l'occlusion. Etant donné un ensemble de mises en relation deux à deux des jonctions en T, il existe un moyen très simple de vérifier que la seconde règle de construction est satisfaite, à savoir qu'il existe un ensemble de lignes de niveau reliant deux à deux les jonctions en T sans qu'il y ait de croisement. Chaque jonction en T appartient à la courbe de Jordan formant la frontière de l'occlusion. Deux jonctions en T mises en relation induisent un partage de la courbe de Jordan en deux arcs qui ne se touchent qu'à leurs extrémités. On ne pourra mettre en relation deux nouvelles jonctions en T que si elles appartiennent au même arc. Il est en effet facile de vérifier que dans le cas contraire deux lignes de niveau quelconques reliant

les jonctions vont nécessairement se croiser. Ainsi, toute solution admissible respecte un principe de causalité en ce sens que la donnée d'une mise en relation de deux jonctions en T contraint toute mise en relation supplémentaire. On dira que deux couples de jonctions en T sont compatibles s'il existe deux lignes de niveau associées qui ne se croisent pas.

Si l'on désigne par $L_{i,j}$ une ligne de niveau admissible reliant les jonctions i et j, on peut lui associer l'énergie

$$C_{i,j} = \int_{L_{i,j}} (\alpha + \beta|\sigma(s)|)ds, \quad \alpha, \beta > 0$$

où $\sigma(s)$ est la courbure le long de la ligne de niveau $L_{i,j}$ et α, β deux constantes données. Le terme $\int_{L_{i,j}} |\sigma(s)|ds$ désigne la variation totale de l'angle le long de la ligne de niveau à laquelle on ajoute implicitement les angles en i et j entre $L_{i,j}$ et la ligne de niveau parvenant à l'occlusion que l'on désire prolonger. Parmi toutes les lignes de niveau appartenant au domaine délimité par l'occlusion et reliant les jonctions en T i et j, la géodésique est celle qui minimise la quantité $C_{i,j}$. On entend ici par géodésique la courbe reliant i et j, entièrement contenue dans l'occlusion et de longueur minimale. Puisque l'occlusion a été supposée simplement connexe, cette géodésique est unique. Par ailleurs, deux couples de jonctions en T compatibles définissent deux géodésiques qui ne se croisent pas.

Considérons maintenant tous les ensembles de lignes de niveau réalisant les connections des jonctions à T deux à deux et satisfaisant les règles de construction. Dans le plan continu, il existe une infinité de tels ensembles, dans la mesure où l'on peut passer de l'un à l'autre par simple modification de la géométrie des lignes de niveau à l'intérieur de l'occlusion sans toucher aux extrémités (voir figure 3.9).

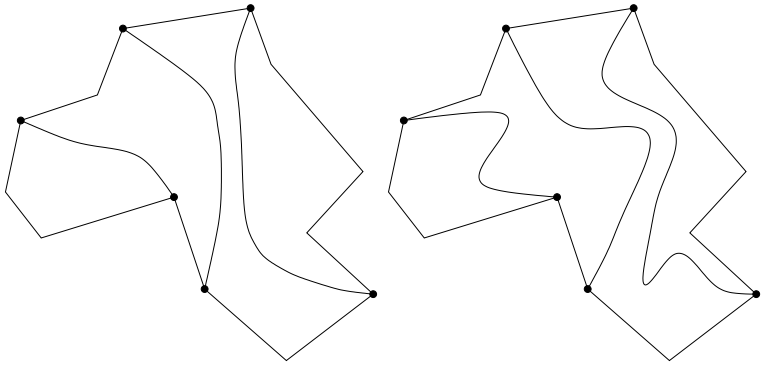

FIG. 3.9: *Deux solutions admissibles différentes associées à un même appariement des jonctions en T*

Désignons par E l'énergie d'une solution admissible, définie comme la somme des $C_{i,j}$ sur tous les couples (i, j) mis en relation. Parmi tous les ensembles admissibles de lignes

de niveau, la solution admissible de plus faible énergie est celle qui fait intervenir les seules géodésiques. Par suite, pour déterminer la solution optimale au problème de désocclusion, il suffit d'énumérer l'ensemble des bijections vérifiant les deux principes de construction, de calculer pour chacune la solution admissible composée seulement de géodésiques et de retenir parmi toutes ces solutions admissibles celle qui a la plus faible énergie.

Détermination d'une géodésique

Nous allons à présent décrire la méthode utilisée pour calculer l'énergie de la géodésique reliant deux jonctions en T compatibles. Cette méthode nécessite au préalable une triangulation de la ligne polygonale simple qui constitue la frontière de l'occlusion. Une triangulation peut être en théorie réalisée en $\mathcal{O}(N)$, où N est le nombre de sommets de la frontière, grâce à l'algorithme de Chazelle [11]. Cet algorithme est cependant tellement complexe qu'il n'a jusqu'à présent jamais pu être implémenté. Nous nous sommes contentés de l'algorithme dit de "ear-clipping" qui dans sa version la plus simple a une complexité en $\mathcal{O}(N^3)$. Il est cependant possible de ramener la complexité à $\mathcal{O}(N^2)$ par un simple réordonnancement des calculs et l'utilisation de listes chaînées [33].

Désignons par $v_1, \ldots, v_N$ les sommets du polygone $\mathcal{P}$ représentant la frontière de l'occlusion $\mathcal{D}$. Tout sommet où le polygone présente une convexité est dit *convexe*. On dit que trois sommets consécutifs v_{i-1}, v_i, v_{i+1} forment une *oreille* (ear) de $\mathcal{P}$ si le segment $[v_{i-1}, v_{i+1}]$ appartient à $\mathcal{D}$ et ne rencontre $\mathcal{P}$ qu'en v_{i-1} et v_{i+1}. Ceci impose bien sûr que v_i soit un sommet strictement convexe et que le segment $[v_{i-1}, v_{i+1}]$ ne rencontre aucune arête de $\mathcal{P}$ si ce n'est aux points v_{i-1} et v_{i+1}. La méthode de *ear-clipping* dans sa version la plus simple consiste à trouver une "oreille" (v_{i-1}, v_i, v_{i+1}) (il en existe nécessairement une [33]) dans le polygone $\mathcal{P}_1 = \mathcal{P} = \{v_1, \ldots, v_N\}$. On définit alors un nouveau polygone $\mathcal{P}_2 = \{v_1, \ldots, v_{i-1}, v_{i+1}, \ldots, v_N\}$ comportant $N-1$ sommets et on itère le processus de "ear-clipping" jusqu'à ce qu'il ne reste plus qu'un triangle (voir figure 3.10).

Les différentes "oreilles" que l'on a successivement éliminées forment une triangulation du polygone initial. On peut vérifier que la complexité nécessaire pour déterminer si trois sommets consécutifs constituent une "oreille" est en $\mathcal{O}(N)$. Au pire, chaque étape de l'algorithme nécessite donc $\mathcal{O}(N^2)$ opérations et la méthode de "ear-clipping" que nous venons de décrire est par conséquent en $\mathcal{O}(N^3)$. Il est cependant facile de vérifier que la suppression d'une "oreille" à une étape n'affecte au pire que deux autres "oreilles" du polygone. Un algorithme moins coûteux [33] peut donc être utilisé qui consiste à calculer toutes les "oreilles" à la première étape ($\mathcal{O}(N^2)$ opérations) puis à mettre à jour au plus deux "oreilles" aux étapes suivantes. Le nombre total d'opérations devient alors de l'ordre de $\mathcal{O}(N^2)$. Enfin, il nous faut signaler l'existence d'une méthode encore moins coûteuse mais plus complexe qui nécessite $\mathcal{O}(N \log N)$ opérations [33].

Une fois la triangulation du polygone effectuée, la méthode de Hershberger et Snoeyink

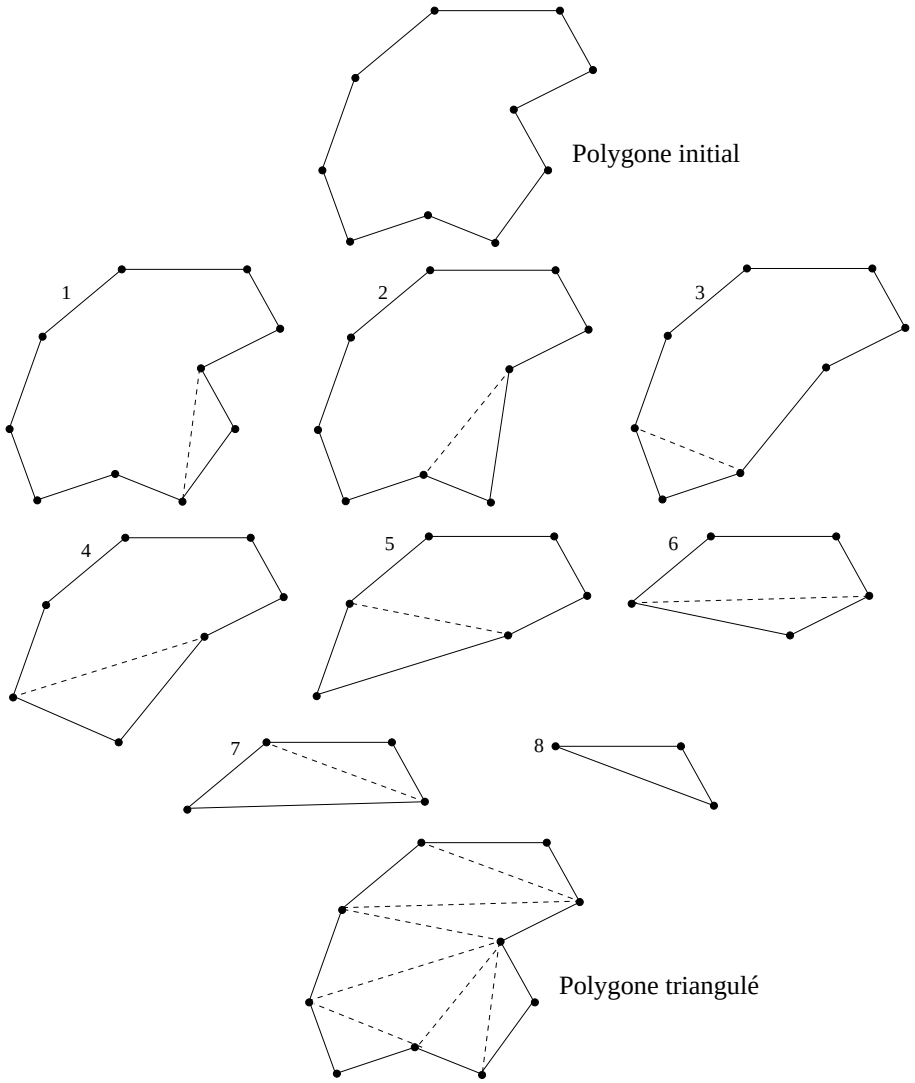

FIG. 3.10: *Triangulation d'un polygone*

[17, 27] permet de calculer la géodésique reliant deux sommets a et b de la frontière en $\mathcal{O}(N)$ opérations. Cette méthode repose sur l'algorithme de la "cheminée" (*funnel algorithm*) dû à Lee et Preparata [21]. Nous reprenons ici la description qui en est faite dans [27]. Connaissant deux triangles T_1 et T_n dont a et b sont des sommets, la première étape de l'algorithme consiste à déterminer la séquence de triangles qui relient T_1 et T_n. Puis chaque triangle est traité de façon itérative jusqu'à l'obtention d'un plus court chemin entre a et b. Une itération consiste en l'opération suivante : on connaît grâce à l'étape précédente le plus court chemin entre a et un point intermédiaire r (voir figure 3.11), ainsi que les plus courts chemins entre r et les points s et t où stu est le triangle à traiter. Cette structure forme une "cheminée" de racine r et de base st. En ajoutant le triangle stu on

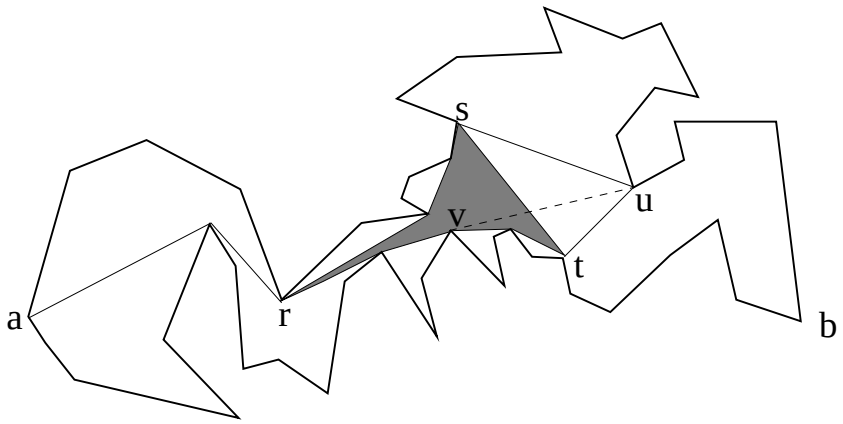

FIG. 3.11: *Algorithme de la "cheminée"*

coupe la "cheminée" en deux à l'aide du plus court chemin entre r et u qui est sur notre exemple la ligne polygonale rvu. Les deux nouvelles cheminées ont respectivement pour base su et tu. On conserve pour l'itération suivante la cheminée qui est incluse dans la séquence de triangles reliant a à b, c'est-à-dire ici la cheminée de base tu. Le résultat final est obtenu dans le pire des cas en $\mathcal{O}(N)$ opérations. En pratique, nous avons utilisé une implémentation de cet algorithme due à Joe Mitchell [28].

Minimisation de l'énergie par programmation dynamique

A présent que nous sommes en mesure de calculer le coût de connection de deux jonctions en T compatibles i et j, voyons comment déterminer un ensemble optimal de connections, c'est-à-dire un ensemble d'énergie minimale. La programmation dynamique est la méthode qui semble la mieux adaptée à la propriété de causalité que satisfont des connections successives de jonctions en T. Appelons $(t_1, t_2, \ldots, t_{2m})$ l'ensemble des jonctions en T à traiter et rappelons qu'il y a toujours un nombre pair de jonctions en T par niveau. La programmation dynamique repose sur le calcul itératif des énergies optimales $E_{i,i+k}$ qui correspondent aux énergies de connections optimales deux à deux de toutes les jonctions en T dans l'intervalle $[i, i+k]$. Ces énergies n'ont bien sûr de sens que pour k pair pour la simple raison qu'il n'est pas possible de connecter deux à deux un nombre impair de jonctions en T! On désignera par $C_{i,j}$ l'énergie de la géodésique reliant i et j, qui peut être infinie si i et j ne sont pas compatibles. Les étapes successives de la programmation dynamique adaptée à la désocclusion sont les suivantes.

Etape 1 : Traitement des intervalles de longueur 2; on calcule successivement les énergies

$$E_{1,2} = C_{1,2},\ E_{2,3} = C_{2,3},\ \ldots,\ E_{i,i+1} = C_{i,i+1},\ \ldots,\ E_{2m,1} = C_{2m,1}$$

Etape 2 : Traitement des intervalles de longueur 4; connaissant déjà les énergies $E_{i,i+1}$ on

calcule successivement

$$\begin{aligned} E_{1,4} &= \min\{C_{1,4} + E_{2,3}\,;\, E_{1,2} + E_{3,4}\} \\ &\vdots \\ E_{i,i+3} &= \min\{C_{i,i+3} + E_{i+1,i+2}\,;\, E_{i,i+1} + E_{i+2,i+3}\} \\ &\vdots \\ E_{2m,3} &= \min\{C_{2m,3} + E_{1,2}\,;\, E_{2m,1} + E_{2,3}\} \end{aligned}$$

Etape 3 : Traitement des intervalles de longueur 6

$$\begin{aligned} E_{1,6} &= \min\{C_{1,6} + E_{2,5}\,;\, E_{1,2} + E_{3,6}\,;\, E_{1,4} + E_{5,6}\} \\ &\vdots \\ E_{i,i+5} &= \min\{C_{i,i+5} + E_{i+1,i+4}\,;\, E_{i,i+1} + E_{i+2,i+5}\,;\, E_{i,i+3} + E_{i+4,i+5}\} \\ &\vdots \\ E_{2m,5} &= \min\{C_{2m,5} + E_{1,4}\,;\, E_{2m,1} + E_{2,5}\,;\, E_{2m,3} + E_{4,5}\} \end{aligned}$$

Etape k : Traitement des intervalles de longueur 2k

$$\begin{aligned} E_{1,2k} &= \min\{C_{1,2k} + E_{2,2k-1}\,;\, E_{1,2} + E_{3,2k}\,;\, E_{1,4} + E_{5,2k}\,;\, \ldots\,;\, E_{1,2k-2} + E_{2k-1,2k}\} \\ &\vdots \\ E_{i,i+2k-1} &= \min\{C_{i,i+2k-1} + E_{i+1,i+2k-2}\,;\, E_{i,i+1} + E_{i+2,i+2k-1}\,;\, \ldots\,; \\ &\qquad\qquad E_{i,i+2k-3} + E_{i+2k-2,i+2k-1}\} \\ &\vdots \\ E_{2m,2k-1} &= \min\{C_{2m,2k-1} + E_{1,2k-2}\,;\, E_{2m,1} + E_{2,2k-1}\,;\, \ldots\,;\, E_{2m,2k-3} + E_{2k-2,2k-1}\} \end{aligned}$$

Etape m : $E_{1,2m}$ est l'énergie optimale cherchée.

$$E_{1,2m} = \min\{C_{1,2m} + E_{2,2m-1}\,;\, E_{1,2} + E_{3,2m}\,;\, E_{1,4} + E_{5,2m}\,;\, \ldots\,;\, E_{1,2m-2} + E_{2m-1,2m}\}$$

Si l'on désigne par $M = 2m$ le nombre de jonctions en T et N le nombre de sommets du polygone qui constitue la frontière de l'occlusion, on peut vérifier que la complexité de cet algorithme de programmation dynamique est de l'ordre de $\mathcal{O}(NM^2 + M^3)$ sachant que le calcul de chaque énergie $C_{i,i+2k}$ nécessite $\mathcal{O}(M)$ opérations d'après ce qui a été dit précédemment. Lorsque l'occlusion est convexe, il est clair que les géodésiques se réduisent à des lignes droites et la complexité de la programmation dynamique est ramenée à $\mathcal{O}(M^3)$. Ce coût reste important mais il faut le comparer au coût d'une méthode de type exhaustif basée sur une simple énumération de toutes les connections possibles. Une telle méthode nécessite un nombre d'opérations en $\mathcal{O}(M!)$ et est donc quasiment impossible à mettre en œuvre dès que l'occlusion atteint une taille suffisamment importante.

Nous avons choisi pour l'implémentation de cette méthode d'utiliser une fonction *Energie(i,i+k)* qui calcule de façon récursive l'énergie de l'intervalle $[i, i+k]$. En clair, nous

allons chercher à déterminer *Energie(1,2m)*, qui va nécessiter le calcul de *Energie(2,2m-1)*, *Energie(3,2m-1)*, etc., qui vont elle-mêmes nécessiter le calcul de l'énergie sur des intervalles plus petits. Cette méthode est strictement équivalente à celle que nous venons de décrire, à ceci près que les calculs inutiles seront évités. En effet, si nous devons calculer par exemple $E_{i,i+3}+E_{i+4,i+2k-1}$, et que l'on trouve $E_{i,i+3} = +\infty$, il est bien sûr inutile de chercher à calculer $E_{i+4,i+2k-1}$. De la même façon, il n'est pas nécessaire de continuer le calcul si $E_{i,i+3}$ est supérieure à un minimum obtenu précédemment. Le nombre d'opérations est théoriquement le même que dans la méthode directe, mais en pratique plus réduit car beaucoup de jonctions en T sont incompatibles et par conséquent de nombreuses énergies sont infinies.

Désocclusion par propagation géodésique des niveaux restaurés

Une fois connu l'ensemble optimal de connections, c'est-à-dire l'ensemble des appariements optimaux de jonctions en T, il ne reste plus qu'à "colorier" l'occlusion. Ceci peut se faire très simplement en deux étapes. La première consiste à tracer l'une après l'autre les géodésiques de longueur positive reliant deux jonctions en T définissant une paire optimale. On trace en fait une ligne d'épaisseur 2 pixels où sont représentés les deux niveaux de gris associés à la la ligne reconstruite. Afin de prendre en compte les problèmes de recouvrement, une méthode simple consiste à tracer une première ligne entre deux jonctions en T formant une paire optimale et voisines immédiates (il existe au moins une telle paire), puis à décrire dans le sens trigonométrique la frontière de l'occlusion et à tracer successivement les géodésiques optimales en coloriant systématiquement la partie droite de la ligne, tandis que la partie gauche ne sera coloriée qu'en ses points qui ne l'ont pas encore été précédemment (voir figure 3.12). Une fois que toutes les géodésiques ont été tracées, on réalise la désocclusion par une simple propagation géodésique des valeurs, c'est-à-dire une dilatation restreinte à l'occlusion.

Nous reprenons ci-dessous les grandes lignes de l'algorithme de désocclusion que nous venons de décrire.

Etape 1 : détermination de la ligne polygonale décrivant la frontière de l'occlusion.

Etape 2 : énumération dans le sens trigonométrique des jonctions en T appartenant à la frontière; chaque jonction est déterminée par sa position sur la frontière, ses coordonnées, les niveaux de gris auxquels elle est associée et la direction moyenne de la ligne de niveau correspondante.

Etape 3 : triangulation de la frontière.

Etape 4 : détermination par programmation dynamique de l'ensemble des appariements de jonctions en T qui a la plus faible énergie.

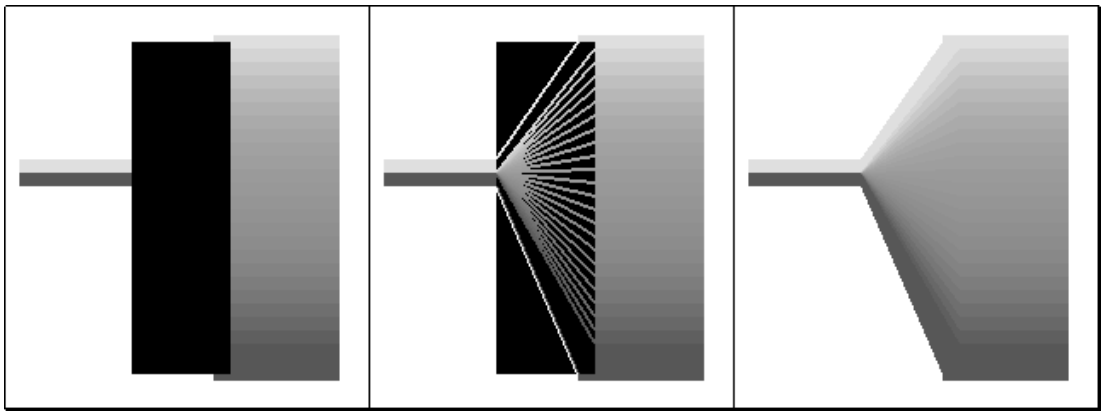

FIG. 3.12: *A gauche, l'image originale occultée par un rectangle noir, au milieu les geodésiques réalisant les appariements optimaux et à droite l'image après désocclusion*

Etape 5 : tracé des géodésiques associées à ces appariements.

Etape 6 : propagation géodésique à l'intérieur de l'occlusion des niveaux de gris définis par les lignes reconstruites. Ces deux dernières étapes nécessitent un nombre d'opérations qui dépend linéairement du nombre de pixels de l'occlusion.

Le coût algorithmique de cette méthode est de l'ordre de

$$\mathcal{O}(N^2 + NM^2 + M^3 + P)$$

où N est le nombre de sommets de la ligne polygonale qui constitue la frontière de l'occlusion, M est le nombre de jonctions en T et P est le nombre de pixels de l'occlusion.

3.4 Résultats expérimentaux

La figure 3.13 illustre l'expérience suivante : partant d'une image altérée par un bruit occlusif, la première étape consiste à identifier les points bruités comme ceux qui seraient modifiés par le filtre de grains (voir section 2.7). Puis, considérant ces points bruités comme des occlusions, on leur applique l'algorithme de désocclusion décrit à la section précédente.

La figure 3.14 illustre le fait que notre méthode de désocclusion peut s'appliquer à la restauration de vieilles photographies. La qualité du résultat ne semble pas altérée par l'utilisation de simples géodésiques pour prolonger les lignes de niveau. Par ailleurs, nous avons associé le processus de désocclusion au filtre de grains qui permet de réduire le bruit dans l'image.

L'expérience présentée dans la figure 3.15 montre que notre méthode permet de restaurer des discontinuités d'une façon compatible avec la théorie de Kanizsa, ce qui n'est

Fig. 3.13: *à gauche une image altérée par un bruit impulsionnel (fréquence = 10%) à droite : les occlusions sont détectées comme étant les ensembles non invariants par le filtre de grains, puis supprimées par désocclusion.*

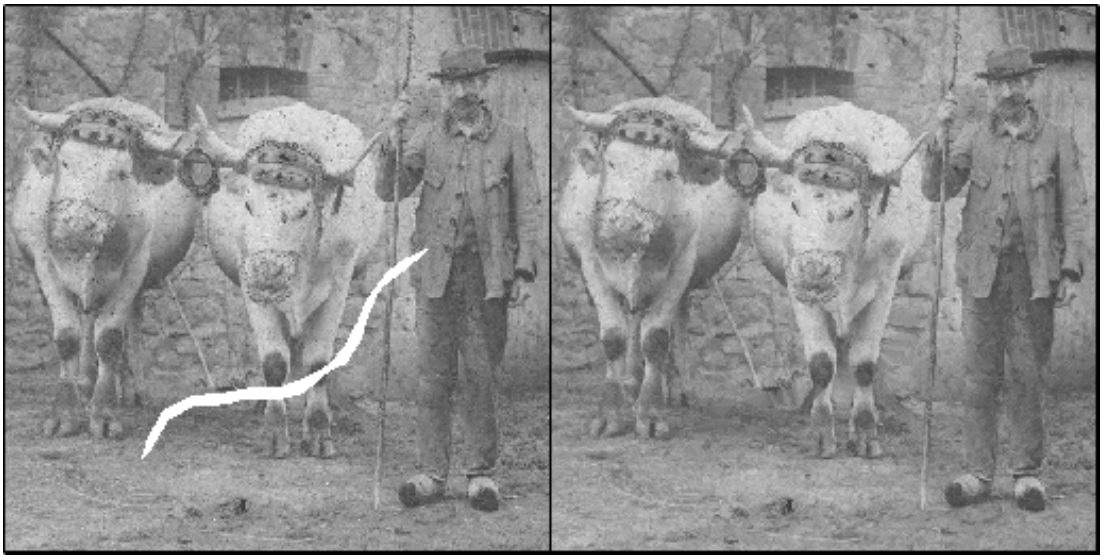

Fig. 3.14: *à gauche une vieille photographie bruitée et tachée. A droite : l'image restaurée par application conjointe du filtre de grains et de la méthode de désocclusion*

pas le cas de l'interpolation régulière par l'équation AMLE (voir section 3.1). Rappelons cependant que cette dernière méthode a été conçue initialement pour l'interpolation entre les lignes de niveau et non pour les prolonger.

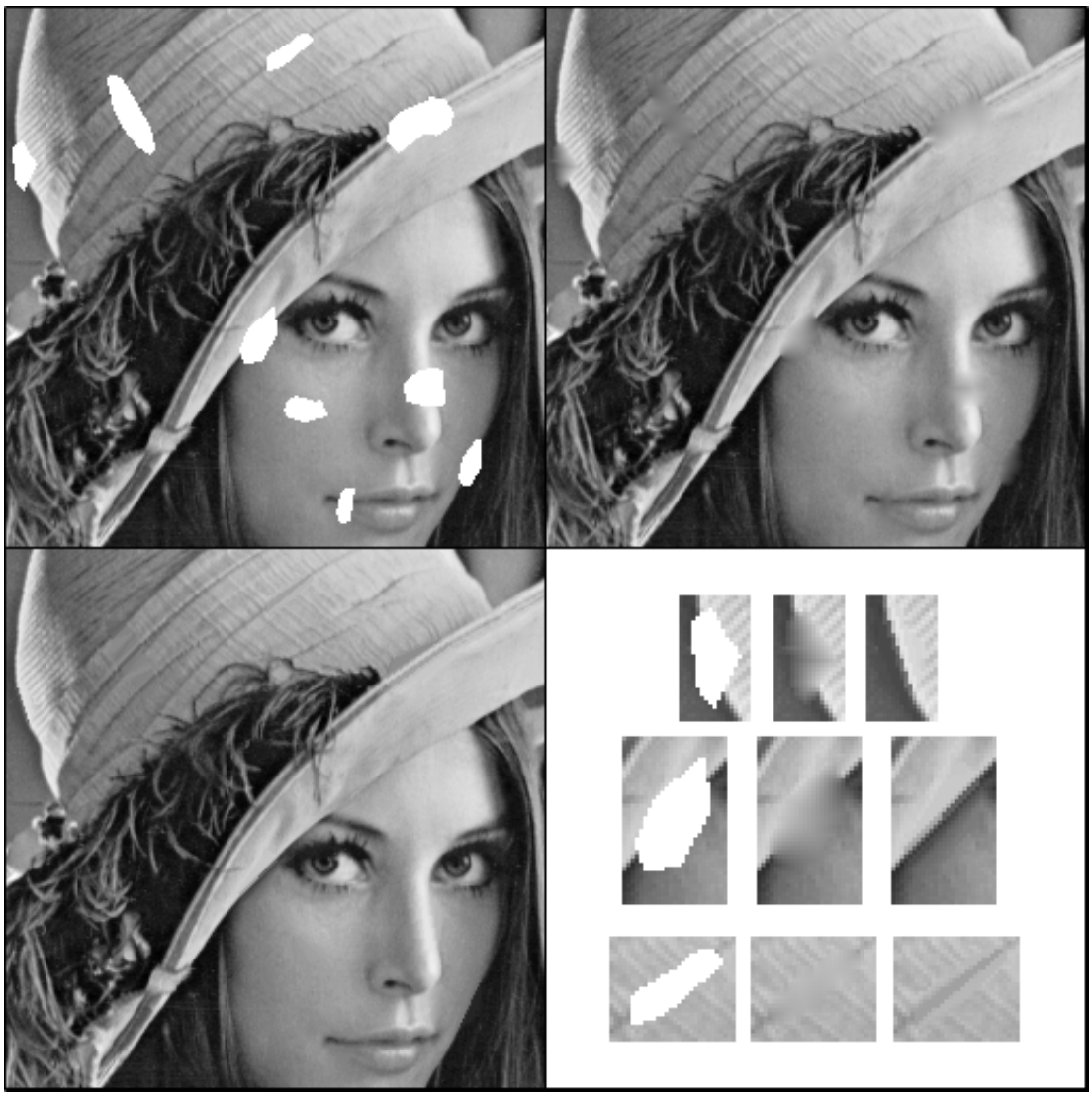

FIG. 3.15: *En haut à gauche, l'image originale où les occlusions sont en blanc. En haut à droite, le résultat de l'interpolation régulière par l'équation AMLE [9]. Les parties régulières de l'image sont bien restaurées mais les discontinuités ont été perdues. En bas à gauche, le résultat de la désocclusion par notre méthode variationnelle. Les discontinuités ont bien été restaurées. En bas à droite, agrandissements de certaines occlusions et des résultats obtenus par les deux méthodes.*

La figure 3.16 montre le résultat obtenu par désocclusion à partir d'une image dans laquelle 70% de l'information est manquante. Le résultat est surprenant car on a pu reconstruire, certes de façon imparfaite, une information à peine visible dans l'image occultée initiale. Remarquons cependant que notre approche, purement géométrique, ne permet pas une bonne restauration des parties texturées. Ceci est essentiellement dû au fait que

nous travaillons à une échelle plus grande que l'échelle de définition des textures présentes dans l'image.

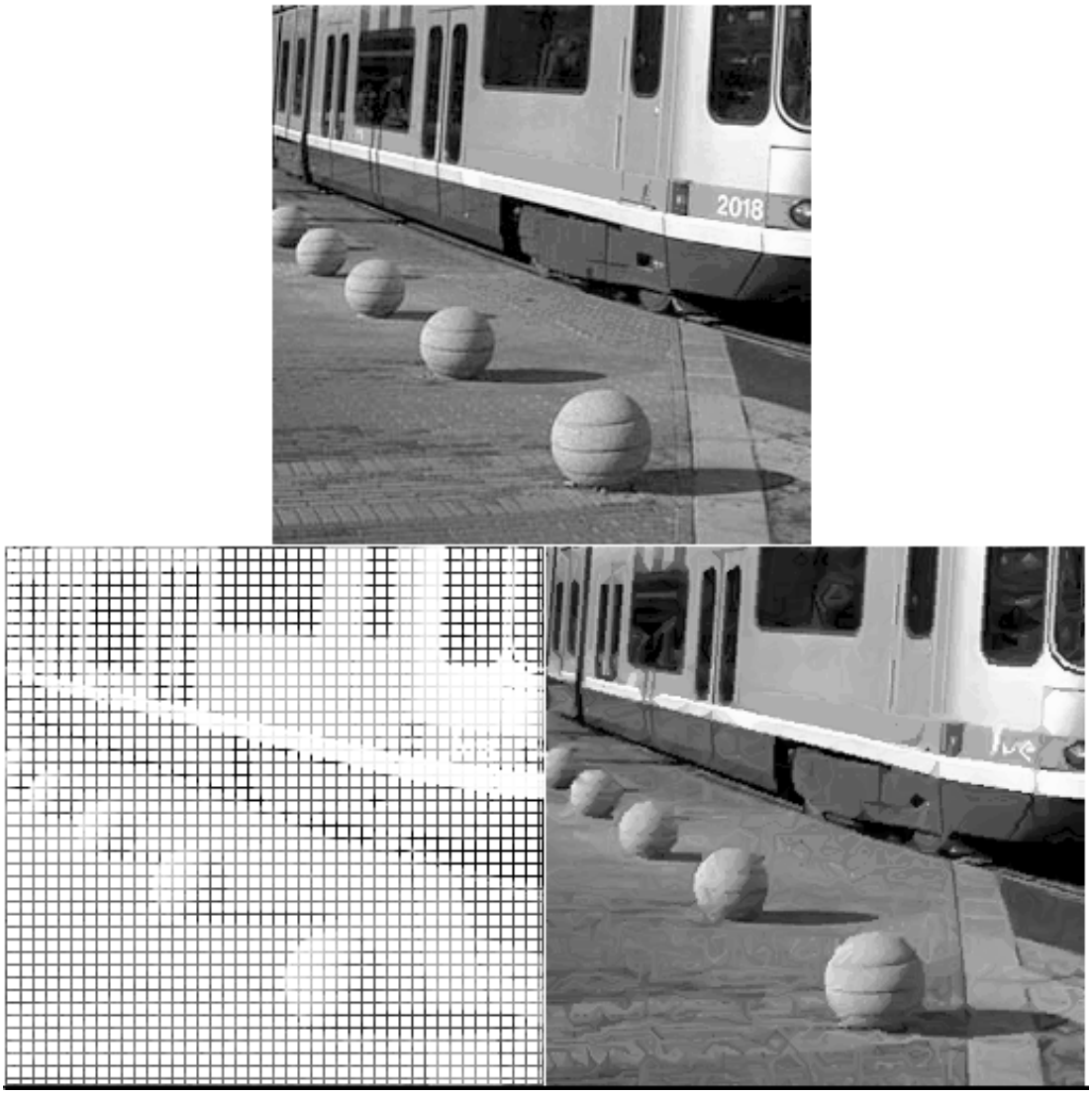

Fig. 3.16: *En haut, l'image originale; en bas à gauche, l'image obtenue en ne conservant sur chaque ligne et sur chaque colonne qu'un pixel sur six. Les occlusions sont les carrés blancs de taille* 5×5 *pixels; en bas à droite, l'image reconstruite par désocclusion.*

Enfin, les expériences qui suivent illustrent l'utilisation que l'on peut faire de notre méthode de désocclusion pour tenter de résoudre des problèmes issus de l'imagerie satellitaire. En particulier, les images prises d'un satellite présentent souvent plusieurs lignes manquantes du fait de problèmes de balayage lors de la saisie. Bernard Rougé, du Centre National d'Etudes Spatiales, nous a suggéré d'utiliser la désocclusion pour tenter de res-

taurer ces lignes manquantes. Nous avons représenté dans la figure 3.17 une simulation d'image satellitaire où manquent des groupes de 2, 3 et 4 lignes et les images obtenues par interpolation régulière et par désocclusion. L'histogramme de chaque image a été égalisé de façon à permettre une meilleure lisibilité. Les résultats apparaissent plus clairement lorsque l'image traitée a une dynamique importante et c'est pourquoi nous présentons dans la figure 3.18 la même expérience effectuée sur l'image de Lena.

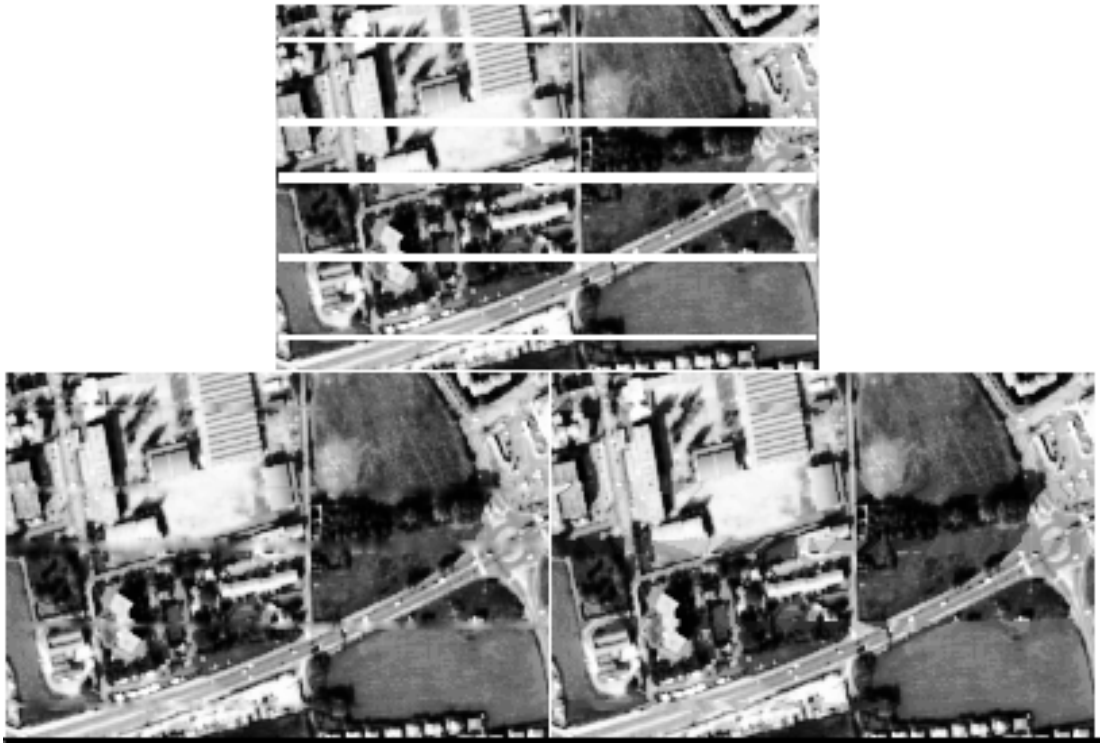

FIG. 3.17: *En haut une simulation d'image satellitaire où manquent des groupes de* 2, 3 *et* 4 *lignes. En bas à gauche, l'image restaurée par interpolation régulière à l'aide de l'équation AMLE. En bas à droite le résultat obtenu par notre méthode de désocclusion. L'histogramme de chaque image a été égalisé.*

Guy Lesthievent, du Centre National d'Etudes Spatiales, a eu l'idée d'utiliser notre algorithme de désocclusion pour éliminer les dégradations d'images du satellite SPOT dues à des pertes d'information lors de la transmission. Ces pertes se manifestent par la présence de taches dans l'image (figure 3.19) dont la position est généralement connue et que l'on peut ainsi très efficacement restaurer.

Fig. 3.18: *En haut, l'image originale et la même image après suppression de groupes de* 2, 3 *et* 4 *lignes. En bas à gauche, l'image restaurée par interpolation régulière à l'aide de l'équation AMLE. En bas à droite, l'image restaurée par notre méthode de désocclusion.*

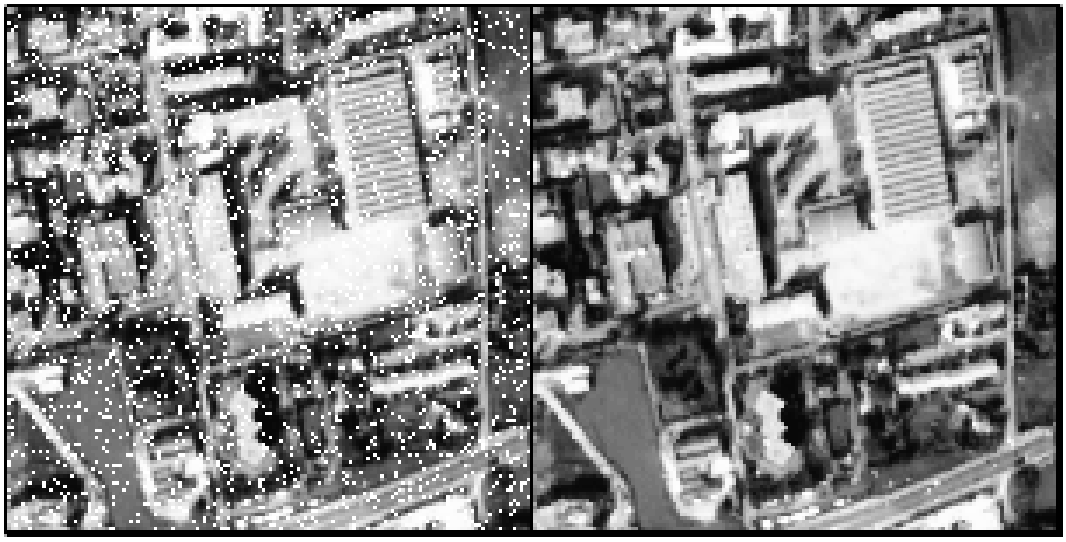

FIG. 3.19: *A gauche une simulation d'une image satellitaire CNES altérée par une perte d'information lors de la transmission; à droite le résultat obtenu après désocclusion de chacune des taches.*

Appendix A

Total variation increasing through median filtering

What follows is related to the counter-example of Section 2.3.3. We shall find by a numerical approximation the geometry of the level lines of $v := \mathrm{med}_1^+ u$. Since we are interested in the set of points such that $A(x,y) > \frac{\pi}{2}$, it is equivalent to find the points (x,y) at which the function $F(x,y) = A(x,y) - \frac{\pi}{2}$ is positive. With respect to the position of (x,y) we shall denote $F(x,y)$ by

$$F(x,y) = \begin{cases} F_1(x,y) & \text{if} \quad x\tan\theta_0 \le y \le -x\tan\theta_0 + h \\ F_2(x,y) & \text{if} \quad |y| \le x\tan\theta_0,\ y \le h - x\tan\theta_0,\ x^2 + (h-y)^2 \le 1 \\ & \quad \text{and } x\tan\theta_0 + h - y \le 1 \\ F_3(x,y) & \text{if} \quad |y| \le x\tan\theta_0,\ y \le h - x\tan\theta_0,\ x^2 + (h-y)^2 > 1 \\ & \quad \text{and } x\tan\theta_0 + h - y \le 1 \\ F_4(x,y) & \text{if} \quad |y| \le x\tan\theta_0,\ y \le h - x\tan\theta_0,\ x^2 + (h-y)^2 > 1 \\ & \quad \text{and } 1 < x\tan\theta_0 + h - y < \frac{1}{\cos\theta_0} \\ F_5(x,y) & \text{if} \quad |y| \le x\tan\theta_0,\ y \le h - x\tan\theta_0,\ x^2 + (h-y)^2 > 1 \\ & \quad \text{and } x\tan\theta_0 + h - y \ge \frac{1}{\cos\theta_0} \\ F_6(x,y) & \text{if} \quad y \le -x\tan\theta_0,\ x^2 + (h-y)^2 > 1 \text{ and } x\tan\theta_0 + h - y \le 1 \\ F_7(x,y) & \text{if} \quad y \le -x\tan\theta_0,\ x^2 + (h-y)^2 > 1 \\ & \quad \text{and } 1 < x\tan\theta_0 + h - y < \frac{1}{\cos\theta_0} \\ F_8(x,y) & \text{if} \quad y \le -x\tan\theta_0,\ x^2 + (h-y)^2 > 1,\ x\tan\theta_0 + h - y \ge \frac{1}{\cos\theta_0} \\ & \quad \text{and } x \le \cos\theta_0 \\ F_9(x,y) & \text{if} \quad y \le -x\tan\theta_0 \text{ and } x \ge \cos\theta_0 \end{cases}$$

This enumeration is not complete, but enough to describe the solution to our problem. From figure A.1 we deduce that

$$F_1(x,y) = \frac{\pi}{2} - (A_1 + A_2 + A_3 + A_4 + 2A_5)$$

Define the area $A(\alpha) \equiv A(\alpha, \theta_0) = \frac{1}{2}(\theta_1 + \alpha \cos\theta_1)$ where $\theta_1 > 0$ satisfies

$$\begin{cases} \beta^2 &= \alpha^2 + 1 - 2\alpha \sin\theta_1 \\ 1 &= \alpha^2 + \beta^2 + 2\alpha\beta \sin\theta_0 \end{cases}$$

so that $\cos\theta_1 = \cos\theta_0 \left(\sqrt{1 - \alpha^2 \cos^2\theta_0} - \alpha \sin\theta_0\right)$. Therefore

$$\begin{cases} A_1 &= A(y - x\tan\theta_0) \\ A_2 &= A(h - y - x\tan\theta_0) \\ A_3 &= A(y + x\tan\theta_0) \\ A_4 &= A(h - y + x\tan\theta_0) \\ A_5 &= x^2 \tan\theta_0 \end{cases}$$

From the expression of $F_1(x, y)$, it must be emphasized that $F(x, y) = 0$ is a transcendental

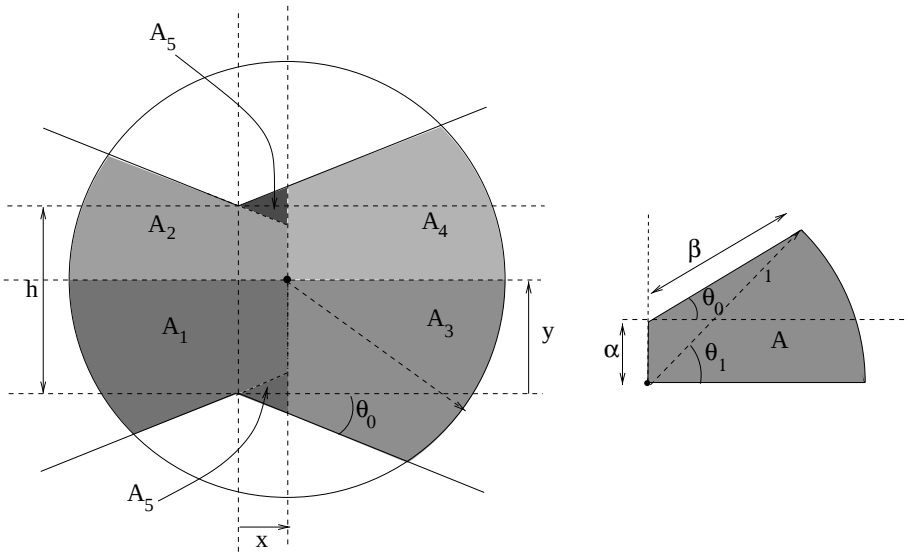

Figure A.1: Configuration related to $F_1(x, y)$

equation for which only a numerical solution can be computed. It arises from figure A.2 that

$$F_2(x, y) = \frac{\pi}{2} - (A_6 + A_8 + A_9 + A_{10} + A_3 + A_4 + A_5)$$

with

$$\begin{cases} A_6 + A_7 + A_8 = \frac{\theta_2}{2} \\ A_7 + A_8 = \frac{1}{2}\sqrt{x^2 + y^2}\sin\theta_2 \\ A_8 + A_9 = \frac{1}{2}(x^2 \tan\theta_0 + xy) \\ A_{10} = A(h - y - x\tan\theta_0) + \frac{1}{2}\arctan\frac{y}{x} \end{cases}$$

Since

$$F_2(x, y) = \tfrac{\pi}{2} - ((A_6 + A_7 + A_8) - (A_7 + A_8) + (A_8 + A_9) + A_{10} + A_3 + A_4 + A_5)$$

it is only necessary to compute θ_2. Let us examine figure A.2b and remark that

$$\left\{ \begin{array}{rcl} z^2 & = & 1 + x^2 + y^2 - 2\sqrt{x^2+y^2}\cos\theta_2 \\ 1 & = & z^2 + x^2 + y^2 + 2z\sqrt{x^2+y^2}\cos(\theta_0 - \arctan\frac{y}{x}) \end{array} \right.$$

so that $\cos\theta_2 = \delta\sin^2\theta_3 + \cos\theta_3\sqrt{1-\delta^2\sin^2\theta_3}$ with $\delta = \sqrt{x^2+y^2}$ and $\theta_3 = \theta_0 - \arctan\frac{y}{x}$. Remark that $|y| < x\tan\theta_0$ and $x < \cos\theta_0$ are sufficient conditions for θ_2 to be defined.

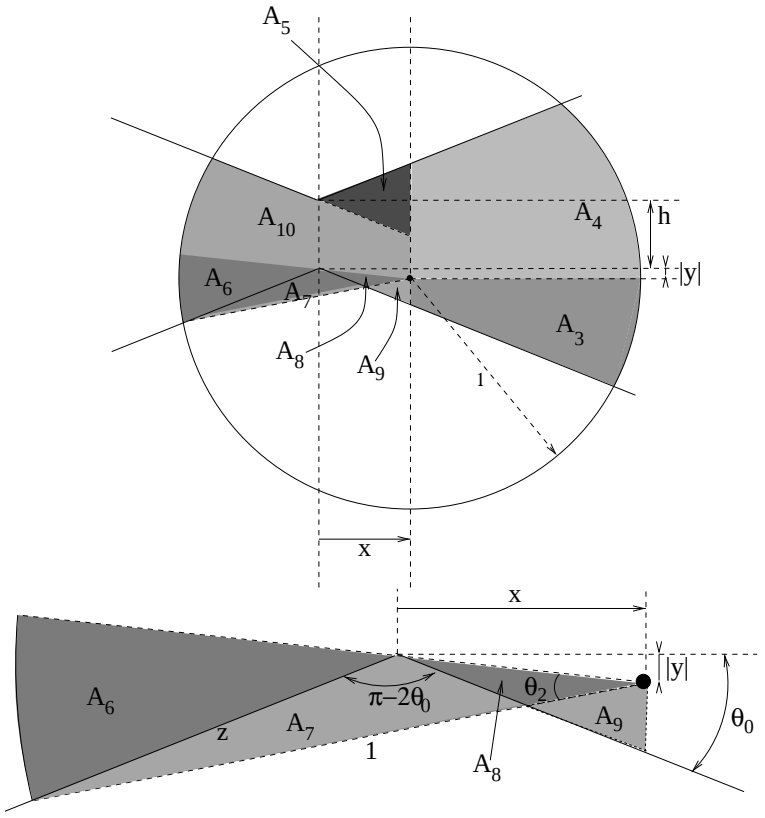

Figure A.2: Configuration related to $F_2(x,y)$

Like illustrated in figure A.3 we can write

$$F_3(x,y) = \frac{\pi}{2} - (A_3 + A_4 + A_{11} + A_{12})$$

with $A_{12} = A_6 + A_8 + A_9$. Define $B(\alpha) \equiv B(\alpha,\theta_0) = \frac{1}{2}(\theta_4 + \alpha\sin\theta_4)$ where

$$\left\{ \begin{array}{l} \beta^2 = \alpha^2 + 1 - 2\alpha\sin\theta_4 \\ 1 = \alpha^2 + \beta^2 - 2\alpha\beta\sin\theta_0 \end{array} \right.$$

so that

$$\cos\theta_4 = \cos\theta_0\left(\sqrt{1-\alpha^2\cos^2\theta_0} + \alpha\sin\theta_0\right)$$

Therefore $B(\alpha, \theta_0) = A(\alpha, -\theta_0)$. Thus

$$A_{11} = B(h - y + x\tan\theta_0) + \frac{1}{2}\arctan\frac{y}{x} = A(h - y + x\tan\theta_0, -\theta_0) + \frac{1}{2}\arctan\frac{y}{x}$$

and $F_3(x, y)$ follows. From figure A.4 we deduce that

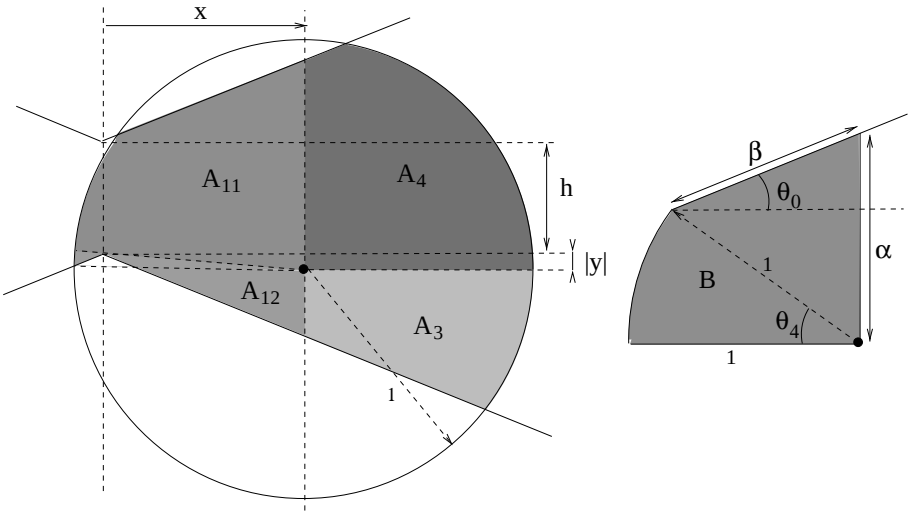

Figure A.3: Configuration related to $F_3(x, y)$

$$F_4(x, y) = \frac{\pi}{2} - (A_3 + + A_{12} + A_{13})$$

where $A_{13} = \frac{\pi}{2} - A_{14} + \frac{1}{2}\arctan\frac{y}{x}$ and $A_{14} = \frac{1}{2}(\theta_5 - \sin\theta_5)$. Since

$$\begin{cases} 1 = \alpha^2 + \delta^2 - 2\alpha\delta\cos\theta_0 \\ 1 = \beta^2 + \delta^2 - 2\beta\delta\cos\theta_0 \end{cases}$$

with $\delta = \frac{h-y}{\tan\theta_0} + x$, we deduce that $\beta - \alpha = 2\sqrt{1 - \delta^2\sin^2\theta_0}$.
From $\frac{1}{2}\sin\theta_5 = \delta\sin\theta_0\sqrt{1 - \delta^2\sin^2\theta_0}$ we get

$$\sin\theta_5 = 2\delta\sin\theta_0\sqrt{1 - \delta^2\sin^2\theta_0}$$

and $F_4(x, y)$ follows. $F_5(x, y)$ can be deduced from $F_4(x, y)$ by simply letting $A_{14} = 0$.

Figure A.5 yields

$$F_7(x, y) = A_{14} + A_{15} - x^2\tan\theta_0 + A_{16} + A_{17} + \frac{\pi}{4}$$

with

$$\begin{cases} A_{15} &= B(|y| + x\tan\theta_0) \\ A_{16} &= \frac{1}{2}(\frac{\pi}{2} - \theta_6) \\ A_{17} &= \frac{1}{2}\delta\sin\theta_6 \end{cases}$$

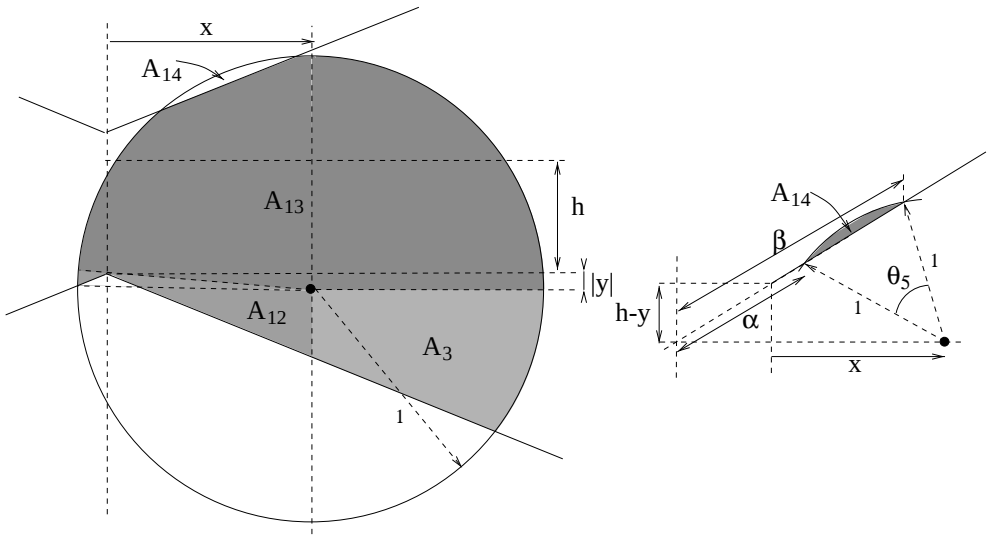

Figure A.4: Configuration related to $F_4(x, y)$

and $\delta = \frac{|y|}{\tan\theta_0} - x$. It is easily seen that

$$\begin{cases} z^2 = 1 + \delta^2 - 2\delta\cos\theta_6 \\ 1 = z^2 + \delta^2 + 2z\delta\cos\theta_0 \end{cases}$$

and thus

$$\cos\theta_6 = \delta\sin^2\theta_0 + \cos\theta_0\sqrt{1 - \delta^2\sin^2\theta_0}$$

so that $F_7(x, y)$ is known. $F_6(x, y)$ is a simple combination of $F_7(x, y)$ and $F_1(x, y)$ since

$$F_6(x, y) = \frac{\pi}{2} - (A_2 + A_4 + A_5) + A_{15} - x^2\tan\theta_0 + A_{16} + A_{17} + \frac{\pi}{4}$$

It is finally easily seen that $F_8(x, y) = A_{15} - x^2\tan\theta_0 + A_{16} + A_{17} + \frac{\pi}{4}$ and $F_9(x, y) > \frac{\pi}{2}$ Let $h = 0.5$. Figure A.6 shows the value of θ_0 such that $F_1(0,\, 0.25) = 0$. A numerical root finding gives the approximate result $\theta_0 \approx 0.33756$. For such a θ_0, one has represented in figure A.7 the graph of $\Gamma = \{(x, y) \in \mathbb{R}^+ \times (-\infty, \frac{h}{2}],\ F(x, y) = 0\}$. It is the lower-right boundary of $\{(x, y),\ \mathrm{med}_{B_1} u > 0\}$. Γ is first a decreasing curve that crosses the line $\mathcal{D}$ with equation $y = -x\tan\theta_0$ at $(x_0, y_0) \approx (0.72,\, -0.25)$, and then increases until coinciding with $\mathcal{D}$ as soon as $x \geq \cos\theta_0 \approx 0.9436$. The figure is a numerical confirmation that

$$|D\,\mathrm{med}_{B_1} u| > |Du|$$

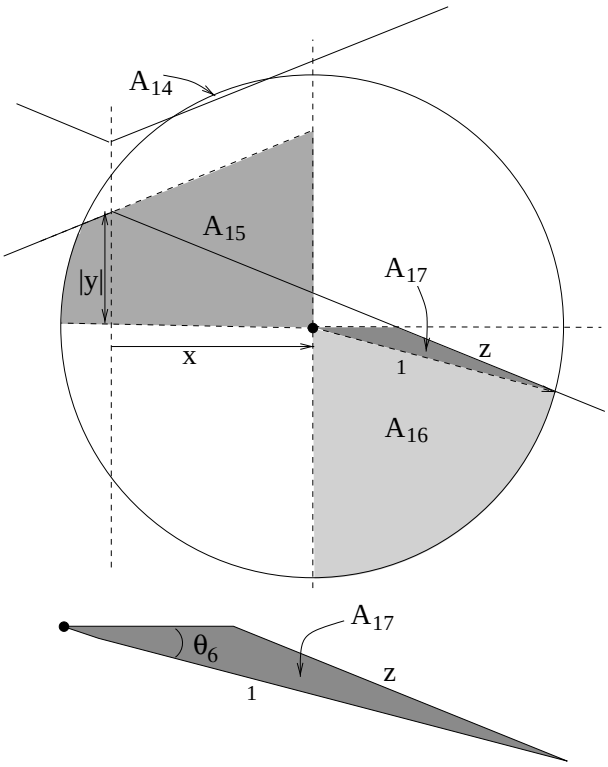

Figure A.5: Configuration related to $F_7(x, y)$

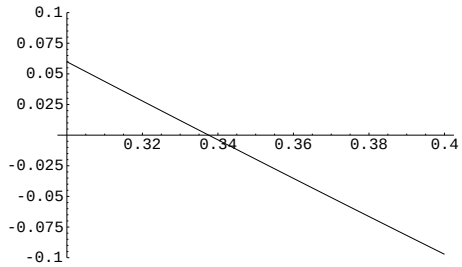

Figure A.6: Graph of $F(0,\ 0.25)$ with respect to different values of θ_0 ($h = 0.5$)

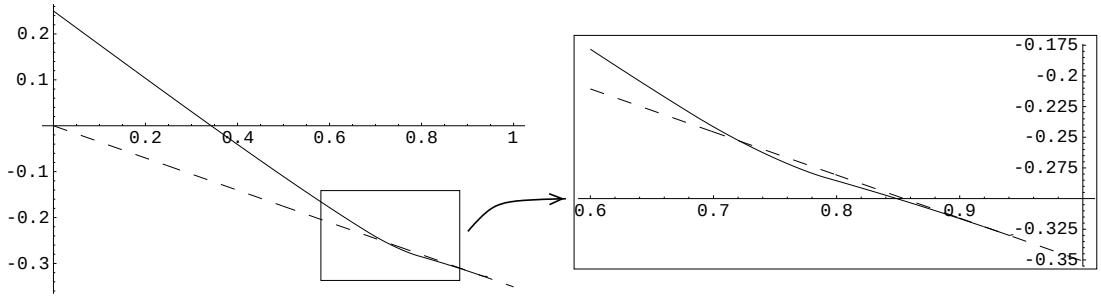

Figure A.7: Left – graph of $\Gamma = \{(x, y) \in \mathbb{R}^+ \times (-\infty, \frac{h}{2}],\ F(x, y) = 0\}$ ($h = 0.5$)
Right – zoom in around the point where Γ intersects $\{(x, y),\ y = -x \tan \theta_0\}$

Annexe B

Etude asymptotique d'un filtre non morphologique à voisinage

Considérons l'opérateur T_h^r dépendant de $h, r \in \mathbb{R}_+^*$ qui à toute fonction mesurable $u : \mathbb{R}^2 \to \mathbb{R}$ associe pour tout $x_0 \in \mathbb{R}^2$

$$T_h^r\ u(x_0) = \mathrm{med}_{x \in W_{r,h}^u(x_0)}\ u(y)$$

avec $W_{r,h}^u(x_0) = \{x \in D(x_0, h)\ :\ |u(x) - u(x_0)| \leq rh\}$. En d'autres termes, ce filtre fait intervenir un voisinage de points dont la luminosité est d'autant plus proche de celle du point central que le rayon du disque est petit, ce qui revient à dire que l'analyse locale en espace est couplée à une analyse locale en niveaux de gris. Ce filtre n'est clairement pas invariant par changement de contraste mais il est facile de vérifier qu'il est invariant par transformation euclidienne. On peut montrer par ailleurs que

$$T_h^r(u - u(x_0))(x_0) = T_h^r u(x_0) - u(x_0)$$

et donc supposer sans perte de généralité que $u(x_0) = 0$. Supposons par ailleurs que $u \in \mathrm{C}^3(\mathbb{R}^2)$ et que x_0 n'est pas un point critique de u. Dans la mesure où T_h^r est invariant par transformation euclidienne, on peut sans perte de généralité placer l'origine du repère en x_0 et choisir les vecteurs de base $(\vec{i}, \vec{j})$ de sorte que $\vec{i} = \frac{Du}{|Du|}(x_0)$ et $\vec{j} = \frac{Du^\perp}{|Du|}(x_0)$. On a alors pour tout (x, y) au voisinage de $(0, 0)$ dans le nouveau repère :

$$u(x, y) = px + ax^2 + by^2 + cxy + \circ(|\vec{x}|^2)$$

$$\text{où } p = |Du(0)|,\ a = \tfrac{1}{2}\tfrac{\partial^2 u}{\partial x^2}(0),\ b = \tfrac{1}{2}\tfrac{\partial^2 u}{\partial y^2}(0) \text{ et } c = \tfrac{1}{2}\tfrac{\partial^2 u}{\partial x \partial y}(0).$$

et l'on peut vérifier que $b = \frac{1}{2}|Du|\mathrm{curv}(u)(0)$. Etudions à présent le comportement asymptotique du filtre lorsque l'on suppose en outre que $a = c = 0$ et $b \neq 0$, c'est-à-dire que les lignes de niveau de u au voisinage de l'origine sont des paraboles symétriques par rapport à l'axe des abscisses. On a alors la proposition suivante :

Proposition *Soit u une fonction C^3 de $\mathbb{R}^2$ dans $\mathbb{R}$.*
En tout point régulier (x_0, y_0) où il existe un repère dans lequel au voisinage de (x_0, y_0)

$$u(x,y) = u(x_0,y_0) + x|Du(x_0,y_0)| + \frac{y^2}{2}|Du|\mathrm{curv}(u)(x_0,y_0) + \circ(|(x-x_0, y-y_0)|^2)$$

on a pour tout h suffisamment petit et $r < |Du(x_0,y_0)|$:

$$\underset{\substack{(x,y)\in D_h(x_0,y_0)\\ |u(x,y)-u(x_0,y_0)|\leq rh}}{\mathrm{med}\, u(x,y)} = u(x_0,y_0) + \frac{1-v^3}{6}|Du|\mathrm{curv}(u)(x_0,y_0)h^2 + \circ(h^2)$$

$$\text{où} \qquad v = \sqrt{1 - \frac{r^2}{|Du(x_0,y_0)|^2}}$$

PROOF : En supposant $u(x_0, y_0) = 0$ comme on l'a vu précédemment, on peut vérifier que

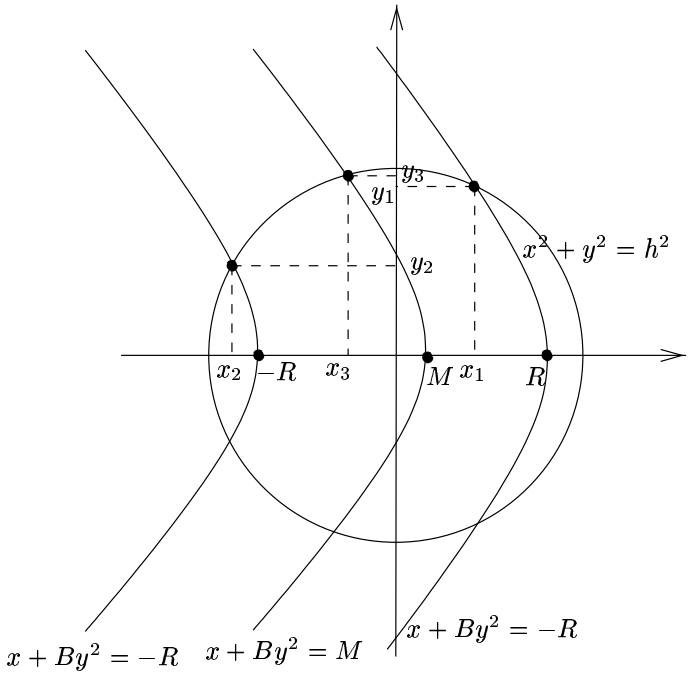

tous les points du voisinage considéré appartiennent au domaine (voir figure ci-dessus) délimité par les trois paraboles d'équations :

$$\begin{aligned} px + by^2 &= rh \\ px + by^2 &= m \\ px + by^2 &= -rh \end{aligned}$$

Afin que les points d'intersection des deux paraboles extrêmes avec l'axe des abscisses appartiennent au disque, nous allons supposer que $r \leq p$. Signalons que lorsque $r > p$

alors pour h suffisamment petit, $r > hb$ et les deux paraboles extrêmes n'ont pas d'intersection avec le disque. On est dans ce cas ramené au filtre médian classique qui est asymptotiquement équivalent à l'équation

$$\frac{\partial u}{\partial t} = \frac{1}{6}|Du|\text{curv}(u)$$

En posant $R = \frac{rh}{p}$, $B = \frac{b}{p}$ et $M = \frac{m}{p}$ les équations des paraboles deviennent :

$$\begin{aligned} x + By^2 &= R \\ x + By^2 &= M \\ x + By^2 &= -R \end{aligned}$$

L'abscisse x_1 indiquée sur la figure est solution du système $\begin{cases} x + By^2 = R \\ x^2 + y^2 = h^2 \end{cases}$

Pour h suffisamment petit x_1 existe et

$$x_1 = \frac{1 \pm \sqrt{1 + 4B(Bh^2 - R)}}{2B}$$

Or $-h \leq x_1 \leq h$ d'où $-1 - 2Bh \leq \pm\sqrt{1 + 4B(Bh^2 - R)} \leq -1 + 2Bh$, ce qui, lorsque h est suffisamment petit, n'est possible que si le terme central est négatif. On a donc comme unique solution :

$$x_1 = \frac{1 - \sqrt{1 + 4B(Bh^2 - R)}}{2B}$$

D'où $x_1 = \frac{1}{2B}[1 - (1 + 2B(Bh^2 - R) - 2B^2(Bh^2 - R)^2 + \circ(h^2)]$, puis

$$x_1 = R - Bh^2 + BR^2 + \circ(h^2) \tag{B.1}$$

De façon analogue, on montre que :

$$x_2 = -R - Bh^2 + BR^2 + \circ(h^2) \tag{B.2}$$

On a par ailleurs $x_3 = \frac{1-\sqrt{1+4B(Bh^2-M)}}{2B}$. En supposant que $M = \mathcal{O}(h^2)$, on obtient :

$$x_3 = M - Bh^2 + \circ(h^3) \tag{B.3}$$

L'ordonnée y_1 est solution de l'équation $B^2y^4 + (1 - 2BR)y^2 + R^2 - h^2 = 0$. Pour des raisons de signe, on a nécessairement :

$$\begin{aligned} y_1^2 &= \frac{2BR - 1 + \sqrt{1 - 4BR + 4B^2h^2}}{2B^2} \\ &= h^2 - R^2 + 2BRh^2 - 2BR^3 + \circ(h^3) \\ &= (h^2 - R^2)(1 + 2BR + \circ(h)) \end{aligned}$$

On en déduit que $y_1 = \sqrt{h^2 - R^2}(1 + BR + \circ(h))$, c'est-à-dire

$$y_1 = vh(1 + BR) + \circ(h^2) \qquad \text{avec } v = \sqrt{1 - \frac{R^2}{h^2}} = \sqrt{1 - \frac{r^2}{p^2}} \tag{B.4}$$

De façon analogue on obtient :

$$y_2 = vh(1 - BR) + \circ(h^2) \tag{B.5}$$

On a par ailleurs

$$y_3^2 = \frac{2BM - 1 + \sqrt{1 - 4BM + 4B^2h^2}}{2B^2}$$

Avec l'hypothèse précédente $M = \mathcal{O}(h^2)$ on obtient $y_3^2 = h^2 + \circ(h^3)$, d'où :

$$y_3 = h + \circ(h^2) \tag{B.6}$$

La valeur médiane que nous voulons déterminer est celle pour laquelle les deux aires suivantes sont égales.

$$\mathcal{A}_1 = \int_{x_1}^{R} \sqrt{\frac{R-x}{B}}dx + \int_{x_3}^{x_1} \sqrt{h^2 - x^2}dx - \int_{x_3}^{M} \sqrt{\frac{M-x}{B}}dx$$

$$\mathcal{A}_2 = \int_{x_3}^{M} \sqrt{\frac{M-x}{B}}dx + \int_{x_2}^{x_3} \sqrt{h^2 - x^2}dx - \int_{x_2}^{-R} \sqrt{\frac{-R-x}{B}}dx$$

On obtient immédiatement

$$\mathcal{A}_1 = \frac{2B}{3}(y_1^3 - y_3^3) + \int_{x_3}^{x_1} \sqrt{h^2 - x^2}dx \tag{B.7}$$

et

$$\mathcal{A}_2 = \frac{2B}{3}(y_3^3 - y_2^3) + \int_{x_2}^{x_3} \sqrt{h^2 - x^2}dx \tag{B.8}$$

Or, on déduit des équations (B.4), (B.5), et (B.6) :

$$\begin{aligned} y_1^3 &= v^3h^3(1 + 3BR) + \circ(h^4) \\ y_2^3 &= v^3h^3(1 - 3BR) + \circ(h^4) \\ y_3^3 &= h^3 + \circ(h^4) \end{aligned}$$

D'où

$$y_1^3 - y_3^3 = h^3(v^3 - 1) + \circ(h^3) \tag{B.9}$$

et

$$y_3^3 - y_2^3 = h^3(1 - v^3) + \circ(h^3) \tag{B.10}$$

Par ailleurs, en posant $x = hcos\theta$, $\theta_1 = \arccos\frac{x_1}{h}$ et $\theta_3 = \arccos\frac{x_3}{h}$, on obtient :

$$\begin{aligned}
\int_{x_3}^{x_1} \sqrt{h^2 - x^2}dx &= \int_{\theta_1}^{\theta_3} h^2 \sin^2\theta d\theta \\
&= \frac{h^2}{2}[\theta_3 - \theta_1 + \frac{1}{2}(\sin 2\theta_1 - \sin 2\theta_3)] \\
&= \frac{h^2}{2}(\theta_3 - \theta_1 + \sin\theta_1\cos\theta_1 - \sin\theta_3\cos\theta_3) \\
&= \frac{h^2}{2}(\theta_3 - \theta_1) + \frac{1}{2}(x_1\sqrt{h^2 - x_1^2} - x_3\sqrt{h^2 - x_3^2}) \qquad \text{(B.11)}
\end{aligned}$$

Or

$$\begin{aligned}
\theta_3 - \theta_1 &= \arccos(\cos(\theta_3 - \theta_1)) \\
&= \arccos(\cos\theta_3\cos\theta_1 + \sin\theta_3\sin\theta_1) \\
&= \arccos\frac{x_1x_3 + \sqrt{h^2 - x_1^2}\sqrt{h^2 - x_3^2}}{h^2} \qquad \text{(B.12)}
\end{aligned}$$

Les équations (B.1) et (B.3) nous donnent :

$$\begin{aligned}
x_1x_3 &= (R - Bh^2 + BR^2 + \circ(h^2))(M - Bh^2 + \circ(h^3)) \\
&= MR - BRh^2 + \circ(h^3) \qquad \text{(B.13)}
\end{aligned}$$

Par ailleurs $x_1^2 = R^2(1 + 2BR - \frac{2Bh^2}{R}) + \circ(h^3)$
D'où

$$\begin{aligned}
\sqrt{h^2 - x_1^2} &= \sqrt{h^2 - R^2 + 2BR(h^2 - R^2) + \circ(h^3)} \\
&= \sqrt{h^2 - R^2}\sqrt{1 + 2BR + \circ(h)} \\
&= hv(1 + BR) + \circ(h^2)
\end{aligned}$$

De façon analogue

$$\begin{aligned}
\sqrt{h^2 - x_3^2} &= \sqrt{h^2 - M^2 + 2BMh^2 - B^2h^4 + \circ(h^5)} \\
&= h - \frac{M^2}{2h} + BMh - \frac{B^2h^3}{2} + \circ(h^4)
\end{aligned}$$

D'où $\sqrt{h^2 - x_1^2}\sqrt{h^2 - x_3^2} = vh^2 + vBRh^2 + \circ(h^3)$, ce qui, avec l'équation (B.13) implique :

$$x_1x_3 + \sqrt{h^2 - x_1^2}\sqrt{h^2 - x_3^2} = vh^2 + MR + BRh^2(v - 1) + \circ(h^3)$$

L'équation (B.12) devient donc $\theta_3 - \theta_1 = \arccos(v + \frac{MR}{h^2} + BR(v - 1) + \circ(h))$
Or $\arccos(v + \epsilon) = \arccos v - \frac{\epsilon}{\sqrt{1-v^2}} + \circ(\epsilon)$ et $\frac{1}{\sqrt{1-v^2}} = \frac{h}{R}$
D'où $\theta_3 - \theta_1 = \arccos v - \frac{M}{h} - Bh(v - 1) + \circ(h)$, puis

$$\frac{h^2}{2}(\theta_3 - \theta_1) = \frac{h^2}{2}\arccos v - \frac{Mh}{2} - \frac{v - 1}{2}Bh^3 + \circ(h^3) \qquad \text{(B.14)}$$

Interessons-nous maintenant à la deuxième partie du second membre de (B.11). On a :

$$\begin{aligned} x_1\sqrt{h^2-x_1^2} &= hv(1+BR+\circ(h))(R-Bh^2+BR^2+\circ(h^2)) \\ &= hv(R+2BR^2-Bh^2)+\circ(h^3) \end{aligned}$$

et

$$\begin{aligned} x_3\sqrt{h^2-x_3^2} &= (M-Bh^2+\circ(h^3))(h-\frac{M^2}{2h}+BMh-\frac{B^2h^3}{2}+\circ(h^4)) \\ &= Mh-Bh^3+\circ(h^4) \end{aligned} \tag{B.15}$$

D'où

$$\frac{1}{2}(x_1\sqrt{h^2-x_1^2}-x_3\sqrt{h^2-x_3^2}) = \frac{hvR}{2}+BR^2hv-\frac{Mh}{2}-\frac{v-1}{2}Bh^3+\circ(h^3)$$

Par conséquent

$$\int_{x_3}^{x_1}\sqrt{h^2-x^2}dx = \frac{h^2}{2}\arccos v+\frac{hvR}{2}+BR^2hv-Mh+(1-v)Bh^3+\circ(h^3)$$

On obtient ensuite à partir des équations (B.7) et (B.10) :

$$\begin{aligned} \mathcal{A}_1 &= \frac{2B}{3}h^3(v^3-1)+\frac{h^2}{2}\arccos v+\frac{hvR}{2} \\ &\quad +BR^2hv-Mh+(1-v)Bh^3+\circ(h^3) \end{aligned} \tag{B.16}$$

$\mathcal{A}_2$ peut être déterminée de façon analogue et nous ne donnons ci-dessous que les principaux résultats intermédiaires :
Avec $\theta_2 = \arccos\frac{x_2}{h}$ et $\theta_3 = \arccos\frac{x_3}{h}$, on montre que

$$\begin{aligned} \int_{x_2}^{x_3}\sqrt{h^2-x^2}dx &= \frac{h^2}{2}(\arccos\frac{x_2x_3+\sqrt{h^2-x_2^2}\sqrt{h^2-x_3^2}}{h^2}) \\ &\quad +\frac{1}{2}(x_3\sqrt{h^2-x_3^2}-x_2\sqrt{h^2-x_2^2}) \end{aligned}$$

Or

$$\begin{aligned} x_2x_3 &= -MR+BRh^2+\circ(h^3) \\ \sqrt{h^2-x_2^2} &= hv(1-BR)+\circ(h^2) \\ \sqrt{h^2-x_2^2}\sqrt{h^2-x_3^2} &= vh^2-vBRh^2+\circ(h^3) \end{aligned}$$

d'où

$$x_2x_3+\sqrt{h^2-x_2^2}\sqrt{h^2-x_3^2} = vh^2-MR-BRh^2(v-1)+\circ(h^3)$$

On en déduit :

$$\frac{h^2}{2}(\theta_2 - \theta_1) = \frac{h^2}{2}\arccos v + \frac{Mh}{2} + \frac{v-1}{2}Bh^3 + \circ(h^3)$$

Par ailleurs

$$\begin{aligned} x_2\sqrt{h^2 - x_2^2} &= hv(1 - BR + \circ(h))(-R - Bh^2 + BR^2 + \circ(h^2)) \\ &= hv(-R - Bh^2 + 2BR^2) + \circ(h^3) \end{aligned}$$

d'où, avec l'équation (B.15)

$$\frac{1}{2}(x_3\sqrt{h^2 - x_3^2} - x_2\sqrt{h^2 - x_2^2}) = \frac{hvR}{2} - BR^2hv + \frac{Mh}{2} + \frac{v-1}{2}Bh^3 + \circ(h^3)$$

On peut alors conclure

$$\int_{x_2}^{x_3} \sqrt{h^2 - x^2}dx = \frac{h^2}{2}\arccos v + \frac{hvR}{2} - BR^2hv + Mh + (v-1)Bh^3 + \circ(h^3)$$

Puis

$$\begin{aligned} \mathcal{A}_2 &= \frac{2B}{3}h^3(1 - v^3) + \frac{h^2}{2}\arccos v + \frac{hvR}{2} \\ &\qquad -BR^2hv + Mh + (v-1)Bh^3 + \circ(h^3) \end{aligned} \tag{B.17}$$

La valeur médiane cherchée est celle pour laquelle $\mathcal{A}_1 = \mathcal{A}_2$, ce qui implique en égalisant les équations (B.16) et (B.17):

$$M = \frac{2B}{3}h^2(v^3 - 1) + BR^2v + (1 - v)Bh^2 + \circ(h^2)$$

Or $R^2 = h^2(1 - v^2)$ d'où :

$$M = \frac{1 - v^3}{3}Bh^2 + \circ(h^2)$$

En revenant aux notations initiales, on obtient :

$$m = \frac{1 - v^3}{3}bh^2 + \circ(h^2)$$

Or $b = \frac{1}{2}|Du|\mathrm{curv}(u)$ d'où :

$$m = \frac{1 - v^3}{6}|Du|\mathrm{curv}(u)h^2 + \circ(h^2)$$

On peut alors conclure, en revenant au repère et aux niveaux de gris initiaux :

$$\underset{\substack{(x,y)\in D_h(x_0,y_0) \\ |u(x,y)-u(x_0,y_0)|\leq rh}}{\mathrm{med}\, u(x,y)} = u(x_0,y_0) + \frac{1 - v^3}{6}|Du|\mathrm{curv}(u)(x_0,y_0)h^2 + \circ(h^2)$$

□

Bibliographie

[1] L. Alvarez, F. Guichard, P.L. Lions, and J.M. Morel. Axiomatisation et nouveaux opérateurs de la morphologie mathématique. *C.R. Acad. Sci Paris*, 315, Série I:265–268, 1992.

[2] L. Ambrosio. Minimizing movements. *Lecture notes, University of Padova, Italy*, 1994.

[3] L. Ambrosio, N. Fusco, and D. Pallara. *Functions of bounded variation and free discontinuity problems.* Oxford University Press, 1999.

[4] G. Bellettini, G. Dal Maso, and M. Paolini. Semicontinuity and relaxation properties of a curvature depending functional in 2D. *Ann. Scuola Norm. Sup. Pisa Cl. Sci.*, 20(4):247–297, 1993.

[5] H. Brezis. *Analyse fonctionnnelle.* Masson, Paris, 1983.

[6] J.F. Canny. A computational approach to edge detection. *IEEE Trans. Pattern Analysis and Machine Intelligence*, 8:769–798, 1986.

[7] V. Caselles, T. Coll, and J.M. Morel. A Kanizsa programme. Technical Report 9539, CEREMADE, Université Paris-Dauphine, France, 1995.

[8] V. Caselles and J.M. Morel. The connected components of sets of finite perimeter in the plane. *Preprint*, 1998.

[9] V. Caselles, J.M. Morel, and C. Sbert. An axiomatic approach to image interpolation. *IEEE, Special Issue on Differential Equations*, 1998.

[10] A. Chambolle and P.L. Lions. Image recovery via total variation minimization and related problems. *Numerische Mathematik*, 76:167–188, 1997.

[11] B. Chazelle. Triangulating a simple polygon in linear time. *Discrete Comput. Geometry*, 6:485–524, 1991.

[12] G. Dolzmann and S. Müller. Microstructures with finite surface energy : the two-well problem. *Arch. Rational Mech. Anal.*, 132:101–141, 1995.

[13] L.C. Evans and R.F. Gariepy. Measure theory and fine properties of functions. In *Studies in Advanced Mathematics*. CRC Press Inc., 1992.

[14] H. Federer. *Geometric Measure Theory*. Springer-Verlag, Berlin, 1969.

[15] E. Giusti. *Minimal surfaces and functions of bounded variation*. Birkhäuser, 1984.

[16] F. Guichard and J.M. Morel. Partial differential equations and image iterative filtering. Technical Report 9535, CEREMADE, Université Paris-Dauphine, France, 1995.

[17] J. Hershberger and J. Snoeyink. Computing minimum length paths of a given homotopy class. *Comput. Geom Theory Appl.*, 4:63–98, 1994.

[18] G. Kanizsa. *Vedere e pensare*. Il Mulino, Bologna, 1991.

[19] G. Kanizsa. *Grammaire du Voir*. Diderot, Paris, 1996.

[20] B. Kirchheim. Lipschitz minimizers of the 3-well problem having gradients of bounded variation. *Preprint*, 1998.

[21] D.T. Lee and F. Preparata. Euclidean shortest paths in the presence of rectilinear barriers. *Networks*, 14:393–410, 1984.

[22] J. Malik and P. Perona. A scale space and edge detection using anisotropic diffusion. In *Proc. IEEE Comp. Soc. Workshop on Comp. Vision, Miami*, pages 16–22, 1987.

[23] D. Marr. *Vision*. Freeman and Co, 1982.

[24] D. Marr and E. Hildreth. Theory of edge detection. In *Proc. Royal Soc. London*, volume B 207, pages 187–217, 1980.

[25] G. Matheron. *Random sets and integral geometry*. John Wiley and Sons, New York, 1975.

[26] Y. Meyer. *Les ondelettes : algorithmes et applications*. Armand Colin, Paris, 1993.

[27] J.S.B. Mitchell. Geometric shortest paths and network optimization. In J.-R. Sack and J. Urrutia, editors, *Handbook of Computational Geometry*. Elsevier Science, 1998.

[28] J.S.B. Mitchell. Personal communication. 1998.

[29] P. Monasse and F. Guichard. Fast computation of a contrast-invariant image representation. *submitted to IEEE Trans. on Image Processing*, 1998.

[30] A.P. Morse. The behaviour of a function on its critical set. *Annals of Mathematics*, 40:62–70, 1939.

[31] D. Mumford. Elastica and computer vision. In C. Bajaj, editor, *Algebraic geometry and applications*. Springer-Verlag, Heidelberg, 1992.

[32] M. Nitzberg, D. Mumford, and T. Shiota. Filtering, Segmentation and Depth. In *Lecture Notes in Computer Science*, volume 662. Springer-Verlag, Berlin Heidelberg, 1993.

[33] J. O'Rourke. *Computational Geometry in C.* Cambridge University Press, 1998.

[34] L. Rudin and S. Osher. Total variation based image restoration with free local constraints. In *Proc. of the IEEE ICIP-94, Austin, Texas*, volume 1, pages 31–35, 1994.

[35] M. Schmitt. Geodesic arcs in non-euclidean metrics : application to the propagation function. *Revue d'Intelligence Artificielle*, 3 (2):43–76, 1989.

[36] J. Serra. *Image analysis and mathematical morphology.* Academic Press, London, 1982.

[37] E. Sharon, A. Brandt, and R. Basri. Completion energies and scale. *IEEE Transactions on Pattern Analysis and Machine Intelligence, forthcoming.*

[38] S.M. Smith and J.M. Brady. Susan - a new approach to low level image processing. *International Journal of Computer Vision*, 1997.

[39] L. Vincent. Morphological area openings and closings for gray-scale images. In *Proc. of the Workshop "Shape in Picture", 1992, Driebergen, The Netherlands*, pages 197–208. Springer-Berlin, 1994.

[40] M. Wertheimer. Untersuchung zur Lehre der Gestalt. *Psychologische Forshung*, IX:301–350, 1923.

[41] A.P. Witkin. Scale-space filtering. In *Proc. of IJCAI, Karlsruhe*, pages 1019–1021, 1983.

[42] L.P. Yaroslavsky. *Digital Picture Processing - An Introduction.* Springer Verlag, 1985.

[43] L.P. Yaroslavsky and M. Eden. *Fundamentals of digital optics.* Birkhäuser, Boston, 1996.

[44] W.P. Ziemer. *Weakly differentiable functions : Sobolev spaces and functions of bounded variation.* Springer-Verlag, New-York, 1989.